Dipl.-Ing. Gabriel Urrutia Benet
Department of Food Biotechnology and Food Process Engineering
Berlin University of Technology

HIGH-PRESSURE LOW-TEMPERATURE PROCESSING OF FOODS: IMPACT OF METASTABLE PHASES ON PROCESS AND QUALITY PARAMETERS

PhD Thesis
Berlin, December 2005

HIGH-PRESSURE LOW-TEMPERATURE PROCESSING OF FOODS: IMPACT OF METASTABLE PHASES ON PROCESS AND QUALITY PARAMETERS

vorgelegt von
Diplom-Ingenieur
Gabriel Urrutia Benet
aus Valencia, Spanien

von der Fakultät III – Prozeßwissenchaften
der Technische Universität Berlin
zur Erlangung des akademischen Grades

Doktor der Ingenieurwissenschaften
- Dr.-Ing. -

genehmigte Dissertation

Promotionsausschuss:
Vorsitzender: Prof. Dr. Tressl
Berichter: Prof. Dr. D. Knorr
Berichter: Prof. Dr. A. Le Bail

Tag der wissenschaftliche Aussprache: 2. Dezember 2005.

Berlin 2005
D83

“No hay libro tan malo que no tenga algo bueno”

Bachiller Carrasco en “El ingenioso hidalgo Don Quijote de la Mancha”
Miguel de Cervantes Saavedra.

Acknowledgements

I would like to thank Prof. Dr. Dipl.-Ing. Dietrich Knorr for the continuous support, confidence, scientific advice and, especially, for his amazing motivation and implication.

My gratitude is also expressed to Prof. Alain Le Bail, and Prof. Tressl, for their critical corrections and for being part of the evaluation committee during the thesis defence.

This thesis has been possible thanks to the financial support of the European Commission, through the project QLK1-CT-2002-02230, SAFE ICE: Low-temperature pressure processing of foods: safety and quality aspects, process parameters and consumer acceptance. But not only the financial support, but also the opportunity to be in close contact and cross-collaboration with some of the most influential scientists in the field of high-pressure low-temperature processing: Dr. Karin Autio, Dr. Pedro D. Sanz, Prof. Dr. ir. Marc Hendrickx, Prof. Dr. Alain Le Bail, Prof. Dr. Stanley Brul and MSc. Jacek Arabas.

This thesis has been also possible thanks to the collaboration with the scientists: Martina Lille, Ritva Heinonen, Antonio Molina, Laura Otero, Carlos de Elvira, Sandy van Buggenhout, Abdelah Ousegui, Nicolas Chapleau, Tong Shen, Janusz Szczepek, Andrzej Kakolewski and many others, to whom I express my thanks.

I also would like to express my gratitude to the colleagues at the Berlin University of Technology, Department of Food Biotechnology and Food Process Engineering, specially, to Dipl.-Ing. Cornelius Luscher, Dr. Oliver Schlüter, Dr. Volker Heinz, Dipl.-Ing. Julia Schneider, Dr. Terez Balogh and, particularly, to Dipl.-Ing. Stefan Boguslawski. My gratitude to Mrs. Irene Hemmerich, Mr. Martin Bunzeit, Mrs. Gisela Martens, Mr. Marcel Pohl and Mr. Pierre Stephan for their patience and support.

A very special thanks to Karn Pannetier, who made an excellent and patient work reviewing the English version of the text.

This work could not be possible without my parents and family, who gave me their support, confidence and love.

This work is dedicated to Hendrikje.

List of symbols

A	Cross-sectional area
a,b,c	Mathematical model parameters
Cp	Specific heat
d	Derivate
F	Force used during the compression
Fo	Adimensional number of Fourier
g	Gram
h	Hour
H or h	Enthalpy of fusion
h_0	height of the sample before compression
Hz	Herz
I to XII	Roman numerals for the identification of ice polymorphs
kg	Kilogram
kJ	Kilo Joule
L	Litres
L,a,b	Lightness, saturation and hue in the colour CIE-Lab-System
m	Meter
m	Mass
min	Minutes
MPa	Mega Pascal
P	Pressure
Q	Calorimetric energy
R	Radius
s or sec	Seconds
T	Temperature
t	Time
v	Specific volume
W	Watts
x	Position coordinate
α	Isobaric expansion coefficient
Δ	Increment or gradient
λ	Thermal conductivity
ρ	Density
Δh	Deformation
Δh	difference of height in sample before and during compression
ε_C	True compressive strain
ε_f	Failure strain
σ_C	True compressive stress
σ_f	Failure stress
∂	Partial derivative
°C	Degrees Centigrade
“	Inches

List of sub/superscripts

0 (sub)	Parameter value before processing
exp (sup)	Experimental
f (sub)	Freezing
i (sub)	Position step in iteration equations
i (sub)	Ice
l (sub)	Liquid
m (sub)	Melting
max (sub)	Maximum value
min (sub)	Minimum value

s (sub)	Solid
t (sub)	Time step in iteration equations
w (sub)	Liquid water

List of abbreviations

HP	High pressure
HPLT	high pressure and low temperature
PE	Polyethylene
PEF	Pulsed electric field
PPO	Polyphenoloxidase

Table list.

Figure list.

Abstract.

High pressure (HP) has been successfully used during the last two decades in food industry as an alternative to conventional thermal preservation methods, given the increasing demand for improved nutritional and sensory characteristics of foods. Freezing and chilling are still nowadays two of the most used preservation methods of foods, providing long term stability to products. Freezing and subsequent thawing are, nevertheless, responsible of undesirable changes in the texture and sensory properties of foods. Pressure markedly influences ice-water transitions and the use of HP in the Low-Temperature domain (HPLT) has opened great potentialities for improving the kinetics of freezing and thawing processes. High pressure treatment has several advantages including independence of size and geometry of the samples during processing, reduction of microbial and enzyme activities, retention of nutrients and the availability of a waste free technology. In this work, the kinetics of phase transitions up to 500 MPa (in the domain of ice I, ice III and ice V) have been studied and the existence of both liquid and solid metastable phases has been proven experimentally and used to analyze the influence of critical parameters to obtain controlled and optimized freezing and thawing paths, in terms of processing time reduction, and product quality and safety enhancement. A complete data base has been created for the phase diagram of potato tissue (taken as model of vegetal tissue), standards of definitions of possible processes in the HPLT domain has been suggested and a modelling work, including definition of processing times, bench mark tests and temperature profile reproduction and prediction has been addressed. A HPLT microscopic cell has been used to observe directly phase transition phenomena in different tissues, revealing new questions and challenges. The effect of pressure freezing/thawing on activities of food spoilage enzymes such as polyphenoloxidase, the degree of permeabilization, cell viability and degree of cell injury (using selective growth media) after various freezing methods and subsequent thawing for microbial model systems (Bacillus subtilis) and the direct impact of HPLT processes of food quality related aspects (colour, texture measurement, microstructure, drip loss) have been studied on both laboratory and pilot scale facilities, with the final aim of developing process and product concepts and performing a feasibility study on scale-up of the high pressure system for proposed processes.

Kurzfassung.

Hochdruck wird seit etwa 20 Jahren in der Lebensmittelindustrie als eine Alternative zu konventionellen thermischen Prozessen eingesetzt, bedingt durch die zunehmende Nachfrage nach Lebensmitteln mit verbessertem Nährwert und besseren sensorischen Eigenschaften. Gefrieren und Kühlen sind heutzutage zwei der am meisten angewendeten Konservierungsmethoden, die eine Lagerfähigkeit von Lebensmitteln ermöglichen. Gefrieren und Auftauen verursachen jedoch unerwünschte Veränderungen der Textur und der sensorischen Eigenschaften von Lebensmitteln. Druck beeinflußt Eis-Wasser-Phasenübergänge und seine Anwendung im Tieftemperaturbereich (HPLT, High-Pressure Low-Temperature) bietet große Möglichkeiten die Kinetik von Gefrier- und Auftauprozessen zu verbessern. Eine Hochdruckbehandlung bietet verschiedene Vorteile, wie die Unabhängigkeit von Größe und Form der Proben während der Behandlung, die Reduzierung mikrobieller und enzymatischer Aktivität, den Erhalt von Nährstoffen und die Möglichkeit abfallfrei zu arbeiten. In dieser Arbeit wurde die Kinetik der Phasenübergänge bis 500 MPa untersucht (in den Bereichen von Eis I, Eis III und Eis V) und die Existenz sowohl flüssiger als auch fester metastabiler Phasen experimentell nachgewiesen. Des Weiteren wurden Parameter untersucht, um kontrollierte Gefrier- und Auftauvorgänge festzulegen, die hinsichtlich einer Verkürzung der Prozesszeiten, der Produktsicherheit und der Produktqualität optimiert wurden. Eine vollständige Datensammlung für das Phasendiagramm von Kartoffeln, als Modell für pflanzliche Zellgewebe, wurde erstellt und Standards für die Definition möglicher Prozesse im HPLT – Gebiet wurden vorgeschlagen. Eine mathematische Modellierung der Prozesse wurde vorgenommen, einschließlich der Definition von Prozesszeiten, Benchmark-Tests und der Reproduktion und Vorhersage von Temperaturprofilen. Eine HPLT – Mikroskopiezelle wurde verwendet, Phasenübergangsphänomene in verschiedenen Matrices direkt zu beobachten, was neue Fragen und Herausforderungen aufwirft. Der Einfluß von Gefrieren und Tauen unter Druck auf die Aktivität von Verderb erregenden Enzymen wie Polyphenoloxidase, auf den Permeabilizationsgrad, sowie auf die Vitalität von Bakterien und das Ausmaß ihrer Verletzung (mittels Selektivmedium am Beispiel *Bacillus subtilis*) wurden untersucht. Diese Auswirkungen sowie der direkte Einfluß von HPLT – Prozessen auf lebensmittelrelevante Aspekte wie Farbe, Textur, Mikrostruktur und Abtropfverlust wurde sowohl im Labor- wie im Technikumsmaßstab erfaßt, mit dem Ziel Prozesse und Produktkonzepte zu entwickeln und die Anwendbarkeit derartiger Prozesse im Sinne eines Scale-up des Systems zu bewerten.

Resumen.

La tecnología de alta presión (High-Pressure, HP) ha venido siendo utilizada con éxito las dos últimas décadas en la industria alimentaria como alternativa a los métodos convencionales de conservación de alimentos, dado la creciente demanda de alimentos de alta calidad nutricional y sensorial. La congelación y la refrigeración (chilling) son aún hoy en día dos de los métodos de conservación más utilizados industrialmente, capaces de proporcionar estabilidad a largo término. Pero los procesos de congelación y descongelación son responsables de un detrimento en las propiedades sensoriales y estructurales (textura) de alimentos. La aplicación de alta presión tiene una influencia única en las transiciones de fase de agua y hielo y el uso de alta presión a temperaturas bajo cero (High-Pressure Low-Temperature, HPLT) ha abierto nuevas posibilidades para la mejora de la cinética de los procesos de congelación y descongelación. El tratamiento de alimentos a alta presión tiene varias ventajas intrínsecas, como son su isotropía (independencia de tamaño y geometría de los alimentos), la retención de propiedades nutricionales y el uso de una tecnología libre de aguas residuales. En la presente tesis doctoral, la cinética de las transiciones de fase a presiones de hasta 500 Mpa (en el dominio de las modificaciones de hielo I, III y V) ha sido estudiada y la existencia de fases meta-estables líquidas y sólidas ha sido experimentalmente comprobada. La comprensión de estas fases meta-estables ha sido la clave para estudiar nuevas posibilidades en los procesos de congelación y descongelación en HPLT, mediante las cuales se han reducido los tiempos de procesado y se han mejorado las propiedades de los productos tratados en cuanto a calidad y seguridad. Los resultados presentados en esta tesis incluyen la obtención de un base de datos completa sobre el diagrama de fases de patata (como ejemplo de tejido vegetal); la formulación de un estándar de definiciones de los posibles procesos en el dominio HPLT, el desarrollo de un modelo matemático, apoyado en la definición de tiempos de proceso y de transición de fases y en ensayos “bench-mark” entre tres laboratorios, para la reproducción y predicción de los perfiles de temperatura y presión; la obtención de imágenes de transición de fases en diferentes tejidos gracias al uso de una celda óptica HPLT acoplada a un microscopio invertido. Se han estudiado a escala laboratorio y piloto los efectos de procesos de congelación y descongelación a alta presión sobre la actividad de enzimas responsables de degradación en alimentos, como polifenoloxidasa, sobre la viabilidad celular y el grado de destrucción celular en medios de cultivo selectivos para sistemas microbiológicos (Bacillus subtilis) y sobre el impacto de estos procesos en propiedades relacionadas con la calidad de los alimentos (color, textura, microestructura, pérdida de agua). El objetivo de estos estudios fue en última instancia el desarrollo de conceptos de proceso y producto a escala industrial, a través de estudios de viabilidad y escalado en los procesos propuestos.

1. Introduction

Food process engineering deals with the transformation of vegetal and animal raw materials to consumer ready products, its main objective being to minimize the changes on the fresh-like characteristics and to achieve a microbial activity control that enables the supply of safe products. Together with pasteurization, freezing is the most used method for food preservation, based on the transformation from the liquid to solid state of the water content of food materials. The traditional problems associated with freezing processes, like the loss of texture, changes in colour and flavour, and the insufficient microbial control can be potentially solved through the application of high pressure during freezing and thawing processes. Taking advantage of the melting point depression under pressure, new possibilities are opened up for freezing and thawing processes under pressure.

Freezing, the preservation technology which is the most used industrially and the oldest used by humans for food preservation, provides long term stability to foods, avoiding microbial growth due to the reduction of water activity as long as water is kept in frozen state. “Freezing” technology is understood under the global process concerning freezing, frozen storage and thawing, and each step must be properly conducted to obtain optimum results when preserving foods. The largest “freezing” industry is, therefore, the one offering already thawed final products to consumers, the whole process (freezing + frozen storage + thawing) being carried out at an industrial scale. There exists, nevertheless, an emerging market of frozen products to be frozen stored and thawed domestically, stimulated during the late eighties after the commercialization on a big scale of domestic microwaves. This market of frozen products is, data from year 2003 in the USA, of $29.2 billion.

Nevertheless, the freezing industry still deals with serious problems in terms of food quality, being the most common undesirable changes in a product’s texture and sensory properties. It is well-known that, generally, slow freezing of foods allows osmotic transfer of water through the cell membrane and the growth of large extra-cellular ice crystals, causing extensive structural changes. On the other hand, enzyme and microbiological activity may be increased due to solute concentration. Independently of the freezing rate, the hexagonal ice modification I is obtained at atmospheric pressure, leading to a volume increase of about 9%, that leads to stress and mechanical damage affecting the texture of (specially plant) tissues.

The technology of high pressure was well-known already one century ago, applied for microbial inactivation (food control and preservation) at room and high temperatures (not at subzero temperatures). After the extensive and exhaustive work carried out during the first decades of the 20th century by Professor Bridgman in the field of high pressure food technology, the subject has been waiting for more than 70 years to focus the attention of scientists and industrial partners again. During the late eighties and during the nineties, the application of high pressure for food preservation appeared as the most promising of the new generation of non-thermal preservation technologies, being the one most studied among others like pulsed electric fields, pulsed light, ultrasonics, oscillating magnetic fields, etc. The success of high, hydrostatic pressure applied to food preservation has been demonstrated during the last 5 years through the best indicator possible: industrial interest on this emerging technology has been translated into a total estimated industrial high-pressure equipments of 82 (data September 2004), working all around the world, 64 of them (the 78%) being installed during the last 5 years. For different products (from meat, fish and sea-food, vegetables, juices, etc.), different sizes (50 to 300 litres) and different pressure (from 100 to 650 MPa) and temperature (from 4 to 60°C) levels, but in all cases, following the same principle: high hydrostatic pressure is able to inactivate micro-organisms (therefore to obtain a good microbial control of foods) in already packed products without the need for high temperatures. The two problems of traditional thermal preservation (mainly

pasteurization) are, therefore solved: (i) The two problems of traditional thermal preservation are, therefore, solved with the substitution of use of high-pressure instead of high-temperature: (i) the problem of the microbial contamination after temperature treatment during packaging and (ii) the problem of the dramatic texture, colour, flavour, vitamin content, etc. loss. The products obtained through the use of HP instead other thermal preservation methods, meet better the characteristics demanded by consumers of fresh-like, safe and high-quality products. "The application of high pressure in the low temperature range (subzero levels, where solid phases are present) was not studied seriously until the late nineties. The unique properties of water under pressure, especially the decrease of the freezing point reaching a minimum at around -22°C at 209 MPa, attracted the attention of scientists, opening a new technological potentiality to apply high hydrostatic pressure to freezing and thawing processes. The first direct consequences of the effect of pressure in the phase diagram of water are, apart from the freezing point depression, the reduction of the enthalpy of crystallization and the possibility of: (i) for freezing purposes, the use of pressure release as the driving force for an instantaneous (high percentage of instantaneously frozen water and low crystal size), isotropic (uniform crystal distribution within the whole volume) freezing process and (ii) for thawing purposes, the increment of temperature gradients between the sample and heating medium.

The effects of the combination of high pressure and low temperature (HPLT), being low temperature understood as subzero levels, have been studied on proteins, fats, sugars, vitamins and micro-organisms, as well as on freezing and thawing processes on plant and animal tissues. The study of the possible processes was, nevertheless, limited to the domain of ice I, that is, to pressures up to 210 MPa and temperatures down to -22°C. After nearly a decade of research, the benefits of HPLT processes on food products were repeated, but no novelty could attract the attention of industry to implement the technology for real products in a real market. The size of samples in the research publications (mostly laboratory scale), the products studied (mostly gels, emulsions, suspensions) and the scarce data on enzymatic and microbial effects of HPLT processes in real products might be the reason.

The aim of the research carried out in the frame of this doctoral thesis has been the extension of the applicability of high hydrostatic pressure for freezing, thawing and storing purposes to the domains of ice III and ice V, ice modifications with higher density than water. This means the study of possible processes for pressures higher than 210 MPa and temperatures lower than -22°C. The main goal was the development of industrial processing concepts and the study of consumer oriented, quality control parameters in real products (the potato was taken as an example of vegetal tissue). The work focused on the understanding of the basics of kinetics of phase transitions in water based products to the development of new processing concepts taking into account the new possibilities opened through the systematic understanding of the kinetics of freezing and thawing under pressure. The main findings presented in this thesis are:

a) the comprehension of the freezing kinetics in the HPLT domain, including higher ice modifications. A complete data base of phase transition individual events (phase transition points and nucleation points) has been obtained, after the systematic performance of freezing experiments at different constant pressure levels for a model product, potato, representing a vegetal tissue of high interest (chapter 4.1.1)

b) the study of the kinetics of thawing processes in the HPLT domain, with special attention to those processes in the domain of ice III. The different possible paths to be followed and the critical parameters to obtain controlled thawing paths have been experimentally obtained and a detailed explanation of the phenomena occurring during the different thawing processes has been

developed; the appearance of ice III during thawing of ice I could be controlled and/or avoided with the definition of these critical parameters (chapter 4.1.2)

c) the definition of new processes, like pressure-induced freezing at room temperature, or pressure-shift thawing, storage of liquids at subzero temperatures (chapter 4.1.3)

d) the experimental demonstration and definition of both liquid and solid metastable phases in the domain of ice III. The extension of phase transition curves for both ice I and ice V into the domain of ice III, the definition of the phenomenon of super-cooling under pressure and the definition of a new term "areas of nucleation" permitted the development of a new theory in which freezing and thawing processes were able to be performed implying ice I in the thermodynamic stable domain of ice III, therefore increasing the temperature gradients used up to now (chapter 4.1.4)

e) the exhaustive definition and a suggested terminology of all possible processes with and without phase transition (including solid-solid phase transitions) in the HPLT domain (chapter 4.1.5)

f) the study of thermodynamics and modelling of freezing and thawing at high pressure, including the definition of processing times (chapter 4.2.1) and the experimental determination of latent heat of fusion for potato samples in collaboration with ENITIAA (Nantes, France) (chapter 4.2.2), both information groups to be used in the development of a mathematical model in which a single step schema based on the use of Microsoft Excel® and Visual Basic to define the nucleation areas of each ice modification and using the nucleation events to re-feed the iteration schema with the new phase (change from liquid to solid, for freezing processes, for example) (chapter 4.2.3)

g) in relation to the mathematical model work, the different processing times defined (freezing time, phase transition time, thawing time) for different processes, delimitating the initial and final points to be used, and therefore, unifying criteria to facilitate comparison between different laboratories' results has been used to compare results from three different laboratories: in collaboration with the Instituto del Frío (Madrid, Spain) and the ENITIAA (Nantes, France), the experimental demonstration of the use of such time definitions in a bench mark test, performed in three different laboratories, working with four different facilities at different scales (chapter 4.2.4)

h) in collaboration with UNIPRESS (Warsaw, Poland), the comprehension of the phase transition phenomena in the HPLT domain through direct observation of different tissues with the help of a developed high pressure low temperature microscopic cell, in which nucleation and melting phenomena are directly observable under a microscope (chapter 4.3)

i) in collaboration with Unilever Research and Development (Vlaardingen, The Netherlands), the evaluation of the response of micro-organisms under high pressure and low temperature conditions, with special attention to the region at which metastable phases are described, in the example of Bacillus subtilis (chapter 4.4)

j) a case study of quality-related parameters of processed potatoes in both laboratory and pilot scale, in collaboration with ENITIAA (Nantes, France) and VTT Biotechnology (Espoo, Finland). Parameters like colour, texture, drip loss and microstructure (thanks to an embedding technique) have been evaluated for both laboratory and pilot scale, and the activity of the enzyme polyphenoloxidase (PPO) in the case of pilot scale have been evaluated after HPLT freezing and thawing processes with potatoes (chapter 4.5), and finally,

k) the study of texture characteristics and melting rates of high pressure treated ice cream, with the aim of enhance texture properties (chapter 4.6).

This research has been possible thanks to the economical support and, mainly, thanks to the scientific collaboration between the partners of the European Commission supported project QLK1-CT-2002-02230 - SAFE ICE: Low-temperature pressure processing of foods: safety and quality aspects, process parameters and consumer acceptance. The partners of this project: VTT Biotechnology (Espoo, Finland), Instituto del Frío (Madrid, Spain), Katholieke Universitait Leuven (Leuven, Belgium), ENITIAA (Nantes, France), Unilever Research and Development (Vlaardingen, The Netherlands) and UNIPRESS (Warsaw, Poland), have been in close collaboration with the Department of Food Biotechnology & Process Engineering of the Berlin University of Technology and thanks to this collaboration, the promising results obtained during last three years of research, summarized in this doctoral thesis, have been possible.

2. Theory of the HPLT technology

2.1. Historical review

2.1.1. Food preservation and the role of non-thermal emerging technologies

Food processing involves the transformation of raw animal or plant materials into consumer-ready products, with the objective of stabilizing food products by preventing or reducing negative changes in quality. Without these processes, we would neither be able to store food from time of plenty to time of need, nor be able to transport food over long distances (Lund, 2003). Processing aims are therefore essentially concentrated on adapting products to the requirements of nutritional physiology. This can mean eliminating substances foreign to foods, improving raw material by concentrating desirable or depleting undesirable constituents and, in particular, the mildest possible processing to maintain the original properties of the food to the greatest possible degree, or even improve them (Behsnilian, Regier and Stahl, 2003). Within this framework, avoiding or minimising microbiological contamination as well as limiting food quality losses due to enzymatic reactions by thermal processing, e.g. by blanching, pasteurisation or sterilisation, play major roles in food production. To consumers, the most important attributes of a food product are its sensory characteristics (e.g. texture, flavour, aroma, shape and colour). These determine an individual's preference for specific products and minor differences between brands of similar products can have a substantial influence on acceptability.

A goal of food manufacturers is to develop and employ processing technologies that retain or create desirable sensory qualities or reduce undesirable changes in food due to processing (Hogan et al., 2005). Physical (e.g. heating, freezing, dehydration and packaging) and chemical (e.g. reduction of pH or use of preservatives) preservation methods continue to be used extensively and technological advances to improve the efficiency and effectiveness of these processes are being made at a rapid rate. The basis of these traditional methods involves reducing microbial growth and metabolism to prevent undesirable chemical changes in food. One of the most common methods of food preservation used today is thermal treatment (e.g. pasteurization, sterilization). Traditionally, most preserved foods are thermally processed by subjecting the food to a temperature of 60 to 100°C for a few seconds to minutes (Jay, 1992). During this period, a large amount of energy is transferred to the food. This energy may trigger unwanted reactions in the food, leading to undesirable changes or formation of by-products. For example, thermally processed milk may have a cooked flavour accompanied by a loss of vitamins, essential nutrients and flavours. Although heating food effectively reduces levels of micro-organisms such as bacteria, such processing can alter the natural taste and flavour of food and destroy vitamins.

The fact that not only the shelf life but also the quality of food is important to consumers gave birth to the concept of preserving foods using non-thermal methods (Barbosa-Cánovas et al., 1998). Therefore, alternative or novel food processing technologies are being explored and implemented to provide safe, fresher-tasting, nutritive foods without the use of heat or chemical preservatives, foods that have fresh-like characteristics and satisfy new consumer demand (Goularte et al., 2004). Innovative non-thermal processes for preservation of food have attracted the attention of many food manufacturers. In the search for new processing methods, particularly for certain products, the application of high-pressure (HP) processing has shown considerable potential as an alternative technology to heat treatments, in terms of assuring safety and quality attributes in minimally-processed food products (Palou et al., 1999).

Examples of these non-thermal emerging technologies are: high pressure processing, pulsed electric fields, ultrasonics, high intensity pulsed light, irradiation/ionisation and oscillating magnetic fields. Although a lot of research has focused on these new preservation technologies, very few of these methods have been implemented by the

food industry until now. High hydrostatic pressure and pulsed electrical fields have been the most investigated ones (Devlieghere et al., 2004).

Details on high-pressure processing are given in the next section.

Pulsed electric field (PEF) pasteurization is a non-thermal process which destroys contaminating bacteria in short bursts (< 1 sec) of high voltage. Exposure to PEF destabilizes cell membranes and with sufficient intensity and duration of treatment, membranes are irreversibly damaged, important cellular compounds leak out, and cells die (Jeyamkondan et al., 1999, Simpson et al., 1999). At lower PEF doses, these effects on cell membranes have been exploited by genetic engineers to induce hybridization of cells and introduction of DNA fragments into cells (Jeyamkondan et al., 1999). Bacterial spores, Gram positive cells (including L. monocytogenes), and cells in stationary phase of growth are more resistant to the effects of PEF (Barsotti and Cheftel, 1999). For L. monocytogenes suspended in milk, a continuous flow PEF system resulted in a 3 log reduction in bacterial numbers at 25°C and a 4 log decrease at 50°C (Reina et al., 1998). As yet, this new technology has been applied primarily to liquids such as juices, milk, yogurt, beaten eggs, sauces, and soups (Qin et al., 1995). A PEF system has also been used to destroy E. coli in a homogeneous semisolid medium (potato dextrose agar) (Zhang et al., 1994). Pumpable food pastes such as vegetable or fruit purées and minced meat are also possible candidates for this type of pasteurization (Barsotti and Cheftel, 1999). Bacteria in dry powders (flour, spices), however, appear to be less susceptible to PEF compared to those in liquids (Jeyamkondan et al., 1999). Further research is needed to determine the potential for the use of PEF for the pasteurization of viscous and particulate foods.

2.1.2. HP technology applied to food preservation

The first reference of the application of HP to food preservation was published by Hite (1899). Milk was subjected to pressures of 650 MPa and a reduction in the viable numbers of microbes was obtained. Bridgman (1914) reported the coagulation of egg albumin by HP and reported different product properties as compared to gels obtained by heat coagulation. Astonishingly, the research on HP technology applied to the food industry had to wait until the late eighties to attract the attention of researchers: see Hoover et al. (1989), Hayashi (1989), Hayashi et al. (1992), Farr (1990), Deuchi and Hayashi (1990, 1991, 1992a and 1992b), Cheftel (1991 and 1992), Knorr (1993) among others.

For the last 15 years, the use of HPP has been explored extensively in the food industry and related research institutions due to the increased demand by consumers for improved nutritional and sensory characteristics of food without the loss of the "fresh" taste. In the late nineties, HPP was extensively used in Japan and a variety of food products like jams and fruit-juices were processed (Cheftel, 1995). There have been 10 to 15 types of pressurized foods on the Japanese market, but several have disappeared, and those that remain are so specific that they would be of little interest to European or American markets. Nevertheless, interest in HPP derives from its ability to deliver foods with fresh-like tastes without added preservatives. Examples of the first commercial pressurized products in Europe or US are: (1) orange juice by UltiFruit®, the Pernod Ricard Company, France; (2) acidified avocado purée (guacamole) by the Avomex Company in the US (Texas/Mexico); and (3) sliced ham (both cured-cooked and raw-cooked) by Espuña, Spain. The European "Novel Foods" Directive (May 1997) has introduced regulatory problems and slowed the introduction of new pressurized products and still means a great limitation for the normalization, label regularization and wide commercialization of HP treated products (Tewari et al., 1999).

High hydrostatic pressure has been already successfully implemented in the food technology field. Pressure-treated food products have been found since 1990 in the Japanese market (Knorr, 1995), and since 1996 the first pressure-processed products reached the markets of the European Union and the USA. The application of high pressure in food technology lies mostly on pasteurisation of juices, marmalades, and

other fruit and vegetable products, to achieve a better quality of products after processing, as compared to conventional thermal processes (Cheftel et al. 1997). The use of pressure as an alternative to thermal processing leads to lower temperature levels during processing, and this means a lower influence on the properties of the raw materials.:

A summary of the applications of HP technology to food preservation is given in Table 2.1:

Table 2.1. Application of HP in retention of sensory and nutritional characteristics of fruits and vegetables.

Reference	Product	Pressure (MPa)	Holding-time (min)	Temp. (°C)	Objective of the work
Eshtiaghi and Knorr (1993)	Potato cubes	400	15	5-50	Microbial safety, softness, functionality
Maggi *et al.* (1994)	Apricot nectar, Distilled water	600-900	1-20	20	*Byssochlamys fulva*, *B. nivea*, *Neosartorya fischeri*, *Talaromyces flavus*
Kimura *et al.* (1994)	Jams	-	-	-	Quality [volatile flavour components, anthocyanins, browning index, furfural, sucrose, vitamin C, microbiological stabilization
Moio *et al.* (1995)	White and red grape must	304-811	1-5	25	Microbiological stabilization
Dumay et al. (1996)	Dairy creams and model oil/water solutions	450	15-30	10-40	Size distribution of fat globules and oil droplets, emulsion stability and viscosity
Dong *et a/.* (1996)	*Angelica keiskei* juice	??	7	25	Sensory and shelf life
Kloczko and Radomski (1996)	Fresh apples, pears, bananas, parsley, potatoes, celery, juices	300, 370	6, 15	25	Preservation, aroma, flavour, microbial quality
Pehrsson (1996)	Citrus juice	500-700	1-1.5	0-5	Freshness
Donsi *et al.* (1996)	Orange juice	350	1	30	Microbial activity and chemical composition
Gow and Hsin (1996)	"Guava purèe"	400, 600	15	25	Quality and shelf life
Gomes and Ledward (1996)	Mushrooms and potatoes	100-800	20-40-60	1-20	Polyphenoloxidase activity
Rovere *et al.* (1997)	Chopped tomatoes	400, 600 or 800	3, 5 or 7	-	Colour, sugar content, pH
Severini *et al.* (1997)	Extra virgin olive and seed oils	700	10	25	Lipid oxidation
Butz et al. (1997)	Fruit and vegetable juices	400,600, 800	10	25,35, 50,100	Peroxidase activity and antimutagenic effect

Messens et al. (1997)	Milk, meat, egg and soy proteins	Up to 1000	15-30	room	Functionality of food proteins
Sancho et al. (1999)	Hydrosoluble vitamins (B1, B6 and C)	200-400-600	30	room	Vitamin retention, nutritional quality of matrices
Tedford et al. (1999)	ovalbumin, lysozyme and β-lactoglobulin	300,600	30	32,40	Structural changes of food proteins
Trujillo et al. (2000)	Cheese	300-600	25	2-25	Microbial control (Escherichia coli)
Reyns et al. (2000)	Yeast	120-320	15	-5/45	Foodborne yeast sensitivity to high pressure
Brul et al. (2000)	S. cerevisiae	200-300	15	25	Inactivation of S. cerevisiae
O'Reilly et al. (2001)	Cheese	400-450	5	25	Rennet coagulation time, rate of curd formation and cheese yield.
Wuytack and Michiels (2001)	Bacillus subtilus spores	100,600	10	40	Bacillus subtilus spores inactivation
Wilkinson et al. (2001)	Poliovirus	200,400, 600	15-60	25	Respiratory adenovirus inactivation
Yan and Barbosa-Cánovas (2001)	Agglomerated food powders	100-500	5	25	Food powders density measurement by means of high hydrostatic pressure
Ananta et al. (2001)	Bacillus Stearother-mophilus spores	50-600	Up to 100	60-120	Inactivation of Bacillus Stearothermophilus spores from mashed broccoli and cocoa mass
Butz et al. (2002)	Vegetables	100-600	5-60	25-95	Carrot, tomato and broccoli content of vitamins, antioxidants, antimutagens, effect on water retention, glucose retardation, changes in extractability
Lakshma-nan et al. (2003)	Salmon	-	-	-	Review article
Zhang et al. (2003	Soybean glycinin	0-600	0-35	-	Conformational changes of soybean glycinin
Minerich and Labuza (2003)	-	400-600	1-10	7-24	Development of a pressure indicator
Krebbers et al. (2003)	Tomato puree	Up to 700	30 seconds	Up to 90	Consistency, viscosity, colour, lycopene content, enzyme activity and micro-organisms
Dobiáš et al. (2004)	Polymer packaging	600	60	-	Mechanical properties, transparency, water vapour permeability, migration, etc.

Voldřich et al. (2004)	Apple juice	200-600	60	17-25	Resistance of vegetative cells and ascospores of heat resistant mould Talaromyces avellaneus
Dogan and Erkmen (2004)	Broth, milk, peach, orange juices	200-700	1-105	-	Inactivation kinetics of Listeria monocytogenes
Linton et al. (2004)	Minced chicken	500	15	40	Aerobic plate counts, psychrotrophic counts and anaerobic counts
Bauer et al. (2004)	Starch granules	300	60	-	Optical in situ analysis with a high pressure cell
Moerman (2005)	Pork Marengo	400	30	20-50	Inactivation of vegetative micro-organisms, aerobic and anaerobic spores
Suthanthangjai et al. (2005)	Raspberry	200,400, 600,800	15	18-22	Colour stability by anthcyanin content
Deliza et al. (2005)	Fruit juices	-	-	-	Review: consumer acceptance
Zhu et al. (2005)	Pork muscle	62,115, 157,199	-	-5/-20	HP calorimetry evaluation of crystal ratio
Torres and Velázquez (2005)	-	-	-	-	Review: commercial opportunities and research challenges
López-Rubio et al. (2005)	EVOH-based food packaging	400-800	5-10	40-75	Oxygen barrier and morphological properties
Van der Plancken et al. (2005)	Egg white proteins	400-700	20	10,25, 60	Turbidity, solubility, residual denaturation enthalpy, surface hydrophobicity, sulfhydryl content, susceptibility to enzymatic hydrolysis and trypsin inhibition activity).

2.1.3. Principles of HP technology

Three principles are the theory basis of the HP technology:

- Le Chatelier principle: Any phenomenon (phase transition, chemical reaction, change in molecular configuration) accompanied by a decrease in volume will be enhanced by pressure increase (Leadley and Williams, 1997, also cited in Zhu, 2004). Thus, HPP affects any phenomenon in food systems where a volume-change is involved and flavours phenomena which result in a volume decrease. The HPP affects non-covalent bonds (hydrogen, ionic, and hydrophobic bonds) substantially as some non-covalent bonds are very sensitive to pressure, which means that low molecular weight food components (responsible for nutritional and sensory characteristics) are not affected, whereas high molecular weight components (whose tertiary structure is important for functionality-determination) are sensitive. Some specific covalent bonds are also modified by pressure.
- Isostatic principle: Pressure is instantaneously and uniformly transmitted independent of the size and the geometry of the food (Balny and Masson, 1993).
- Microscopic Ordering Principle: At a constant temperature, an increase in pressure increases the degree of ordering of the molecules of a substance (Heremans, 1992).

2.1.4. Effect of high pressure on micro-organisms

The effectiveness of any food preservation technique is primarily evaluated on the basis of its ability to eradicate pathogenic micro-organisms present and so to enhance the product's safety; a secondary objective is inactivation of spoilage micro-organisms to improve the shelf-life of the food (McClements et al., 2001). Growth of micro-organisms in foods can cause spoilage by producing unacceptable changes in taste, odour, appearance and texture (Hogan et al., 2005).

Micro-organisms are a heterogeneous group of organisms, different members of which are capable of growth at temperatures from well below freezing (extreme psychrophiles) to temperatures above 100°C (extreme thermophiles). However, each species has a particular temperature range in which it can grow best; this range is determined largely by the influence of temperature on cell membranes and enzymes, and growth is restricted to those temperatures at which cellular enzymes and membranes can function. As with heat, large differences in pressure resistance can be apparent among various strains of the same species (Hogan et al., 2005). Figure 2.1 shows the pressure/temperature combinations used for different processes.

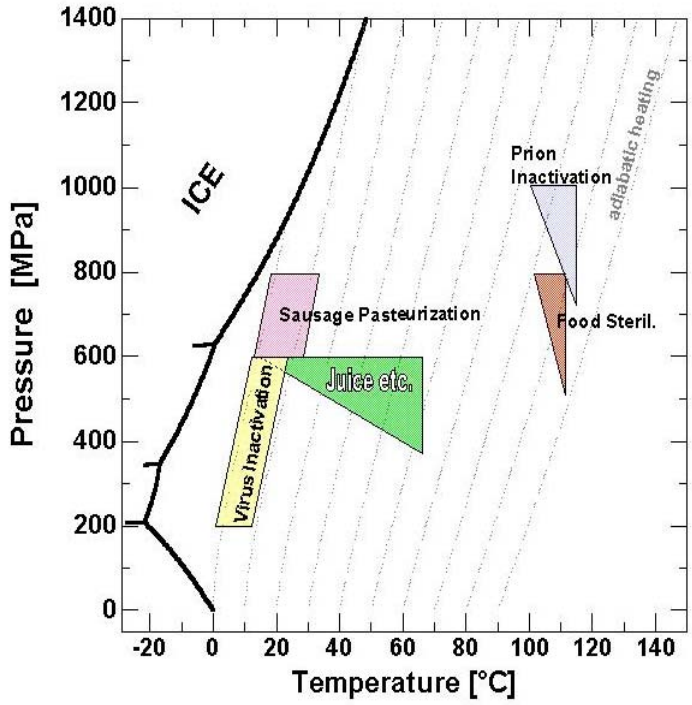

Figure 2.1. Temperature and pressure combinations for different preservation processes and products, on the phase diagram of water (V. Heinz, personal communication).

Effect of high pressure on bacteria and bacterial spores

Although it has been known for over a century that HP can inactivate micro-organisms, further investigation is necessary to determine the mechanisms of inactivation. It is now known that HP can damage membranes, denature enzymes and cause changes in cell morphology (Hoover et al., 1989 and Mackey et al., 1994). Hoover et al. (1989) proposed that, in a similar way to thermal inactivation, HP does not disable one specific site, but acts on a variety of targets depending on the pressure applied.

Cell membranes are thought to be a primary target for HP inactivation of bacteria (Cheftel, 1995 and Smelt, 1998), and evidence for this is provided by the relationship between pressure resistance and membrane fluidity (Smelt et al., 2002). Furthermore, it has been suggested that susceptibility to HP of Gram-negative compared to Gram-positive bacteria is due to the complexity of Gram-negative cell membranes (Shigehisa

et al., 1991). HP disrupts membrane function and causes leakage through the inner and outer membranes, as demonstrated for HP-treated cells by their increased sensitivity to sodium chloride and bile salts (Chilton et al., 1997), uptake of propidium iodide and ethidium bromide (Mackey et al., 1995), and leakage of ATP (Smelt et al., 1994). Membrane perturbation is attributed to the promotion of phase transitions in the phospholipid bilayer from liquid to more tightly packed gel phases (Marquis, 1976). HP can also denature or displace membrane-bound enzymes.

In addition, HP induces changes in morphology and internal organisation of cells, including cell lengthening, contraction of the cell wall and pore formation, separation of the cell membrane from the cell wall, and compression of gas vacuoles (Cheftel, 1995). Altered distributions of DNA and ribosomes (Chilton et al., 1997), and ribosome destruction (Isaacs et al., 1995) have also been observed in HP-treated cells, and a correlation between cell death and ribosome damage has been suggested (Niven et al., 1999). Although nucleic acids are more resistant than proteins to HP (Marquis, 1976), condensation of nuclear material has been observed following treatment at very high pressures (Mackey et al., 1994 and Wouters et al., 1998). There is also evidence that HP can cause degradation of bacterial DNA, due to the action of endonucleases not normally in contact with DNA (Chilton et al., 1997).

Many studies have shown that pressures in the range of 300–600 MPa can inactivate many fungi and vegetative bacteria (Smelt, 1998); however micro-organisms can differ widely in their intrinsic susceptibility to HP. Bacteria, in particular, demonstrate a wide range of resistance to HP. Gram-negative bacteria tend to be more sensitive to HP than Gram-positive species (Farkas and Hoover, 2000 and Smelt, 1998), but there are many exceptions to this generalisation, for example, certain strains of E. coli O157 are exceptionally pressure resistant (Patterson et al., 1995). The HP-resistance of bacteria is dependent on many factors, including strain (Alpas et al., 1999, Benito et al., 1999 and Linton et al., 2001), growth phase (McClements et al., 2001 and Pagan & Mackey, 2000), growth temperature (McClements et al., 2001), and the composition of surrounding matrices (Patterson et al., 1995 and Simpson & Gilmour, 1997). Bacterial spores are very resistant to inactivation by HP; for example, spores of Clostridium botulinum strains can survive extreme treatment conditions (827 MPa for 30 min at 75 °C; Farkas & Hoover, 2000). However, the use of oscillatory HP treatments, where a lower HP induces spores to germinate, allowing their inactivation by a subsequent cycle at a higher HP, has proved successful (Hayakawa et al., 1994 and Sale et al., 1970).

Effect of high pressure on viruses

Viruses are a structurally diverse group of organisms that also differ widely in their sensitivities to HP (Table 1). For example, feline calicivirus (a norovirus surrogate) is inactivated by treatment at 275 MPa for 5 min (Kingsley et al., 2002). In contrast, poliovirus is very resistant to HP, with no significant reductions in infectivity reported after relatively severe treatments, such as 600 MPa at 20 °C for 60 min (Wilkinson et al., 2001). The reason for the disparate resistance of viruses to HP is not known. It has been suggested that the resistance of poliovirus may be related to the size and shape of the virus particle (Wilkinson et al., 2001) or its high thermodynamic stability (Oliveira et al., 1999).

The mode of inactivation of viruses by HP has not been fully elucidated. It is known that HP causes macromolecules to dissociate and much of the published data concerns the use of HP as a tool to investigate virus assembly. HP induced dissociation of viruses may be fully reversible or irreversible, depending on the virus and treatment conditions and typically more extreme treatments lead to irreversible changes in virus conformation (Gaspar et al., 1997 and Silva & Weber, 1988).

2.1.5. HP market for food preservation

From the first commercialization of HP processed products (orange juice by UltiFruit®, acidified avocado purée (guacamole) by Avomex Company and sliced ham by Espuña, to the very latest new commercialization, published by Hormel Foods, introducing the True Taste™ technology[1], a large number of products have been commercialized, but still none of them labelled as HP-processed products. It cannot be forgotten that the European "Novel Foods" Directive (May, 1997) has introduced regulatory hurdles and slowed down the introduction of new pressure-treated products (Tewari et al., 1999). However, the evaluation of this legislation was envisaged after 5 years and since this process is not completed now the further progress with regard to new applications of high pressure in the low temperature region remains somewhat unclear. But, it can be expected that the relatively moderate pressures (for relevant processes mainly below 300 MPa) to be applied helps simplify the demanded proof of substantial equivalence before introducing a high pressure product to the food market, since this pressure range is just slightly above the pressure level reached in commercialised processes (e.g. homogenisation of ice cream at 200 MPa). Based on the results of this study substantial equivalence of high pressure – low temperature processed and conventionally processed foods can be assumed for the materials investigated. Nevertheless, further studies on this topic might be necessary for acceptance of the European executives.

---

[1] May 25, 2005

BREAD READY® sliced meats with TrueTaste™ technology are raising the standard for today's sliced meats.

BREAD READY® sliced meats have always offered pre-sliced convenience, portion control and excellent flavor. Now, thanks to an advanced high pressure processing technology, this HORMEL® product line can offer all that and much more – while eliminating the need for chemical preservatives commonly found in other sliced meats. BREAD READY® sliced meats with TrueTaste™ technology employ controlled water pressure to kill potentially harmful pathogens and spoilage organisms, thus eliminating the need for any chemical preservatives, including sodium lactate, potassium lactate and sodium diacetate. This gives BREAD READY® meats an even cleaner, fresher flavor; without the metallic or salty aftertaste created by chemical preservatives. Also, by killing the potentially harmful bacteria – versus just slowing their growth – TrueTaste™ technology has doubled the shelf life of BREAD READY® sliced meats. This extended shelf life, in turn, allows for greater inventory flexibility. These are welcome improvements not available via chemical preservatives that have long been a standard means to inhibit bacteria growth and ensure a modest shelf life. Going forward, this new Hormel Foods' technology clearly raises the industry standard for sliced meats by providing dramatically improved food safety, a cleaner meat flavor with no metallic aftertaste, plus a refrigerated shelf life that goes well beyond the current industry norm.

Hormel Foods' proprietary TrueTaste™ technology is an all-natural, USDA-approved process that goes beyond inhibiting bacterial growth. It actually kills bacteria, without affecting the meat's true taste, texture, appearance or nutritional value. After the BREAD READY® meats have been sliced and packaged, the entire sealed package is placed in a TrueTaste™ technology chamber where it is surrounded by water. By exerting equal pressure from all sides, the cellular activity of the pathogens is interrupted, causing them to die. However, the meat flavor and all meat properties (such as vitamins) retain their full integrity. Also, because the package is sealed, new germs cannot be re-introduced due to slicing or handling. Ultimately, the entire line of BREAD READY® sliced meats with TrueTaste™ technology deliver a truer meat flavor, greater inventory flexibility and the utmost in food safety.

Hormel Foods is the first food processor in the country to employ large-scale high pressure pasteurization (utilizing controlled water pressure) to extend the un-opened shelf life and bolster food safety in sliced meats. "It's going to be a big step in preservation technology," commented Martin Cole, director of the National Center for Food Safety and Technology at the Illinois Institute of Technology. Extensive testing has proven that when BREAD READY® sliced meats arrive at the operator's door, they are among the absolute safest meats in the industry. For additional information on BREAD READY® sliced meats with TrueTaste™ technology, simply call 1-800-723-8000.

Some examples of commercialized products are given:

Espuña, Spain.

Equipment: Hyperbar – ACB pressure systems, France

Technical data: internal diameter = 0.28m; length = 5 to 5.20m; internal volume = 255 to 320 L; maximal pressure = 400 to 600 MPa; pressurization time = 10 min; pressure transmitting medium = water; maximum temperature of water = 15°C; cycles/day = 23; total cycles carried out (1998 to 2004) = 36,000; production = 2400 kg/day

Products: mainly sliced cooked ham. Since 1998 Espuña has been using HP for the whole range of sliced cooked ham (high water activity) products. Since February 2002, new ready products were developed (tapas: small cooked sausages, small kebabs, etc.) and they are all HP treated to improve their microbial safety. In the case of low water activity products (dry cured products), the use of HP is not really effective against microorganisms at 400 MPa (pressure level used for high water activity products). The use of 600 MPa for low water activity products enhanced these results.

Jumex, Mexico

Equipment: Hyperbar – ACB pressure systems, France

Technical data: internal diameter = 0.28m; length = 6.84m; internal volume = 2 x 420 L; maximal pressure = 500 MPa; production = 3000 L/h

Products: fruit juices

Many other products could be detailed here. In Table 2.2, a list of commercialized products using HP technology is given. Figure 2.2 shows some of these products.

Table 2.2. Commercial products treated by HP (source: NC-Hyperbaric; personal communication from C. Tonello).

Company	Country	Year	Product	Treatment
Meat products				
Fuji Chiku	Japan	1994	Raw-salted pork ham	250 MPa, 20°C, 3h
Espuña	Spain	1998	Sliced cooked ham & tapas	400 MPa, 15°C, 10-20min
	USA	2001	Sliced cooked products and prosciutto ham	
	USA	2002	Poultry products	

	USA	2002	Pre-cooked chicken and beef strips	
Campofrío	Spain	2002	Sliced cooked chicken, ham and turkey, Serrano dry ham	600 MPa, 20°C, 3min, 300 L
Vismara	Italy	2004	Prosciutto ham, salami, mortadella & pancetta	600 MPa, 20°C, 300 L
Itoham	Japan	2004	Dry & cooked meat	600 MPa, 20°C, 150 L
Abraham	Germany	2005	Dry & smoked ham	600 MPa, 20°C, 150 L
Maple Leaf	Canada	2005	Leaf	600 MPa, 20°C, 55 L

Juices and beverages

Meiji	Japan	1990	Fruit concentrates, jams and gelatines	400 MPa, 10-20min, 150L/h
Pokka	Japan	1991	Fruit juices	200 MPa, 10-15min, 600L/h
Pampryl	France	1994	Orange juice	Confidential
Jumex	Mexico	2001	Fruit juices	500 MPa, 2 x 420L, 3000L/h
	USA	2000	Orange juice	
	Lebanon	2001	Fruit juices	
	UK	2001	Citrus juices and smoothies	
	USA	2001	Apple juice	
	Portugal	2001	Apple juice	
	Italy	2001	Fruit and vegetable juices	
	Ireland	2001	Fruit juices and smoothies	
	USA	2002	Orange juices and lemonade	
	Czech Rep.	2004	Broccoli and apple juice	

Vegetal products

Meiji	Japan	1990	Vegetable sauces	400 MPa, 10-20min, 150L/h
Echigo Seika	Japan	1994	Pre-cooked hypoallergenic rice	400 MPa, 10min, 45-70°C
Avomex	USA	1997	Guacamole sauce	600 MPa, 2 x 215L
Solofrutta	Italy	2001	Fruit jams	
	Mexico	2002	Avocado products	
	Mexico	2002	Guacamole	
	Mexico	2003	Avocado products	
	USA	2003	Sliced onions	

	Canada	2003	Apple products	
	USA	2004	Soya products	

Shellfish and fish

Kibin	Japan	1995	Vieiras de Santiago	Confidential
	USA	1999	Oysters	
	Japan	2000	Kipper	
	Japan	2000	Salmon	
	USA	2001	Oysters	
	USA	2001	Oysters	
	USA	2001	Oysters	
	Australia	2002	Oysters	
	Canada	2004	Seafood	
	New Zealand	2004	Seafood	
Giezzi	Italy	2004	Desalted cod	
Ocean choice	Canada	2004	Lobster	275 MPa, 20°C, 1min, 300 L
Campofrío	Spain	2005	Ready-to-eat salmon and kake	600 MPa, 20°C, 3min, 300 L

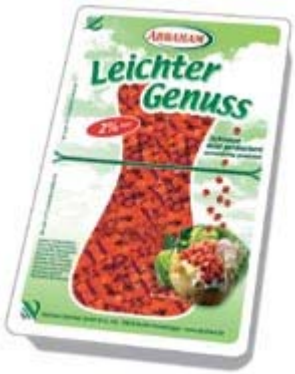


PERDUE
Short Cuts
Carved Chicken Breast
Original Roasted


Avocado's Number
Guacamole


FRESHER LASTING


SOLOFRUTTA
Mela


AVOCADO
Pico de Gallo
100% FRESH
ALL NATURAL!


GUSTIVIVI
MELA
PERA
SUSINA


ulti
JUS DE
PAMPLEMOUSSES
FRAICHEMENT
PRESSÉ


PINEAPPLE, BANANA &
MANGO FRUIT SMOOTHIE

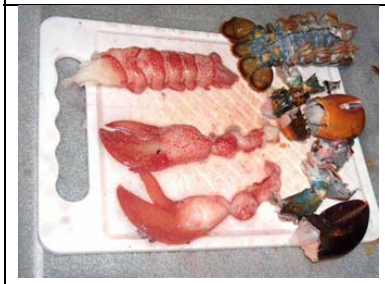


OYSTERS
ARE
BACK!

Figure 2.2. Some examples of commercialized products treated with HP.

The number of HP equipments installed and in industrial usearound the world is estimated at a total of 82. Figure 2.3 shows the evolution with the years and the continent in which the facilities are installed or the industrial sector (source, C. Tonello, NC Hyperbaric, personal communication).

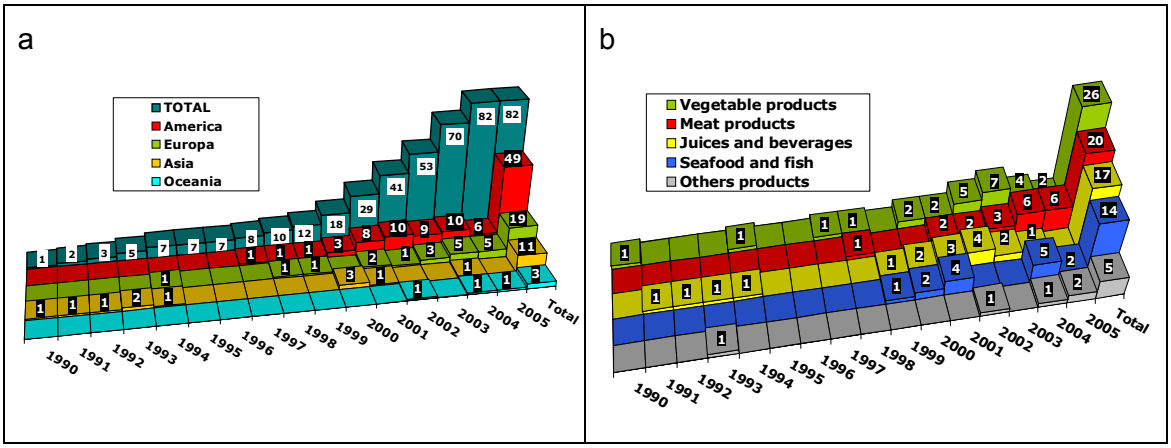

Figure 2.3. Industrial HP equipment numbers versus year of installation and continent (a) or industrial sector (b). Data from Nicolás-Correa Hyperbaric company, Spain (personal communication from Mrs. C. Tonello).

2.1.6. Food freezing and thawing industry

Basics of freezing process

The physico-chemical processes that occur during a freezing process can be explained with the help of Figure 2.4 in which the time-temperature relationship for freezing of pure water (ABCDE) and aqueous solutions (AB'C'D') is shown. The first thermal event that can be seen from such a diagram is super-cooling below the freezing point before the induction of crystallization, from A to B or B' . This is a non-equilibrium, metastable state which is analogous to an activation energy necessary for the nucleation process. Pure water can be super-cooled by several degrees before the nucleation phenomenon begins.

Once the critical mass of nuclei is reached, the system nucleates at point B or B' in the figure and releases its latent heat faster than heat is being removed from the system. In aqueous solutions, however, B' is not as low as B, since the added solute will promote heterogeneous nucleation, thereby accelerating the nucleation process. The temperature increases instantly to the initial freezing temperature, T_f, of the solution at Point C or C'. The presence of solutes results in the depression of the freezing point based on Raoult's Law, which relates the vapour pressure of the solution to that of pure solvent based on solute concentration. Note that C' is not as high as C, because the initial freezing point is depressed as a result of the solute. Hence, the solute has greatly decreased the amount of super-cooling for two reasons: faster nucleation and lowered

freezing point. In very concentrated solutions, it is sometimes even difficult to induce super-cooling.

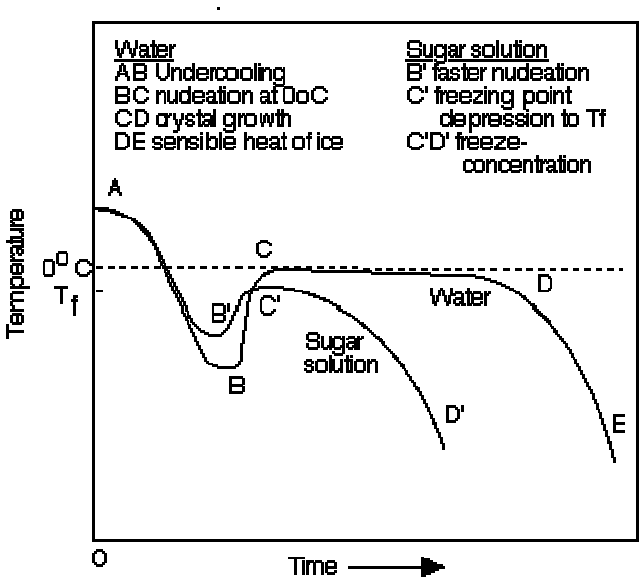

Figure 2.4. Basics of freezing process for water and sugar solution. Adapted from Goff, D. (2005), with permission.

In pure water, the time line from C to D in the figure reflects the time during which crystal growth is occurring. Fast freezing rates promote the formation of many small ice crystals during this period. The partially frozen mixture will not cool until all of the "freezable" water has crystallized; hence, the line CD occurs at nearly constant temperature. After crystallization is completed, the temperature drops from D to E as sensible heat is released. This time space C to D is defined as the freezing plateau (Goff, D., 2005).

Freezing and thawing in foods

The freezing process consist of freezing, frozen storage and thawing, each of which must be properly conducted to obtain optimum results when preserving foods and living specimens (Schlüter, 2004). Freezing involves lowering the product temperature to -18°C or below (Fennema et al., 1973)[2]. The temperature reduction process can be divided into three distinct phases: a pre-cooling or chilling phase in which the material is cooled from its initial temperature to the freezing point, a phase change period (the freezing plateau) which represents the phase transition, and a tempering phase in which the products reaches the final established temperature (Delgado and Sun, 2001).

At temperatures below 0°C there is a significant reduction in growth rates for micro-organisms and in the corresponding deterioration of the product due to microbial activity. The same temperature influence applies to most other reactions that might normally occur in the product, such as enzymatic and oxidative reactions (Schlüter, 2004). In addition, the formation of ice crystals within the product changes the availability of water to participate in reactions. As the temperature is reduced and more water is converted into a solid state, less water is available to support deteriorative reactions (Singh and Heldman, 2001). Thus frozen products benefit from two stabilising

[2] This definition is based on the Council Directive of 21 December 1988 on the approximation of the laws of the Member States relating to quick-frozen foodstuffs for human consumption (89/108/EEC). The article 1 states that “For the purposes of this Directive 'quick-frozen foodstuffs' means foodstuffs which have undergone a suitable freezing process known as 'quick-freezing' whereby the zone of maximum crystallization is crossed as rapidly as possible, depending on the type of product, and the resulting temperature of the product (after thermal stabilization) is continuously maintained at a level of -18 °C or lower at all points.

factors: reduced temperature and reduced effective moisture content. The primary advantage of frozen products is that of guaranteed long-term stability. At the higher temperatures of storage or shelf-stable products, chemical change is much more rapid, and high quality life is much shorter.

The general principles of food freezing have been detailed in many books and articles (Fennema, 1973; Bello et al., 1982; Jeremiah, 1996; Erikson and Hung, 1997; Rao and Hartel, 1998; Reid, 1998a,b; Kennedy, 1998; Vali, 1995,etc.). It is well-known that “slow freezing” induces the formation of large ice crystals that may cause mechanical damage, while “rapid” freezing enhances nucleation and the formation of many smaller crystals. Slow freezing of cellular tissues (especially from fruits and vegetables) leads to large extra-cellular ice crystals, thus to an increased extra-cellular concentration of solutes, and therefore, to cell dehydration and death through osmotic plasmolysis and membrane damage. Upon thawing, extra-cellular ice does not re-enter the cells and may cause extensive drip and texture softening. Detrimental reactions are also enhanced by solute concentration effects and closer enzyme-substrate interactions. Rapid freezing of cellular tissues induces simultaneously extra- and intracellular ice crystals, the latter promoting cell death through disruption of the cytoplasmic gel and organelles. Very rapid freezing (e.g., in liquid nitrogen) may also cause macroscopic cracks due to non-homogeneous volume expansion. Thus, freezing processes and conditions have been optimized for different types of foods, taking into account a whole range of parameters from initial quality to packaging, storage conditions, turnover, and consumer preferences. Thawing conditions are also critical, since phenomena like recrystallization can occur, with detrimental effects (Cheftel et al, 2000).

Freezing and thawing industry

The birth of the modern frozen food industry is normally regarded as having taken place when Birdseye introduced the double-belt contact freezer in 1928 and later the multi-plate freezer. Subsequently events of significance were the development of individual quick freezing (IQF) by introducing in-line freezers such as the fluidised bed freezer and cryogenic freezing equipment (Mallet, 1994, Thevernot, 1979). Frozen foods might have died off altogether if not for the onset of World War II. When Japan overran south-east Asia, it captured a large portion of the world’s tin resources and the U.S. government placed stringent controls on canners in an effort to conserve this vital wartime metal. This opened the door for frozens, which used less crucial materials such as paperboard, waxed paper and cellophane. Furthermore, retail shelves emptied as canned goods went to war, so major grocery chains eagerly pressed frozens into service to fill the gaps. Additionally, since frozens did not use metal, their purchase by consumers required fewer ration points than canned products.

The 1940s were host to another milestone in the growth of the frozen food industry: the introduction of frozen concentrated orange juice. This product really marked the first volume item for the frozen food industry, but was soon followed by another: frozen breaded seafood.

The 1950s were significant for the frozen food industry because it marked the introduction of a product that grew to be synonymous with the term frozen food: the TV Dinner. For the first time, a complete meal was available in frozen form to families who wished to dine quickly and easily at the table or in front of the TV, as the name implied. These dinners included an entree/meat item, a starch and a vegetable, and sometimes a dessert.

The 1960s were lean years for the frozen food industry, but not in the traditional sense. The 1960s were characterized by a new "diet" craze in the USA and Europe, and from this craze such products as Lean Cuisine and Weight Watchers were born. The industry continued to experience growth until the early 70s, when the USA was gripped by one of the worst recessions in history, and an inflationary spiral that led the government to institute severe price controls.

The introduction of the microwave oven for home use allowed consumers to prepare frozen foods in record time, and solved the dilemma of families who now had two working parents. Teamed with the microwave oven, frozen food's new buzzword became "convenience," and consumers were quick to respond. TV dinners were replaced by "frozen entrees" and upscale dinners, with more taste and variety, and the option to prepare dinner in minutes using the microwave.

The 1990s ushered in an era of "healthy" eating. Frozen foods were quick to adapt to this new life-style of western world, and brands like Healthy Choice, Lean Cuisine, Weight Watchers, and many others thrived. Consumers were hungry not only for taste, but for healthy ingredients, and regulations requiring full disclosure of ingredients made consumers more health conscious than ever before. Words like "lite," "low-salt," "low-fat," and "low-cholesterol" were the new adjectives of choice on frozen meals (National Frozen and Refrigerated Foods Association, NFRA, http://www.nfraweb.org/).

The different freezing technologies industrially used up-to-now can be categorized in many ways: by batch or in-line operation, by heat transfer systems (air, contact, cryogenic) or by product suitability (Schlüter, 2004). To reduce freezing time and water loss during the process, a cryomechanical process was developed for freezing of products with low mechanical resistance (strawberries, raspberries, shrimps), products that otherwise change their appearance (chicken, scallops) or products that tend to stick or clump (diced potatoes) (Londhal and Goranson, 1995). Cryomechanical freezing consists of the association of two freezing systems: an on-line cryogenic immersion freezer combined with a mechanical freezer (air-blast) to compete freezing (Agnelli and Mascheroni, 2001). However, some products may crack or even shatter if the freezing rate is too high, or if the products are exposed directly to extremely low-temperature freezing media. (Hung and Kim, 1996).

Table 2.3 shows the situation of frozen products sales in the USA for year 2003. The sales of frozen vegetables, even being of a great value ($2,8 billion), has an increase of only +0,3%. The quality of frozen vegetables might me the responsible. Therefore, there is a big opportunity for HPLT processing given the quality enhancement obtained and the consumer's demand of high quality, fresh-like products.

Table 2.3. Industry sales of frozen products in the USA, in 2003. (Source: Information Resources, Inc. 2003).

	Sales	% Change vs. 2002
Total Frozen Food Sales	$29.2 billion	1.6
Bread Dough	$590 million	2.6
Breakfast Foods	$1.06 billion	-0.6
Novelties	$2.5 billion	5.8
Ice Cream	$4.8 billion	-2.1
Frozen Dessert/Fruit/Toppings	$764 million	2.3
Juices/Drinks	$611 million	-13.2
Pizza/Snacks	$3.57 billion	2.5
Hors D'Oeuvers/Snacks	$825 million	2.3
Pizza	$2.74 billion	2.8
Total Prepared Foods	$6.35 billion	0.4
Frozen Dinners	$1.27 billion	2.4
Frozen Entrees	$3.67 billion	-2.1
Hand-held Entrees (non-breakfast)	$1.08 billion	7.9
Pot Pies	$325 million	2.3
Meat/Seafood	$4.87 billion	8.4
Meat	$1.12 billion	9.8
Poultry	$2.1 billion	6.8
Seafood	$1.65 billion	8.6
Vegetables	$2.8 billion	0.3
Broccoli	$194 million	1.5

Corn/Corn on the Cob	$324 million	-6.3
Beans	$220 million	3.6
Mixed Vegetables	$455 million	-2.9
Peas	$203 million	-2.5
Potatoes	$858 million	-1.1

The case of ice cream, with $4,8 billion sales, but with a growth of -2,1% shows the case of a product with a stabilized market that could be re-activated through the introduction of quality enhancement factors by new technologies, or through the use of simplified or cheaper processes, like the one suggested in this thesis (chapter 5) of combining the freezing and the homogenization step of ice cream production in a single step at high-pressure. The case of prepared foods is of special interest, taking into account the great quantity and variety of products involved: dough, vegetables, meat, sauces, etc. It is also the case of a product that is susceptible to be treated in frozen and in chilled state and the opportunities of HP applied to chilled products has not still been investigated. The most interesting case is the one of meat and seafood. Both products imply nearly $5 billion sales, with an increment of +8,4% (!). In this case, new process ideas like meat tenderization with the use of solid-solid phase transitions is of special interest given the rapidly growing market.

2.1.7. Problems and limitations of food freezing and thawing industry

Freezing:

Freezing provides long term stability to foods. At the same time, freezing and subsequent thawing of foods cause undesirable changes in their texture and sensory properties. Studies of the effects of freezing and thawing rates on food quality led to the current trend of rapid freezing and thawing or, more economically, to a combination of slow and rapid freezing and thawing (George, 1993). In fact, the optimum freezing rate for foods is system-dependent. Generally, slow freezing of tissue material allows osmotic transfer of water through the cell membrane and the growth of large extra-cellular ice crystals, causing extensive structural changes and a shrunken appearance of cells (Fennema, 1975; Reid, 1990; George, 1993; Shagian and Goff, 1996). Other problems, like increased enzyme and microbiological activity may result from increased solute concentration. Rapid cooling, on the other hand, results in numerous smaller ice crystals (intra- and extra-cellular), and leads to better product quality with a frozen appearance, one that is similar to the unfrozen material. Independent of the freezing rate, freezing to ice I (the ice modification existing at atmospheric pressure) is accompanied by a volume expansion of about 9%. The resulting non-uniform volume change may cause stress and possible mechanical damage affecting the texture of plant tissues. Furthermore, the freeze concentration which accompanies freezing causes change in the pH, ionic strength, viscosity and several other properties of the unfrozen matrix. In addition, water structure and water-solute interaction may change and macromolecules may be forced close together creating more chance for detrimental chemical reactions. This can cause damage in susceptible products (Fennema, 1975).

There are four contributory processes that are particularly important when considering the mechanisms of freezing damage in plant tissues, namely chill damage, solute-concentration damage, dehydratation damage and damage from ice crystals (Reid, 1993). Damage to the internal membrane allows enzymes and substrates which are normally separated, to mix. This results in a wide range of chemical reactions leading to breakdown of the cells and the development of off-flavours and colours (Edwards, 1995). Colour changes can result in irreversible browning or darkening of the tissues. The enzyme related to this biochemical reaction is polyphenoloxidase (PPO), which can be found in most plant tissues but in especially high amounts in mushrooms and potato tubers. Consequently, heat treatment (e.g. blanching) is partially used prior to freezing to inactivate the enzymes and certain micro-organisms (Cano, 1996).

Thawing:

The conventional conductive or convective industrial thawing of foods with water and/or air requires substantial amounts of time and energy, produces large volumes of wasted drinking water (e.g. approx. 7 m^3 per ton of frozen fish) and in addition can often result in reduced microbial and sensory qualities. Microwave thawing which became a viable tool in households has not found its entry into the industrial scale due to energy costs, low penetration depth and temperature gradients within products (Zhao et al., 1998).

During thawing, additional time is spent at a temperature just below the initial freezing temperature. This has detrimental effects on food quality, as re-crystallization (or clustering of existing small ice crystals in bigger ones; these phenomena are discussed in chapter 4.3, through the microscopic results) and growth of micro-organisms are more likely at this temperature than at any other subfreezing temperature. In addition, many deteriorative chemical reactions like protein insolubilization and lipid oxidation are surprisingly fast. Another phenomenon associated with thawing is the collapse of product structure with loss of the cells water-holding capacity, i.e., drip loss. Thus, thawing poses greater potential damage to food quality than freezing in the frozen food chain (Fennema, 1975). Hence, there is a need for rapid thawing processes with minimized quality loss. It has been observed that a rapid rate of thawing reduces the loss of liquid retention properties and can improve colour and flavour preservation in plant tissue (Kalichevsky et al., 1995).

Thawing of high moisture products such as tomatoes and courgettes can result in a spongy texture, which may result in their rejection. This is due to the destruction of the ultrastructure of plant cells and a loss of moisture during thawing, brought about by ice crystal growth in the thawing zone. As a consequence, water and enzymes are released through the broken cell walls. Those enzymes which had become inactive owing to the low temperature will also start working again (Edwards and Hall, 1988).

With respect to the microbial quality, the thawing process restores the potential for the proliferation of both pathogenic and spoilage microorganisms. During thawing, the surface of large frozen products will reach higher temperatures sooner and will be exposed longer than interior portions of the product (Golden and Arroyo-Gallyioun, 1997). In a hygienically acceptable thawing process, the product surface time-temperature history prevents microbial proliferation from exceeding acceptable limits. Regulatory authorities generally advocate that commercial thawing be undertaken at low temperatures (<10 °C) to ensure that the hygienic status of the product is not compromised by the growth of mesophilic pathogens (Devine et al., 1996). However, the potential health or quality hazard poses by specific thawing regimes requires individual assessment (Lowry et al., 1989).

2.1.8. HPLT applied to food freezing, thawing and chilling

The preservation field is not the only application of high hydrostatic pressure in food technology. A wide range of possibilities are offered by the combination of high pressure with low temperature: the phase transitions of water and food products under such HPLT (High-Pressure-Low-Temperature) conditions, the modification of the behaviour of proteins, both for biotechnology and nutritional purposes (probiotics control and microbial inactivation) and the reduction of chemical and enzymatic reactions (both responsible of degradation of foods) are some of the fields in which HPLT is showing new promising opportunities and challenges.

Pressure markedly influences ice-water transitions, and the use of high pressure technology has distinct potentialities for improving the kinetics of freezing or thawing, and the characteristics of ice crystals.

Recent investigations to improve freezing and/or thawing processes of foods showed an increasing interest in the use of high hydrostatic pressure to support phase transitions (Cheftel *et al*., 2000, Teramoto and Fuchigami, 2000, Denys *et al*., 2002, Cheftel *et al*., 2002, Li and Sun, 2002). Fundamental research has already been

carried out by P.W. Bridgman (1912), who presented an extensive data set for the phase diagram of pure water at the beginning of the last century.

With the commercialization of high-pressure processes, pressure may now be used as a "third dimension", together with temperature and time, in order to improve food quality and safety (Schubring et al., 2003). The primary goal of an effective freezing process is the rapid initiation of ice nucleation and the minimization of crystal growth (Préstamo et al., 2005). Research on high pressure-assisted thawing of frozen fish and meat has shown the possibilities to significantly reduce the thawing time (e.g., Deuchi and Hayashi, 1991; Murakami *et al*., 1992; Zhao *et al*., 1998; Massaux *et al*., 1999a) as well as to minimise the drip volume after thawing (Murakami *et al*., 1992) and subsequent cooking (Massaux *et al*., 1999b; Chevalier *et al*., 1999; Okamoto and Suzuki, 2001; Rouillé *et al*., 2002).

A summary of the early contributions (up to 1998) in the filed of HPLT technology to food freezing and thawing is given in Table 2.4:

Table 2.4. First reported applications of HPLT for freezing and thawing purposes.

Reference	Product	Pressure (MPa)	Holding-time (min)	Temp. (°C)	Objective of the work
Hoa et al. (1982)	-	1-800	-	+30/-40	Technical requirements to work under pressure at low temperatures
Knauf and Mendgen (1988)	Leaf	210	-	-	Rust-infected leaf structure preservation using a new Balzers® high pressure freezer.
Knauf et al. (1989)	Bean leaves	?	-	-30/-90	Study of the haustorial host-parasite interface in rust-infected bean leaves. Using Balzers®.
Djaczenko et al. (1990)	Cell suspensions	220	-	N_2 contact	"Unprecendent quality of cell fine structure preservation was achieved". Using Balzers®.
Lechaire et al. (1993)	Collagen gels	220	-	N_2 contact	Comparison after slam or high pressure freezing of collagen gels structure. Using Balzers®.
Morason et al. (1993)	Fat body cells	?	-	N_2 contact	Comparative ultrastructure of fat body cells after chemical fixation and high pressure freezing. Using Balzers®.
Richter (1994)	"Biological specimens"	230	50 ms	N_2 contact	High-density morphologies ice II and ice III presence. Using Balzers®.
Kalichevsky et al. (1995)	-	-	-	-	Review article
Dubochet (1995)	-	-	-	-	Cryoelectron microscopy. Review article. Using Balzers®.
Sanz et al. (1997)	Water	Up to 216	Up to 100	-25	Basics and mathematical modeling
Martino et al. (1998)	Pork	200	-	-20	Size and location of ice crystals

2.2. Phase diagram of water

2.2.1. Phase diagram of water at low temperature

The phase diagram of water as a function of temperature and pressure delimits distinct crystalline ice forms with different specific volumes, melting temperatures and latent heats of fusion (Cheftel et al., 2000). The effects of pressure (Figure 2.5) are, together with the decrease of the freezing point (until a minimum of –22°C at 209 MPa), the reduction of the enthalpy of crystallisation (from 334 kJ/kg at atmospheric pressure to 193 kJ/kg at 209 MPa) and the crystallisation (from 209 MPa) of higher ice modifications, like ice III or ice V, with higher density than the liquid water (Schlüter et al., 1998). The water substance exhibits a range of solid phases, and all of these are referred to as forms of 'ice'. Ice possesses 12 different crystal structures, plus two amorphous states. At ordinary (low) pressures the stable phase is termed ice I. There are two closely related variants: hexagonal ice Ih, whose crystal symmetry is reflected in the shape of snowflakes, and cubic ice Ic. Ice Ih is obtained by freezing water; ice Ic is formed by depositing vapour at low temperatures (-130 °C). Amorphous ice can be obtained by depositing vapour at still lower temperatures and by compressing ice Ih at liquid nitrogen temperature. In addition to the elemental phases are clathrate hydrates.

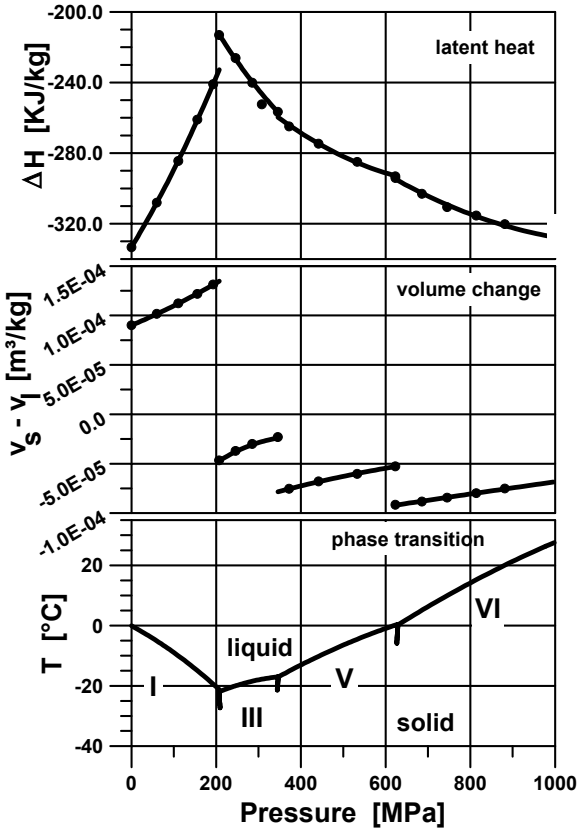

Figure 2.5. Influence of pressure on the enthalpy of fusion, the specific volume changes and the phase transition temperatures (Heinz et al., 1998).

Generally, the effect of pressure, P, on the melting temperature, T_m, of compounds is described by the Clausius-Clapeyron equation (2.1):

$$\frac{dT_m}{dP} = T_m \frac{\Delta V}{\Delta H} \qquad (2.1)$$

where ΔV is the volume change and ΔH the latent heat change. Hexagonal ice (ice Ih, common solid state of water) contracts on melting, making ΔV negative and dTm/dP also negative as seen in the pT-diagram (Figure 2.5). The expansion on freezing is not unique to ice I; it occurs also in silicon and germanium which have similar low-density

structures in the solid state (Petrenko and Withworth, 1999). For all other solid phases of water that have a boundary in which the ice is denser than the liquid and the phase boundary line slopes the other way. However, internationally adopted empirical equations for the melting curves of the phases of ice are given by Wagner et al. (Wagner et al., 1994). The volume change (liquid-solid), the latent heat of fusion and the phase transition temperatures are plotted versus pressure in Figure 2.5. Besides the depression in the freezing point, a reduction in the enthalpy of crystallisation can also be observed in a range up to 210 MPa. Experimental data obtained by Bridgman (1912) and Karino et al. (1994) for water-ice and ice-ice transitions are shown in Table 2.5.

The first high pressure phases were discovered almost a century ago by Tammann (1900) in a programme to study the pressure-volume-temperature relationships of various materials, and he named 'ice II' and 'ice III'. His discovery was extended in experiments by Bridgman (1912), in which pressures of 2 GPa were reached and led to the discovery of ices V and VI, as shown in Figure 2.6. Ice IV was not assigned by Bridgman until 1935 (Bridgman, 1935), because of uncertainty with regard to some unstable forms, the existence of which was suspected by Tammann (1900). The phases of ice have been labelled with the Roman numerals I-XII in the approximate order in which they were produced experimentally. Each phase (except IV, IX, and XII) is stable over a certain range of temperature and pressure, but it is a feature of the ice systems that many phases are metastable well outside their regions of stability (Petrenko and Withworth, 1999).

Table 2.5. Thermodynamic properties of the phase transitions of water.*

Phase transition	Transition temperature T (°C)	Transition pressure P (MPa)	Volume change ΔV (cm^3g^{-1})	Enthalpy change ΔH ($kJkg^{-1}$)
Liquid ➔ ice I	0	0.1	+0.0900	-334
	-5	59.8	+0.1016	-308
	-10	110.9	+0.1122	-285
	-15	156.0	+0.1218	-262
	-20	193.3	+0.1313	-241
Liquid ➔ ice III	-22	207.5	-0.0466	-213
	-20	246.2	-0.0371	-226
	-17	346.3	-0.0241	-257
Liquid ➔ ice V	-20	308.0	-0.0828	-253
	-15	372.8	-0.0754	-265
	-10	442.4	-0.0679	-276
	-5	533.7	-0.0603	-285
	0	623.9	-0.0527	-293
Liquid ➔ ice VI	-10	518.0	-0.0960	-264
	0	623.9	-0.0916	-295
	10	749.5	-0.0844	-311
	20	882.9	-0.0751	-320
Ice I ➔ ice II	-35	212.3	-0.2177	-42.5
Ice I ➔ ice III	-30	211.5	-0.1919	+14.6
	-20	206.3	-0.1773	+23.4
Ice II ➔ ice III	-25	330.6	+0.0148	+68.2
Ice II ➔ ice V	-25	350.2	+0.0401	+66.5
Ice III ➔ ice V	-25	341.1	+0.0546	-3.64
	-20	345.5	+0.0547	-3.72
Ice V ➔ ice VI	0	626.0	-0.0389	-0.76
	-20	624.4	-0.0381	-0.83

*data obtained from Bridgman *et al*. (1912) and Karino *et al*. (1994)

There is often some difficulty in nucleating a new phase, so that one phase can continue to exist where another phase would have a lower free energy. Extended lines in the pT-diagram of water represent the equilibrium between two phases within the region of stability of another. For example, if ice III has not formed, ice Ih can convert to liquid on the extrapolation of the ice Ih-liquid line (Bridgman, 1912). When the liquid is cooled there is often supercooling and the phase eventually formed may depend on the nucleation site rather than which of several phases has the lower free energy (Petrenko and Withworth, 1999). Appropriate nucleating agents can promote the formation of a certain ice polymorph (Evans, 1967a).

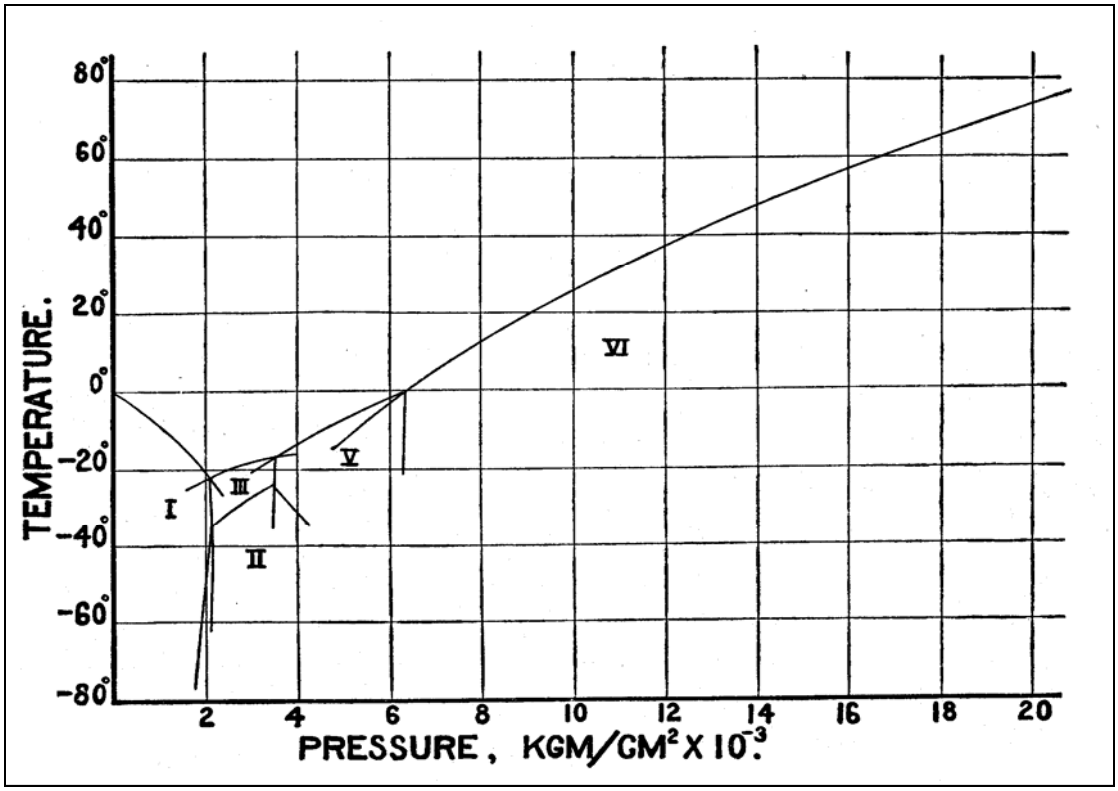

Figure 2.6. Phase diagram of water, after Bridgman (1912).

In principle, no solid (ordered) phase can exist in the liquid (disordered) domain, but the liquid phase can remain for some time (as a metastable state) in a crystalline domain: this phenomenon, called **supercooling**, is enhanced in the case of homogeneous nucleation (ultra pure water, absence of nucleation catalysis by surface effect). The homogeneous ice I nucleation temperature decreases from -40°C at 0.1 MPa to -92°C at 209 MPa (Lüdemann, 1994) The kinetics of conversion from one phase to another one appears to partly depend on the temperature. The conversion of ice III to ice I is reported to be explosive near -22°C and 207 MPa (vicinity of the triple point) but slower at -30°C (Bridgman, 1912). Pressure shifting between ice III and ice I has been envisaged as a method for disrupting microorganisms, but it would probably also disrupt cells and tissues, since the volume increase exceeds 17% (Kalichevsky et al., 1995). A recent study from Luscher et al. (2004) indicated that inactivation of the gram-positive bacterium Listeria innocua is more effective after it had undergone Ice I-III solid-solid phase transition.

Representative values of volume changes between the different ice modifications are shown on the phase diagram of water of the area of study in Figure 2.7.

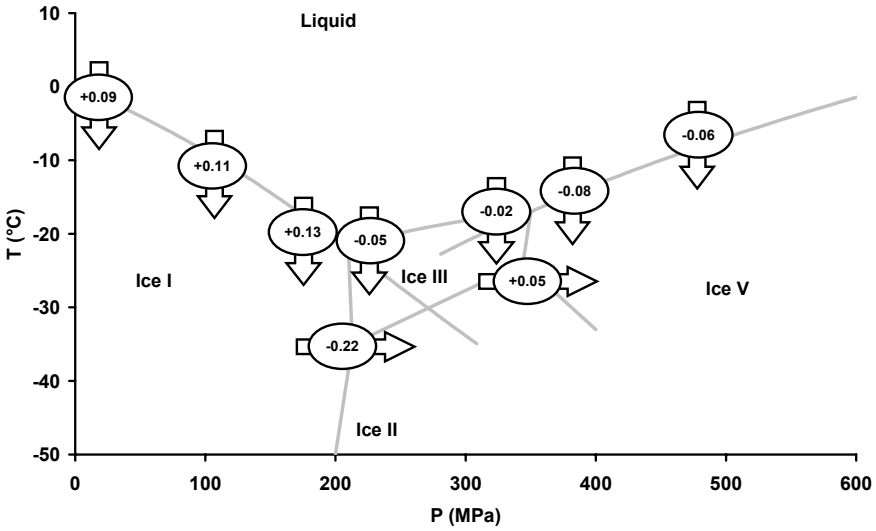

Figure 2.7. Representative volume changes (cm^3/g) between phases on the phase diagram of water (from the data in Table 2.5).

The structure of liquid water, ice Ih and ice III are shown in Figure 2.8, together with the volume changes between the phases.

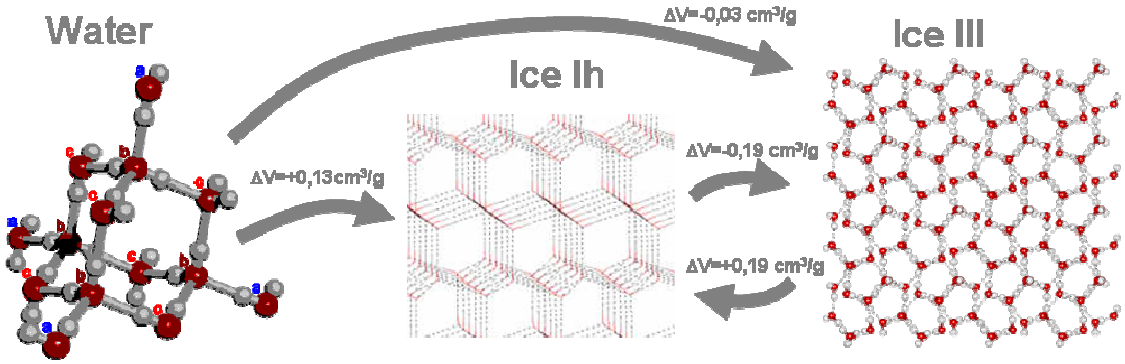

Figure 2.8. Structure of liquid water, ice Ih and ice III and specific volume changes between phases (adapted from http://www.lsbu.ac.uk/water/index.html).

2.2.2. Metastable phases: description and consequences

Bridgman found, however, that although ice I, ice III and ice VI could be readily crystallized from the liquid at the appropriate pressure, ice IV and ice V were obtained from the liquid only with great difficulty, their appearance, according to Bridgman, being a matter of "caprice". Thus, in the pressure range of about 350 to 450 MPa, the ice which crystallizes from the liquid may be ice IV, ice V, ice VI or mixtures thereof (Evans, 1967a). Bridgman finally prepared ice V by decompressing ice VI, but even this inconvenient route was only sometimes successful, the transformation from ice VI to ice V apparently being dependent on the nature of the containing vessel. The preparation of ice IV was even more capricious because ice IV is a metastable phase which exists wholly within the stability range of ice III and ice V (Evans, 1967a).

As can be seen, Evans (1967a) already introduced the concept of "metastable phase" when reviewing the selective nucleation of "high-pressure ices". The next reference to this term, related to the phase diagram of water, is found by Petrenko and Withworth (1999), who concluded that each phase (except IV, IX, and XII) is stable over a certain range of temperature and pressure, but it is a feature of the ice systems that many phases are metastable well outside their regions of stability. These authors state that Ice II is formed by compressing ice Ih at –60 to –80 °C (or by decompression of ice V at –30 °C), and if heated it transforms to ice III which has a totally different arrangement

of oxygen atoms. Ice II is not easily formed on cooling ice III, which remains metastable and finally orders to ice IX (Petrenko and Withworth, 1999).

It is obvious that the lack of understanding of the phenomena occurring during phase transitions led to the cited authors to write terms like “capricious” or to make the nature of the vessel responsible for obtaining particular ice modifications. The present work demonstrates that a proper understanding of the kinetics of phase transition phenomena at high pressure permits the delimitation – being for each material different – of the metastable regions and permits the definition of the critical parameters to obtain controlled freezing and thawing paths, also in the region in which metastable phases are observed. Additionally, it is demonstrated that microbial inactivation, enzyme activity control and quality-related parameters are enhanced when performing freezing and thawing processes in the range of metastable phases.

Different ice modifications were obtained during freezing processes at several pressure levels from atmospheric pressure up to 300 MPa (Schlüter et al., 2004). In the pressure range between 210 and 240 MPa, a metastable ice I modification area was observed, as the nucleation of ice I crystals in the thermodynamically stable region of ice III was reached. On the other hand, different factors, like initial temperature and final pressure, were discussed to obtain controlled thawing paths and the existence of a solid ice I metastable phase in the domain of ice III was proved. A significant degree of supercooling was obtained before freezing the tissue water to ice III which has to be considered when designing pressure supported freezing processes. The phenomenon of supercooling is, actually, another case of metastable phase, in this case a metastable liquid in the stable domain of ice that has not yet nucleated. All these terms are discussed in chapter 5.1.5.

The existence of these liquid and solid metastable phases opened a new range of possibilities for freezing and thawing processes in the HPLT domain. The temperature gradients for thawing could be increased, thanks to the prolongation of the ice I melting curve into the domain of ice III; the initial nucleation temperature for pressure-shift freezing could be reduce, being therefore increased the percentage of instantaneously ice crystal formed, etc. More details are given in section 5.1.

2.3. State of the art of HPLT

2.3.1. Summary of contributions

Effects of HPLT processes on food constituents and structures

Proteins:

High pressure influences the bonds which stabilise the spatial structure of proteins. Depending on the pressure level, the protein structures are modified reversibly or irreversibly i.e. denatured. Influencing factors are the pressure, the temperature, the protein structure, the pH and the composition of the solvent. In the case of enzymes, which of course are also proteins, the change in structure (denaturing) can cause the properties of the enzymes to be affected. The activity of the enzyme can be either decreased or increased. Proteins can also be modified in a targeted way by high pressure treatment however. For example, the formation of protein gels, which are very smooth and elastic, is made possible by structural changes. The use of such gels for new products, e.g. in the desserts sector, is conceivable. The fact that muscle flesh and fish become tender by high pressure treatment can also be utilised in foodstuff technology.

Kanda et al. (1992) reported that applying PSF to tofu (soy protein) at 200 MPa and -18°C, after thawing, less exudation and a texture nearer to that of unfrozen tofu, than that of samples blast-frozen in air at -20°C and atmospheric pressure, and ice crystals had a smaller size (1-3μm) after PSF than after air-blast freezing (30-100μm). Fuchigami and co-workers (1996, 1997 and 1998) studied the texture of tofu after keeping samples for 90 minutes at different pressures, up to 700 MPa and -20°C. The

results are nevertheless unclear, as some samples could be frozen, some others not, and the sample temperature was not measured during the high pressure treatments. Barry et al. (1998a and 1998b) reported a better preservation of structure of β-lactoglobulin gels when PSF was applied (at 207 MPa and -19°C), compared to atmospheric pressure (whether in still air at -43°C or in gaseous nitrogen at -80°C). Dumoulin et al. (1998) reported that subzero temperatures decreased the minimum pressure level required for gelation of protein gels (ovalbumin and soy proteins) and resulted in more porous and exudative gels than those obtained by pressure processing at higher temperatures. In the case of egg yolk, subzero temperatures prevented pressure-induced gelation. Kolakowski et al. (2001) reported an enhancement of exposure of the hydrophobic zones of β-lactoglobulin to water when lowering the temperature under pressure. They concluded that it is likely that low temperatures minimize the loss of native structure induced by pressurization and reduce subsequent aggregation reactions under high pressure.

Fats:

The action of high pressure can modify behaviour during melting and crystallisation of fats. Fats crystallise out under the action of pressure because the specific volume of crystallised fat is smaller than that of liquid fat. This also occurs in emulsion drops, the emulsion remaining stable. High pressure treatment also influences the chemical composition of fats. The extent to which fat decay is delayed or promoted by oxidation depends on the composition of the foodstuffs and the treatment conditions.

Sugars:

The molecular structure of simple carbohydrates (sugars) is not modified by high pressure treatment. However, it is possible that the properties of carbohydrates are affected, e.g. their ability to bond water. Starch in an aqueous environment can be made into a paste under pressure. Starch gelled under pressure shows a lower degree of retrogradation during storage compared with one gelled under heat and its digestibility is additionally improved. Such gels can be used as substitutes for fats. The enzymatic breakdown of carbohydrates can proceed differently in foodstuffs treated under high pressure to that in untreated foodstuffs. Non-enzymatic browning reactions (Maillard reactions) such as often occur during pasteurisation by heat are suppressed by a high pressure treatment, so that fewer colouring and flavouring substances are formed.

Vitamins:

Studies show that vitamins A, B1, B2, B6 and C are stable over short exposure times. The vitamin C content e.g. in orange juice treated under high pressure is approximately the same as that in untreated juice.

The water-soluble antioxidative potential of orange juice, for which L-ascorbic acid and phenolic compounds are mainly responsible, is also largely retained after high pressure treatment. The carotenoid content of an orange-carrot-lemon nectar is affected only little, if at all, by high pressure treatment. Colourings and flavour substances are likewise stable given suitable process conditions. Flavouring substances are also retained virtually unchanged during the high pressure treatment.

Microorganisms:

Since enzymes and proteins are also important constituents of microorganisms, their modification can also have an effect here. Microorganisms have different sensitivities to pressure. While yeasts, moulds and vegetative microorganisms can be inactivated at a relatively low pressure, this only happens in some viruses and bacterial spores when they are exposed to very high pressures or are also additionally heat-treated.

Spores can be made to germinate under low pressure, in order to kill the germinated spores under a higher pressure. Complete destruction of Bacillus subtilis, both of the

vegetative organisms and of the spores, has been achieved at temperatures of about 70ºC and pressures of about 200 MPa.

A vast amount of data exists on the kinetics of pressure inactivation of vegetative micro-organisms (Cheftel, 1995) at ambient and elevated temperatures (Heinz and Knorr, 1996; Heinz et al., 1998). In contrast, limited information has been gathered so far concerning microbial inactivation by means of high pressure in the low temperature range. Empirical data have shown that high pressure processing at low to ambient temperatures yielded improved microbial inactivation and better sensorial characteristics of vegetables (George, 2000; Brul et al.; 2000; Smelt et al., 2001). Preliminary data on selected pathogenic organisms suggest more effective inactivation under pressure at low (-10 to 5°C) temperatures as compared to ambient (20 to 40°C) ones (George, 2000).

To examine the influence of HP treatments on Listeria innocua in the area of stability of liquid water the inactivation kinetics at 200 MPa, 0 °C and at 300 MPa, 0 °C and -10 °C, were examined (Luscher et al., 2004). Due to the experimental method freezing occurred during the pre-tempering pressure release at 300 MPa and -10 °C. During the experiments at 0 °C freezing was avoided by slow pressure release. The influence of partial freezing on the inactivation was neglected as complete freezing at ambient pressure did not cause considerable inactivation. The inactivation was generally low at 200 MPa, even after 30 minutes, however a 300 MPa, 0 °C the inactivation was progressing more rapidly. The inactivation was considerably higher at -10 °C than at 0 °C. All inactivation kinetics showed approximately linear inactivation kinetics running through the point of origin. Deviations from the point of origin could be explained by the application of pressure during the pressure build-up and pressure release time.

In the frame of the present work, the inactivation of Bacillus subtilis has been studied at HPLT conditions; the temperature lowering alone has hardly any effect on the inactivation of Bacillus subtilis cells. High pressure alone has a minor effect on cell viability. The combination of high pressure and low temperature, especially when it led to phase transitions, turned out to be most effective in inhibiting outgrowth of the Bacillus cells. Solid-solid phase transitions seemed to be of special interest. The change of the ice crystal configuration (ice I to ice III transition) may induce denaturation of the cellular protein, which damages the integrity of the cell membrane, and could lead to enhanced inactivation of crucial intracellular enzymes. In addition, partial thawing of structures inside the cells may occur as well.

Up-to-now, storage processes of foodstuffs at subzero temperatures under pressure have not been carried out. The data on enzyme inactivation at subzero temperatures (Indrawati, et al., 1998, Indrawati, et al., 2000) suggest that denaturation of some enzymes under pressure might be enhanced by low temperature. Recently published data show that HPLT processes up to 210 MPa and -20°C are not enough to inactivate PPO enzymes from potato pieces treated by PSF, being pressure maintained over a period of 1,5 to 3 hours (Préstamo et al., 2005).

The results obtained by Urrutia et al. (2006) showed that, for the enzymatic activity of PPO in HP treated potatoes, a slight inactivation (up to 10%) was achieved at pressure levels of 280 MPa for freezing and 290 MPa for thawing. These results are in agreement with those presented by Indrawati et al. (1998), who found only a slight, reversible inactivation of mushroom PPO (around 15% at 200 MPa and -15°C). Both results should be compared carefully, given that the activity examined in this work is measured directly from a potato tissue and not from extracts or enzyme solutions, where no influence of cell damage plays a role on the measured activity.

Effects of HPLT processes on plant and animal tissues

Koch et al. (1996) observed that pressure-shift freezing of potato cubes resulted in less damage to the cell structure, less drip loss, and less enzymatic browning than conventionally frozen cubes. Fuchigami et al. (1996, 1997a, 1997b) reported that

improvements in texture and histological damage are achieved in pressure-shift frozen carrots. Otero et al. (1998) compared the damage to the microstructure of eggplants frozen by conventional air freezing and by pressure-shift freezing. Pressure-shift frozen samples had the appearance of fresh samples, and no differences between centre and surface cell structure were observed (indicating uniform nucleation). Otero *et al*. (2000) confirmed beneficial effects of pressure-shift freezing on whole peaches and mangoes when compared to air-blast frozen samples. The authors reported that the cell damage at sample centre was much less in pressure-shift frozen samples than in air blast frozen, evidenced from scanning electron microscopic analysis. This beneficial effect might result from the formation of smaller ice crystals due to enhanced supercooling and homogeneous nucleation during pressure release.

The group of Le Bail studied the effects of PSF processes on the drip loss and physical properties of whiting fish, Norway lobster and turbot fish (Chevalier et al., 1999; Chevalier et al., 2000; Chevalier et al., 2000). In all cases, a HP vessel of 3000mL was used, processing in each case, approximately, 500g of sample. Whiting fish was thawed at high-pressure (pressure-assisted thawing) at 50/100/150/200 MPa. Norway lobster PSF at 200 MPa and -18°C, and turbot fish PSF at 140 MPa and -14°C.

The group of Sanz reported the microstructure of pork, eggplant, and mango and peach after processing with PSF at 200 MPa and -20°C (Martino, et al., 1998; Otero, et al., 1998; Otero et al., 2000). In all cases, the vessel volume was 2350mL and the sample volume, around 500mL. The group of Knorr described the impact of pressure assisted thawing on the quality of fillets from various fish species (redfish, salmon, whiting, haddock, rainbow trout and cod) through their sensory evaluation, texture, drip loss, colour, etc. (Schubring et al., 2003). They treated the samples at 200 MPa in a 600mL HP vessel, processing in each batch 250 g of sample. Finally, Zhu, Ramaswamy and Simpson (2004) reported the effect of high-pressure versus conventional thawing on colour, drip loss and texture of Atlantic salmon. About 90g of fish sample were HP processed in a 4568mL vessel, performing a pressure-assisted-thawing process at 100/150/200 MPa.

Investigations on high pressure-assisted thawing of frozen fish and meat have shown the possibilities of significantly reducing the time required for thawing (e.g., Deuchi & Hayashi, 1992a; Murakami et al., 1992; Zhao et al., 1998; Massaux et al., 1999a) as well as minimising the drip volume after thawing (Murakami et al., 1992) and subsequent cooking (Massaux et al., 1999b; Chevalier et al., 1999; Okamoto & Suzuki, 2001; Rouillé et al., 2002). Therefore, major advantages of high pressure-assisted thawing reducing the drip loss and lowering the processing time can be seen. However, high pressure treatment is also connected to colour and texture changes. These are obviously dependent on the amount of pressure applied as well as on the time of pressurisation. While almost no changes in colour and penetration force of the pressure-thawed (210 MPa) product beef were observed (Zhao et al., 1998), discoloration and toughening of pork meat were observed and increased with the working pressure (Massaux et al. 1999a). Therefore, it is concluded that the freezing-thawing process under a pressure of 100 MPa seems to be an interesting treatment for pork meat because there is no exudate, and only slight discoloration and toughness of meat (Massaux et al. 1999b). On the other hand, it is reported that discoloration of the pork meat induced by high pressure-thawing was not recognisable to the naked eye up to the pressurisation of 200 MPa. Furthermore, meat tenderisation was found to be induced during high pressure treatment. When frozen pork was pressurised at 200 MPa, the most desirable results were obtained. Over 200 MPa however, unfavourable changes were brought about by high pressure (Okamoto et al., 2001).

2.3.2. Equipment considerations

Vessels used to contain high pressures (greater than 70 MPa) have been used for many years in many industries such as cannons and small arms, processing polyethylene, materials processing and high pressure water jet cutting for example.

Most high pressure commercial applications use vessels that operate at pressures no greater than about 400 MPa. Some of these vessels such as those used in polyethylene processing and water jet cutting are subjected to high cycle fatigue loading. Some weapons and some metals processing operating pressures are as high as and even greater than 700 MPa. This latter group of high pressure vessels is not usually subjected to high cycle fatigue loading.

The key components of a high-pressure system are the pressure vessel, pressurizing system, and ancillary components (Figure 2.9). A high-pressure vessel, in which products under treatment are subjected to pressure, is the key component of this technology. Pressure vessels are generally made of low-alloy steel and are routinely used in the ceramic and metal industries. However, in the case of food applications, a unique requirement for the high-pressure vessel is that it must undergo several thousand processing cycles per year to process large volumes of foods. The large number of required pressurized and depressurized cycles increases metal fatigue and reduces the life of the vessel. Furthermore, the vessel itself must be protected from any corrosion due either to the food material itself or to any liquids used for cleaning, and must be easy to clean.

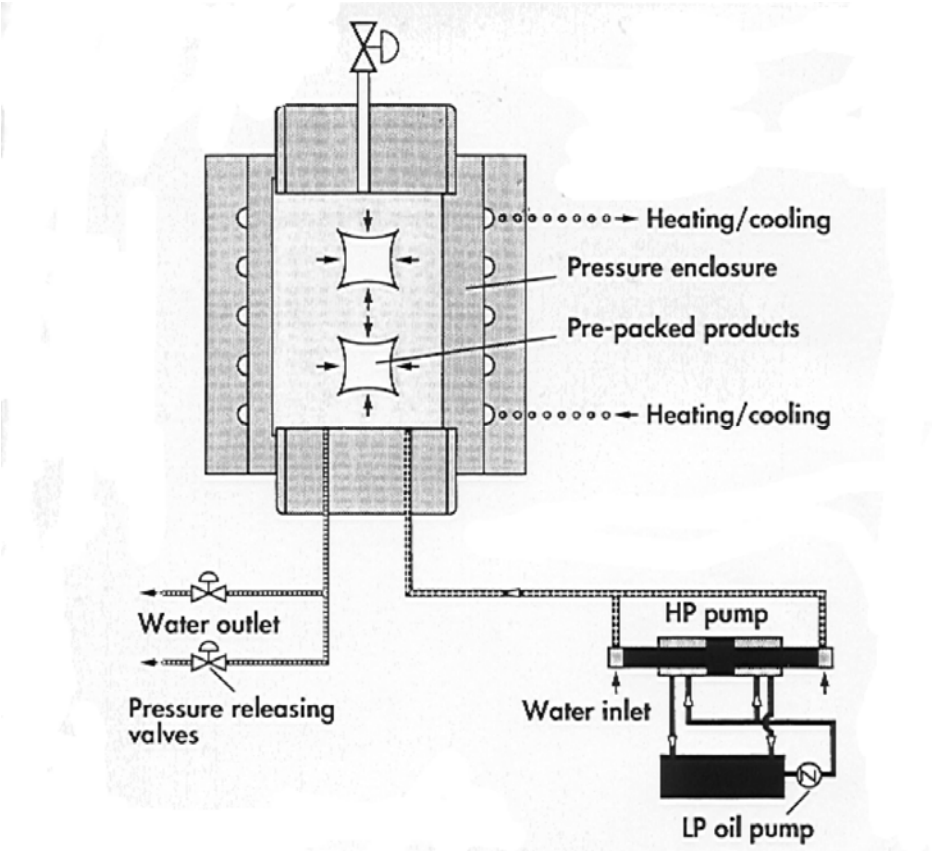

Figure 2.9. A typical high-pressure processing system for treating pre-packaged foods (source http://www.fao.org/ag/ags/agsi/Nonthermal/nonthermal_1.htm).

Two types of pressurization systems defined as indirect and direct, are commonly employed in the industry (Figure 2.10).

In an indirect pressurization system, the pressurizing medium (e.g., water) is first pumped through an intensifier, into the pressure vessel. The intensifier is a high-pressure pump used to increase the pressure to desired levels. The intensifier is separate from the high-pressure vessel. This system requires high-pressure tubing and appropriate fittings to convey the pressurized medium to the pressure vessel.

In a direct pressurization system, the pressure intensifier is located within the pressure vessel. In this system, both the pressure intensifier and the vessel are fabricated as a single unit, and the total size of the vessel can be quite large. A piston is used to

deliver the high pressure to the product. This system requires heavy-duty seals that must withstand repeated opening and closure without leakage. A major limitation of this method is the need for efficient seals between the pressure vessel and the piston.

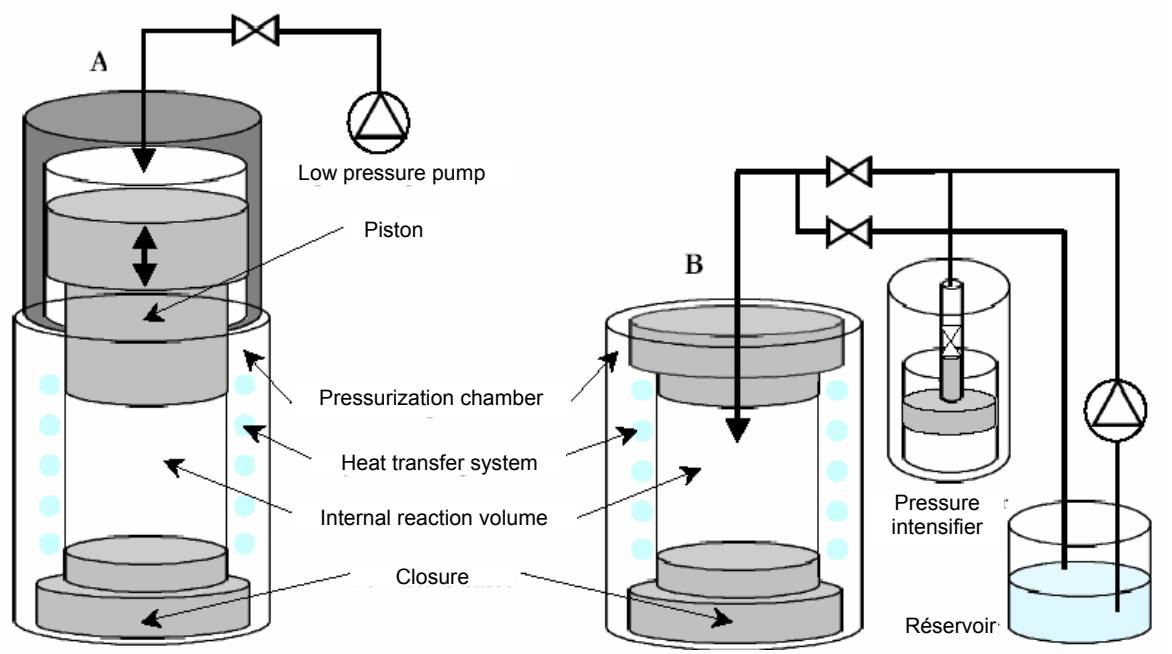

Figure 2.10. Schema of systems for high pressure for direct (A) and indirect (B) compression (source: Nicolas Chapleau, personal communication).

A simplified mode of operation used in a high-pressure processing system is shown in Figure 2.11. In a high-pressure process, the pressure vessel is filled with a food product and pressurized for a desired time, following which it is depressurized.

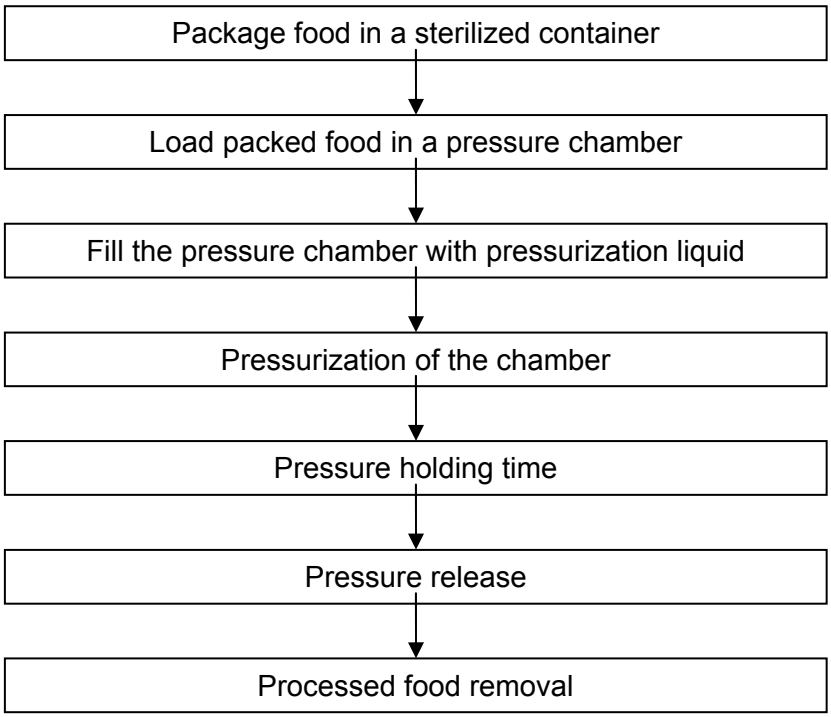

Figure 2.11. A schematic flow diagram of high-pressure processing.

The time required to pressurize the vessel is influenced by the compressibility of the pressure medium and the nature of the food material. If water is used as the pressure-transmitting medium for most food materials, compressibility is similar to that of the pressure medium. Typically, the pressurization time for foods is independent of the

quantity of food placed in the pressure vessel. The presence of air in the food increases the pressurization time, since air is considerably more compressible than water. After pressurization, the food is kept under high pressure for the required process time, which may be for several minutes. Upon completion of the pressure exposure, depressurization can be done quite rapidly. Figure 2.12 shows a typical HP processing cycle time.

Batch operation: High pressure processing in the batch processing mode offers several advantages in that different types of foods can be processed without cross-contamination, there is no need for clean-up between runs, the equipment is relatively simple, and there is no risk of large quantities of foods becoming contaminated in the case of equipment malfunctioning. Several pressure vessels may be operated in a controlled sequence to minimize any time lag associated with the time required for the pressurization of vessels. Most of the high-pressure equipment currently used is operated in the batch mode. Since pressurizing and depressurizing steps can be rapidly accomplished, the low efficiency associated with batch processing may be minimized. Rapid pressurizing and depressurizing cycles also can cause metal fatigue and reduce the life of equipment. Above 4,000 kg/cm^2, the weight of equipment increases significantly, as does its cost.

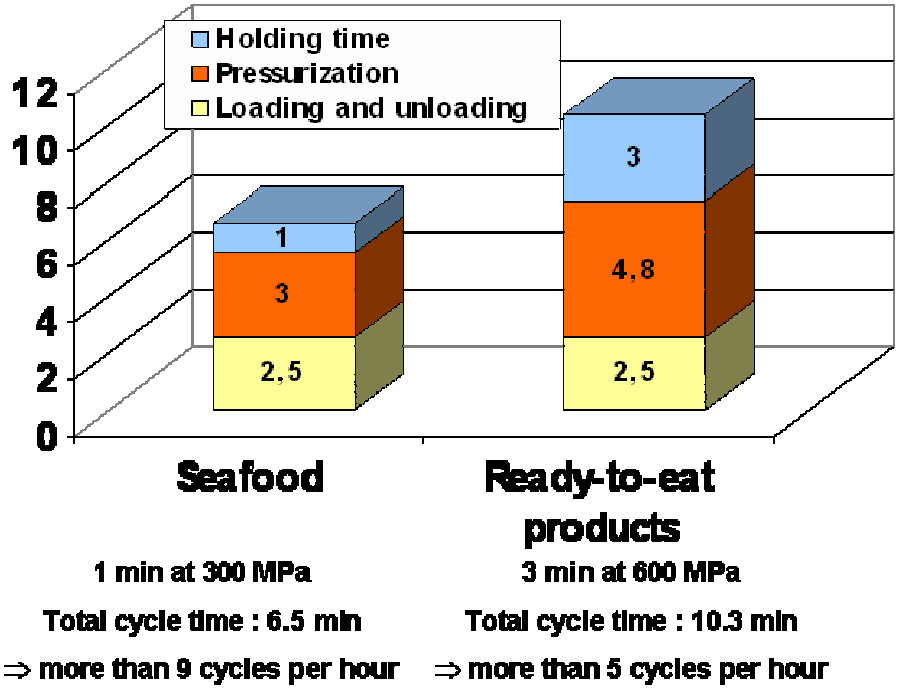

Figure 2.12. Typical processing time cycle (source: NC Hyperbaric; C. Tonello, personal communication).

Semicontinuous Processing Mode: Another approach to high-pressure treatment of liquid foods is the use of a semicontinuous processing mode (Deutchi and Hayashi, 1992b). This system involves a combination of multiple pressure vessels that are sequenced to provide a continuous flow. As shown in Figure 2.13, while one vessel is being pressurized, another may be in a decompression mode. This approach has been commercially used by companies such as the Wakayama plant in Japan, for the treatment of tangerine juice. In this process, three 50 litre pressure cells are sequenced to achieve a production rate of 4 000 litre per hour (Deutchi and Hayashi, 1992b). The pressure system, known as ACB high-pressure liquid processor (GEC Alsthom ACB, France) is equipped with a chamber having an internal volume of 4 litres. The compression process is done with water up to a maximum pressure of 400 MPa. Programmable pressure controllers are used to adjust pressurization and decompression rates. Appropriate temperature controls are used to maintain

temperatures between -20°C and +80°C. This unit has been used in selected processing steps in wine production. The reduction in cost of a semicontinuous process is about 27 percent over a batch process for 500 litres per hour production (Deutchi and Hayashi, 1992b).

Another continuous high-pressure system involves 5 metre long stainless-steel pipes that are wound like a coil with a pressure resistance of 700 MPa (Dunn et al., 1995). An air-driven hydraulic pump is used to introduce the liquid product into the pipes. With the outlet valve closed, the liquid is subjected to pressure. The coiled pipes are placed in thermostatically controlled water baths, in which the temperature is maintained between 5 and 80° C. The outlet valve is gradually opened to release the pressurized product in a continuous manner.

Other innovations in high-pressure system design include the use of pulsating high pressures (Estiaghi et al., 1994). The pressure vessel is similar to those used in cold isostatic pressing. A unique feature of this new system is an air-driven pressure-increasing device that allows instantaneous change in pressure. Additionally, a pressure-reducing valve attached to the pressure vessel is useful in releasing pressurized water. By manipulating the pressure-reducing valve, desired pulsations are obtained. The pressure vessel is contained in a thermostatically controlled water bath. The investigators were able to achieve 500 MPa in 10 seconds. Reduced process times at high pressures were obtained when used in combination with higher temperatures. These studies emphasize the synergistic benefit of pressure and temperature in selected food applications.

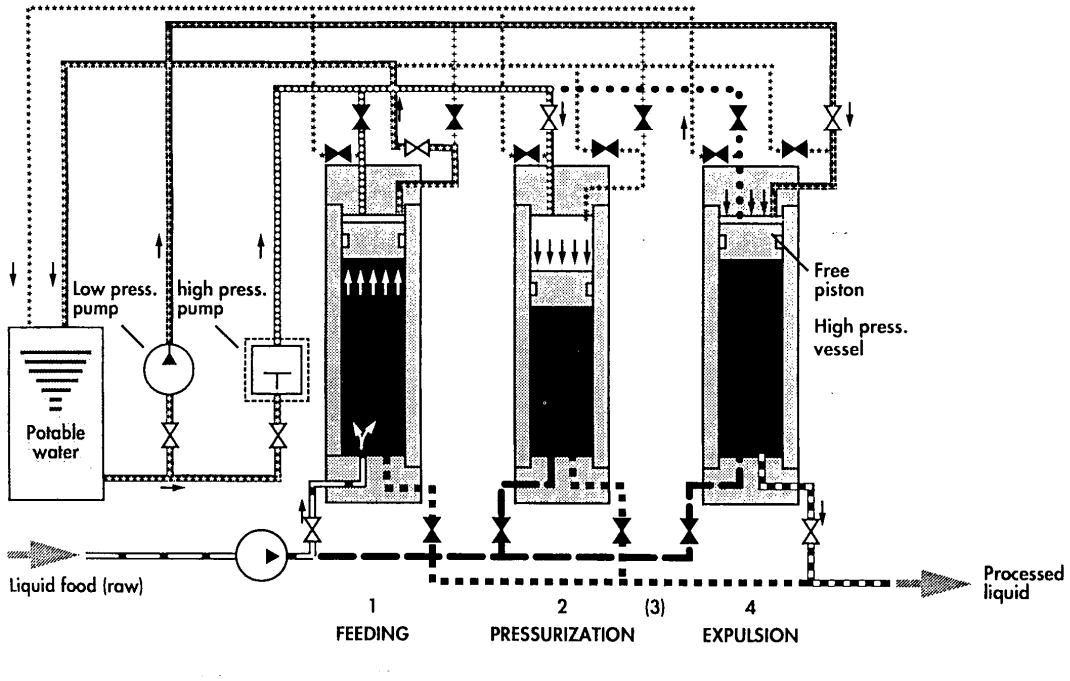

Figure 2.13. A multivessel arrangement for semi-continuous HP processing (source http://www.fao.org/ag/ags/agsi/Nonthermal/nonthermal_1.htm).

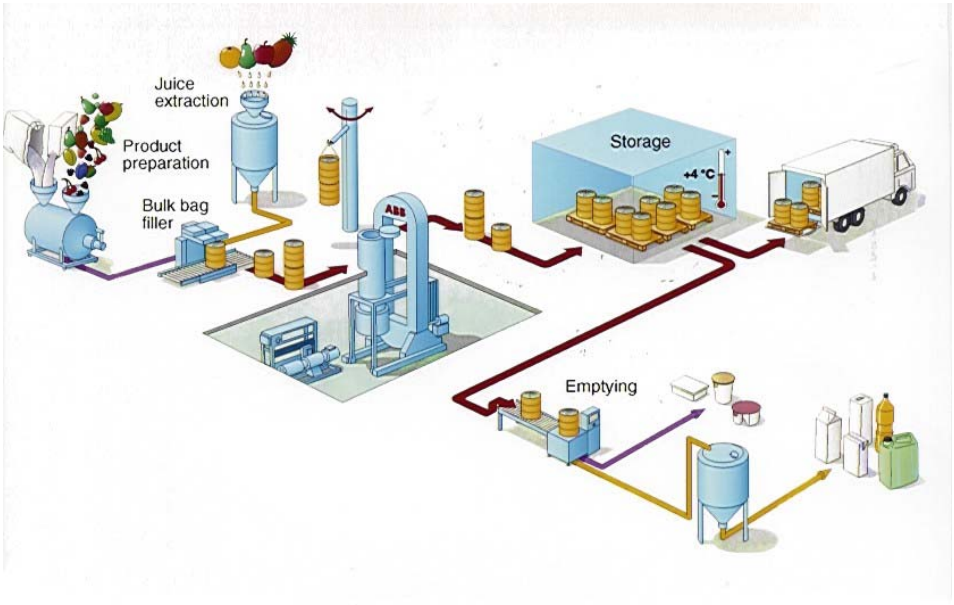

Figure 2.14. A bulk processing line for high-pressure treatment of foods contained in bulk packages. The contents are later transferred into retail packages (source http://www.fao.org/ag/ags/agsi/Nonthermal/nonthermal_1.htm).

The cost of high-pressure processing is dependent upon the combination of pressure, pressure holding time and temperature at which the product is processed (Hayashi et al., 1992). These variables must therefore be carefully selected. The cost per unit of production is lower for a single large production unit than for several small pressure units in parallel (Hayashi et al., 1992). This cost saving is possible because the capital cost of manufacturing a large pressure unit is lower than for manufacturing several small units.

Examples of Industrial-Scale High-Pressure Systems: High-pressure equipment, manufactured by ABB Pressure Systems, AB, has been largely used for synthetic diamond manufacturing, sheet metal forming and for the extrusion of metal. Equipment developed specifically for food processing includes the QUINTUS Food Press (Figure 2.14). The pressure vessel is pre-stressed using a spring steel wire and remains in a pre-stressed state even under pressure. A replaceable liner is inserted into the cylinder for additional safety of operation. The press uses a retractable frame made of pre-stressed wire winding in order to keep the top and bottom closures safely in place (Figure 2.14). As an alternative, food in retail-size packages, placed in a loading basket, may be processed under pressure and later transported directly for retail sales, as shown in Figure 2.15.

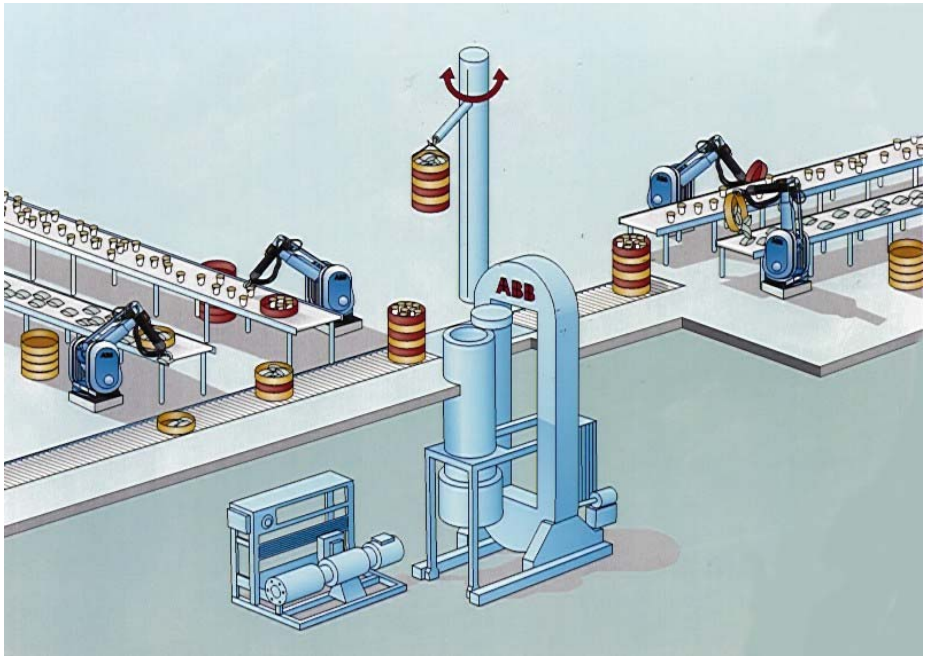

Figure 2.15. High pressure processing of consumer packages (source http://www.fao.org/ag/ags/agsi/Nonthermal/nonthermal_1.htm).

A list of HP equipment suppliers is given:

Alstom (www.alstom.com): Design and prototyping of a high pressure intensifier incorporating shear seal technology.

Avure Technologies Incorporated (www.avure.com): Manufactures both batch presses and continuous systems. Their website offers extensive information about the technology and commercial applications.

Elmhurst Research, Inc (www.elmhurstresearch.com): Designs and manufactures ultra high pressure vessels for general and food processing uses.

Energy Service Co.: Distributes high pressure processing equipment. Contact Andrew Freeman for more information on their high pressure processing products (1010 Vermont Avenue, N.W., Suite 706, Washington, D.C. 20005; Phone – (202)737-6018; FAX – (202)638-1069).

Engineered Pressure Systems Inc. (www.espsi-highpressure.com): Supplies laboratory and industrial scale high pressure processing equipment.

Flow International Corporation (www.fresherunderpressure.com).

Kobelco (www.Kebelco.co.jp/index_e_wi.htm): Offers a whole range of laboratory and industrial high pressure processing equipment.

Mitsubishi Heavy Industries (www.mhi.co.jp/e_hg/e_koatsu/04.html): Manufactures high pressure food processing test systems.

Nicolás Correa Hyperbaric (www.nchyperbaric.com): Manufacturers of HP facilities with horizontal design, 600 MPa maximum pressure and 300 litres maximum volume.

Resato (www.resato.com): Specializes in the design and manufacture of high pressure components, high pressure test equipment, and complete high pressure systems.

Sitec (www.sitec-ho.ch).

Stansted Fluid Power (www.sfp-4-hp.demon.co.uk/home.htm): Manufactures high pressure engineering equipment and systems for a wide range of industrial and research applications.

Stork Food and Dairy Systems (www.fds.storkgroup.com): No specific information is available yet.

Uhde Hockdrucktechnik (www.uhde-hpt.com): Offers high pressure processing equipment for treating food, pharmaceuticals and cosmetics.

Zdas (www.zdas.cz).

Excepting a very reduced number of facilities listed in Table 2.6, all the examples shown above correspond to high pressure equipments for temperatures above 0°C. In the case of HPLT, the special material qualities needed for the pressure vessel, the seal systems and pressure transmitting medium need to be examined and modified accordingly. Obviously, water is no longer applicable in the sub-zero domain and different alternatives have been tested, as shown in Table 2.6.

Table 2.6. Examples of experimental high pressure units in the subzero temperature range (adapted from Schlüter, 2004).

High-Pressure-Low-Temperature Units							Measurement		
Company (Reference)	Material	T range (°C)	P range (MPa)	V_i (mL) diameter (m)	P transmitting medium	Cooling system	T	P	Rate (Hz)
ACB, France Levy (1999)	Stainless steel, copper-beryllium	> -30	< 300	1000 0.080	Propanediol / water (55/45, v/v)	Circuit in vessel wall	2x K	2	<10
Uhde, Germany Amanatidou (2001)	Special steel	> -40	< 360	600 0.056	Glycol/ethanol (80/20, v/v)	Tubes around the vessel	11x T 2x Pt100	1	<10
EPSI, Belgium Denys (1997)	Special steel	> -35	< 600	590 0.050	Polyglicol	Tubes around the vessel	7x K	1	<0.04
Kobe Steel, Japan Fuchigami (1997)	Special steel	> -30	< 400	40 0.025	Polytehylen-eglycol	Immersion	2x	1	?
Unipress, Poland Arabas (1998)	Copper-beryllium	> -50	< 700	5 x 4.1 0.013	Pentane/hexane or silicon oil	Immersion	5x K	5+1	<1
Uhde, Germany Urrutia (2005)	Stainless-steel 1.6580	> -50	< 350		Water/ethanol (50/50, v/v)	Extern jacket	1x K	1	<1

Four patents have been found (after a study made by J. Arabas et al., 2005 – personal communication within the project SAFE ICE) within the period from 1995 to 2004 concerning apparatus for HPLT processing, obtained from the Internet database of the European Patent Office (http://ep.espacenet.com).

A summary of these four patents is given.

Number: US6640696; Date: 2003-11-04

Inventor: Haramoto Nobushiro (JP)

Applicant: Japan Steel Works Ltd.

Title: Device and method for continuous high pressure treatment

Abstract: A device and a method for continuous high-pressure treatment; the method, comprising the steps of increasing the pressure of raw materials (25) in a feed tank (9) by a pressurization pump (1) so as to continuously feed the raw material to treatment containers (6) and (6a) and increasing the flow rate of the pressurizing pump (1) over that of a depressurizing pump (2) or continuously exhausting the raw material from the treatment containers (6) and (6a) through a pressure regulating flow path resistance (59) while depressurizing; the device, comprising pressure releasing bypass circuits (55) disposed in the flow path resistance (59) in parallel with each other, wherein the insides of the treatment containers (6) and (6a) are kept in a specified high-pressure state during the continuous processing

Main claims: Apparatus comprising: a pressurizing pump, depressurizing pump and control means for controlling delivery rates of both pumps, first delivery rate of pressurizing pump is larger than a second delivery rate of depressurizing pump.

Drawing:

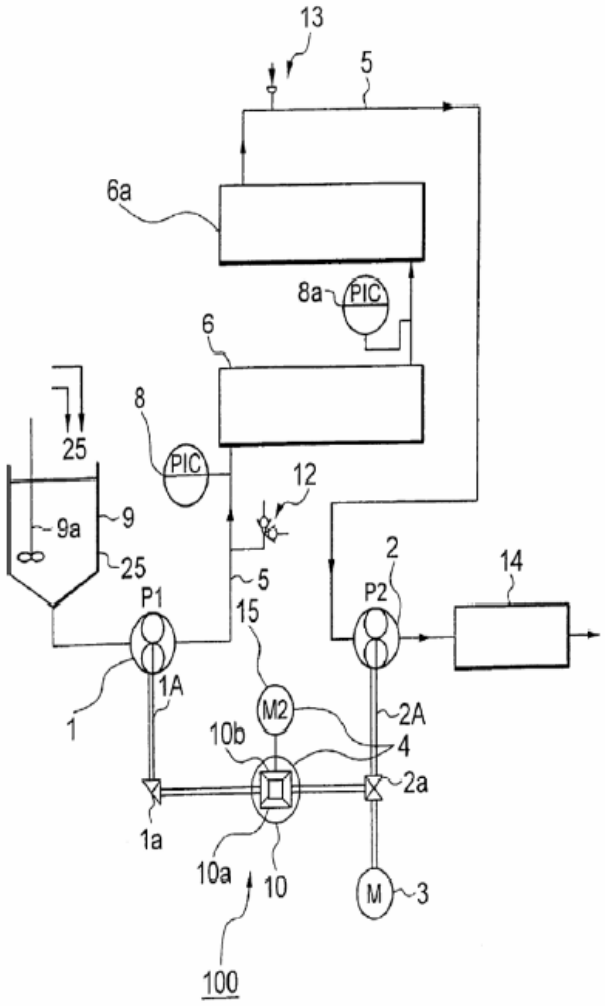

Number: WO02102422; Date: 2002-12-27

Inventor: Lonnebor Nils-Gunnar (SE)

Applicant: Flor Internacional (US)

Title: Method and apparatus for high pressure treatment of substances under controlled temperature conditions

Abstract: A product carrier (10) for use in ultrahigh pressure processing substances is substantially fluidically closed, and is insulated, to prevent heat transfer from the product being treated to the cooler wall of the pressure vessel. The insulating material (18) has compression heating properties, such that as the product is pressurized, the temperature of the insulation increases as does the temperature of the product and pressure media, thereby helping to prevent heat transfer from the product to the surrounding media and pressure vessel.

Main claims: (1) The fluidically closed carrier with insulating material which exhibits an adiabatic compression temperature change under pressure; (2) The method comprising: preheating the product in the product carrier, pressure vessel and pressure media to the selected temperature, prior to pressurizing the product carrier.

Drawing:

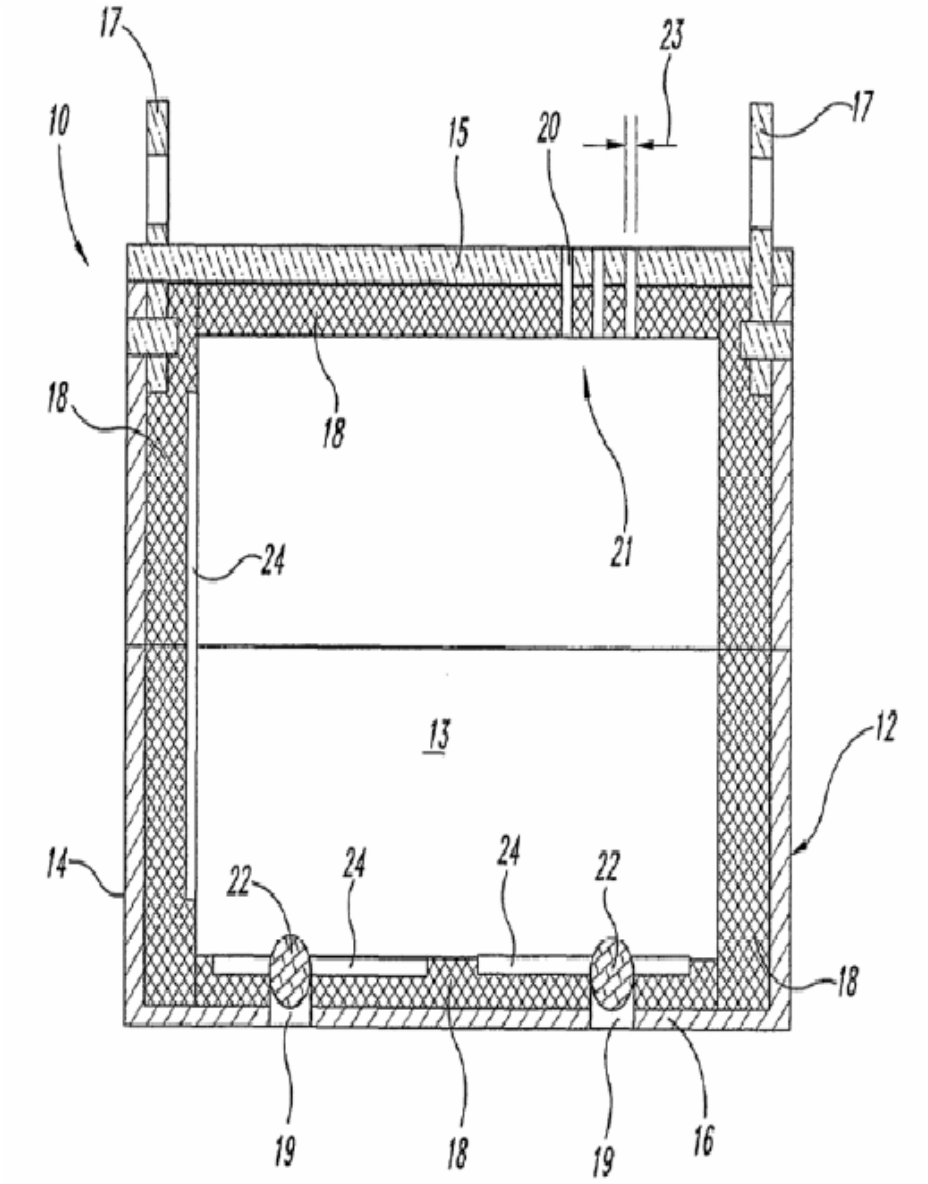

Number: US5475983; Date: 1995-12-19

Inventor: Yamamoto Siichi, Kanda Takeshi (JP)

Applicant: Kobe Steel Ltd. (JP)

Title: Method and apparatus for treating material under pressure

Abstract: Method and apparatus for industrially freezing (or cooling) food or the like under pressure. The method consists of isostatically exerting pressure on the material such as food (14) and the frozen body (15) composed mainly of water through the pressure medium (12) contained in the pressure vessel (1), thereby cooling the material (14). When the temperature of the material (14) decreases below 0 DEG C. at which freezing does not take place under pressure, the pressure is released rapidly so that fine ice crystals are formed in the material (14). The apparatus comprises a pressure vessel (1) having therein a high-pressure chamber (6) which can be supplied with a pressure medium (8), a treating vessel (9), in said high-pressure chamber (6) said treating vessel (9) having therein a treating compartment (13) containing a pressure medium (12) to apply isostatic pressure, and a plurality of trays (16) removably arranged in the treating compartment (13) in its axial direction, each of said trays holding the material (14) and the frozen body (15) composed mainly of water.

Main claims: (1) Method for rapidly cooling material by pressurizing it isostatically together with a frozen body composed mainly of water in a pressure medium. (2) High-pressure chamber which contains treating vessel having therein a treating compartment containing a pressure medium to apply isostatic pressure, and a plurality of trays removably arranged in the treating compartment.

Drawing:

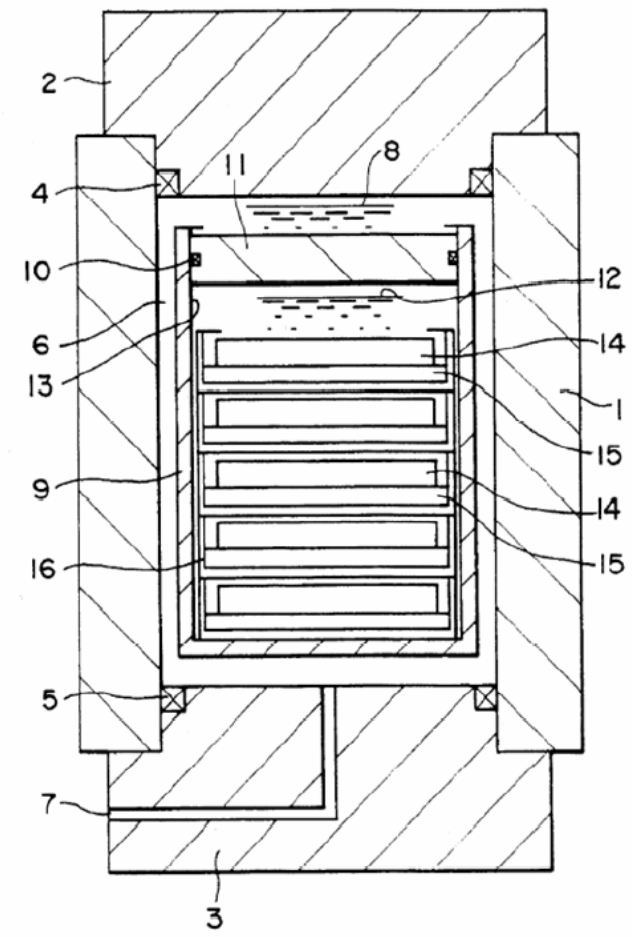

Number: US5213029; Date: 1993-05-25

Inventor: Yutaka Hideki (JP)

Applicant: Kobe Steel Ltd. (JP)

Title: Apparatus for treating food under high pressure

Abstract: An apparatus for treating food under isostatic high pressure applied by a liquid pressure medium which comprises a high-pressure vessel forming therein a treating chamber in which food is placed, a pressure medium tank adjacent to said high-pressure vessel, pipes to deliver a pressure medium from said pressure medium tank to said treating chamber, and a cooling device to hold therein the high-pressure vessel and the pressure medium tank and to cool the high-pressure vessel and the pressure medium tank simultaneously.

Main claims: (1) High-pressure vessel and the pressure medium tank are arranged integrally side by side in a freezer to cool them; (2) Pump, the treating changer and the pressure medium tank are connected by pipes and a stop valve which are arranged in the freezer.

Drawing:

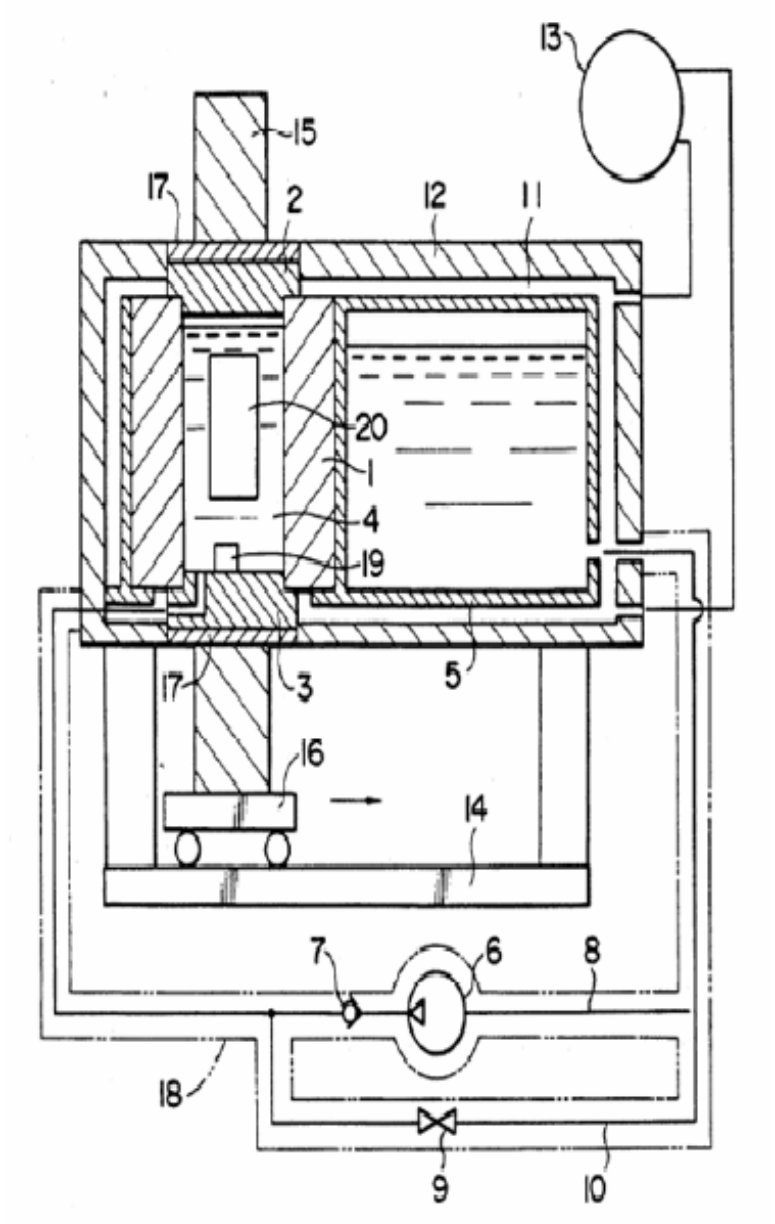

2.3.3. Challenges of HPLT technology

It must be noticed that NO products have been found which are commercialized either after or for a sub-zero temperature treatment. Therefore, there is a lack of investment of HPLT treated products and the opportunity for European companies to take advantage of the years of research in this field for a proper industrialization. Taking into account the fact that most of the HP technology research has been carried out in Europe, when counting the number of equipments installed in America (49) and Europe (19), it seems clear that the research effort in Europe is used in other parts for industrial application. It is still time to call upon the European companies to take the opportunity of the several research centres' expertise, which have been researching under the economical finance of the European Committee.

In the special case of a product such as ice cream, which must necessarily be treated at sub-zero temperatures, a Europe-based company, like Unilever, has already published two patents for the use of High Pressure in the manufacture of ice cream. A summary of these patents is given:

- US Patent 6497913 (2002), Unilever: "Using a homogenizer operating at higher pressures than those conventionally used in ice cream manufacturing, it is possible to generate smaller oil droplets (ca. 0.3μm) in an ice cream mix. This allows stabilization of a larger air : water interface, leading to smaller discrete gas cells which in turn modify (improve) the organoleptic quality of the ice cream. […] very small oil droplets will give inherently stable ice cream mixes which will not generate the desired microstructure unless the desired level of partial coalescence occurs […] This is achieved by […] manipulating the interfacial composition by the appropriate selection of emulsifiers". The pressure used is of 160 MPa and the air bubble mean diameter is reduced from 20-30 to <10 μm.
- US Patent 6156367 (2000), Unilever: "High-Pressure-Process (HPP) of mix with decreased meltdown, thicker, smoother, creamier ice cream in the absence of emulsifiers or stabilizers and / or with zero or low fat content and / or with low levels of snf".

All references (only these two!) found for the application of HP in the sub-zero domain in industry are related to ice cream, both of them being applied to the homogenization step. Anyway, this homogenization process of ice cream mix (mixtures of ingredients before the freezing step) is conventionally done at pressures up to 200 MPa. So, the use of HP for phase transitions is not referenced in the literature.

3. Materials and methods

3.1. HP facilities

3.1.1. HPLT lab single vessel (Berlin)

The facility consists of a high pressure vessel specially designed for subzero operation (Unipress, Warsaw, Poland), connected to a HP pump unit. A schematic drawing of the high pressure equipment is given in Figure 3.1a. The inner volume of the vessel was 3,7 mL, the maximum design pressure 1,0 GPa in a temperature range of –50°C to +150°C. In the HP vessel, potato cylinders are held by a holding tube screwed to the upper plug plate at the bottom of the vessel (Figure 3.1b) and the transient temperature field during the phase transition process is measured by three thermocouples (type K) using a special feed through system (Unipress, Warsaw, Poland). The thermocouples are placed in the centre (± 0.1 mm) and in both diametrical opposite surfaces of the samples with a radial distance of 4.8 mm (± 0.1 mm). As a pressure transmitting medium in the high pressure pump, silicone oil (No. 6165, Huber, Germany) was used. The temperature of the vessel is controlled by immersion either on a cryostat (HAAKE, Germany) or on a thermostat (Lauda, Germany). The temperatures (including the outer vessel wall and the bath temperature) and the system pressures during the experiments are digitally recorded every 0,2 seconds (measure rate is nevertheless adjustable).

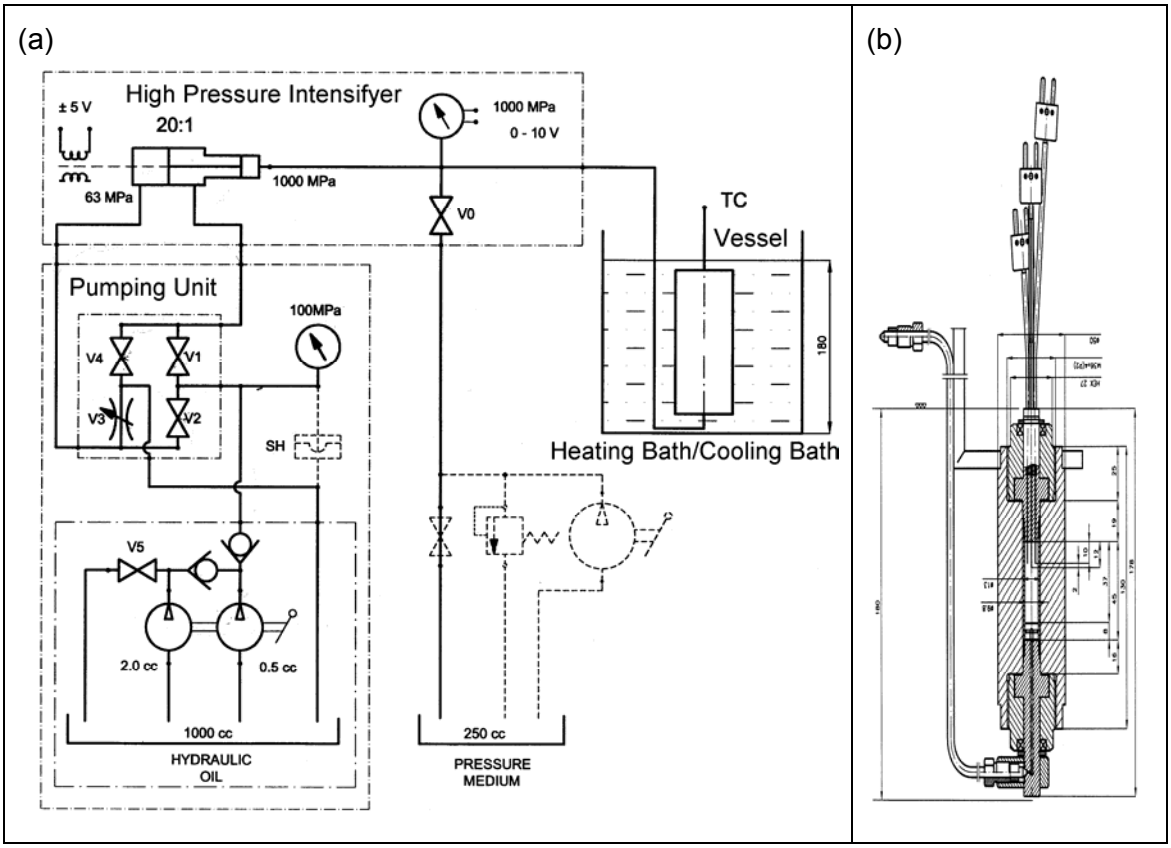

Figure 3.1. a) High pressure apparatus for subzero temperature operation and b) sectional view of the high pressure vessel (UNIPRESS, Warsaw, with permission).

3.1.2. HPLT lab multivessel (Berlin)

The multivessel lab scale unit (Model U111, Unipress, Warsaw, PL) has been designed to conduct kinetic studies (enzyme inactivation or microbial inactivation kinetics) up to pressures of 700 MPa over wide temperature range between –40°C and 100°C. This unit consists of five pressure chambers, which were separately connected to an oil-driven intensifier by five high pressure valves. Each of the vessels had a volume of 4

mL. The chambers are immersed in a water bath equipped with a thermostat. This design allows a simultaneous treatment of five different samples in one pressure build-up step at close to isothermal conditions. Each chamber is equipped with a K-type thermocouple and a pressure sensor to monitor the temperature and pressure history of each sample during the treatment cycle.

3.1.3. HPLT pilot scale vessel (Berlin)

The facility consists of a high pressure vessel of 1.6 litres internal volume (Uhde GmbH, Hagen, Germany), as shown in Figure 3.2. The temperature of the vessel is controlled externally by a cooling jacket connected to flexible tubes containing circulating silicon oil, cooled in a cryostat (Ultra-Kryomat RUK 50-D, Lauda, Germany). The pressure is built up with an air driven pump (DXS HF-602, Haskel, California, USA). The pressure transmitting medium used is 50% v/v mixture of ethanol/water (freezing point < -42°C) because of its non-toxicity, suitable chemical and thermophysical properties within the pressure and temperature range used and its industrial applicability. The temperature of the samples is measured using a type K thermocouple (response time 70ms). Pressure is measured using a pressure transducer (Intersonde HP28, Watford, England).

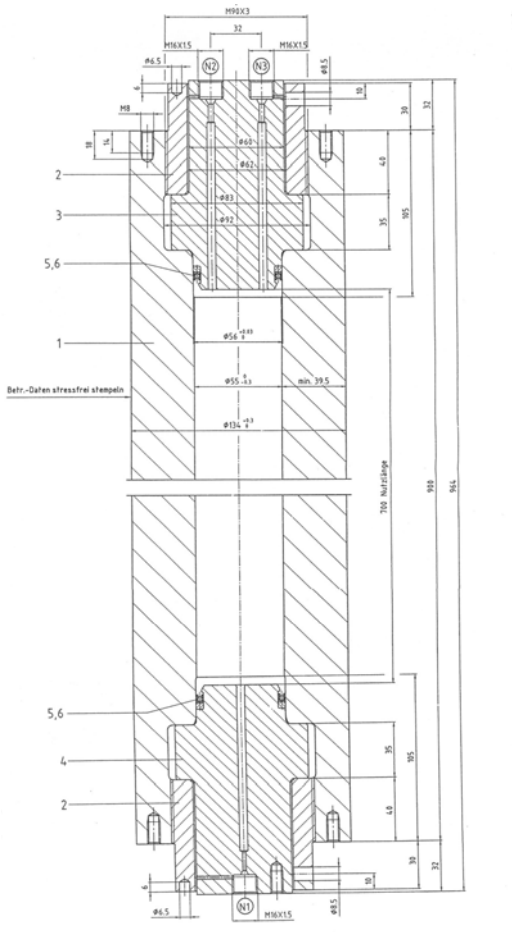

Figure 3.2. High-pressure vessel with capacity of 1,6 litres (Uhde).

3.1.4. HPLT pilot scale vessel (Nantes)

The vessel (Figure 3.3) has an inner diameter of 120 mm and an internal height of 310 mm. A specific lift system, able to manipulate the obturator and the sample to be treated, is used. A circulating glycol is connected to the high pressure vessel. It allows the vessel to be cooled down to -30°C and to be heated up to 80°C.

A mixture of water and ethyl alcohol (50/50 w/w) is used as fluid of pressurization. The facility is equipped with an instrumented obturator allowing the passage of six

calibrated thermocouples (K-type). Three thermocouples (diameter = 1 mm, K-type) were positioned into the samples: one at the surface and one at the centre of the bottom potato, and the third one at the centre of the upper potato. An additional thermocouple (diameter = 0.3 mm, K-type) is positioned at the bottom of the vessel, to measure the temperature of the pressurization fluid.

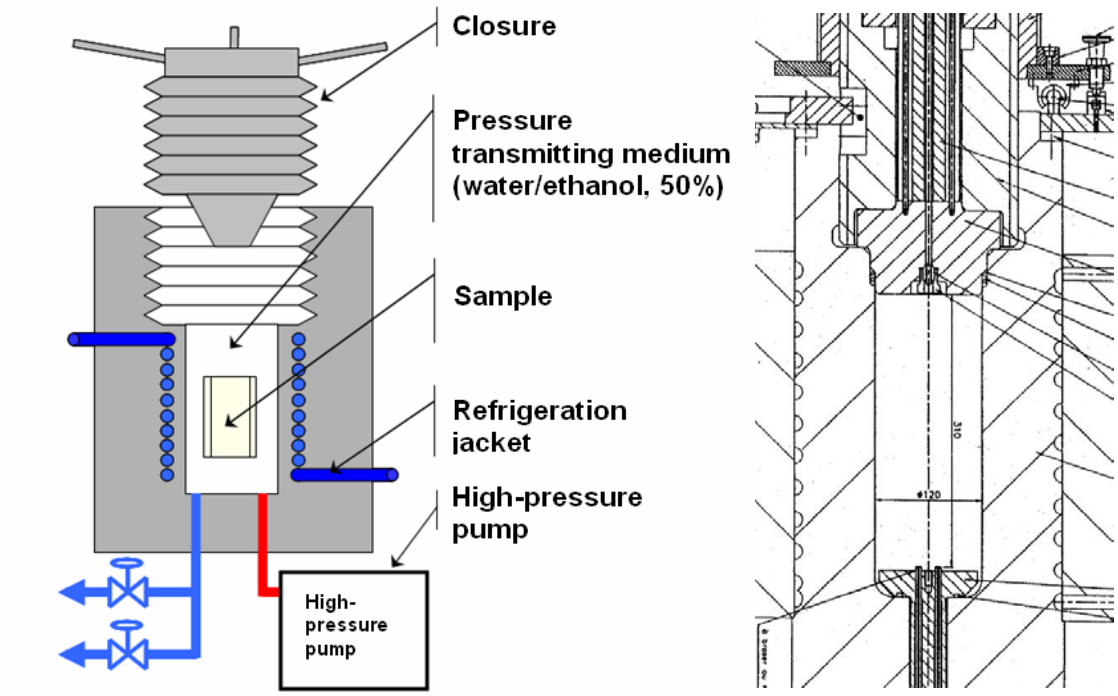

Figure 3.3. High-pressure vessel with capacity of 1,5 litres (ACB).

3.1.5. HPLT calorimeter (Nantes)

A High-Pressure Differential Scanning Calorimeter (HP DSC, Figure 3.4) was used in this study. The experimental system consisted of a differential calorimetry head, a refrigerated circulator, two HP cells, a HP compressor and a computer. The calorimetry head (Pass 27, Sceres, Orsay, France) had two cavities (20 mm diameter x 95 mm depth) used for holding the sample and the reference cells. There were 220 thermocouple junctions installed between the two cavities to amplify the generated temperature differential signal. Two platinum thermometers (Pt 100) were placed under each of the cavities to monitor/control temperature of the calorimeter.

The temperature of the calorimetry heat was controlled through a copper coil wound around the contour of the head (Figure 3.4a) and an oven around the system. The copper coil was connected to the refrigerated circulator (Huber CC250, Offenburg, Germany) with a water-glycol medium. During the experiment, the calorimetric head together with copper coil was thermally insulated in plastic box containing foamed plastics.

The HP cell (made of beryllium copper) contained two plugs with a nitrile O-ring and a threaded bolt for sealing on one side (Figure 3.4b). It was connected to a pressure tube (3.2 mm diameter) on the other side with miniature fittings (M2 Serie, 100 MPa, Harwood Engineering, MA). The pressure within the system was achieved through the HP compressor (400 MPa, 5 cm^3, Nova-Swiss, Effretikon, CH) driven by a step motor (MO63-LE09, Mijno, Fenwick, France) and controlled by the computer. A pressure sensor (200 or 400 MPa, Asco Instruments, Chateaufort, France) was used to monitor and control the pressure. When the pressure required for a test exceeded 180 MPa, the 400-MPa sensor was used during the experiment. A software (Labview 6, National Instruments, Austin, TX) was used for system control and data recording (temperature, pressure and heat flow). Pentane (Sigma, Fallavier, France) was used as

pressurization medium in the system because of its stability on the pressure–temperature domain tested and its properties (low viscosity, no phase change) (Bridgman 1970; Scaife and Lyons 1980).

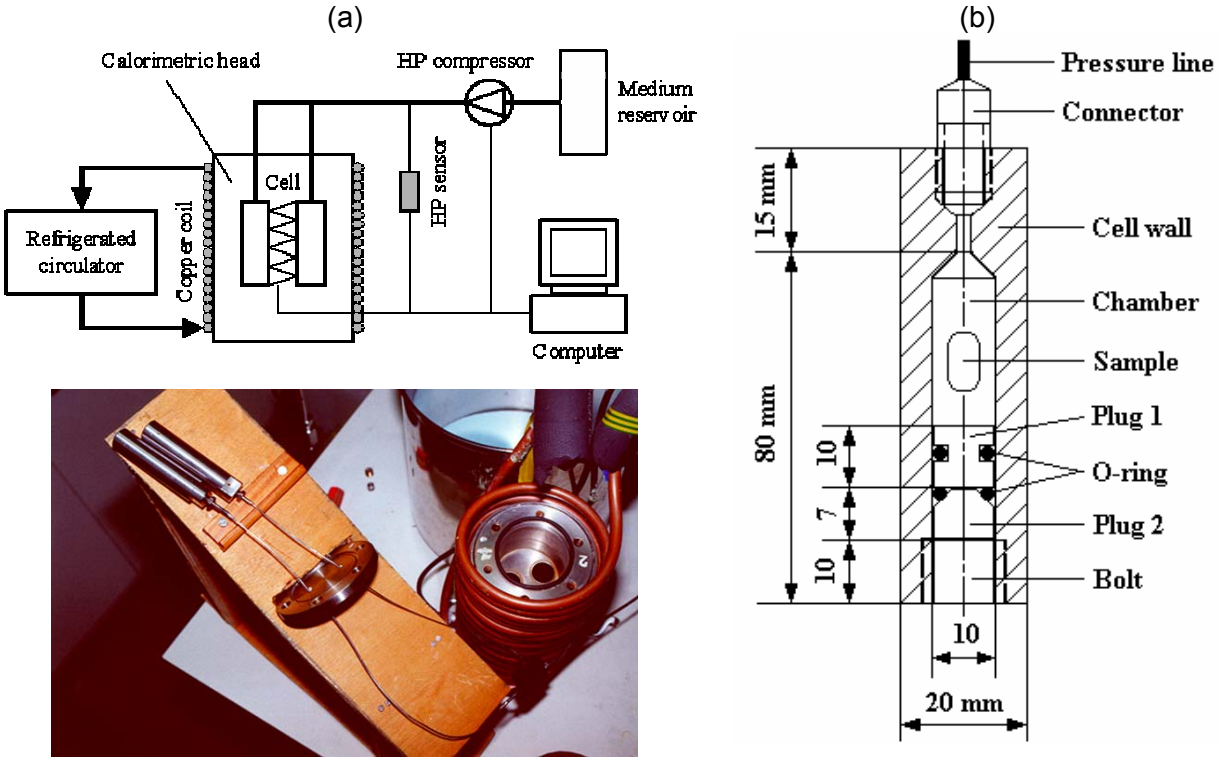

Figure 3.4. Experimental set-up of HP calorimeter: (a) schematic diagram with photography and (b) scheme of the HP cell and sample installation.

3.1.6. HPLT microscopic cell (Warsaw)

The design of the microscopic cell (performed in CATIA v5 CAD system) is shown in Figure 3.5. Figure 3.5a shows the pressure cell, Figure 3.5b the pressure cell equipped with cooling system and Figure 3.5c the pressure cell entirely assembled with the cooling system and insulation enclosure provided with inlets for anti condensation system.

The pressure cell is made of Stainless Steel 15-5PH, with a weight of about 250 g. It is shaped in a nearly cubicoidal form, with a quadratic cross section of 41.4 mm and height of 20 mm. At the bottom of the cell body, a Sapphire cylindrical plate 8x3 mm is built-in, co-operating with the objective of the inverted microscope. In the upper part of the cell (closing screw) a Sapphire cylindrical plate 8x3mm is built-in, co-operating with the condenser of the microscope. Two miniature pressure connections for pressure tubing 1/16” and for high-pressure single or multi-thermocouple probe (the prototype is equipped with a sheathed thermocouple type K, diameter of 0.5 mm and wire type multi-thermocouple with three thermocouples type T) (Figure 3.5a).

The pressure cell is equipped with a cooling system based on four Peltier elements (Melcor CP1.4-35-045L, max. capacity 19 W), assembled at the lateral walls of the cell body (Figure 3.5b). Heat is removed by two heat exchangers connected to an external bath.

The pressure cell with the heat exchangers are covered with an insulation enclosure provided with two inlets for dry gas (Figure 3.5c). Blowing dry Argon (flow lower than 5 dm^3/min) is used to avoid condensation of vapour on the pressure cell and especially at the optical plates. All elements are designed for easy mounting on an inverted microscope (Nikon, Eclipse T100, Warsaw).

(a)

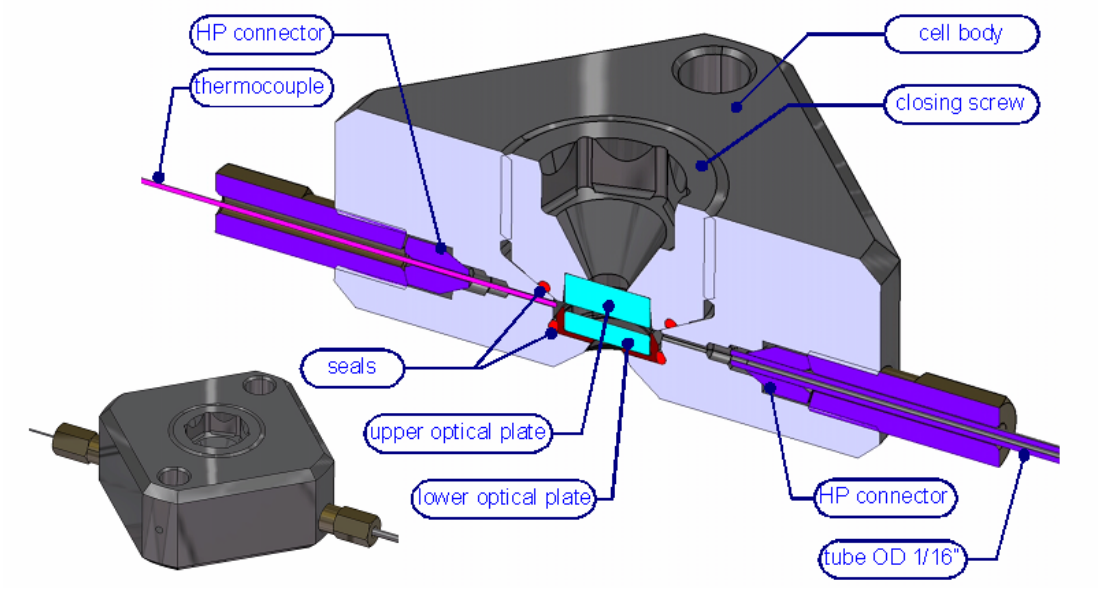

(b)

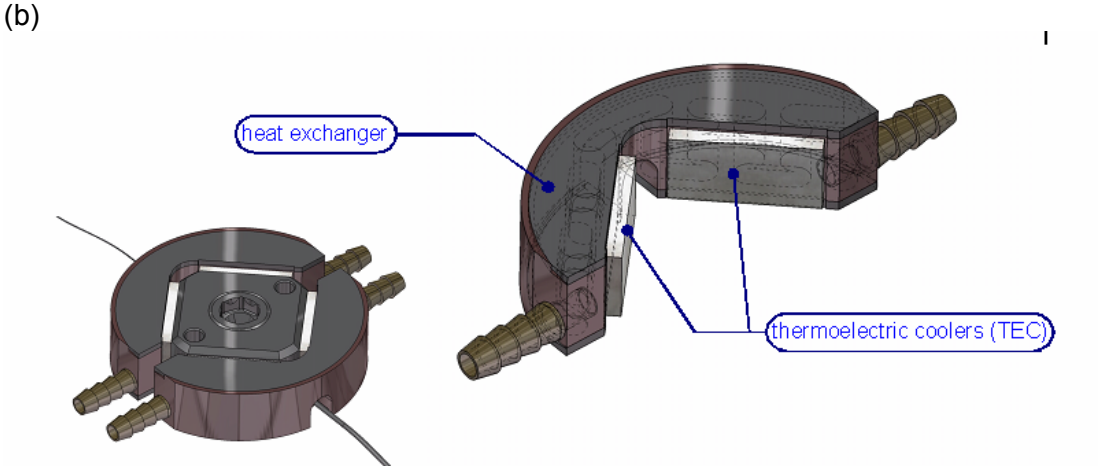

(c)

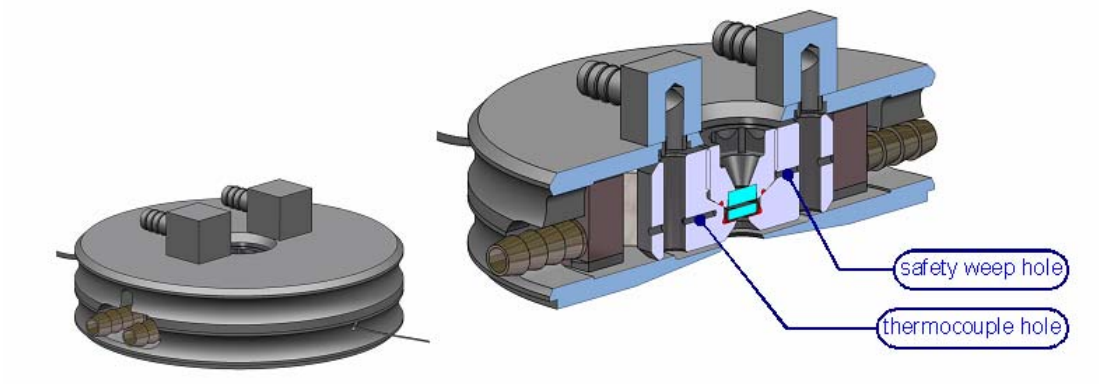

Figure 3.5. Pressure cell (a), with cooling system (b), and insulation enclosure (c). (Source: SAFE ICE project, UNIPRESS, with permission)

3.2. Test samples

3.2.1. Tylose

Tylose (methylcellulose gel) is used as a model food, in two geometry versions: slabs or cylinders. Tylose was provided by MADI S.n.c. (Italy). Tylose samples are vacuum packed in a polyethylene bag. Tylose is used due to its high content of water, easy manipulation and similar thermophysical properties to water.

3.2.2. Potatoes: lab scale, Berlin scale & Nantes scale

Commercial potatoes (variety Bintje, with an initial water content of 77%, wet basis) were selected as food model, due to their homogeneous structure. For the laboratory scale experiments, the samples were cut into cylinder shape samples of 40 mm length and 9,8 mm diameter to perform the freezing experiments. Three holes were bored into the cylinder with a thin needle to insert the tip of a K-type thermocouple into the sample centre and two additional thermocouples near the surface in the sample.

For the pilot scale experiments in the facility in Berlin, potatoes (variety Nicola, category I, calibre Grenaille, mean diameter 35mm, mean height 50mm) were vacuum packed in two different bags for each experiment, each bag containing 6 potatoes. The first and last potatoes of each bag were previously cut: one half was placed in the vacuum bag and the other half separately packed for reference analysis. Working this way, the reference analysis of one half-sample and the analysis after HPLT processing of the other half-sample are comparable, as both results come from the same whole-sample, and the variability of results due to the variability of natural specimens is avoided. The two bags were placed in a polypropylene container especially designed for the high pressure vessel used. An additional potato, not packed, was used at the top of the vessel to measure temperature during processing. Figure 3.6 shows a scheme of the sample preparation in the sample container.

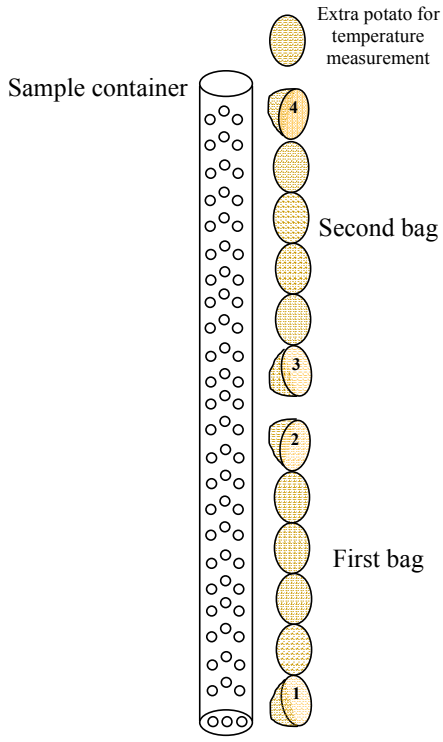

Figure 3.6. Disposition of the potato samples for the pilot scale facility in Berlin.

For the pilot scale experiments in the facility in Nantes, whole potatoes were vacuum packed in PE plastic films and were placed in the HPLT facility, as shown in Figure 3.7a. A total of 6 potatoes were used for each HPLT experiment, in which the top one and the bottom one were individually packed, to be able to introduce thin capillary

tubes inside the potatoes with a type K thermocouple in it. In this way, the temperature was recorded directly from the potatoes (Figure 3.7b).

Figure 3.7. Sample preparation and disposition in the HPLT vessel (a); packaging and thermocouples disposition in samples (b).

3.2.3. Ice cream: Berlin pilot plant scale

Ice cream with a fat content of 9% was packed in PE plastic bags to perform the HPLT experiments in the pilot plant unit from Uhde. Details on the formulation of the product are confidential.

3.2.4. Microorganisms: Bacillus subtilis suspensions

The strain used in all of the experiments was B. subtilis PS832 (VBBBa 1-187, a wild-type trp+ revertant of strain 168, Unilever Food Research Centre) kindly provided by the group of Prof. Peter Setlow (University of Connecticut Health Centre, Farmington, CT USA). This strain is classified as genetically indistinguishable from Bacillus subtilis 168 (Oomes et al. 2004, Kort et al. 2005).

For the microorganisms culture preparation, one aliquot of Bacillus subtilis PS832 overnight culture was transferred into pre-warmed TSB (Trypticase Soy Broth, Tritium Microbiologie B.V. BBL 4311768) with an initial OD600 of 0.02 to 0.04. This broth was incubated for about 2.5 hours to reach the mid-exponential growth phase at an OD600 of 0.4 to 0.6. This step was repeated once to get to the final culture that was used for the experiments. Cells were then harvested by centrifugation at 4°C and 5000×g for 15 minutes. Cell pellets were re-suspended in 50mM ACES, pH 7.0 (N-[2-Acetamido]-2-aminoethene-sulfonic acid, EEC No 230-908-4, SIGMA) buffer, at a final concentration of 10^7-10^8 cells ml^{-1}.

Approximately 3ml of the suspension was placed in a polyethylene pouch and heat-sealed. This pouch was placed in an aluminium pouch and heat-sealed. It was imperative to eliminate any air bubbles from both bags. After sealing samples were immediately stored at –80°C. The cultures were examined for the presence of spores

by heating the cell suspension at 80°C for 10 minutes, followed by colony counting on TSA (tryptic soy agar, Tritium Microbiologie B.V. BBL 4311043). The concentration of the spores in all cultures used in the experiments described here was less than 102 spores ml^{-1}.

3.3. Analysis methods

3.3.1. Analysis of phase transitions

At atmospheric conditions, the precise determination of the product dependent freezing and/or melting points may be possible with the aid of different analytical methods. Compared to Differential Scanning Calorimetry (DSC), a more feasible method of measurement is the Thermistor-Cryoscope method with which the temperature of the sample is recorded over time while cooling below the freezing point. In this case, the crystallization temperature is derived by the relatively long temperature plateau which follows the nucleation on account of latent heat being released. If the latent heat of fusion is dissipated to a large extent, the temperature of the sample decreases in accordance with the defaulted ambient temperature. In the same way the freezing and/or melting point of foods was determined at high hydrostatic pressure. The temperature change in the centre of a sample related to the phase transition can be plotted versus time or pressure. A possibility of representing the product specific pressure dependent freezing and/or melting curve arises for example, from the determination of single freezing points at different pressure levels. The slope of the phase transition line can then be obtained by extrapolation. The temperature stability at the phase boundary offers a different approach to the experimental description of the equilibrium line. Using a suitable measurement system, the shift of the phase transition temperature in the centre of a sample can be recorded during manual change of the system pressure, so that the slope of the phase boundary can be determined. Figure 3.8 shows a typical freezing and thawing curve obtained at a constant pressure of 200 MPa. The projection of the freezing/melting point of potato tissue and the corresponding pressure value to the pT-diagram leads to a single point of the phase transition line. To ensure a comparable cooling/heating rate the bath temperature of the tempering units was set 20 °C below/above the expected melting point at the selected pressure values calculated using the equations given for water (Wagner et al., 1994).

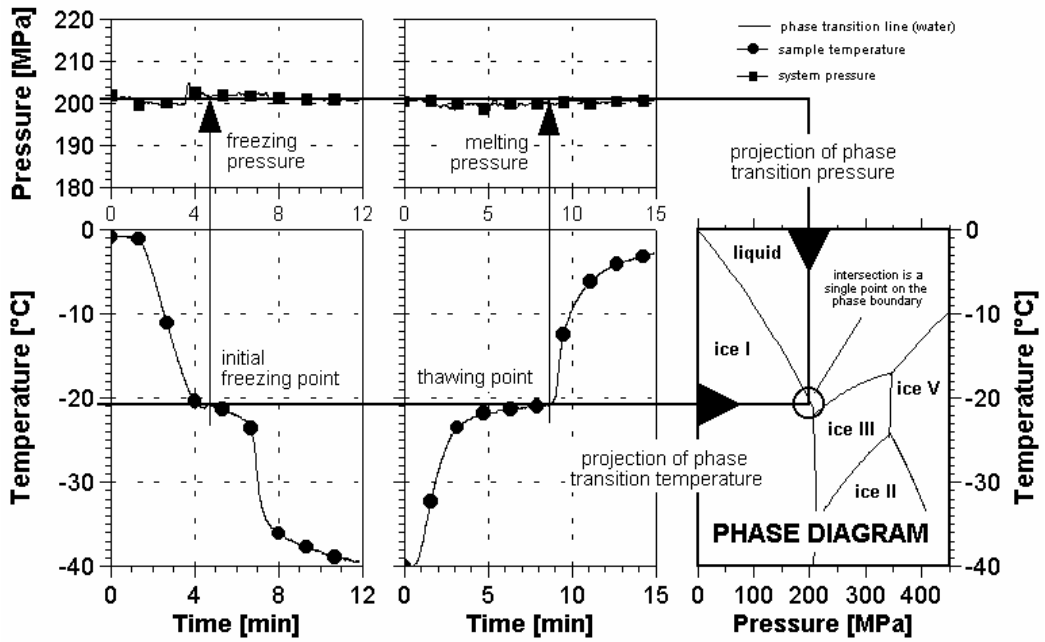

Figure 3.8. Simultaneous detection of temperature and pressure data during freezing and thawing of potato tissue and determination of single phase boundary points by projecting the data pairs to the pT-diagram.

3.3.2. Analysis of calorimetric signal

Calorimetry is a powerful tool to study thermodynamic properties of materials and phase-change phenomena. Normally, calorimetric experiments are carried out with a differential scanning calorimeter (DSC) at a constant (usually atmospheric) pressure using temperature as the working parameter. In HP calorimetry, the cell for holding the sample should be strong enough to resist high pressure. Thus, the cell becomes large in terms of mass and heat capacity, which presents a major challenge to obtain accurate results for temperature scan (T-scan) tests. To overcome this difficulty, an alternative measure of pressure scan (P-scan) at a constant temperature is adopted in HP calorimetry. The pressure can be changed either as a step change (Pruzan et al., 1979) or at a constant rate (Randzio et al., 1994). Several studies have been carried out using P-scan tests for gathering thermal properties of water and aqueous solution (Chourot et al., 2000; Le Bail et al., 2001) and some organic liquids such as hexane, butane-1, benzene, toluene (Fuchs et al., 1979; Pruzan et al., 1979; TerMinassian et al., 1988; Grolier and Randzio 1997) under HP conditions.

Most foods and food products contain a high percentage of moisture. Thermo-physical properties of foods have been generally linked to moisture content, temperature, phase and pressure. Phase transition of water in these foods during HP process can be more complicated than that of pure water. Scientific information related to HP calorimetry of foods is scarce and poorly documented.

Experiments were carried out with pure water (for calibration) and potato cylinders of about 0.5g, vacuum packed in polyethylene bags (80 μm thick multilayer film). For each test, the sample is installed in the sample cell (see Figure 3.4). The reference cell was prepared in the same way as the sample cell but without the sample.

Isothermal pressure-scan (P-scan) experiments were carried out to experimentally obtain the values of latent heat of the sample. After sample installation, the sample and reference cells were placed in the sample and reference cylinders, respectively. The sample was frozen at the set temperature (between -10 and -20°C) in the calorimeter. Once the calorimeter signal showed a stable baseline (close to zero), the pressure was increased from the atmospheric level at a constant rate of 0.5 MPa/min up to a level high enough ensuring the sample melting (e.g., around 160 MPa for P-scan at -10°C) and heat flow signal was recorded every 5 seconds. When the pressure reached the corresponding phase change temperature, ice started melting (see point 1 in Figure 3.9), resulting in a peak of heat flow to compensate the temperature drop. A low P-scan rate was employed (as compared to 1 MPa/min used in previous studies, by Le Bail et al., 2001), in order to obtain a well defined span of the calorimetric peak. Figure 3.9 shows the path followed in a typical P-scan experiment.

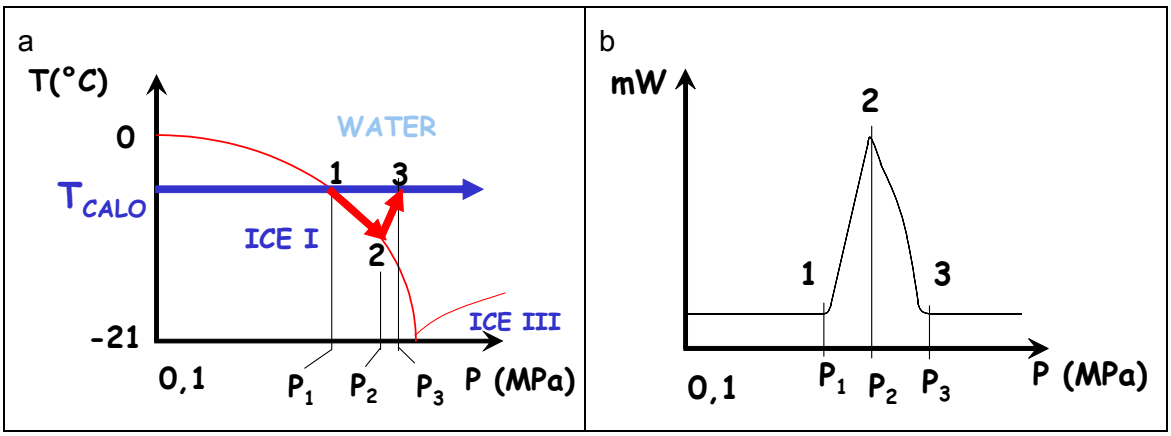

Figure 3.9. Schematic description of isothermal pressure scan for the phase change on the phase diagram of water (a) and the corresponding calorimetric signal (b).

The calorimetric signal can be expressed as a function of pressure and temperature variations as expressed in equation (3.1):

$$\partial Q = C_p \partial T + h \partial P \qquad (3.1)$$

Where C_p is the specific heat and h the latent heat. If a P-scan experiment is performed, the temperature remains constant. Therefore,

$$\frac{dQ}{dt} = \alpha VT \frac{dP}{dt} + h\frac{1}{dt} \approx \alpha VT \frac{\Delta P}{\Delta t} + h\frac{1}{dt} \qquad (3.2)$$

Representing in a same graph the pressure change and the calorimetric signal change with time (Figure 3.10a), the terms from the equation (3.2) can be discussed.

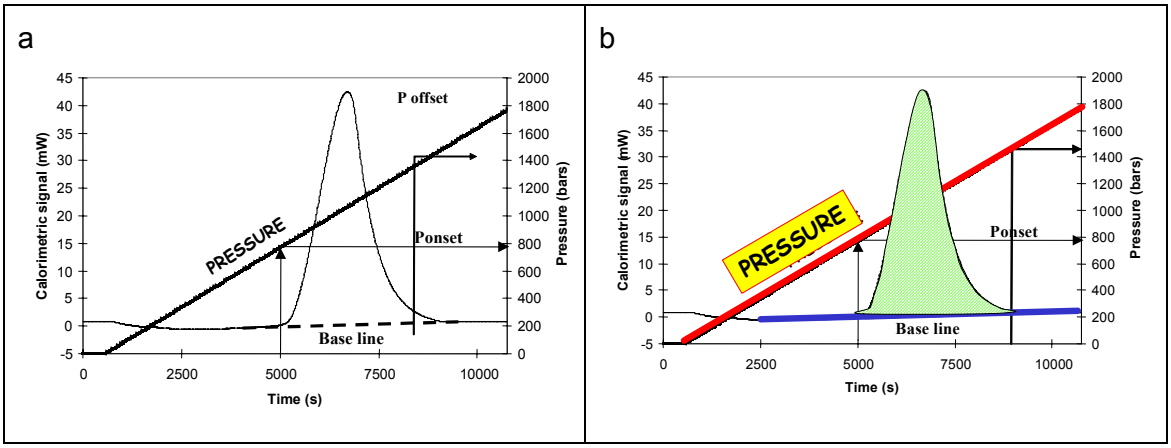

Figure 3.10. Pressure and calorimetric signal change with time.

The first term of equation (3.2) takes into consideration the P increase with time. The second term, expresses the relationship between the calorimetric signal and the latent heat. If this second term is integrated:

$$\frac{dQ}{dt} = h\frac{1}{dt} \xrightarrow{\int} \int dQdt = \int hdt \rightarrow Qdt = \int hdt \qquad (3.3)$$

Therefore, the area under the calorimetric curve corresponds to the latent heat of the sample (lined area in Figure 3.10b).

3.3.3. Mathematical modelling tools

A numerical explicit finite difference scheme was used to describe conductive heat transfer and thermal phenomena during the high pressure supported freezing processes (Schlüter *et al*., 2003). A one-step mathematical model based on the solution of differential equations governing the heat transfer will be applied. This scheme is used to predict the temperature distribution inside the cylindrical potato samples through an explicit one-dimensional finite volume scheme, and then, to predict the phase transition time and overall process time (two variables of relevance with different explanatory values). In this mathematical model, the grid layout uses *n* nodes which are equally distributed in a distance of Δx along the sample radius, *R*, leading to node positions described by $i \cdot \Delta x$. The sample was, then, supposed to have homogeneous temperature in the axial direction.

At each time step, Δt, heat balances were performed for all the elements, resulting, when developed, in an equation where the temperature at time step $t+\Delta t$ and position *x* is a function of temperatures at *t*, for the three former consecutive positions, $x+\Delta x$, *x* and $x-\Delta x$:

$$T_i^{t+\Delta t} = T_i^t + \frac{Fo}{i}\left[\left(T_{i+1}^t - T_i^t\right) + i\left(T_{i+1}^t - 2T_i^t + T_{i-1}^t\right)\right] \quad (3.4)$$

In a similar way, for the central nodes, the following function was defined:

$$T_0^{t+\Delta t} = T_0^t - 4Fo\left(T_0^t - T_1^t\right) \quad (3.5)$$

where:

$$Fo = \text{element thermal diffusivity} \equiv a\frac{\Delta t}{(\Delta x)^2} \equiv \frac{\lambda}{c_p \rho}\frac{\Delta t}{(\Delta x)^2} \quad (3.6)$$

This algorithm requires the determination of thermal conductivity, heat capacity and density of the potato samples at the different experimental conditions. As there are no available data in the literature for potato properties at high pressures, the model itself was used as a tool to return the corresponding values for each experimental condition. Taking a previous set of data obtained from an atmospheric pressure freezing experiment as a starting point, modification coefficients were included into the numerical schema to give back the values that better fit with the experimental curves.

Then, the thermophysical properties for this material must be expressed as a function of the temperature at time step t-Δt. The freezing temperature, T_f, supposes an inhomogeneous point. For this reason, constant values were used for $T \geq T_f$ and the cumulative Weibull distribution (equations 3.7 and 3.8) was used to calculate thermal conductivity and density at temperatures below the freezing point. According to the parameters b and c the shape of the function varies between maximum and minimum values of the quantities under consideration, which were estimated from the literature (Ross *et al.*, 1977, Chizhov, 1993).

$$\lambda(T) = \lambda_{\min} + \left(\lambda_{\max} - \lambda_{\min}\right)\left[1 - \exp\left(-\left(\frac{T - T_f}{b}\right)^c\right)\right] \quad (3.7)$$

$$\rho(T) = \rho_{\min} + \left(\rho_{\max} - \rho_{\min}\right)\left[\exp\left(-\left(\frac{T - T_f}{b}\right)^c\right)\right] \quad (3.8)$$

Following the approach of Cleland and Earle (1984) the heat capacity is modelled by assuming a hypothetical change in specific heat capacity around the freezing temperature. Since the sharp peak in c_p at T_f seems to affect the plateau of the freezing curves (where the phase transition occurs), a modification of the distribution Weibull function was used as follows:

$$c_p(T) = c_{p,\min} + \left(T - T_f - T_{\min}\right)\frac{c_{p,\max} - c_{p,\min}}{T + T_{\min}} + a\left(\frac{T_f - T}{b}\right)^c \frac{c}{T_f - T}\exp\left(-\left(\frac{T_f - T}{b}\right.\right. \quad (3.9)$$

where T_{min} is the minimum temperature reached during each experiment, that is, in practice, the cold bath temperature.

The model used here is applied to freezing processes in which ice III is obtained, with a one-step modelling schema. This model has been implemented in a spread sheet with the help of Visual Basic program tool. The way this model is applied permits that a one-

step calculation follows the experimental jump to the corresponding freezing point, also after significant supercooling as ice III is obtained. This one-step model is then able to calculate nucleation temperatures, freezing times and phase transition times.

3.3.4. Quality analysis: texture, colour, drip loss, microstructure

3.3.4.1. Texture

Potatoes

The texture of fresh and processed samples was measured with a Texture Analyser TA.XT2 (Stable Micro Systems, Godlaming, UK). The samples were cut into cubes (3 x 1,5 x 2 cm) and stress tests were performed with a cylinder. The samples were subjected on one side to compression tests with the cylinder, being the uniaxial compression of 10 mm and the force-deformation data were recorded. The deformation rate was 1 mm/s.

The parameter's true compressive stress (σ_C) and true compressive strain (ε_C) were calculated according to the equations (3.10) and (3.11).

$$\sigma_c\left[\frac{N}{mm^2}\right]=\frac{F[N]}{A[mm^2]} \text{ being } A=\frac{A_0\cdot h_0}{h_0-\Delta h} \tag{3.10}$$

$$\varepsilon_c=ln\left(\frac{h_0}{h_0-\Delta h}\right) \tag{3.11}$$

F (N) being the force used during the compression, A (mm^2) the cross-sectional area of the cylinder at a deformation of Δh, A_0 (mm^2) the cross-sectional area of the cylinder before the compression, h_0 (mm) the height of the sample before compression and Δh (mm) the difference of the height of the sample before compression and during compression.

During the deformation, the true compressive stress increases with the true compressive strain, until a certain point when the tissue cracked, i.e., failure of the tissue occurred. This failure was read off in the true stress-true strain plot by an abrupt decrease in the stress during further compression. The resulting first local maximum in the true stress-true strain plot (calculated with the first derivative) was defined as failure stress (σ_f) and the associated strain was defined as failure strain (ε_f).

Ice cream

Texture profile analysis of ice cream samples was performed in duplicates with the same facility used for potatoes using a double compression test. After the HPLT treatment, samples were kept at least for 2 hours into frozen storage at -25°C and then taken for analysis. Samples were compressed at a depth of 10mm with a cylindrical probe of diameter 2,5mm, at a compression speed of 2 mm/s, at room temperature (Hayes et al., 2003). Four rheological parameters are calculated from the curves: hardness (maximum force during the first cycle of compression), cohesiveness (ratio of the positive force area during the second cycle of compression to that of the first cycle), gumminess (hardness x cohesiveness) and adhesiveness (the negative force during the first compression cycle, representing the work needed to overcome the attractive forces between the surfaces of the probe and the ice cream).

3.3.4.2. Colour

The colour changes of the surface of treated potatoes (half samples, being the other half measured as reference without treatment) were measured with a Chroma-Meter CR-200 (Minolta, Japan) using the CIE-Lab-System, based on the L, a and b parameters of colour. In this system, the L-component describes the lightness in a scale from 0 (black) to 100 (white), and the length and the orientation of the vector in the ab-plane describe the saturation (green to red) and the hue (blue to yellow) of the

spectrum. The Euclidean distance between two Lab-vectors corresponds roughly to the perceptual similarity of two colours. To measure this distance between two points, the parameter ΔE is calculated following the equation (3.12):

$$\Delta E = \sqrt{\left(\Delta L^*\right)^2 + \left(\Delta a^*\right)^2 + \left(\Delta b^*\right)^2} \quad (3.12)$$

being ΔL*, Δa* and Δb* the differences of these parameters for two measurements, in our case the difference between HPLT processed and fresh sample. Each colour measurement was performed immediately after processing (or immediately after cutting for the fresh reference samples) and after 20, 40, 60 and 80 minutes.

3.3.4.3. Drip loss

The half samples (both processed and fresh) were weighed with 0,001g precision immediately after processing (or immediately after cutting for the fresh reference samples) and after 20, 40, 60 and 80 minutes.

3.3.4.4. Microstructure

For the microstructure analysis, an embedding procedure in a resin of cylindrical samples cut from the processed potatoes was performed. For the embedding procedure, samples were cut with a sharp knife after treatment in a cylindrical shape of approximately 9 mm diameter and 3-4 mm height. Then, the samples were fixed in 1% glutaraldehyde in 0,1M phosphate buffer (pH 7) over night at +4°C. After fixation, samples were washed (distilled water 3 x 30min) and dehydrated (50% ethanol 1 x 1h, 70% ethanol 2 x 2h, 95% ethanol 1x 1-2h, and again 95% ethanol over night) at room temperature. After 6-8 hours infiltration with a mixture of absolute ethanol and commercial infiltration solution (Leica Mycrosystems), the final infiltration (only with the commercial infiltration solution) took five days. Extra solution was dried before putting samples to the mould tray. Twelve ml infiltration solution and 800µl hardener was mixed and the solution was immediately used. Samples were oriented into the middle of the mould and left to polymerize over night. Adaptors were used to recover resin embedded samples from the moulds.

Resin embedded samples were cut with a microtome (Leica Jung RM 2055, Nussloch, Germany), with a depth of 5 μm, and died with 0.1% toluidine blue. After drying, images from samples were taken with a microscope (Olympus BX50).

3.3.5. Safety analysis: enzymatic activity measurements

The polyphenol oxidase activity was measured through photometric (at λ:420 nm) determination of the linear increase of the absorbance per time unit. The enzyme activity with 0.1 M catechol in phosphate buffer pH 6.5 and at room temperature was evaluated (Cano et al, 1990) in triplicate. One gram of each sample were rasped and placed to 3 ml of phosphate buffer pH 6.5 then homogenised in ice-bath with Ultra-Turrax (T25-basic, Kika Labortechniek, Germany) at 9500 U/min. The samples stayed in ice-bath for 30 min, then they were centrifuged RC-5B (Sorvall GmbH, Germany) for 10 min., 5000g and at 4°C and the supernatant was kept.

3.3.6. Microbial activity measurements

Samples treated at subzero temperatures were taken out from the deep frozen storage (–80°C) and thawed on ice before colony counting. Samples treated at 10°C were kept on ice for a maximum of 2 hours before colony counting. All of these samples were then diluted in ten-fold series and incubated in TSA at 37°C for 3 days for colony counting. All the experiments were performed, at least, in duplicates.

4. Results and discussion

4.1. Modified phase diagram of water for potato tissue

4.1.1. Freezing processes

Since the first papers reporting the potentials of the pressure-supported freezing and thawing processes for food products appeared, a heterogeneous terminology has been used, due to the novelty of these terms and to the diversity of researchers involved in the new processes, from food technologists and biochemists to engineers and mathematicians. The concepts of high pressure supported, assisted, shift and induced processes have been reviewed and experimental paths have been obtained for different initial pressure-temperature combinations and, after an analytical discussion of the results, a compilation table of terms and paths is proposed. The processes already reported in the literature were reviewed and some other, new processes like pressure-shift thawing, were defined.

The first work suggesting a terminology for the reported processes was presented by Knorr, Schlüter and Heinz (1998) who presented different idealized freezing and thawing paths on the phase diagram of water. According to this report, “pressure-assisted” means that the phase transition occurs under constant pressure “pressure-shift” refers to a phase transition due to a pressure release and “pressure-induced” means a phase transition initiated by a pressure increase and continued at constant pressure. Some authors presented a compilation of processes and, therefore, of terms. Cheftel et al. (2002) reported the following situations related to the phase diagram of water:

- “ *«Freezing under pressure». A food sample may be pressurized, then frozen, leading to the formation of ice I, III, V or VI, depending on the pressure-temperature conditions*”. The description of this term is similar to the term “pressure-assisted freezing” (phase transition occurring at constant pressure).
- “ *«Subzero cooling without ice crystal formation». A food sample may be pressurized e.g. to 112, 207 or 300 MPa, then cooled down under pressure to about –10, -21 or –18 °C, respectively, without ice crystal formation*”. This process was named by Knorr et al. (1998) as "subzero storage without freezing". The term storage, instead of cooling seems to be more precise, as the aim of the process is to store food products under pressure and subzero temperatures for preserving goals. In a general case (independent of time, i.e., with or without storage) the process can be defined as SbC (Subzero cooling). Cooling, without the word freezing implies already clearly that the process has no ice crystal formation associated.
- “ *«Pressure-shift nucleation». Such a food sample cooled below 0 °C under pressure may be subjected to instant pressure release, thus inducing undercooling and uniform ice crystal nucleation throughout sample depth, whatever sample size*”. In this case, the nucleation of small sized uniformly distributed crystals of ice I is described, but it does not refer to a completed phase transition process, as specified by the next term. Moreover, the present paper suggests the use of “supercooling” (Pham, 1989) as a standard term instead of “undercooling” (Cheftel et al., 2002) or “overmelting” for the phenomenon of metastable liquid in solid domains.
- “ *«Pressure-shift nucleation followed by freezing at atmospheric pressure» [..] This process is called pressure-shift freezing (PSF) or freezing by fast pressure release.*” In fact, the pressure-shift nucleation should anyway be followed by ongoing processing. The term of pressure-shift freezing should therefore include the nucleation of ice I due to pressure release, but the nucleation should not be taken as a process itself.

- " «Freezing followed by pressurization, or pressure generation through freezing». A sample can be frozen at atmospheric pressure and then subjected to high pressure (thawing or changes in ice form may occur, depending on the temperature-pressure conditions)." This complex term seems to be unclear: it may make reference to a normal atmospheric freezing (one independent process) followed by a second process in which pressure is increased, with or without melting or ice form changes (i.e., solid-solid phase transitions), but it makes no reference to a new process. On the other hand, it can be understood as the process in which the volume change during freezing of ice I at atmospheric pressure generates a pressure increase during phase transition Hayashi et al. (1998). This process is not a process itself, but a pressure change during atmospheric freezing (AF is the process itself). Therefore, this definition may not be considered.

In the literature, some examples of processes can be found, in which different authors used different heterogeneous definitions and terms. For example, Martino, Otero, Sanz and Zaritzky (1998) reported the size and location of ice crystals in pork frozen by "high-pressure-assisted freezing" as compared to classical methods. In this paper, the reported process involved a pressure release and therefore an instantaneous crystallization occurs. Otero, Solas and Sanz (1998), from the same research group, used the same terminology for a similar process. In both cases, the term "pressure-shift freezing" should be used.

Teramoto and Fuchigami (2000) reported the changes in temperature, texture and structure of konnyaku (konjac glucomannan gel) during "high-pressure-freezing". In their work, changes in pressure and temperatures histories of konnyaku and pressure medium were presented during "high-pressure-freezing" and for "freezing-thawing under pressure". In fact, the terminology used by the authors is consistent, but seems to be not specific enough. Indeed, the processes represented by their experimental curves are freezing and thawing processes under pressure, but it is recommendable to specify the process: assisted, shift, induced, higher ice modifications, etc.

Recent studies on pressure phase transition processes focused mainly on the triple point of water/ice I/ice III at 209 MPa and -22 °C, where the lowest onset temperature for pressure-shift freezing and the highest temperature difference (sample - pressure transmitting medium) by decreasing the melting point of a food sample due to pressurization is expected (Schlüter *et al.*, 2003). Generally, an analogous slope of the melting curve of food compared to that of pure water was assumed (Denys *et al*., 2002 and Sanz and Otero, 2000). Recently the melting curves for potato tissue at pressures up to 450 MPa were described by using existent equations for pure water but modifying relevant parameters. Calculated and experimental melting curves (ice I, ice III, ice V) for potato showed an analogous slope compared to pure water (Schlüter and Knorr., 2002).

To ensure comparability between experiments the effective temperature gradient between sample and cooling medium was set on a certain value for conventional freezing as well as for pressure supported freezing processes. Then, reductions in phase transition time along the melting curve of ice I can be attributed to a decrease in the latent heat values of water with pressure (Fuchigami *et al.*, 1997b, Denys *et al.*, 1997).

Liquid-solid phase transitions for potato cylinders, working along the melting curve of ice I were studied. After the results from Evans (1967a), in which a prolongation of the ice I phase transition curve in the thermodynamically stable domain of ice III was reported, for pressures higher than 209 MPa, ice I is assumed to be obtained. When the pressure-assisted freezing process through prolonged ice I phase transition line is carried out at pressures above 209 MPa (pressure of the triple point liquid/ice I/ice III), further reduction on latent heat of fusion might lead to a shorter phase transition time (shorter time in the plateau of the typical temperature-time freezing curve).

A second type of process were studied, in which the food sample was stepwise subjected to higher pressure levels where ice III formation is expected following a significant degree of supercooling (Evans, 1967b). A higher supercooling phenomenon leads to a reduction of phase transition time, because the temperature gradient (between sample centre and sample wall) is higher, and thus, the amount of ice instantaneously crystallized is higher (Otero and Sanz, 2000). Here, the higher ice modification supposes lower volume changes, and then, lower structural damages to the sample (Luscher *et al*., 2003). A comparison between the pressure-assisted freezing process to higher ice modifications (ice III) and pressure-shift freezing had been also addressed. In this sense, pressure-shift freezing has an adjustable supercooling phenomenon, leading to high nucleation velocities (Otero and Sanz, 2000).

4.1.1.1. Pressure-assisted freezing to ice I.

Freezing at atmospheric pressure (0.1 MPa). This first experiment (Figure 4.1) was thought to be a guide to know the change in phase transition curves between water and potato cylinders, to better predict the plateau temperatures, then to better set up the next experiments, in which one of the critical operating factors is the temperature difference between the plateau and the cooling medium.

This first experiment gave us the difference between melting temperatures of water and potato. The experimental value of the melting point of potato cylinders was found to be –1°C. This –1°C of difference between the phase change curves of water and potato was taken as the starting value of the expected freezing point in the next experiments. Then, the temperature of the freezing medium was always set to a temperature 25°C lower than the expected phase change one.

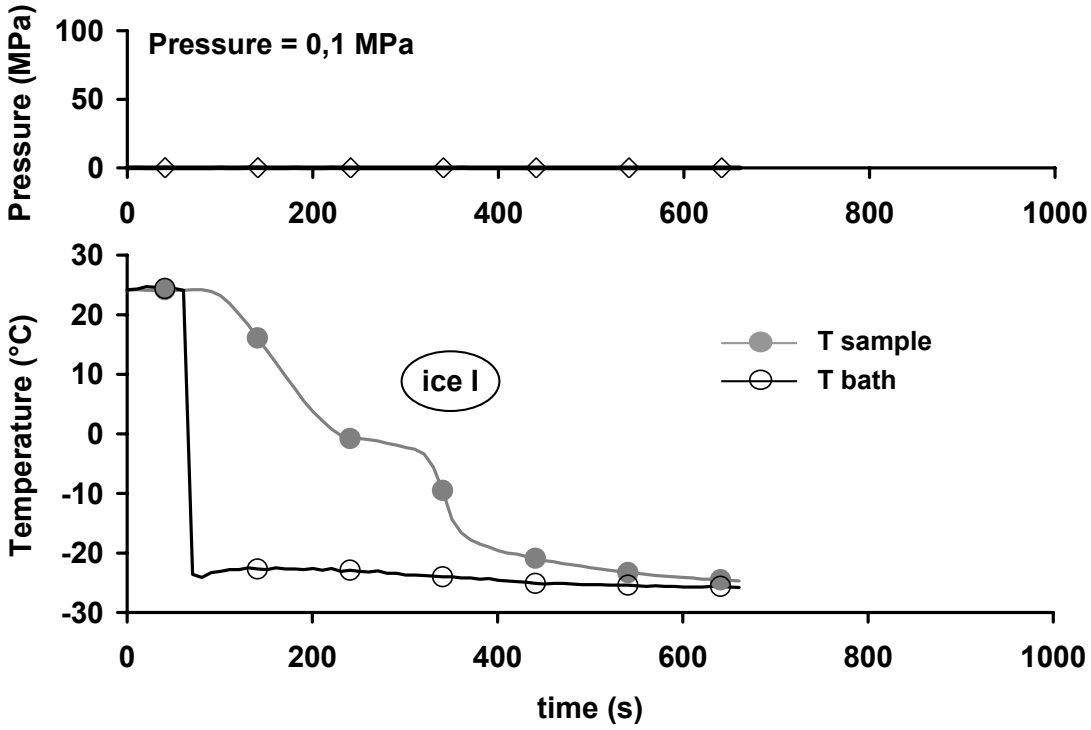

Figure 4.1. Freezing at atmospheric pressure (ice I).

Pressure-assisted freezing at 140 MPa. In order to better compare the effect of the supercooling phenomenon, and the nucleation of a higher ice modification, a conventional pressure-assisted freezing experiment was planned. Here, ice I is obtained (as expected from the phase diagram) after a weak degree of supercooling. In

Figure 4.2, this freezing curve to ice modification I and the mathematical model application are shown.

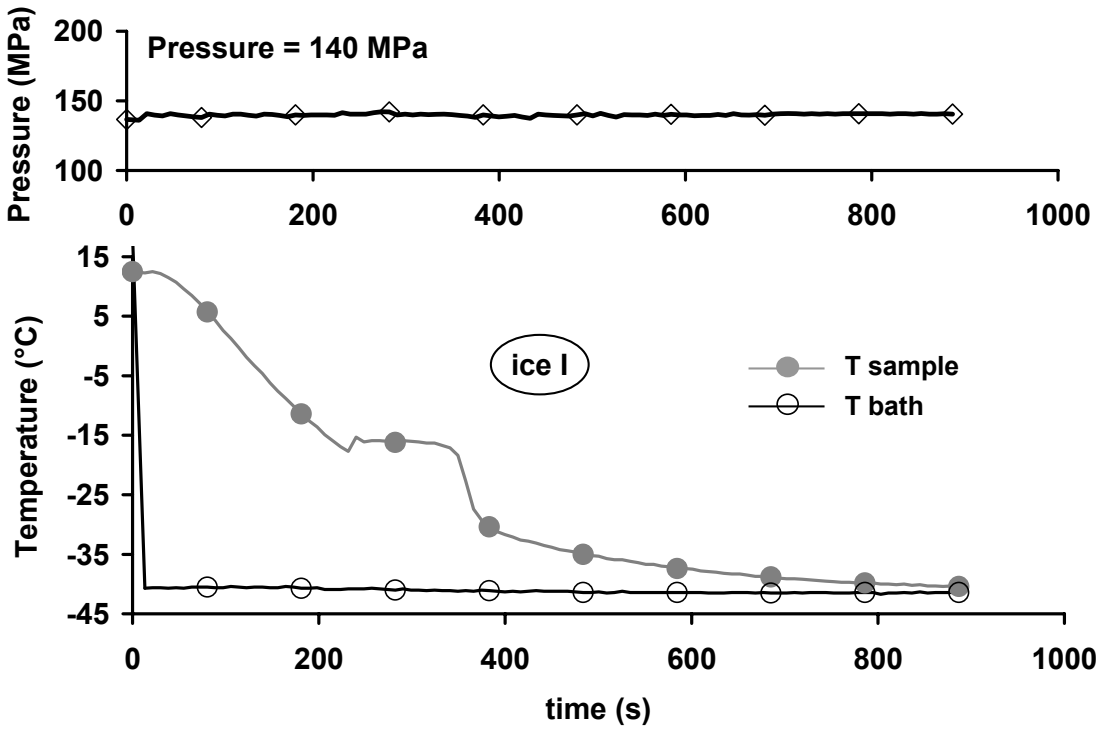

Figure 4.2. Pressure-assisted freezing curve to ice I at 140 MPa.

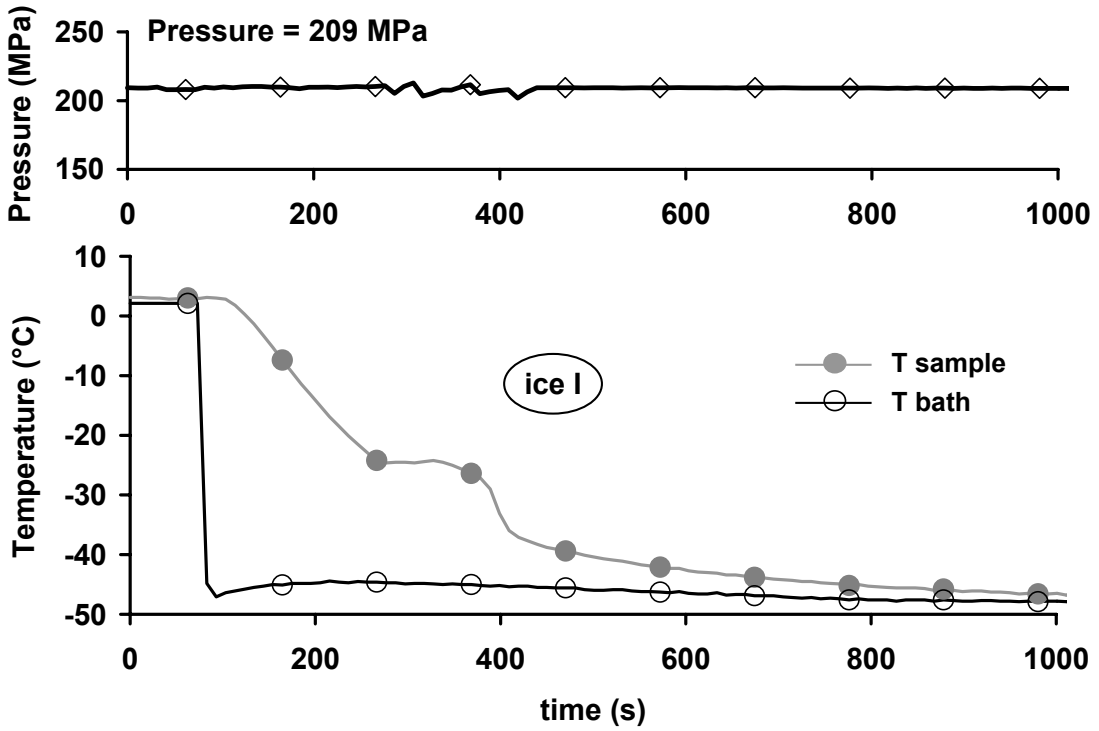

Figure 4.3. Pressure-assisted freezing curve to ice I at 209 MPa.

Pressure-assisted freezing at 209 MPa. After the water phase diagram, the triple point liquid/ice I/ice III is expected to appear at this pressure level. It is assumed that an experiment carried out at 209 MPa leads to formation of the ice modification I as well as the ice modification III. The obtained results, in Figure 4.3, show a freezing

temperature of around –25°C, that is 2°C lower than the expected for potatoes (taking into account the corresponding for water and lowering 1°C). In this case, the higher volume of the sample after freezing, clearly shows that ice I was obtained.

In this near region of the triple point liquid/ice I/ice III, a weak supercooling peak is obtained, and, after short running through the metastable liquid phase, ice I is formed. In this process, as the enthalpy of fusion is lower, the processing time is expected to be also lower, with respect to the same freezing process run into the stable liquid/ice I transition zone (140 MPa). As the highest damages are caused during the phase transition, the lower this transition time, the better the product quality. However, volume changes must also be taken into account, these are higher near the triple point (~13 %) compared to lower pressure levels.

4.1.1.2. Pressure-assisted freezing to ice III.

Pressure-assisted freezing at 255 MPa. At this pressure level, the ice modification III is already clearly reached. In Figure 4.4, this can be observed, as the ice III is clearly obtained, after the supercooling phenomenon, with a clear horizontal temperature plateau. The freezing temperature experimentally recorded was –21.0°C for 255 MPa, that is 1.3°C lower than the corresponding one for pure water, after regression of Wagner data (Wagner *et al*., 1994). So, this temperature is still in the range of difference between potato and water predicted by the atmospheric experiments. A degree of supercooling of 11,3°C is obtained here.

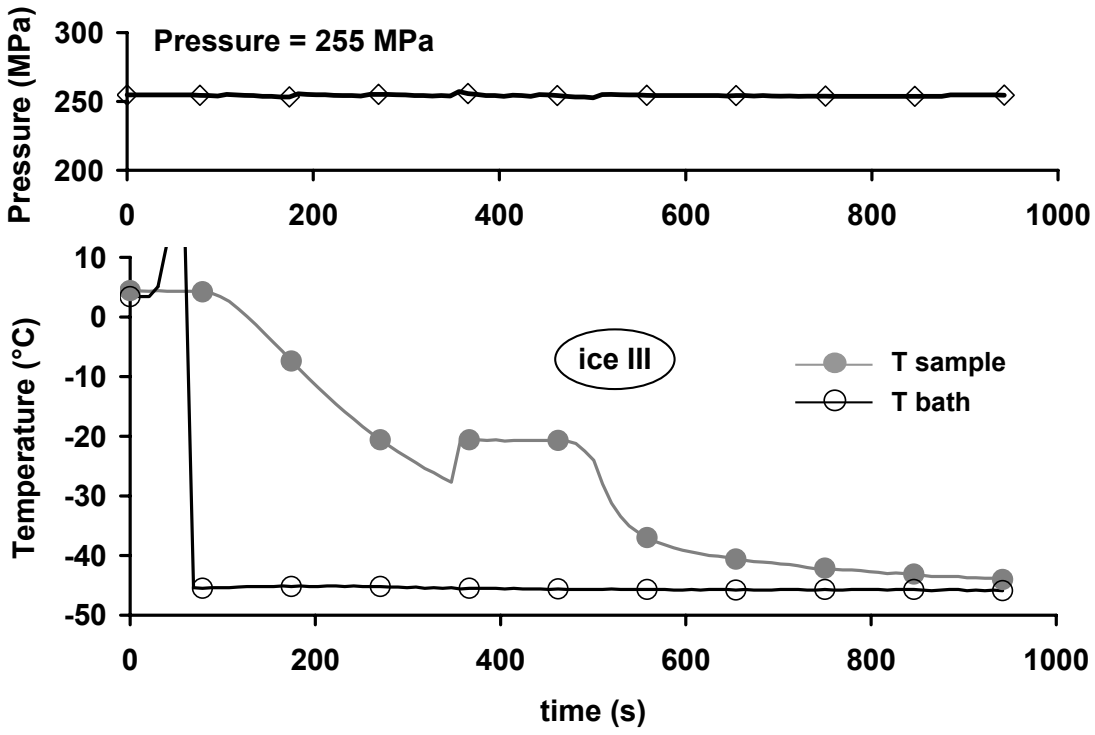

Figure 4.4. Pressure-assisted freezing curve to ice III at 255 MPa.

Pressure-assisted freezing at 270 MPa. With an earlier plateau, and a higher degree of supercooling, again ice III is clearly obtained here (Figure 4.5), with a freezing temperature experimentally recorded of –20.5°C, that is again 1.3°C lower than the corresponding one for pure water (after phase diagram interpolation, see above). The degree of supercooling in this case is around 15.0°C.

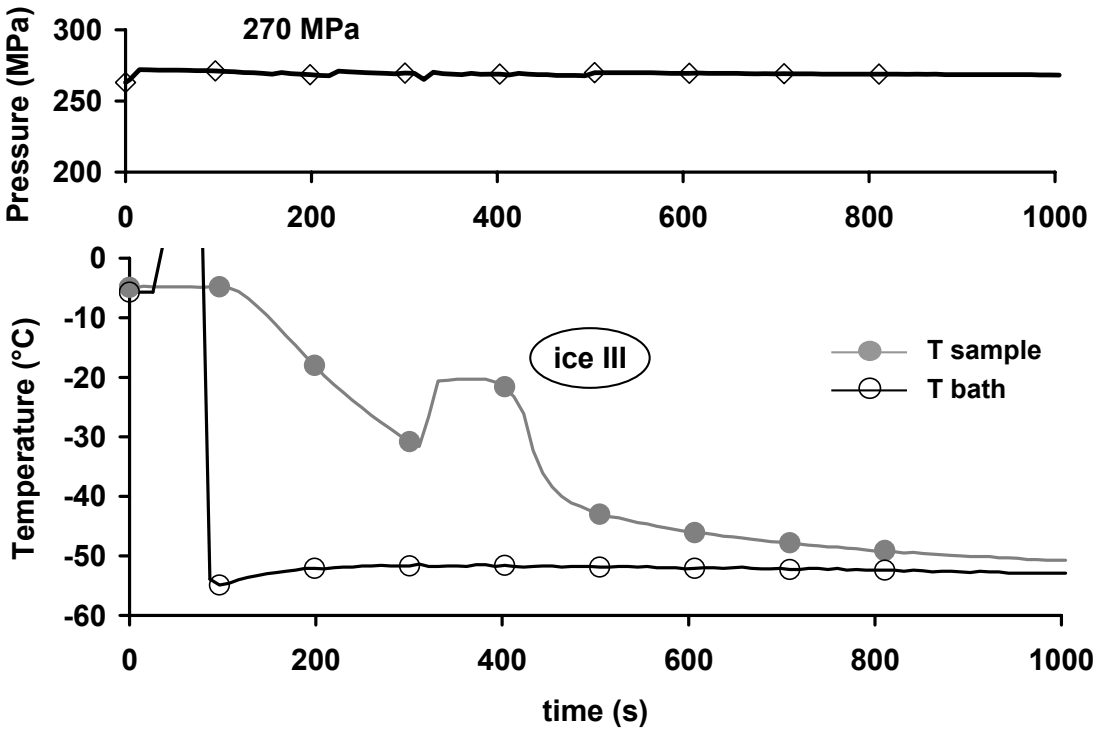

Figure 4.5. Pressure-assisted freezing curve to ice III at 270 MPa.

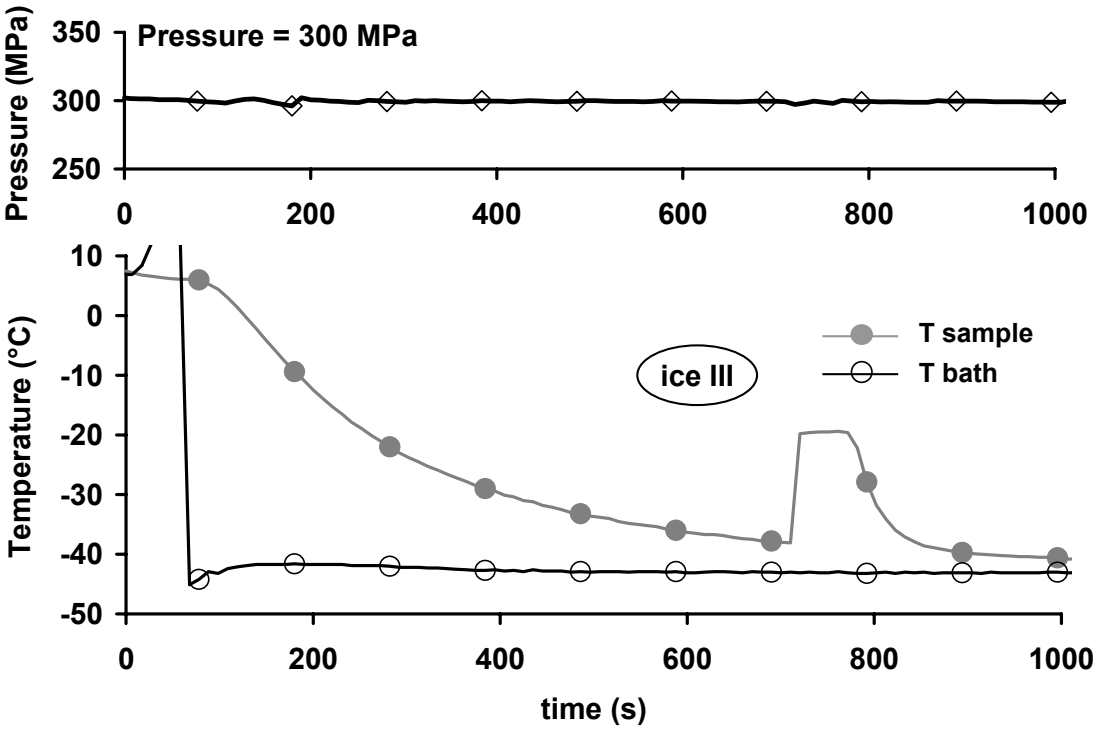

Figure 4.6. Pressure-assisted freezing curve to ice III at 300 MPa.

Pressure-assisted freezing at 300 MPa. In this case, the freezing temperature given by the clear plateau obtained after the nucleation of ice modification III is –20.0 °C, that is 1.8°C lower than the corresponding one for pure water. A degree of supercooling of around 18.5°C, significantly higher than the one obtained at 255 MPa, can be seen in Figure 4.6. It is here remarkable that, between the freezing curves at 255 and 300 MPa, the higher the pressure, the higher the degree of supercooling, and therefore, the

shorter the plateau time. But also, when a higher degree of supercooling occurs, there is a longer tempering or precooling time before nucleation starts. But at 300 MPa, the enthalpy of fusion is higher than the one at 255 MPa (both corresponding to ice III), and then, the phase transition time must be higher. All these effects together lead to a shorter plateau time at higher pressures.

4.1.1.3. Pressure-assisted freezing in metastable phase.

Pressure-assisted freezing at 225 MPa. At this pressure level, the ice modification III is expected to be obtained, as stated by the phase diagram, but according to Evans (1967b), ice I is obtained through the prolonged melting curve ice I. What we actually obtained was a set of experiments in which the instability of this region led to different results. Therefore, in Figure 4.7, Figure 4.8 and Figure 4.9, three different experimental freezing curves are shown in which ice I, ice III or a mixture of both ice modifications are obtained.

The behaviour when ice I is obtained (Figure 4.7) can be explained as follows: in the area where theoretically ice III is to be reached, at this pressure level, a metastable zone of liquid is still obtained, in agreement with the published data from Schlüter and Knorr (2002). Therefore it is assumed that a prolongation of the ice I phase transition curve gives the new freezing points for this area. This assumption can be proved by comparing the experimental freezing point when ice I is still obtained to the one calculated from an extrapolation of the ice I phase transition curve. This comparison gave differences no greater than 2°C and the different experimental results confirm this prolongation of ice I phase transition curve. The corresponding experimental freezing temperatures are, –27.5°C for ice I and –23°C for ice III (the expected being –25.2°C and –22.1°C, respectively).

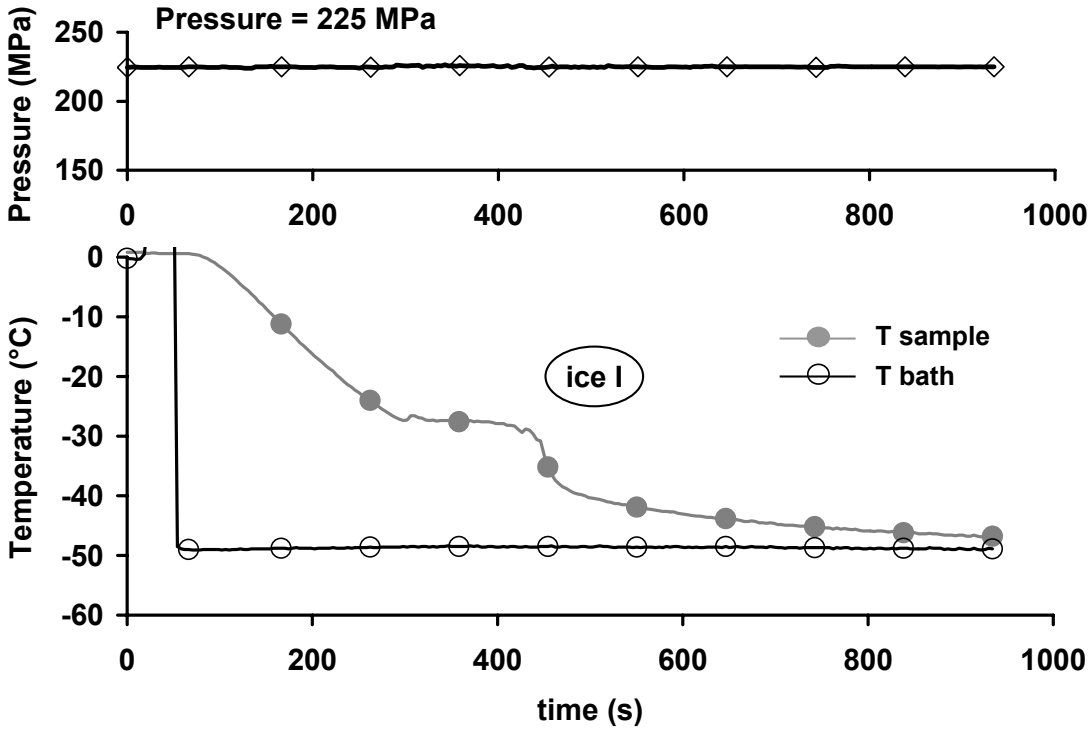

Figure 4.7. Pressure-assisted freezing curve to ice I at 225 MPa.

Additionally, in Figure 4.9 a double plateau is observed. In this case, an explanation becomes more difficult. Nevertheless, a possible reason for this behaviour is that first, as freezing runs, the nucleation temperature corresponding to ice I is reached, and then, this aggregation state is crystallized. But, at the same time, just after ice I nucleation starts, the wall temperature in the sample reaches the nucleation line of ice

III. The whole sample then starts an ice III nucleation, and the second jump to the corresponding ice III plateau is observed.

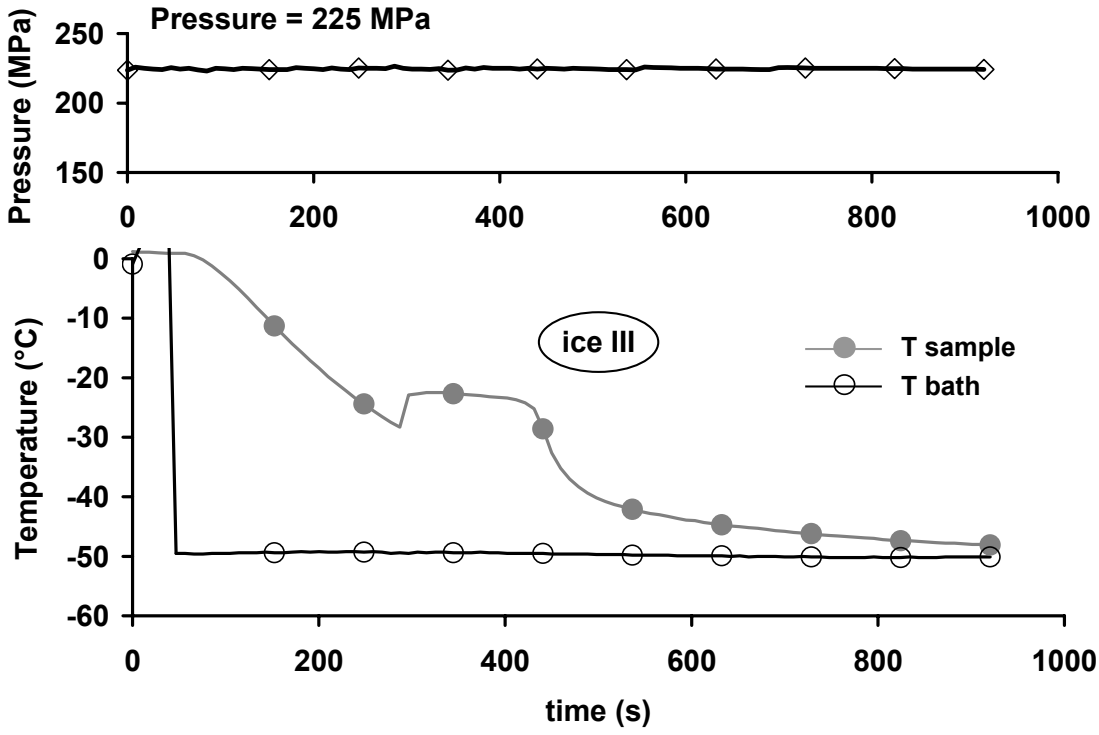

Figure 4.8. Pressure-assisted freezing curve to ice III at 225 MPa.

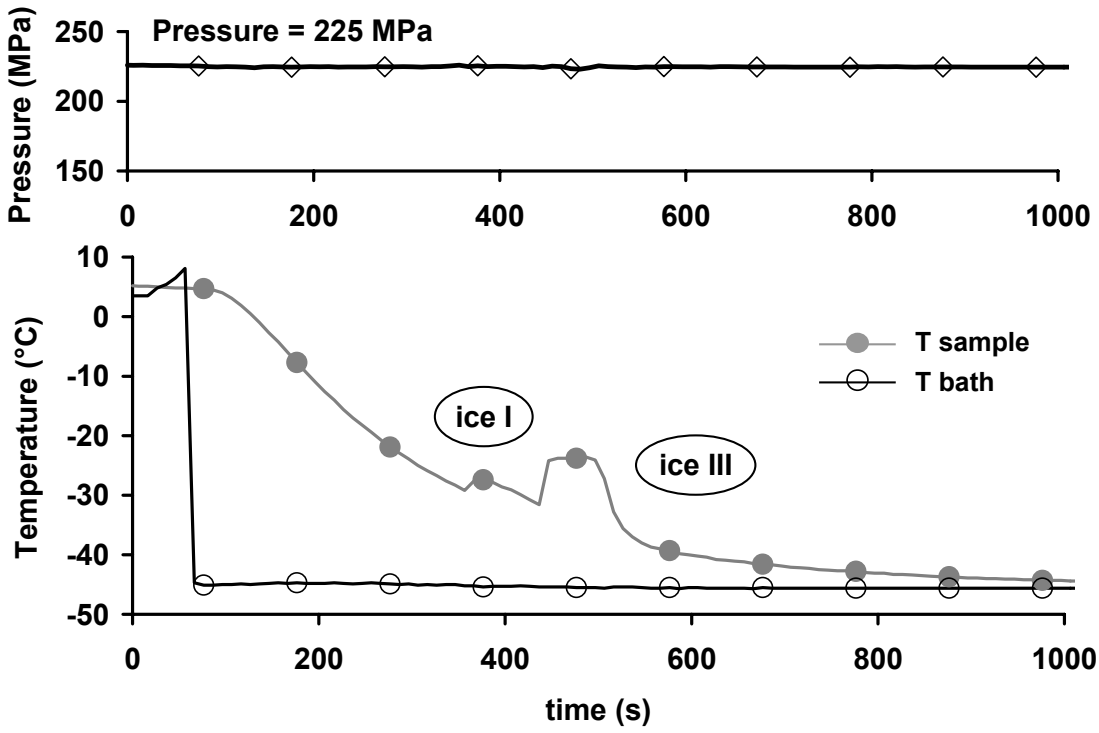

Figure 4.9. Pressure-assisted freezing curve to ice I and to ice III in a double plateau at 225 MPa.

Pressure-assisted freezing at 240 MPa. In the case of 240 MPa, similar results to those shown in Figure 4.9 are obtained (Figure 4.10). A first freezing point, given by a (not specially marked) plateau, is obtained for a temperature assumable for ice

modification I, and after a further supercooling, ice III "plateau" is observed. This double freezing plateau clearly states the evidence of a metastable phase in this region. This metastable phase gives no clear freezing patterns, but unstable freezing curves in which both ice modifications I and III are susceptible to be obtained. No further predictions can be made about which ice modification will first nucleate, when freezing occurs in the metastable area. However, in all experimental cases (especially formation of ice III) nucleation occurs not before cooling below the extended melting curves of ice I or ice III, respectively.

Specially significant is the unstable freezing curve obtained here, as no clear plateau is observed, for ice I, or for ice modification III, and no clear freezing points can be taken from the experimental data, neither from ice I freezing point, nor from ice III. In this experiment for 240 MPa, the expected freezing temperatures are –27.3°C and –21.4°C for ice I and ice III, respectively. The experimental freezing temperatures are slightly cooler than those expected from inter and extrapolation of the potato-adapted phase transition curves: –29.5°C and –23°C for ice III and ice I, respectively.

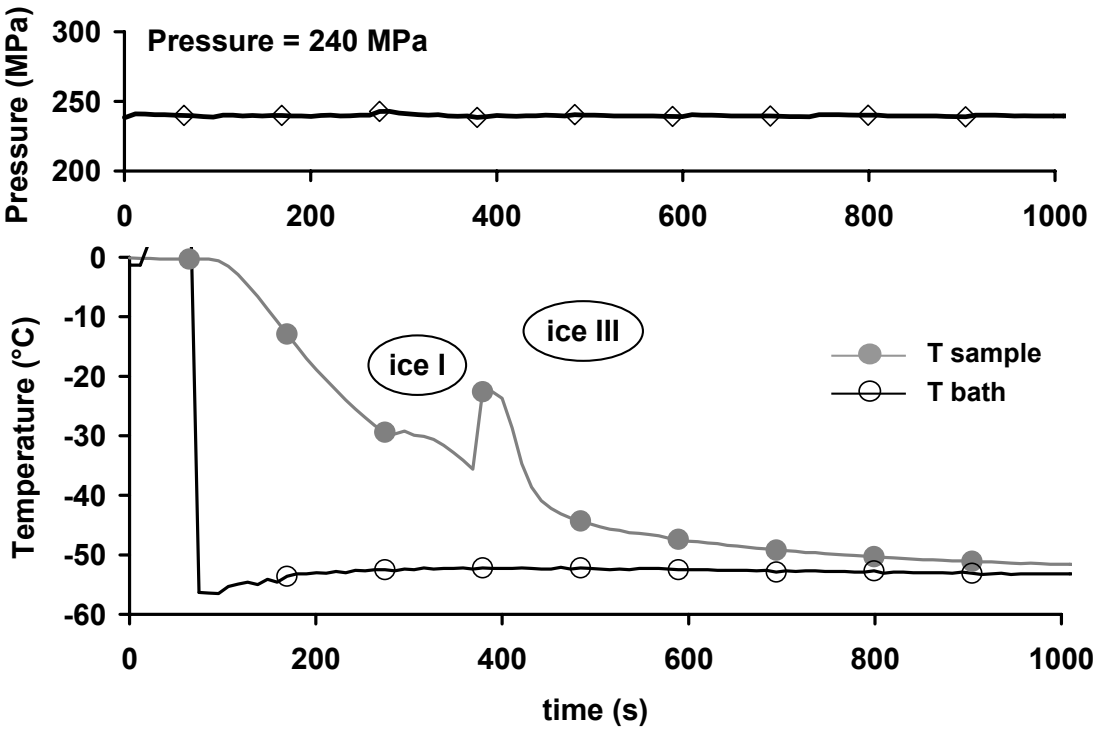

Figure 4.10. Pressure-assisted freezing curve to ice I and to ice III in a double plateau at 240 MPa.

4.1.1.4. Pressure-shift freezing.

An additional experiment was carried out in order to compare a pressure-assisted freezing experiment with the other extended high-pressure operation to frozen food products: pressure-shift freezing. This experiment will provide us with a tool to discuss the effect of the pressure change or the pressure range in which each process is carried out, with respect to the phase transition time, i.e. the freezing plateau time in the freezing curve. The application of this process for potato cylinders is shown in Figure 4.11. In this case, ice I is also obtained, and the pressure release leads to a kind of "supercooling", but now due to pressure-shift and not due to further temperature decrease.

When comparing this experiment with the corresponding at atmospheric pressure, we can clearly state that the freezing time is by pressure-shift higher than by atmospheric

pressure, but the phase transition time is much shorter here, due to this “supercooling” effect (provoked by the pressure release).

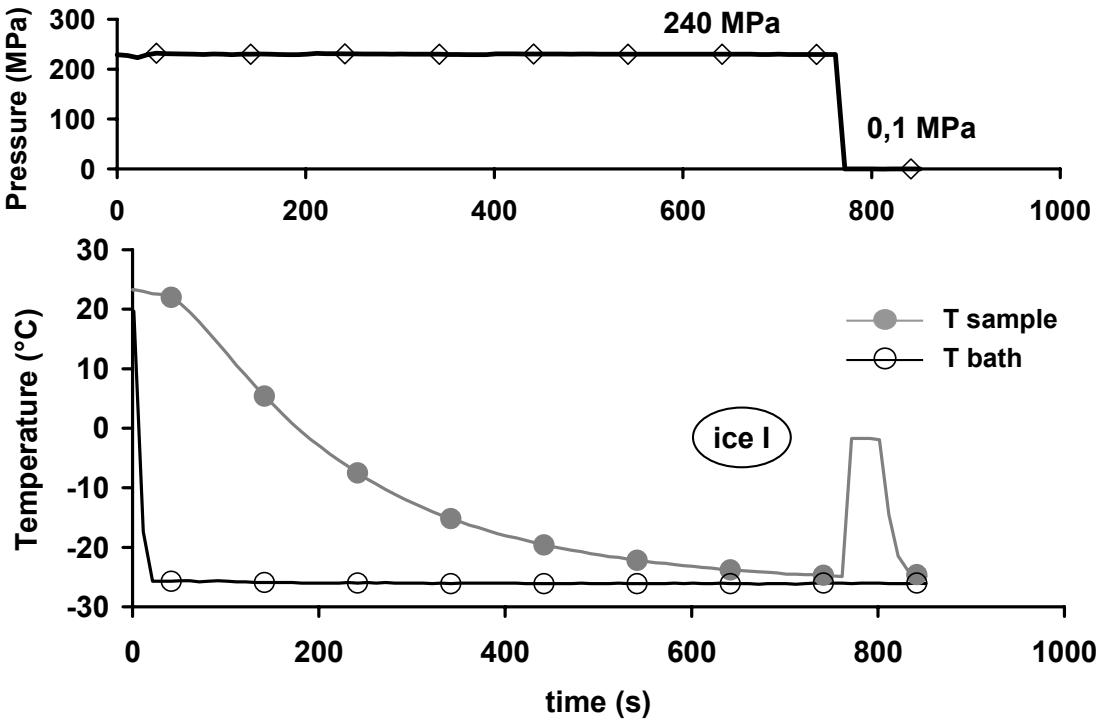

Figure 4.11. Pressure-shift freezing (to ice I) from 240 MPa and -25°C.

When freezing to ice III, a high degree of supercooling is obtained, and, therefore, a higher temperature gradient is reached. This temperature gradient is the one reached between the temperature of sample wall just before nucleation starts and the temperature of the sample centre during phase transition (removal of latent heat). Then, a shorter phase transition time is expected for these experiments.

In the experiments at 225 and 240 MPa, the metastable ice I solid phase is obtained, in a region where ice III is thermodynamically stable and there are two experiments (Figure 4.9 and Figure 4.10) in which a “double plateau” is obtained. That means, during the freezing process, ice I (or a mixture of both ice I and ice III) is first obtained, and then, when the nucleation line of ice III is reached, the freezing curve jumps to the freezing temperature corresponding to ice III. A physical explanation can be given by possible simultaneous existence of different ice modifications according to Hasselton *et al*. (1995) or a liquid – solid (ice I) mixture is first obtained, and this residual liquid in mixture nucleates further to ice III, as the temperature decreases. As the core temperature after the second jump to ice III is higher than the corresponding freezing temperature for ice I, it can be assumed that all the ice I first nucleated undergoes again to liquid and then further nucleation to ice III occurs. A solid (ice I) – solid (ice III) transformation is not indicated by the obtained results since it must be accompanied by a temperature decrease in the thermal history due to the endothermic process.

A fact that should be mentioned is the existence of the supercooling phenomenon when ice III is obtained and the non-existence or the weakness of this supercooling when ice I is obtained. Evans (1967a) described this weakness of supercooling when ice I crystallizes at higher pressure levels. The results he reported showed that nucleation is enhanced by pressure, and the supercooling initially necessary to nucleate ice I falls from –6.5 °C (at pressures below 100 MPa) to virtually zero between 150 and 250 MPa.

4.1.2. Thawing processes

The latest defined process taken from Cheftel et al. (2000) is related to thawing:

- " *«Thawing under pressure». A frozen food sample can be thawed at a subzero temperature at an appropriate pressure level, since the phase transition temperature of ice I is lowered under pressure*". This term refers, actually, to the pressure-assisted thawing processes, in which thawing occurs at constant pressure, and can be performed for different ice modifications, depending on the initial pressure level. The term is only applicable for ice I, but extended definitions for other higher ice modifications have to be taken into account.

Additionally, Zhao, Flores and Olson (1998), in their report of "high hydrostatic pressure effects on rapid thawing of frozen beef", reported a "high hydrostatic pressure thawing process" in which, apart from the terminology used, the thawing process they presented describes a path not found by other authors (e.g., Denys, 2000). In their work, the pressurization was not accompanied by a slight temperature increase due to the work of compression, but by a temperature decrease. The phase transition between ice I and liquid took place without the often reported extension of the phase transition line, and, after a pressure release, the sample temperature increased up to the melting point at atmospheric pressure. Regarding the temperature history it seems that the authors did not thaw the sample, but just started the thawing at the sample surface and did not complete it – therefore, the -still frozen- sample followed the phase transition line after releasing pressure. This might be the reason for observing the stable red colour of the beef, as reported after recrystallization. The divergences between this path and many others presented in the literature (Evans, 1967; Kanda, Kitagawa and Fujinuma, 1993; Knorr et al., 1998) should be taken into account for a proper thawing terminology.

Thawing of foods under high pressure is a new area of research interests, thanks to the depression of the phase transition temperature of water under pressure (Mussa and Le Bail, 2000). The application of high pressure reduces the freezing and melting points of water to a minimum of –22°C at 209 MPa, as pressure opposes the volume increase occurring during the formation of type I ice crystals. That means that the driving force for a thawing process is increased until a maximum, reached at 209 MPa, where the melting curve liquid/ice I goes to the triple point liquid/ice I/ice III. This advantage assumable by the higher driving force must be balanced with quality considerations. Ice I uniquely has a lower density than liquid water, resulting in a volume increase of ~9% on freezing at 0°C, increasing to ~13% at –20°C, which may cause significant tissue and textural damage (Kalichevsky et al., 1995).

As a consequence of the depression in the melting point of water under pressure, the heat flux rate during thawing is enhanced due to the bigger increment between the pressurising fluid temperature and the phase change front in the sample (Chourot et al., 1996). Processing under pressure has been also reported to reduce the latent heat values with increasing pressure up to 210 MPa (in the range of ice I) (Bridgman, 1912, Hobbs, 1974, Schlüter et al., 2003b). These two effects together, produce a reduction in thawing times when compared to those corresponding to atmospheric pressure thawing processes developed at identical temperatures (Takai et al., 1991; Chevalier, et al., 1999). Moreover, some reports show that it may also reduce the drip volume and minimise microbial growth. Nevertheless, very few reports are available regarding the behaviour of microorganisms during high pressure thawing (Yoshioka et al., 1999). Additionally, as the processes are developed at sub-zero temperatures, the microbiological control of products is safer, solving the problem of long time classical thawing processes at moderate and high temperatures, causing undesired microbial growth (Chevalier et al., 1999).

The potential applications of high pressure effects on ice-water transitions during thawing of food products have been already reviewed by Kalichevsky et al. (1995) and Cheftel et al. (2000), among others. Research on high pressure-assisted thawing of frozen fish and meat has shown the possibilities of significantly reducing the thawing time (e.g., Deuchi and Hayashi, 1991; Murakami et al., 1992; Zhao et al., 1998; Massaux et al., 1999a) as well as minimising the drip volume after thawing (Murakami et al., 1992) and subsequent cooking (Massaux et al., 1999b; Chevalier et al., 1999; Okamoto and Suzuki, 2001; Rouillé et al., 2002).

However, very few papers have been published up to now regarding pressure-supported thawing processes above 210 MPa, where higher ice polymorphs might be involved in the process (Zhao et al, 1998, Knorr et al., 1998, Fuchigami et al., 1998), but published data seem to be dubious, as explained later in this paper. Anyway, in the reviewed texts, no discussion has still been addressed about the roll of ice III during the pressure-supported thawing processes. Available published experimental data support the assumption of a thawing process through the extended melting curve liquid/ice I, with increased effective temperature gradient, taking advantage of the metastable state of ice I in the stable area of ice III, as reported in a previous paper (Schlüter et al., 2004).

Knorr et al. (1998) described three types of high-pressure thawing processes (Figure 4.12a): pressure-assisted thawing (ABGH), pressure-induced thawing (ABEFGH) and thawing from ice III (CDEFGH). Theoretically, in the pressure-assisted thawing from ice I, the phase transition occurs under constant pressure by increasing the temperature. In the pressure-induced thawing, the phase transition is initiated by a pressure change and continued at constant pressure. Finally, thawing from ice III is a case of pressure-assisted thawing, but coming from a frozen sample in which the ice modification is ice III.

Together with these proposed “ideal” paths (Figure 4.12b), reported experimental paths obtained from the existing literature (Zhao et al. (1998), Knorr et al. (1998) and Denys (2000)) are shown in Figure 4.12b, corresponding to pressure-assisted and pressure-induced thawing processes.

For the pressure-assisted curve presented by Denys (2000), during pressure build up, sample (agar gel) temperature is supposed to be increased due to the work of compression. Thawing then takes place under (ideally) constant pressure, controlled by thermal gradients between the sample and the pressurising fluid or the thermal medium. But phase transition took place not exactly at constant pressure, but with a slightly decrease, due to the volume decrease associated with ice I/liquid transition (note that density of ice I is lower than the liquid one) (Denys et al., 2000). This result contradicts the curve presented by Zhao et al. (1998) where the sample (beef meat) temperature decreases during pressurisation and, after a (supposed) phase transition ice I/liquid, pressure is released and then, the (supposed) already thawed sample temperature increases nearly parallel to the phase transition line.

In the case of the pressure-induced thawing curve by Denys (2000), the sample temperature decreased with increasing pressure nearly following the phase transition line ice I/liquid, and in divergence from the theoretical curve shown (path ABE in Figure 4.12a), the curve does not cross the phase transition line; however, a drop in sample temperature is observed during pressurisation, indicating that the work of compression is transferred into melting energy along the phase transition line. Therefore, during the temperature decrease, a part from the ice I has already thawed to liquid water. Further discussion about this process will be addressed in the text. Then thawing from ice I is completed after the already mentioned slight pressure decrease at 200MPa.

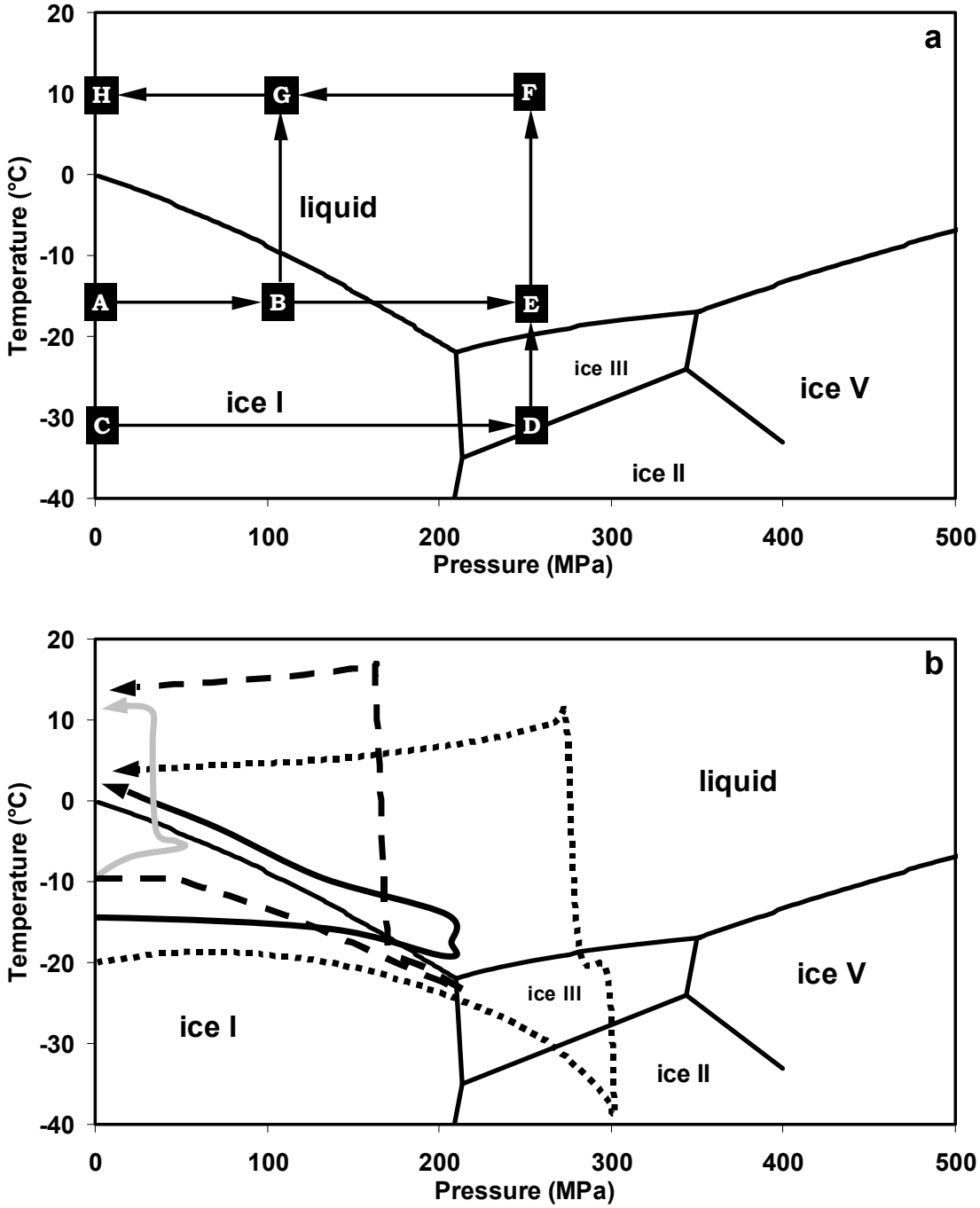

Figure 4.12. (a) Theoretical pressure-supported thawing paths: pressure-assisted thawing (ABGH), pressure-assisted thawing from ice III (CDEFGH) and pressure-induced thawing (ABEFGH); (b) Experimental paths, re-printed after Zhao et al. (1998) (——), Knorr et al. (1998) (▪ ▪ ▪) and Denys (2000) for pressure-assisted (——) and for pressure-induced (— —) thawing.

The curve described by Knorr et al. (1998) again describes the divergence from the ideal pressure-induced thawing process (ABEFGH in Figure 4.12a). Using the Clausius-Clapeyron equation (4.1), the negative slope of the liquid/ice I equilibrium line implies that the signs of volume change ΔV and the latent heat, ΔH, in equation 4.1 are different. In the case of solid-liquid phase transition, ΔH is always positive, whatever the modification of the solid state. Hence, the differences in the slope of the ice I/liquid and ice III/liquid transition lines are due to negative or positive volume change, respectively (Knorr et al., 1998). Moreover, the decrease in pressure clearly indicates a

volume contraction of the sample during melting, which is observable exclusively in ice I. Then, although the ice III is thermodynamically stable when the thawing line crosses the transition one, explained evidences state that, in practice, ice I melts into the liquid phase in the schematic path shown in Figure 4.12b, although at 300MPa ice III is the stable

$$\frac{\partial T}{\partial P} = \frac{\Delta V}{\Delta H} T \tag{4.1}$$

These results suggest that a prolongation of the melting curve of ice I is extended in the domain of ice III. This extended phase transition line was already reported by Schlüter et al. (2003).

Therefore, pressure-assisted thawing should be defined as each pressure-supported thawing process in which no melting of ice takes place during pressurization and, more generally, when phase transition is provoked by a temperature gradient at constant pressure. On the other hand, pressure-induced thawing, should be defined as every process in which a melting of ice is “induced” during the pressurization, leading to a temperature decrease (as a consequence of the negative slope of ice I phase transition line) and followed by further thawing at constant pressure. The real p-T evolution of samples and the physical phenomena occurring during these processes will be discussed in the text.

This chapter claims to clarify a commonly confused nomenclature for the different possible pressure-supported thawing paths and to describe the process steps of pressure-supported thawing processes up to 310 MPa, varying pressure levels, temperature gradient, and also the initial temperature of the samples, leading to different thawing processes. The discussion is based on a dynamic (continuously measured system) study of the processes and the strategies to reach improved thawing process design are discussed.

This section presents also the results of various experimental thawing processes carried out for pressures up to 500 MPa, and for different temperatures and previous freezing characteristics. The aim of the work is to explain the physical phenomena occurring when thawing from ice III or from ice V, to define the new related thawing paths and to suggest a guide to the influence of processing parameters to obtain controlled thawing paths, i.e., to be able to predict which kind of behaviour can be expected from a sample exposed to a pressure-supported thawing process.

The experimental set was organized as follows:

Pressure-supported thawing in the domain of ice I and ice III. A new parameter P_C is defined as a pressure (characteristic for each product) at which the prolongation of ice I phase transition curve and the upper level of the area of nucleation of ice III are crossing. After the reported results of Knorr *et al*. (1998a) and Denys (2000), the phase transition line ice I/liquid is expected not to be crossed during pressurisation and, therefore, the sample temperature decreases, because its latent heat is being used to melt part of the ice into water. Depending on several factors, different thawing paths are likely to be obtained. For pressures below the defined P_C, depending on the initial temperature three different processes can be obtained, as shown in Figure 4.13: pressure-assisted thawing (continuous line), a mixture of assisted and induced thawing of metastable ice I without nucleation of ice III (discontinuous line) or thawing from ice III after solid-solid transition (dotted line). The influence of the combination of initial temperature and pressure should be discussed after the obtained results. On the other hand, when the critical pressure P_C is overcome, the sample temperature follows this extended line, reaching the area of nucleation of ice III. Figure 4.14 schematically shows the described process. It is expected that the sample, after melting some ice I (temperature depression along the phase transition line) reaches a temperature equivalent to the nucleation one of ice III. Then, the part of ice I already melted at

sample surface, should crystallise into ice III and therefore, a temperature jump (equivalent to the jump observed after supercooling in pressure-assisted freezing to ice III) is expected. Depending on the initial temperature, two options are again expected: thawing from ice I or from ice III after a solid-solid phase transition. In the latter case, the pressure level reached is not changing the result of the process.

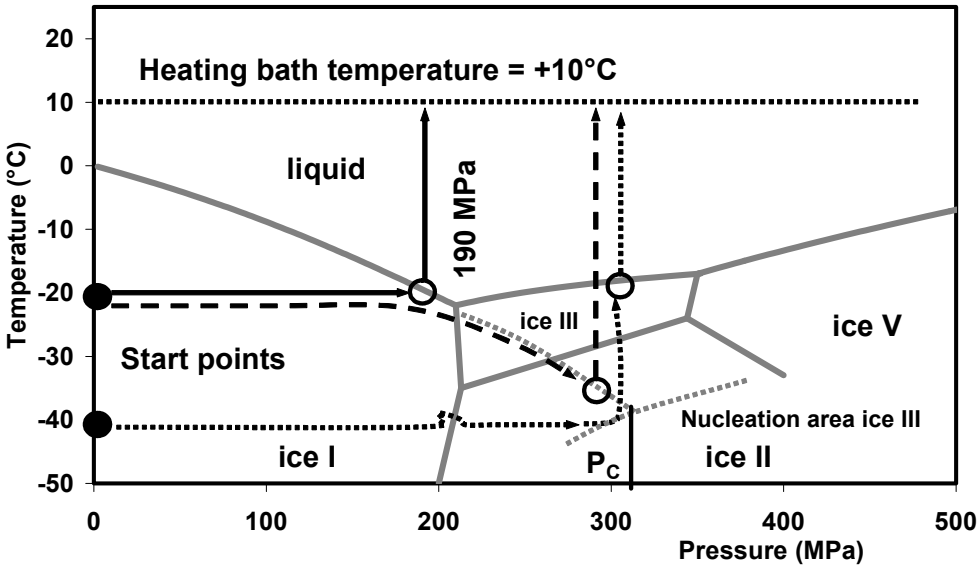

Figure 4.13. Schematic paths for pressure-supported thawing processes in the domain of ice I and ice III, below the critical pressure level: pressure-assisted thawing at constant pressure from ice I (full line), pressure-induced thawing of ice I with partial melting during pressurization (discontinuous line) and pressure-assisted thawing of ice III after solid-solid phase transition ice I to ice III (dotted line).

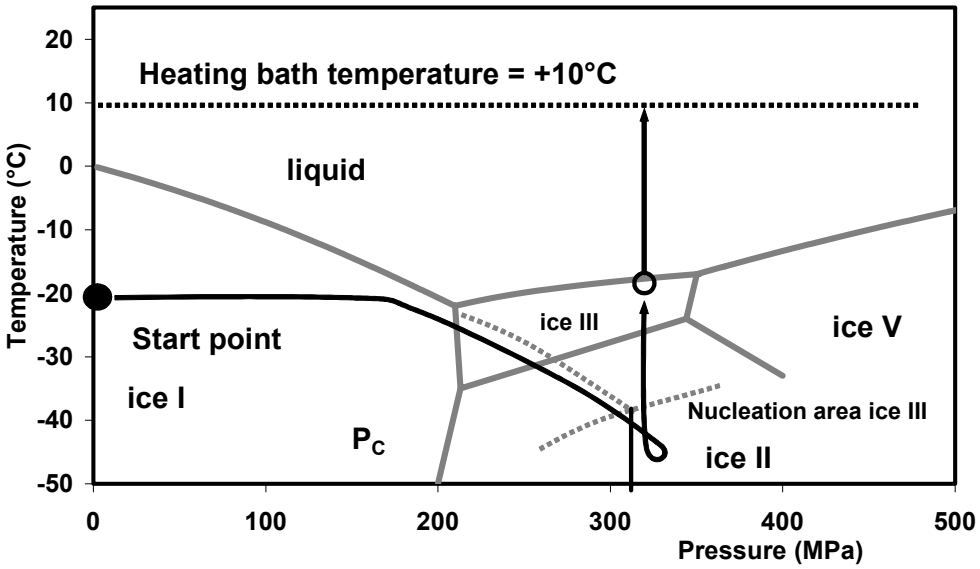

Figure 4.14. Schematic path for a pressure-supported thawing process in the domain of ice I and ice III, reaching the critical pressure level. The partially melted water re-crystallizes into ice III and then pressure-assisted thawing of ice III is completed.

Pressure-supported thawing in the domain of ice V. In this case, the pressure is increased until values corresponding to the domain of ice modification V. In Figure 4.15, the expected thawing path is shown. During pressurisation, the nucleation to ice III of the melted ice I during pressurisation is expected to occur; then, the path follows the phase transition curve between ice III and liquid, until the nucleation line of ice V, or the selected pressure is reached. A pressure level of 500 MPa will be tested. It is expected that nucleation of ice V does not take place, but further comments should be made after analysis of the experimental results.

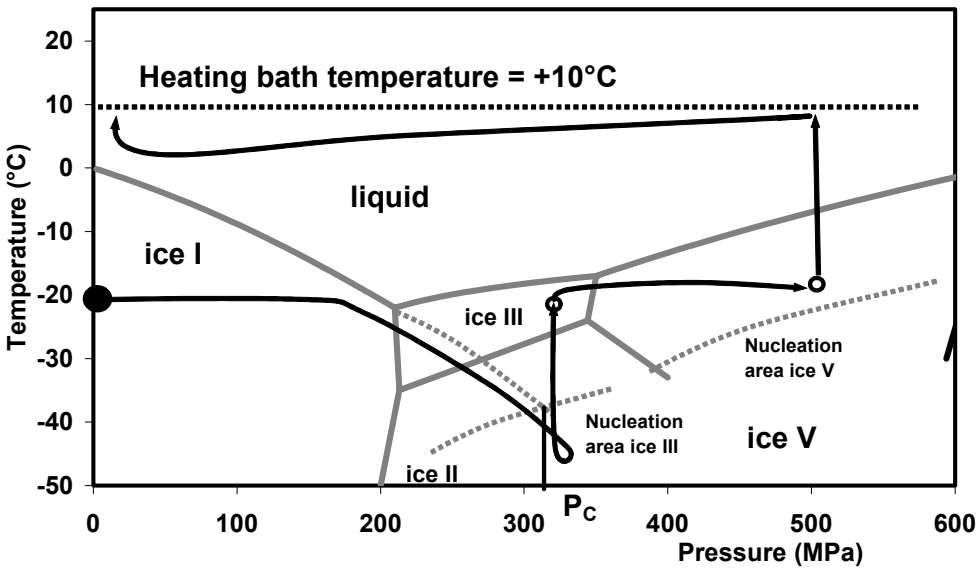

Figure 4.15. Schematic path for pressure-supported thawing in the domain of ice V.

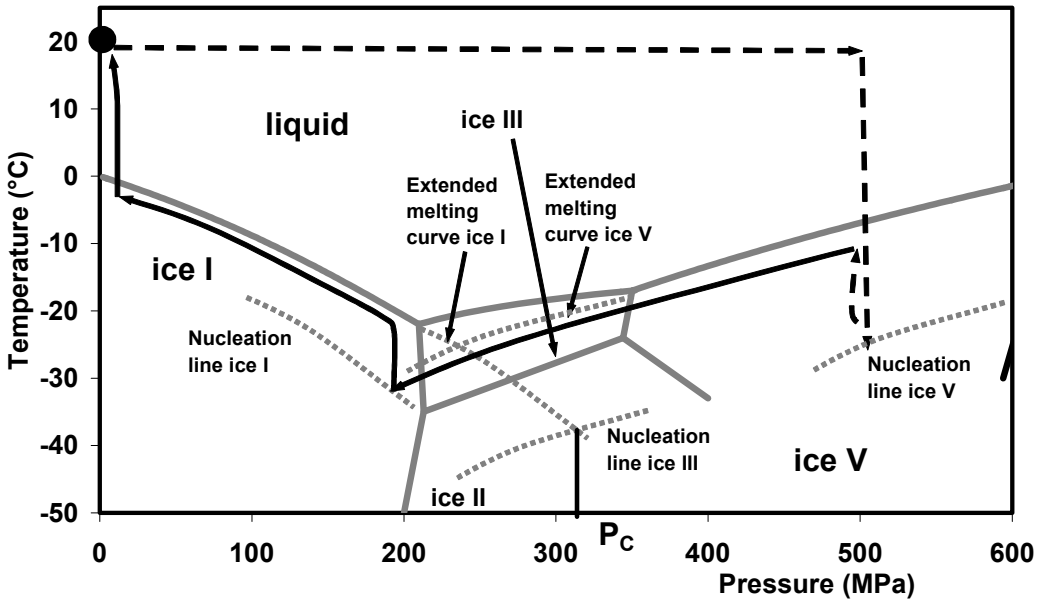

Figure 4.16. Schematic path for pressure-shift thawing process of ice V: the previous freezing process to ice V (discontinuous line) is followed by the pressure release and therefore the thawing of ice V (full line), reaching the area of nucleation of ice I, therefore, re-crystallizing ice I.

Pressure-shift thawing. In a previous paper by Schlüter *et al*., 2004, pressure-shift freezing was defined as a process where crystallisation is induced simultaneously in the entire sample by fast pressure release. Therefore, following the same principle, a thawing process should be possible by fast pressure release. In Figure 4.16, the schematic process for a pressure-shift thawing is shown. In this case, the samples are frozen to higher ice polymorph (ice V) and then instantaneously thawed by rapid pressure release, taking advantage of the positive phase transition lines of higher ice modifications.

4.1.2.1. Thawing in the domain of ice I and ice III

In a given range of initial temperatures, during the pressurisation, the thawing path in the p-T diagram reaches the melting curve of ice I. From this point, as long as pressure increases, the sample temperature decreases, following the unique tendency of this ice I melting curve, because of the partial endothermic melting of ice I in water. Then, depending on the pressure level, the sample can reach the nucleation line of ice III, appearing then ice III at the sample surface (where melted water is first appeared). In this case, a new process can be defined: the **pressure-induced crystallisation of ice III**. But, if pressure remains under this critical value, P_C, after this partial melting of ice I, it is expected that ice I remains stable and the thawing process occurs without the presence of ice III. Nevertheless, the nucleation of ice III is also depending on the initial temperature, because a solid-solid phase transition can also occur during pressurisation. Figure 4.17 summarises the experimental thawing results.

Tf = -40°C Ti = -20°C	Pmax = 300 MPa	Thawing of ice III
Tf = -40°C Ti = -30°C	Pmax = 300 MPa	Thawing of ice III
Tf = -40°C Ti = -40°C	Pmax = 300 MPa	Solid-solid phase transition
Tf = -30°C Ti = -30°C	Pmax = 300 MPa	Thawing of ice I
Tf = -30°C Ti = -30°C	Pmax = 300 MPa	Thawing of ice I (P constant)
Tf = -30°C Ti = -30°C	Pmax = 310 MPa	Thawing of ice III
Tf = -20°C Ti = -20°C	Pmax = 300 MPa	Thawing of ice I
Tf = -20°C Ti = -20°C	Pmax = 300 MPa	Thawing of ice I (P constant)

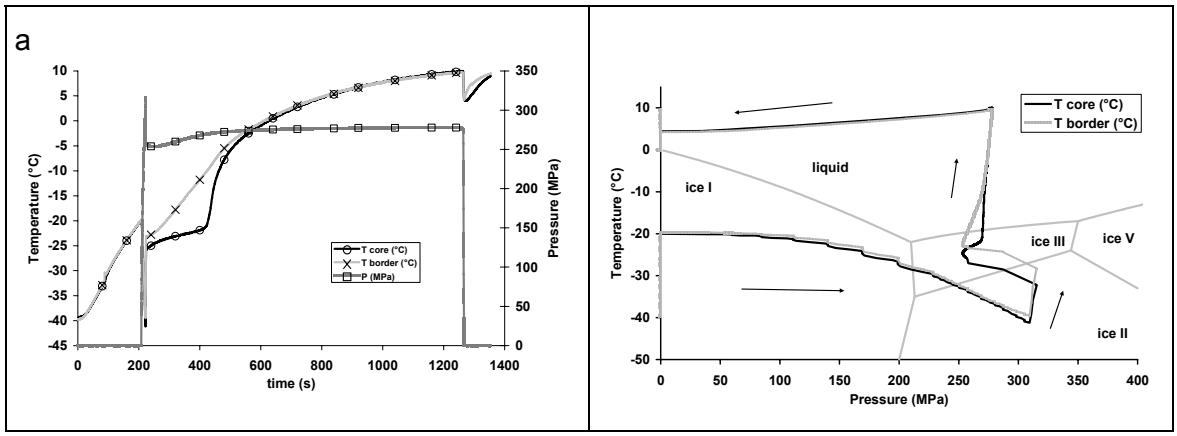

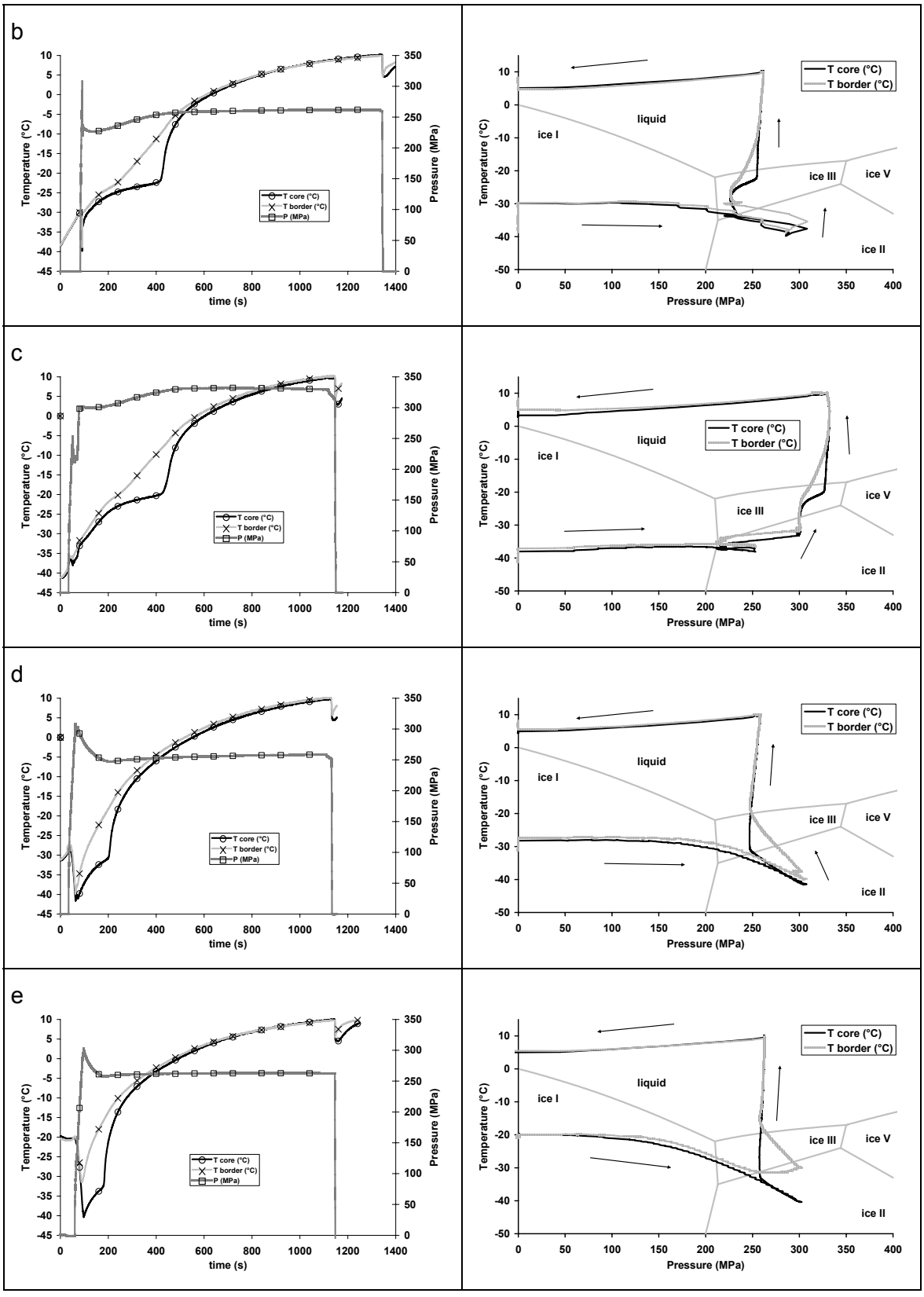
b
c
d
e
Temperature (°C)
Pressure (MPa)
time (s)
T core (°C)
T border (°C)
P (MPa)
liquid
ice I
ice III
ice V
ice II

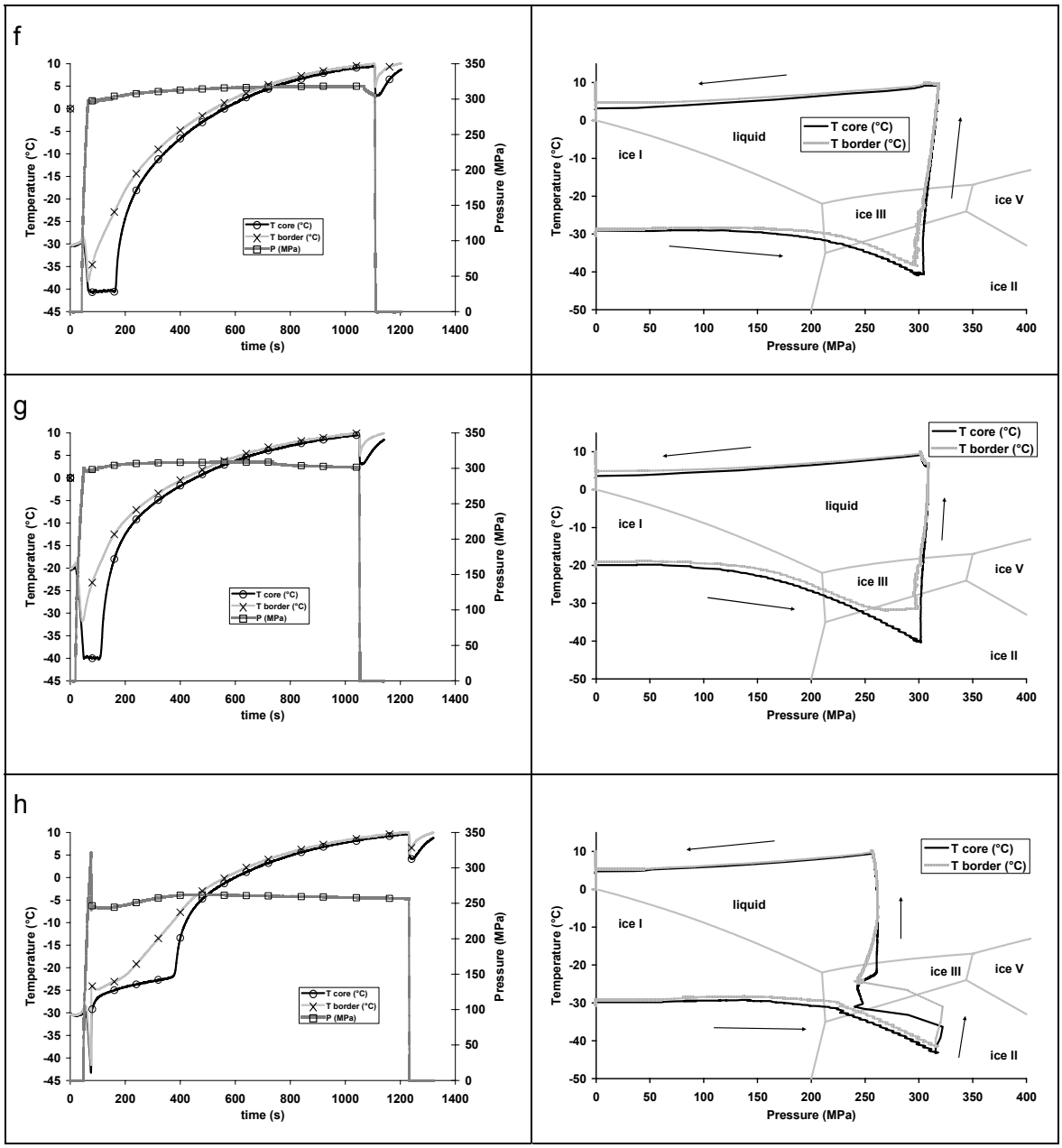

Figure 4.17. Time profiles (left) and processing paths on the phase diagram of water (right) for pressure-induced thawing processes in the domain of ice III, at 300 and 310 MPa.

After the results shown in Figure 4.17, it seems that when a previous freezing process at –40°C was performed, ice III was obtained, either through the re-crystallization of melted water into ice III crystals in the range of 300-310 MPa (case a and b) or through a solid-solid phase transition taken place before reaching this pressure level (case c). On the other hand, when no previous freezing at -40°C was run, that is direct freezing to the initial temperature (-20 or -30°C), ice I was thawed and no nucleation of ice III occurred (cases d, e, g and h), with one exception, case f, in which ice III is re-crystallized. For the cases in which ice I was thawed, two kinds of path can be described: either a classical thawing curve for ice I at higher pressure levels (until the vicinities of 300 MPa), cases e and h) or a jump in the thawing path, cases d and g, in which the sample temperature/pressure seems to tend be changed to the triple point.

Figure 4.17a shows the case of thawing a previously frozen potato sample at –40°C and then tempered to the initial temperature of –20°C. Pressure was then increased and, in the vicinities of 300 MPa, as expected, nucleation of ice III crystals in the

sample surface took place. This nucleation is possible thanks to the already melted ice I into water at the sample surface during pressurisation, as confirmed by the depression on temperature during the pressure increase through the extended ice I phase transition line. After nucleation, the pressure was not further controlled or increased, and the temperature/pressure combination tends to go to the triple point, where all three phases present co-exist. That means, in the moment of crystallisation of ice III, all three phases are coexisting: liquid water, ice I and ice III. After reaching the vicinities of the triple point, the system pressure increased, confirming that ice III was thawing (remember that liquid water has less density than ice III). The case shown in Figure 4.17b is completely similar, with the only difference that the temperature before pressure increase was -30°C.

Figure 4.17c illustrates the case in which after a previous freezing at –40°C starting at the same temperature level, the frozen ice I is led to an solid-solid phase transition to ice III at a pressure level between 200 and 250 MPa. A first slight temperature increase can be seen before the solid-solid phase transition takes place, due to the local work of associated compression. The actual phase transition is identified by a typical pressure and temperature decrease in the time profiles (left) and by a pressure decrease in the processing path (right). After the solid-solid phase transition, ice III is pressure-assisted thawed with a considerable pressure increase, due to the volume increase.

Figure 4.17d and Figure 4.17e are showing comparable thawing paths in which, after a direct freezing to –30°C, pressurisation was stopped at 300 MPa. In both cases, after overcoming 200-210 MPa (the value of pressure in the triple point ice I/ice III/water), the system followed the extension of the phase transition line of ice I and then, a jump following the way back was obtained. This behaviour is evidence of the re-crystallisation of ice I after a partial melting from the same ice I into water during the pressurisation. This re-crystallisation was instantaneous and then, a typical “pressure-assisted” thawing curve was obtained. The non-existence of a pressure increase parallel to the ice III phase transition line during thawing corroborated that ice I was thawing.

Figure 4.17f and Figure 4.17g present the thawing paths obtained after a direct freezing to –30°C, in which was also stopped at 300 MPa. Again, after partial melting following the extension of the phase transition line of ice I, when reaching 300 MPa, the pressure level was controlled and maintained constant. A classical thawing plateau could be therefore observed, at a constant temperature of around -40°C (ice I present at -40°C in real products!).

Finally, Figure 4.17h shows the case in which, after direct freezing at –30°C, the pressure was increased to more than 300 MPa, until re-crystallization of ice III was obtained, at around 310-320 MPa. Then, a classical thawing plateau for ice III was observed.

The general remark confirming that the thawing paths after previous freezing at –40°C lead to ice III solid-solid transformation or ice III nucleation and that the thawing paths with direct freezing lead to ice I thawing or to a jump to the triple point followed by ice I thawing (always when pressure maintained under 300 MPa) should be further discussed and experimentally corroborated. Nevertheless, after the results obtained here, it seems that the thermal history of the sample has a key role in controlling the thawing path to be obtained.

4.1.2.2. Pressure-induced/-assisted thawing in the domain of ice V

In this case, the pressure was increased to 500 MPa, reaching the thermodynamically stable domain of ice V, with an initial temperature of –20 or -30°C. After the nucleation of ice III or the solid-solid phase transition from ice I to ice III (as described in the previous experiments), the thawing is continued up to a pressure of 500 MPa, in the thermodynamically stable domain of ice V. Figure 4.18 shows the experimental temperature profiles and the thawing paths for two experiments: case a shows a

thawing path with an initial temperature of –20°C, while case b shows a thawing path with an initial temperature of –30°C.

a) T initial = –20°C. Ice III thawed

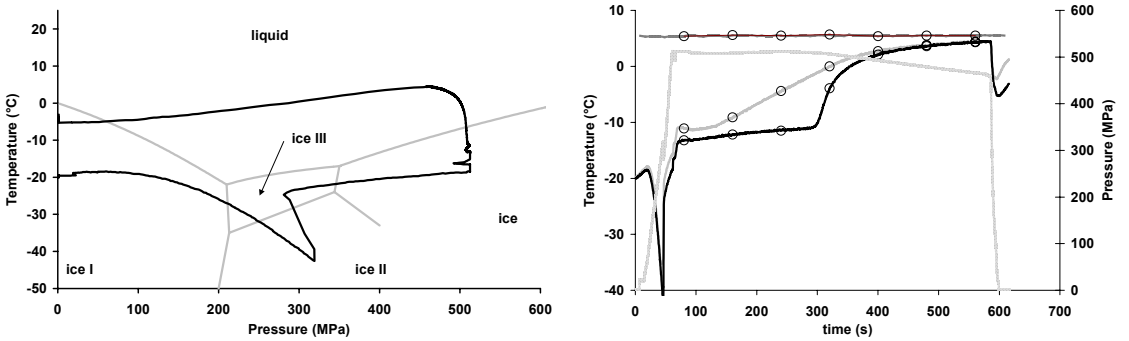

b) T initial = –30°C. Ice V thawed

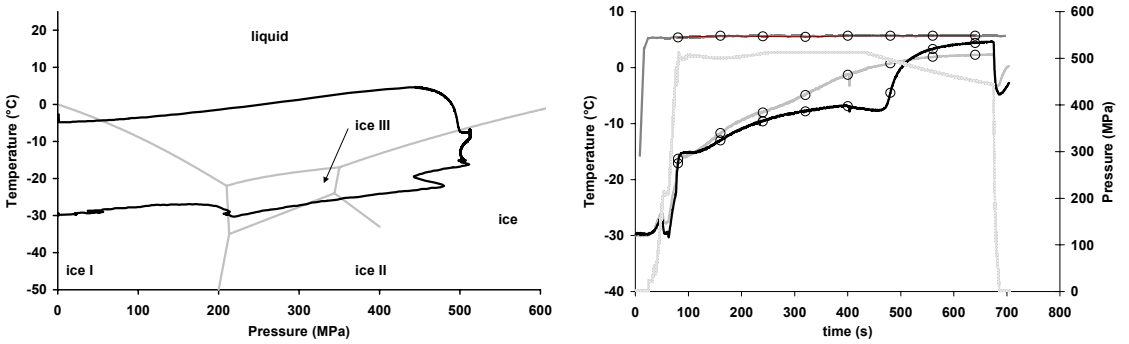

Figure 4.18. Experimental thawing paths (left) and temperature profiles (right) for thawing in the domain of ice V; (a) T initial = -20°C; (b) T initial = -30°C.

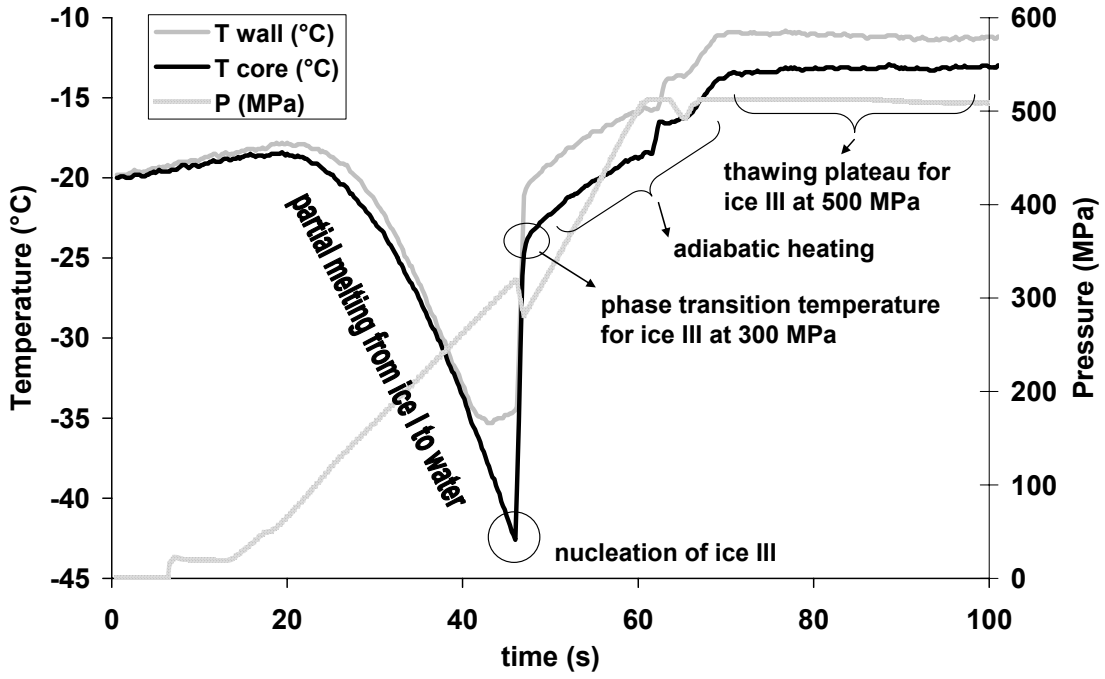

Figure 4.19. Detail of time profile of thawing of metastable ice III at 500 MPa.

In case a, after the re-crystallization of the partial melted water in the sample surface during the pressurization, a mixture of ice III and water is present in the sample and a further pressurization of this mixture leads to a metastable ice III present in the domain

of ice V. This metastable ice III is pressure-assisted thawed at 500 MPa with a phase transition temperature of around -11°C. To better understand and recognize the phenomena occurring during this first case, a detailed thawing profile is given in Figure 4.19.

In the case b, after the solid-solid phase transition from ice I to ice III, pure ice III (and not a mixture of ice III and water) is further pressurized. Therefore, the thawing path follows the parallel line of ice III and then a second solid-solid phase transition to ice V occurs. The solid-solid phase transition from ice I to ice III happens at 210-250 and the area of nucleation of ice III is reached at 300-310 MPa. Similarly, for ice V, the area of nucleation is probably obtained at higher than 500 MPa and solid-solid phase transition happens already at 450-500 MPa. Further research would be needed to clarify this question. To better identify the two solid-solid phase transitions, Figure 4.20 is showing the two thawing path details where these transitions are identified.

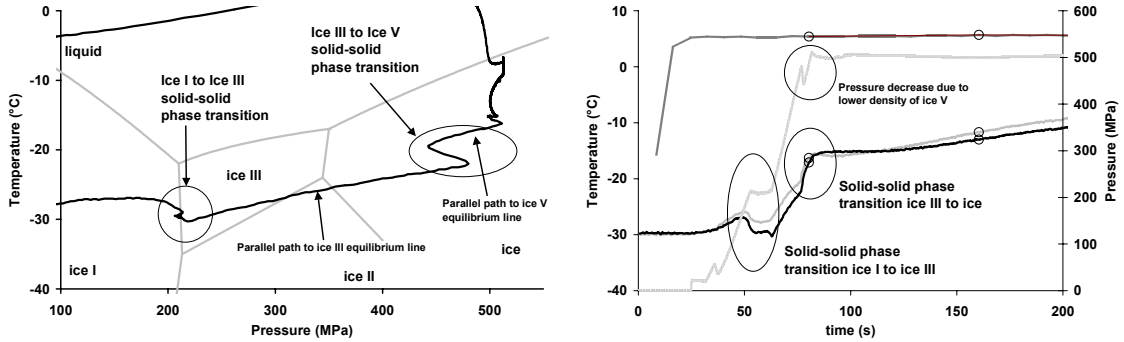

Figure 4.20. Solid-solid phase transition details on thawing at higher pressures into the domain of ice V: case b with T initial = –30°C and no previous freezing.

4.1.2.3. Pressure-shift thawing

As previously defined, (Schlüter *et al*., 2003) pressure-shift freezing is a process where crystallisation is induced simultaneously in the entire sample by fast pressure release. Therefore, when thawing of an entire sample is induced by a fast pressure release, a new process should be defined: pressure-shift thawing. This process is possible to be carried out when the slope of the phase transition line between water and a higher ice modification is positive, therefore, taking the same possibility that the negative slope of ice I/water phase transition line gave to pressure-shift freezing, but now taking into account a positive slope in the phase transition line of ice V/water for pressure-shift thawing. In Figure 4.21, the thawing path and temperature profile are shown.

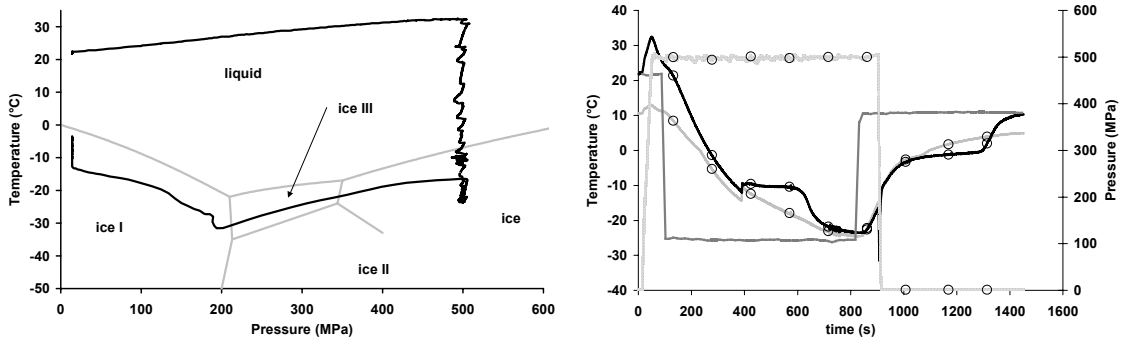

Figure 4.21. Experimental thawing path and temperature profile for pressure-shift thawing.

After performing a classical pressure-assisted freezing to ice V at 500 MPa, pressure is instantaneously released when the freezing *plateau* is completed and the temperature of sample centre has reached a temperature of at least -23°C (12°C bellow the plateau

one, -10°C). Then, the bath temperature was changed to thawing conditions (+10°C) and pressure was released. The sample temperature follows the melting curve of ice V, indicating the co-existence of ice V and water. This curve is followed through an extension into the thermodynamically stable domains of ice III and ice I. The sample thawing path follows this extended melting curve of ice V until the first nucleation area for another ice modification is reached, corresponding, in this case, to ice I, at 195 MPa and -32°C.

To observe this fact better, Figure 4.22 shows the detail of the temperature decrease while the ice V phase transition line is followed and the instantaneous jump when ice I nucleates. The water in sample surface nucleates to ice I, then the crystals appear in the whole sample, as demonstrated in Figure 4.22: both sample surface and sample centre temperatures have the same values just after the nucleation of ice I, showing that nucleation took place uniformly in the whole potato cylinder. Finally, when pressure is completely released, an atmospheric pressure thawing process from ice I to water takes place (thawing temperature around 0°C).

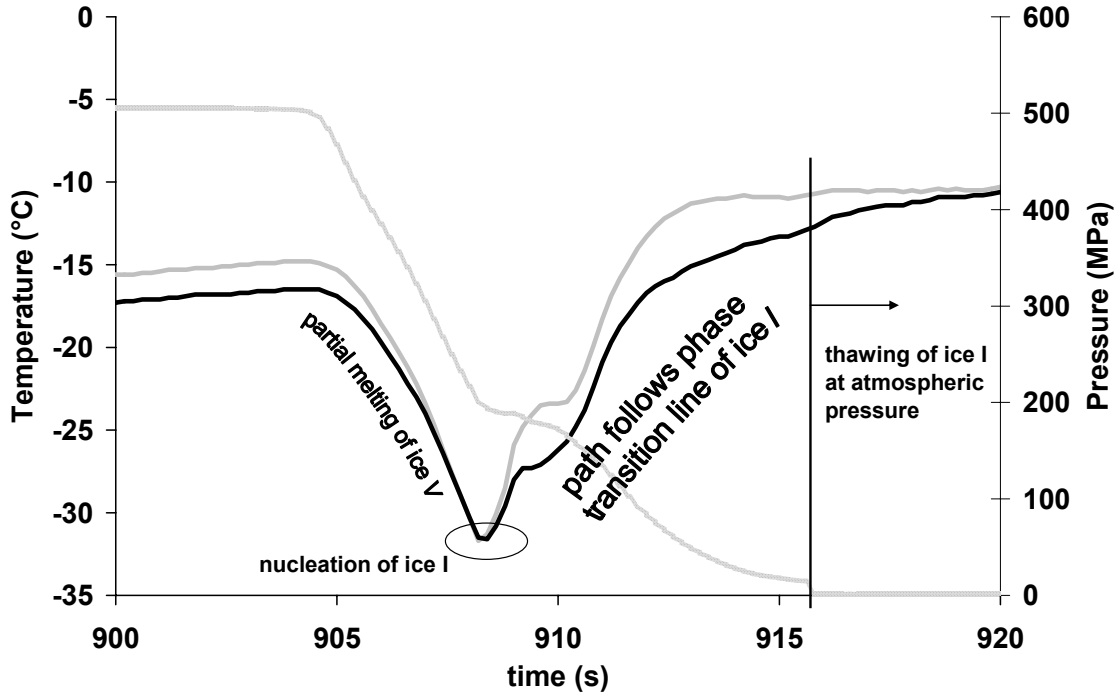

Figure 4.22. Detail of temperature decrease in followed ice V phase transition line and instantaneous nucleation of ice I crystals.

4.1.2.4. Schematic representation of kinetics of thawing

To better understand the physical phenomena involved in the different thawing paths described here, a schematic representation of the potato cylinders during the experimental paths is illustrated in Figure 4.23.

a) Pressure-induced/-assisted thawing with ice III nucleation

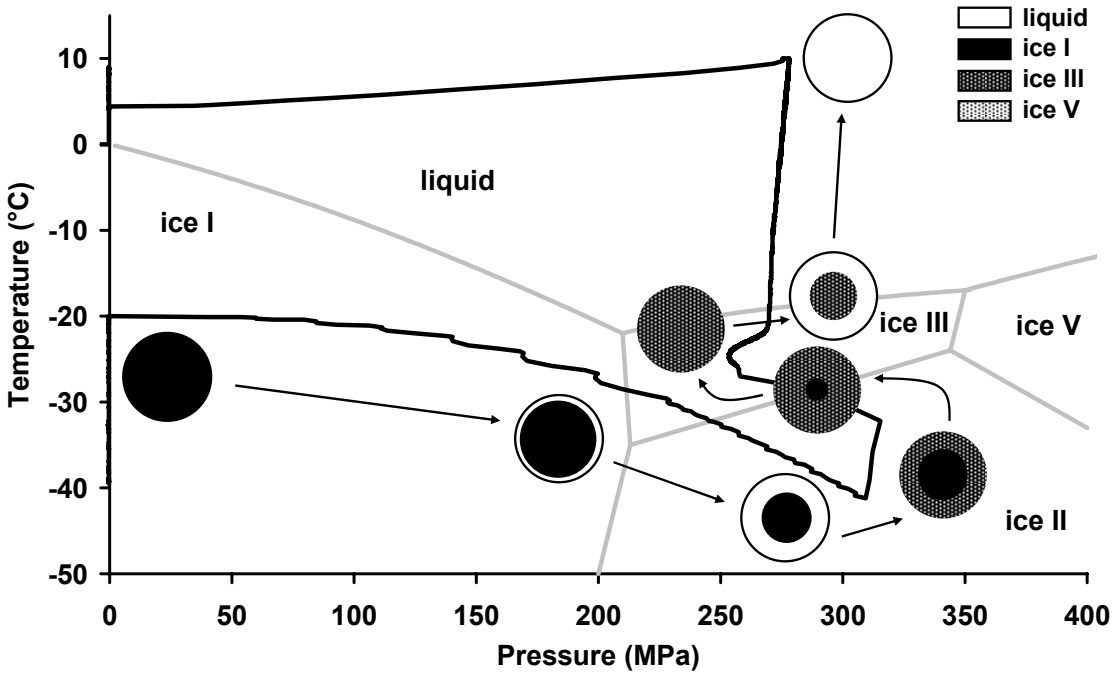

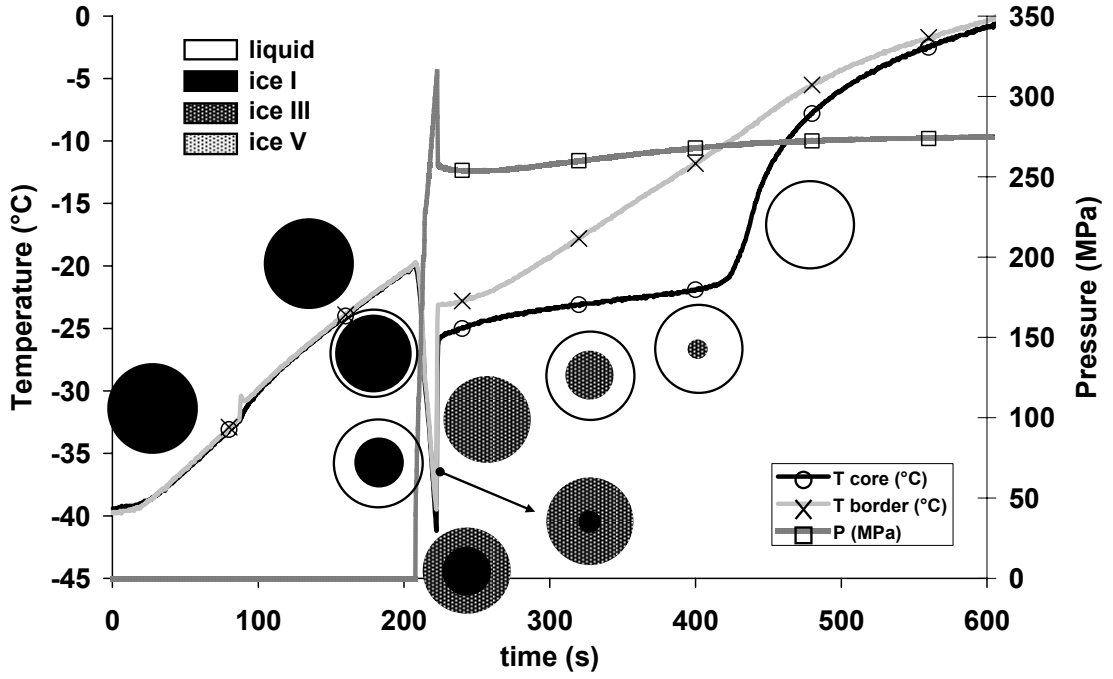

b) Pressure-induced/-assisted thawing of ice I without pressure control

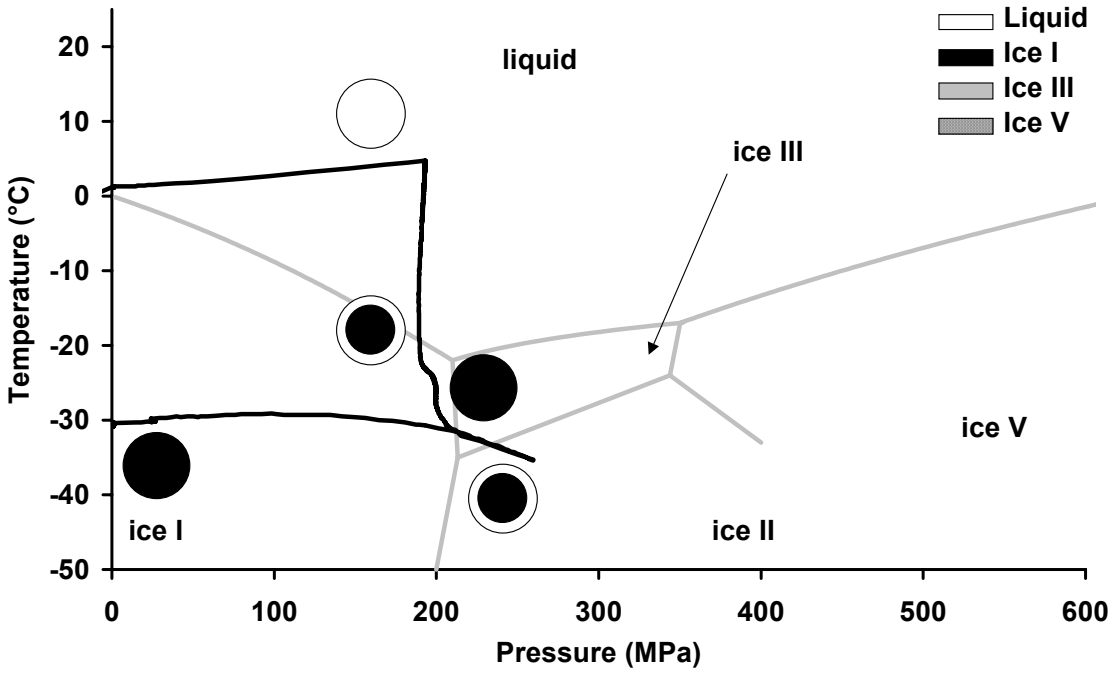

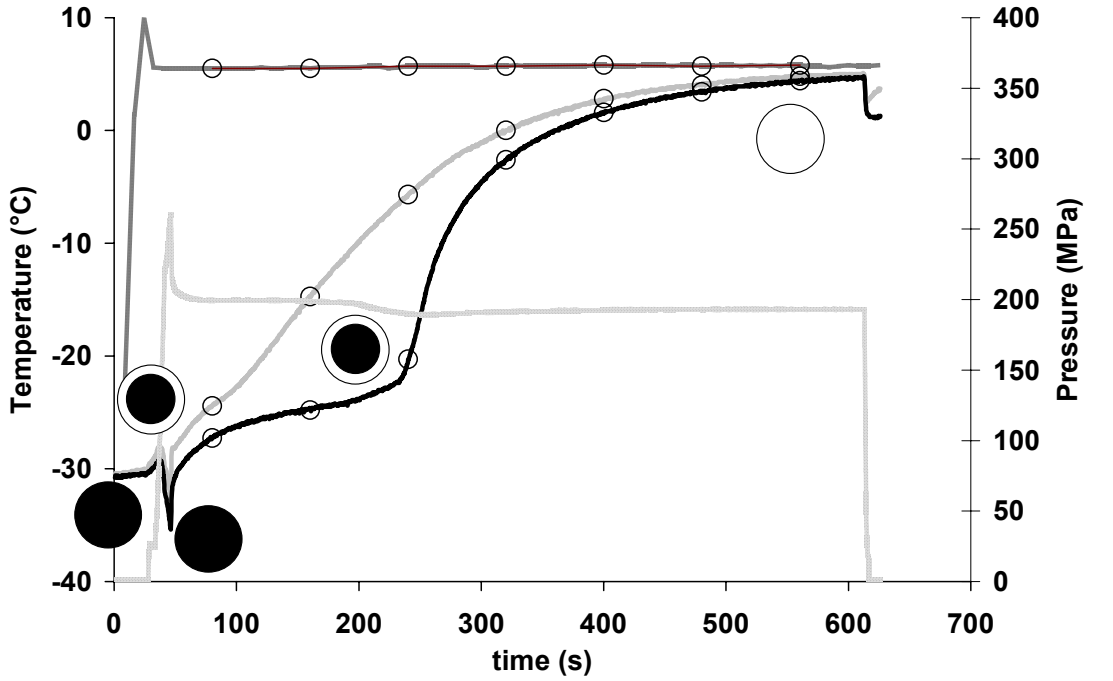

c) Pressure-induced/-assisted thawing of ice I with no nucleation

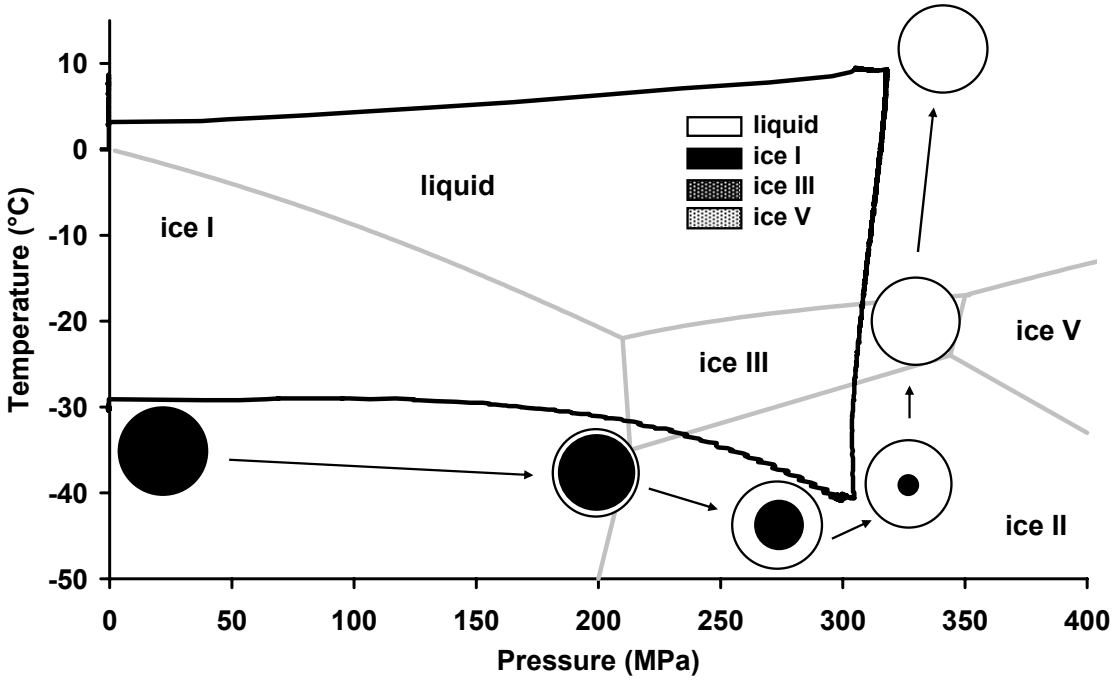

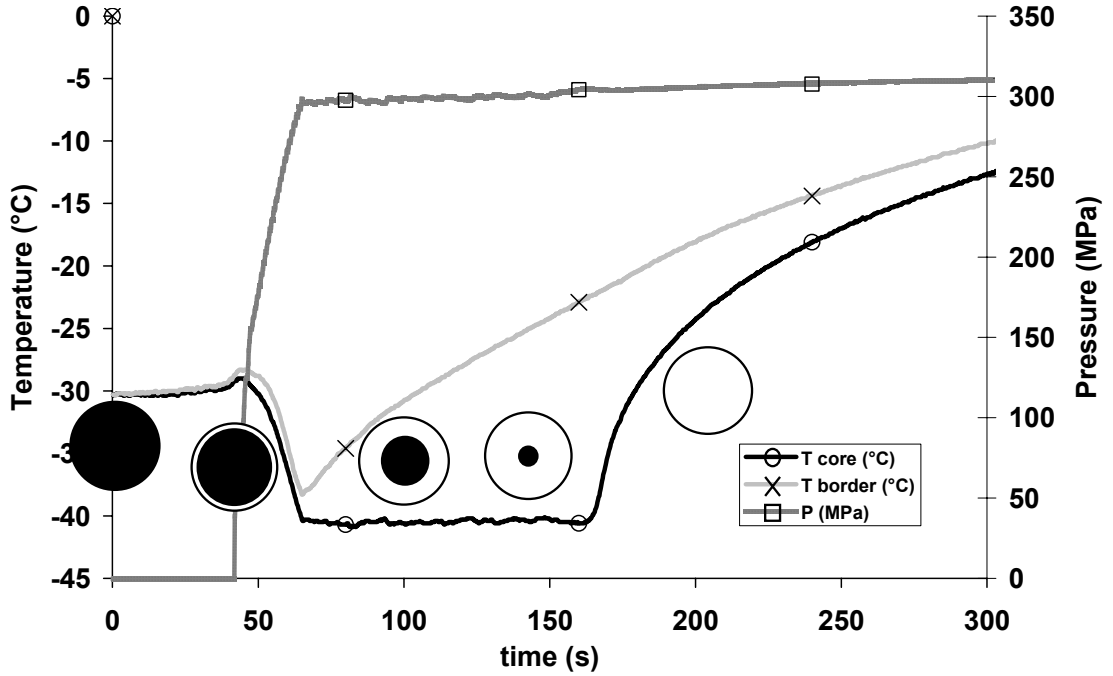

d) Thawing in the domain of ice V with no solid-solid phase transition

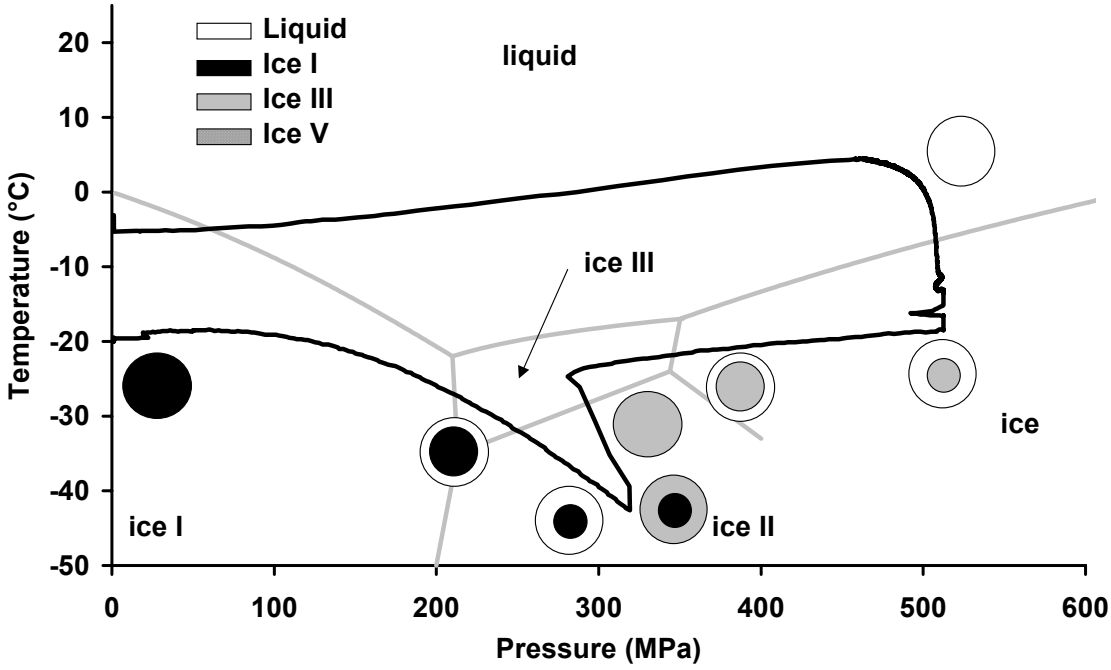

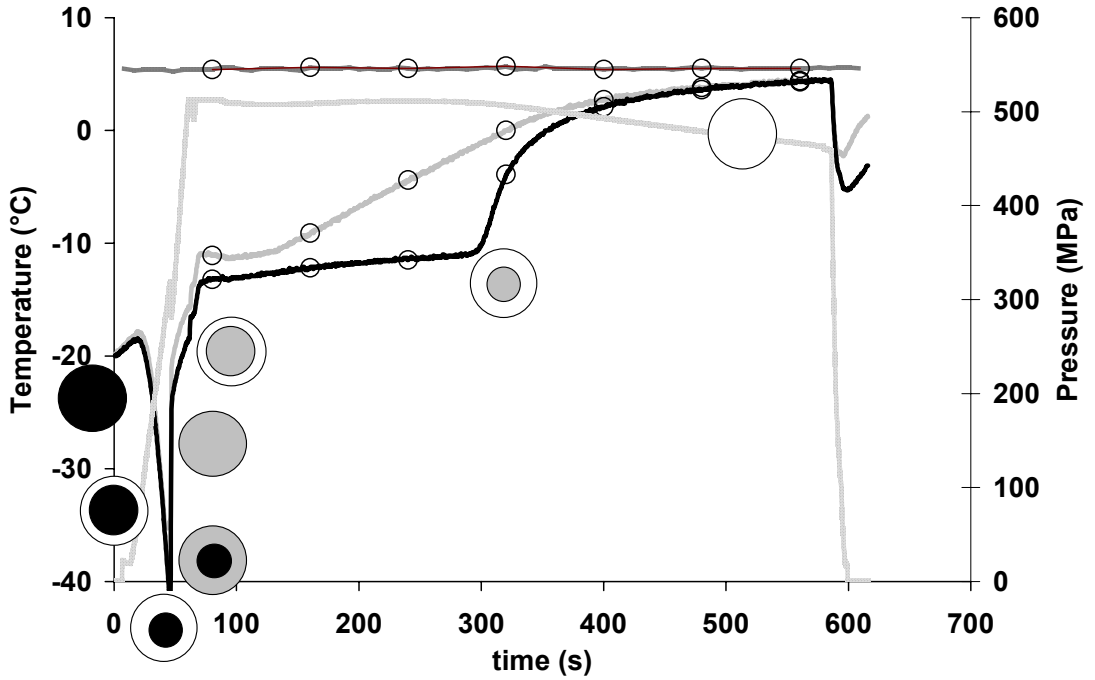

e) Thawing in the domain of ice V with solid-solid phase transition

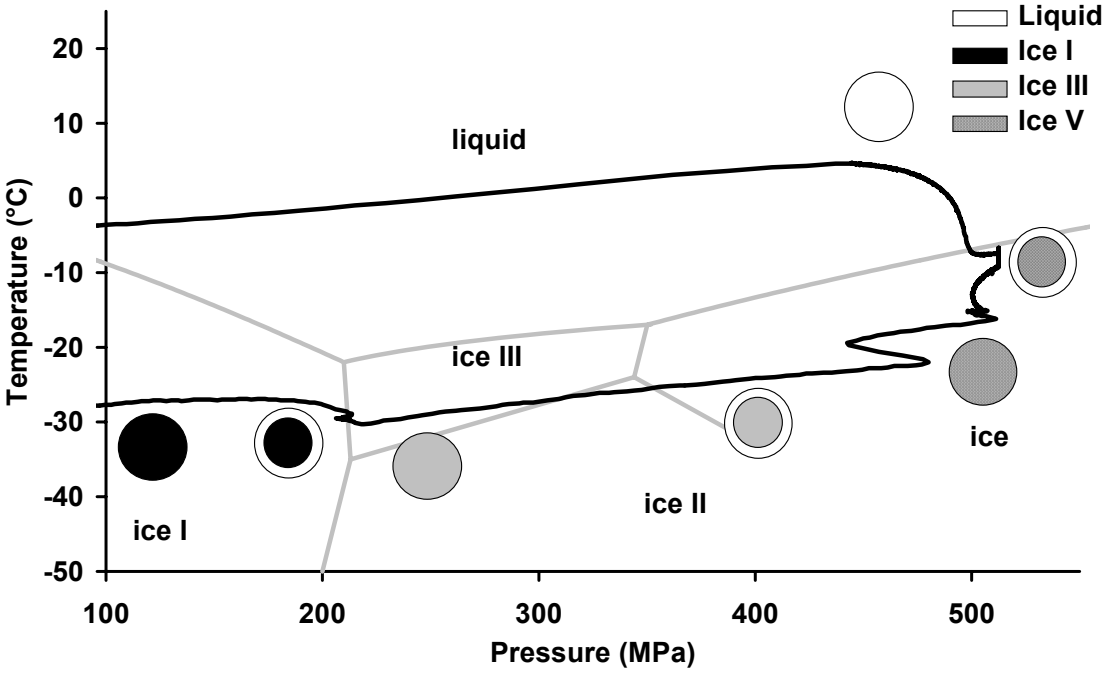

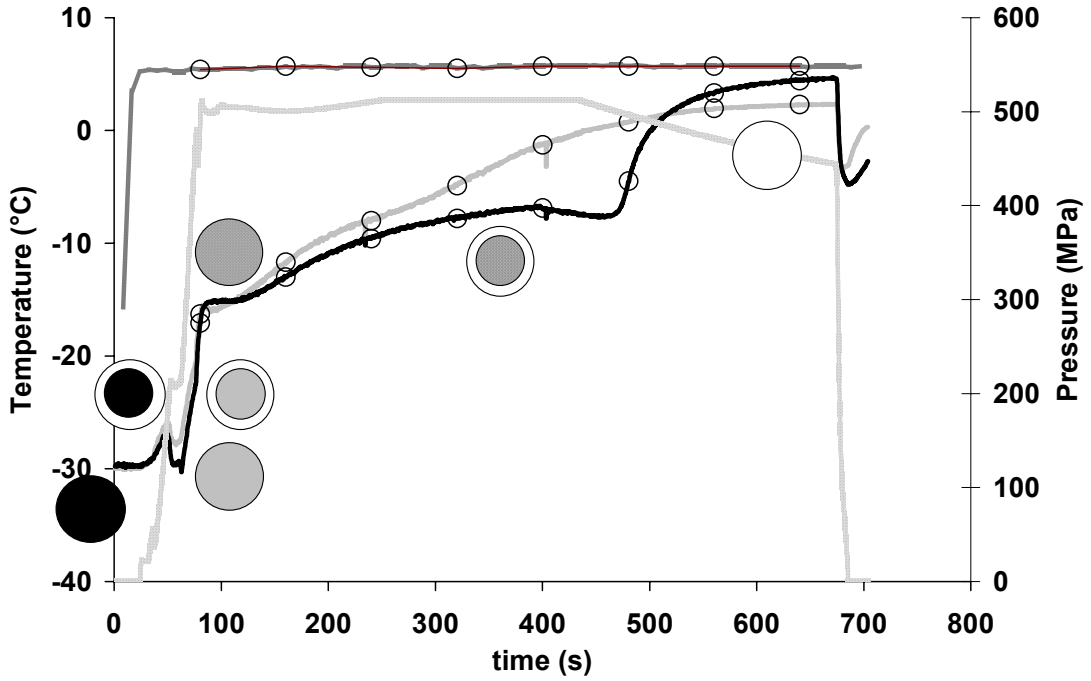

f) Pressure-shift thawing from ice V

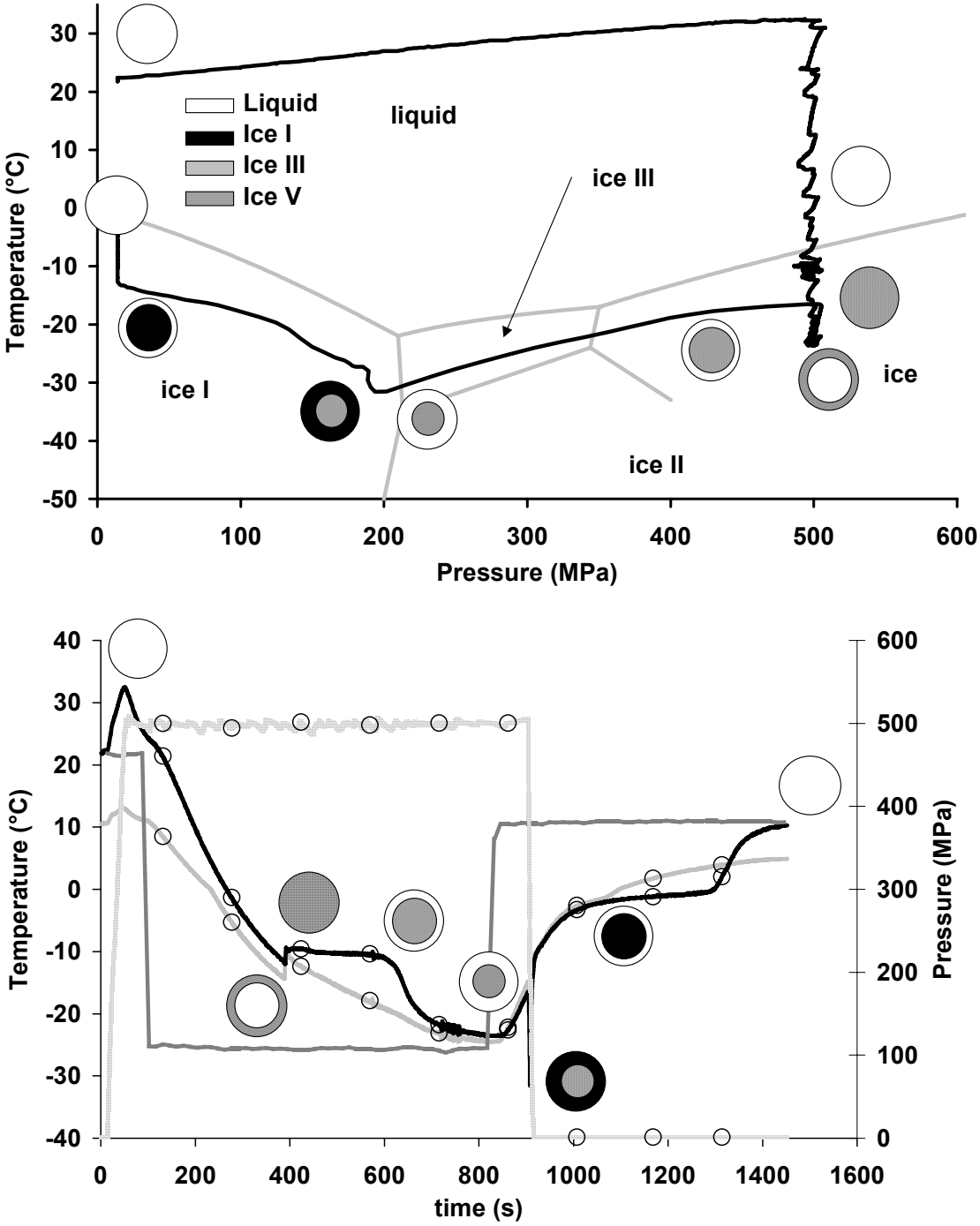

Figure 4.23. Schematic transversal cuts of potato cylinders during thawing paths.

The nucleation of ice III after following the extended melting line of ice I is explained in Figure 4.23a. At the beginning, the sample is completely frozen into ice I, and during pressurisation, ice I is melted into water (represented by an external ring). This external ring of water first nucleates into ice III, and then, the whole sample, quasi-instantaneously, has ice III crystals. Then, the assisted thawing of ice III occurs, thawing first the sample surface and finally, the whole cylinder is represented by liquid water.

Some of the experiments performed (Figure 4.17d and Figure 4.17e) showed a "re-crystallisation" of ice I after a partial melting during pressurisation, describing the

thawing path a “way-back” through the extended ice I line. Figure 4.23b represents this behaviour. At the beginning, the whole sample is frozen into ice I, and then, during pressurisation, the already commented partial melting is schematised. Then, the re-crystallisation of ice I occurs, and, therefore, again the whole sample is shown as ice I. Then, the classical assisted thawing cylinders are shown.

In the case of Figure 4.23c, no nucleation of ice I nor of ice III is obtained. In this case, the frozen sample melts in its surface and, at 300 MPa, a normal assisted thawing occurs.

When the pressure is increased until the domain of ice V is reached, two thawing paths were found. Figure 4.23d and Figure 4.23e represent these two cases. In Figure 4.23d, no solid-solid phase transition took place: the ice I frozen sample is pressurised and therefore, the surface is melted into water. The surface water, when the temperature is low enough, crystallises into ice III and then, the ice III crystals are extended throughout the whole sample. Then, an assisted thawing was obtained, although the pressure level indicates that ice V is the stable ice modification. In Figure 4.23e, after surface melting of ice I into water, a solid-solid phase transition is represented for the whole sample. Then, ice III melts into water as long as the pressure is further increased, and then, a second solid-solid phase transition is represented for the whole sample from ice III to ice V. Then, assisted thawing from ice V is schematised.

Figure 4.23f shows the schematic cylinders for a pressure-shift thawing. In this case, the initial state is liquid, and then, pressure-assisted freezing is performed. In the phase diagram (left), the next step after reaching the selected pressure is the nucleation in sample surface of ice V, and then, temperature increases slightly (after supercooling) and the whole sample is represented as ice V. Then pressure is released, and the sample surface melts into water. This water, when the nucleation area of ice I is reached, crystallises into ice I, and then these ice I crystals are expanded throughout the whole sample. Then, thawing is completed until the sample is liquid again.

4.1.3. Modified phase diagram for potatoes, including the metastable zone.

The freezing curves, together with the corresponding pressure curves (both parameters P and T plotted against time) may give the different singular points of the modified phase diagram for potato, presented in Figure 4.24a.

On the other hand, the nucleation temperatures shown define the extent of the supercooling reached for each pressure level. This supercooling is higher for ice modification III, arriving to values of around –20 °C. This greater degree of supercooling for ice III is obtained as expected, and together with the results of the phase transition times, indicate the consistency of the results, as shorter phase transition times are reached for higher degrees of supercooling.

The differences of the experimental ice III nucleation temperatures, when compared to the better fit for ice I indicates the existence of a non-stable area between the indicated pressure levels (209 to 240 MPa). This non-stable liquid phase before nucleation starts, and the following non-stable ice modification I in the region of stable ice III are the cause of the lower degree of fitting of nucleation points for ice III.

Three different metastable phases are likely to be found in the modified potato phase diagram, in agreement with available data Schlüter and Knorr (2002). For definition, a metastable phase is one that exists in a pressure – temperature combination in which another phase is thermodynamically stable. Given the different metastable phases related to high pressure-supported processes, here their definitions will be established.

Metastable phase A (transient supercooled liquid): when a freezing process is carried out and the supercooling phenomenon appears, until the nucleation line for ice I or ice III is reached, we experimentally still have liquid phase, at temperatures lower than the theoretic phase boundary: in this case, a metastable liquid is reached.

Metastable phase B (long resting supercooled liquid): according to the results of Luscher *et al*. (2003), there is a “long resting” or “significantly stable” region in which the liquid phase is still kept after keeping samples in this pressure/temperature levels for more than 40 hours.

Metastable phase C (thermodynamically non-stable solid phase): at pressures above 209 MPa, when ice modification III is already the thermodynamic stable phase, ice I is still obtained when cooling below its prolonged melting curve. This definition is also applicable to metastable ice V in the region of ice III (see Evans, 1967b, Schlüter and Knorr, 2002, Luscher *et al*., 2003).

In Figure 4.24b, only the metastable phases B and C are represented, as the metastable phase A is present in every case when the nucleation point is below the corresponding phase transition line: in a higher or lower degree, this supercooling phenomenon is always present when carrying out a pressure-assisted freezing operation.

According to the results shown in Figure 4.24b, the position of the metastable areas, both for ice I in the ice III domain and for the long resting liquid, is defined. According to the results presented by Evans (1967b), another prolongation (but in the case of ice V in the domain of ice III) was experimentally obtained, and here schematically represented. The prolongation of the phase transition lines of both ice I and ice V into the domain of ice III leads to a shorter pressure range in which it can be ensured that ice III will nucleate. In this sense, when comparing to the obtained nucleation points for ice I, a high dispersion of nucleation points is shown for ice III. This dispersion enables us to define an area (Figure 4.24b) which upper and lower lines give the limits to ensure or to avoid the nucleation of ice III. In the cooling process, to ensure the nucleation of ice III a lower temperature than the one given by the lower line must be reached, and if this nucleation is to be avoided, the temperature of the sample must always be kept above the upper line of the defined area. Therefore, the best conditions to ensure the nucleation of ice III are working between (approximately) 250 and 300 MPa, and below –40°C.

The existence of the experimentally proofed metastable phases open new processing opportunities, especially for pressure-shift freezing and pressure-induced thawing, the two more promising processes. In this sense, Schlüter (2003) described the need of further studies on the metastable phases of modified phase diagrams to identify controlled and optimised freezing and thawing paths. That means, obtaining the external manipulation of pressure and temperature profiles to obtain desired processes with paths that optimise the process possibilities. In this sense, the extended melting curve of ice I offers the opportunity to study a controlled pressure-induced thawing path in which ice I is thawed from temperatures lower than the triple point by pressure increase and further thawing at constant pressure. Anyway, all these processes are particularly difficult to explain because of the non consistent nomenclature existing in the literature, especially when comparing data from different laboratories.

A complete data base has been created related to the phase diagram of potato. Figure 4.25 is showing the collected data for different ice modifications’ melting points and nucleation points.

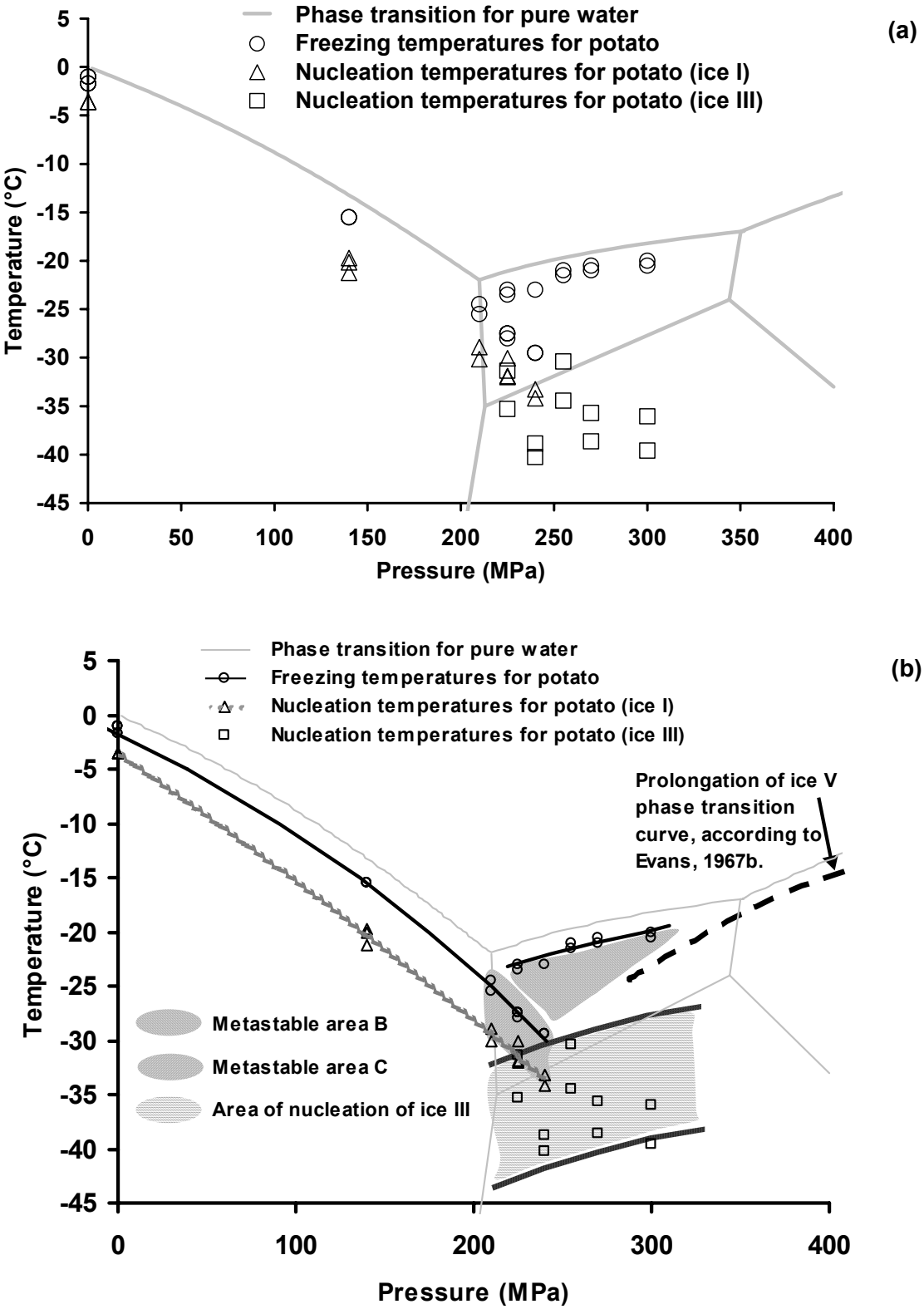

Figure 4.24. (a) Freezing and nucleation points in the modified phase diagram for potato (compared with the one for water); (b) Metastable phases associated with the obtained experimental data.

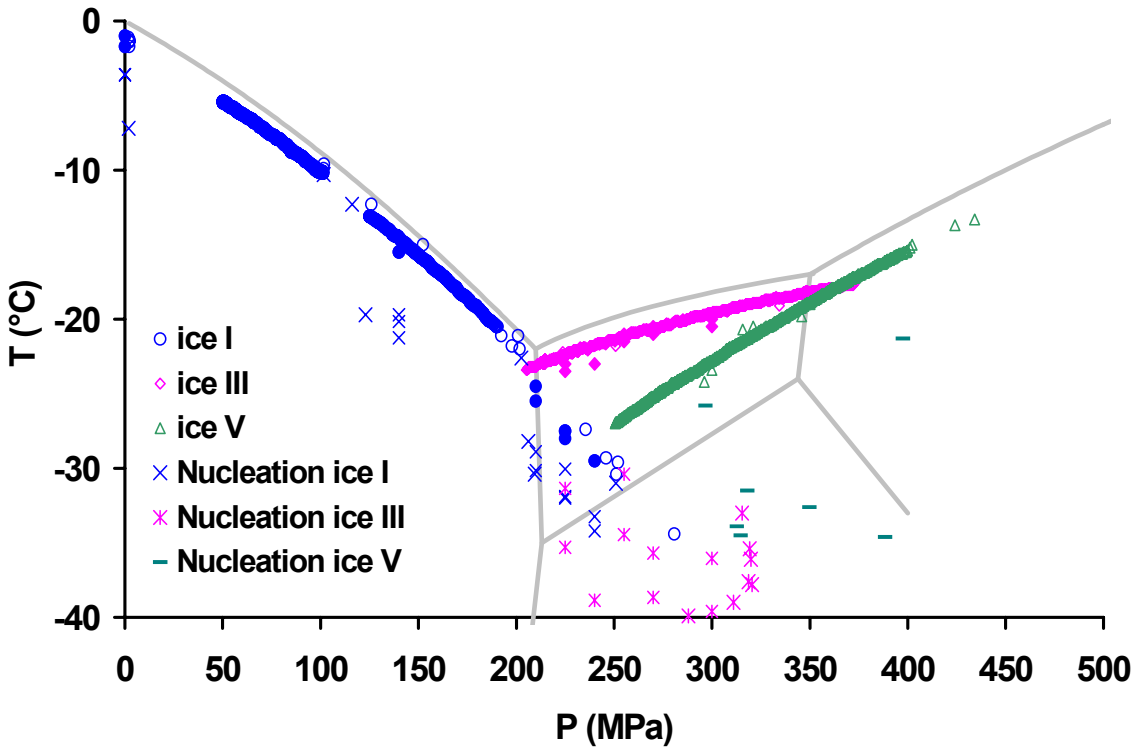

Figure 4.25. Complete phase diagram for potato (with nucleation points for ice I and III).

The phase transition lines and their extensions, together with the new defined concepts of area of nucleation are shown in Figure 4.26, and the liquid and solid metastable phases are represented in Figure 4.27.

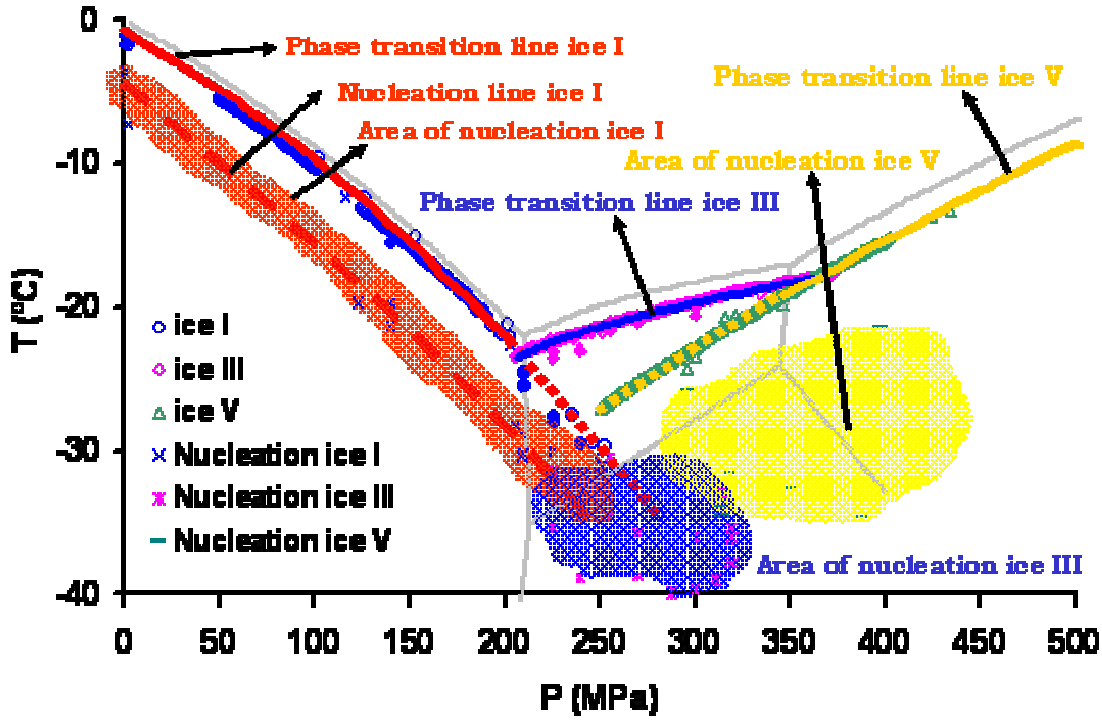

Figure 4.26. Phase transition lines, areas of nucleation and extended phase transition lines on the experimental phase diagram of potato.

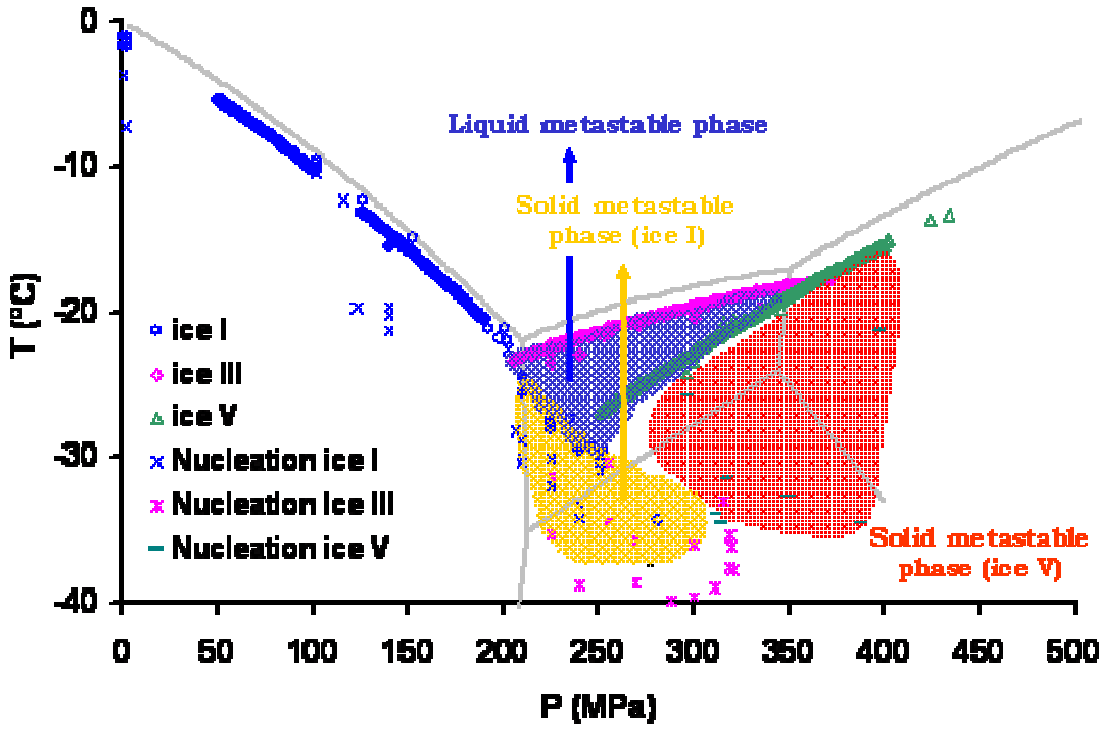

Figure 4.27. Definition of liquid and solid metastable phases on the experimental phase diagram of potato.

4.1.4. Description of possible processes

Taking advantage of the phase diagram of water various pathways of changing the physical state of food can be followed using external manipulations of temperature or pressure (Knorr et al., 1998). Figure 4.28 shows theoretical path-ways together with one specially attractive real path for thawing during pressurisation. The nomenclature used is taking into account the definitions given below (Urrutia et al., 2004).

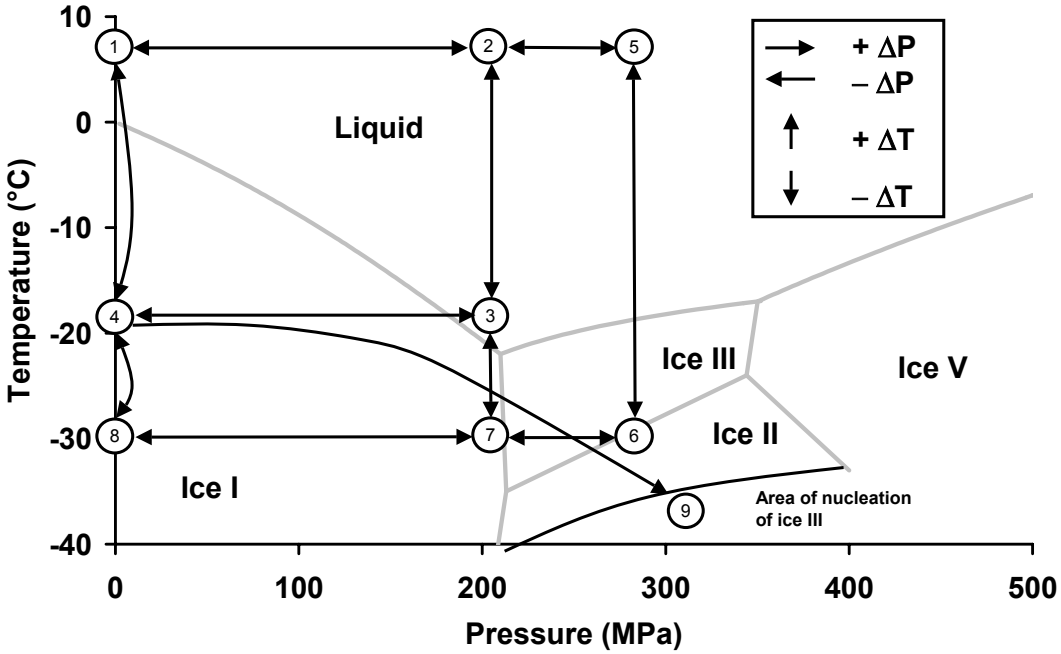

Figure 4.28. Possible processing paths in the phase diagram of water; 1-4-8: Freezing at atmospheric pressure; 1-2-3-7-8: Pressure-assisted freezing; 1-2-3-4-8: Pressure-shift freezing (PSF); 1-2-5-6-7-8: Pressure-assisted freezing to ice III

(followed by pressure release and consequent solid-solid phase transition from ice III to ice I); 8-4-1:Thawing at atmospheric pressure; 8-7-3-2-1: Pressure-assisted thawing (PAT); 8-7-6-5-2-1: Pressure-assisted thawing from ice III (PAT III); 4-3-2-1: Ideal pressure-induced thawing (PIT); 4-9: Real pressure-induced thawing (PIT).

Before describing the different processes, it should be mentioned that the criterion for classifying the paths is based on the **aim** of global processes, in which the initial and final states of the sample are at atmospheric pressure. In some cases, the processes are shown starting from or finishing with a pressurised sample, in order to simplify some definitions. In some cases, the experimental data are showing paths crossing phase transition lines, but without a phase change, neither nucleation nor melting. This kind of behaviour can be explained through the concept of metastable phases, as shown in recent publications (Schlüter et. al., 2004, Luscher et al., 2004). The different definitions are presented below, based on a basic classification as shown in Figure 4.29. In this classification, the main possible processes in the High-Pressure-Low-Temperature (HPLT) region are shown.

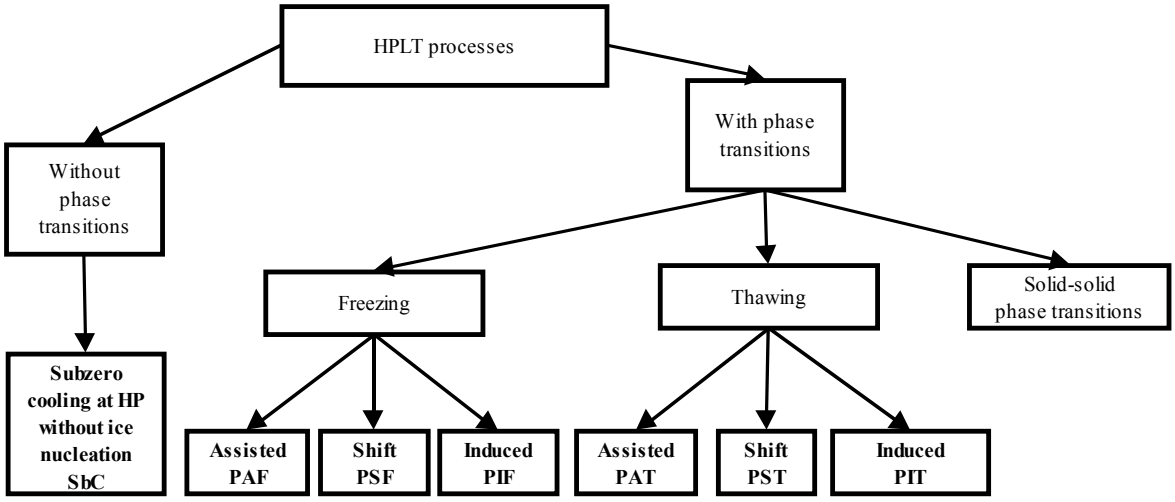

Figure 4.29. Schema of main processes in the HPLT region.

For pure water the International Association for the Properties of Water and Steam (IAPWS) accepted the definition of melting curves given by Wagner et al. (1994). Wagner fitted the parameters of Simon equations to the available experimental data and reaches high conformity for pressures up to 20 GPa. These curves define equilibrium lines between stable phases, but entering a different region of thermodynamic stability does not necessarily induce a phase transition.

The decrease of a product temperature below its freezing/melting point leads to freezing of a before unfrozen sample at ambient pressure as well as at high hydrostatic pressure. Due to soluble components the freezing point of food is decreased when compared to pure water. To start the nucleation of ice crystals often a significant supercooling is required depending on the experimental conditions (cooling rate, physical and chemical properties of the sample, cooling system, etc.). Freezing of a potato cylinder to a higher ice modification can be shown by a typical temperature plateau due to the exothermic thermal event when plotting the sample temperature versus time. The degree of supercooling can be quantified by a sudden temperature increase from the nucleation temperature to the initial freezing point (Figure 4.30).

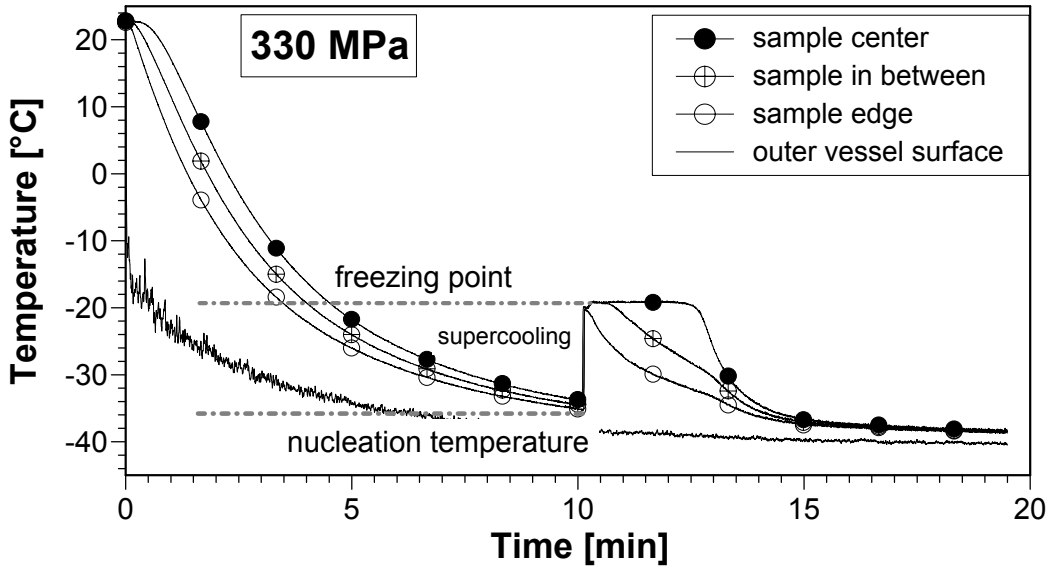

Figure 4.30. Temperature profile during pressure assisted freezing (ice III) of potato tissue.

The melting curves of potato tissue and of pure water show an analogous slope of the phase boundaries when plotted to the *pT*-diagram. Since liquid–solid phase transitions also takes place beyond the triple points (liquid/ice I/ice III and liquid/ice III/ice V) along the extended phase boundaries (Bridgman, 1912; Evans, 1967a) in a region where ice III thermodynamically exists a metastable liquid phase was defined (Schlüter et al., 2004). In this region (Figure 4.31) no nucleation was observed during cooling for all experiments performed. Consequently thermodynamic metastability must be taken into consideration when regarding HPLT processes.

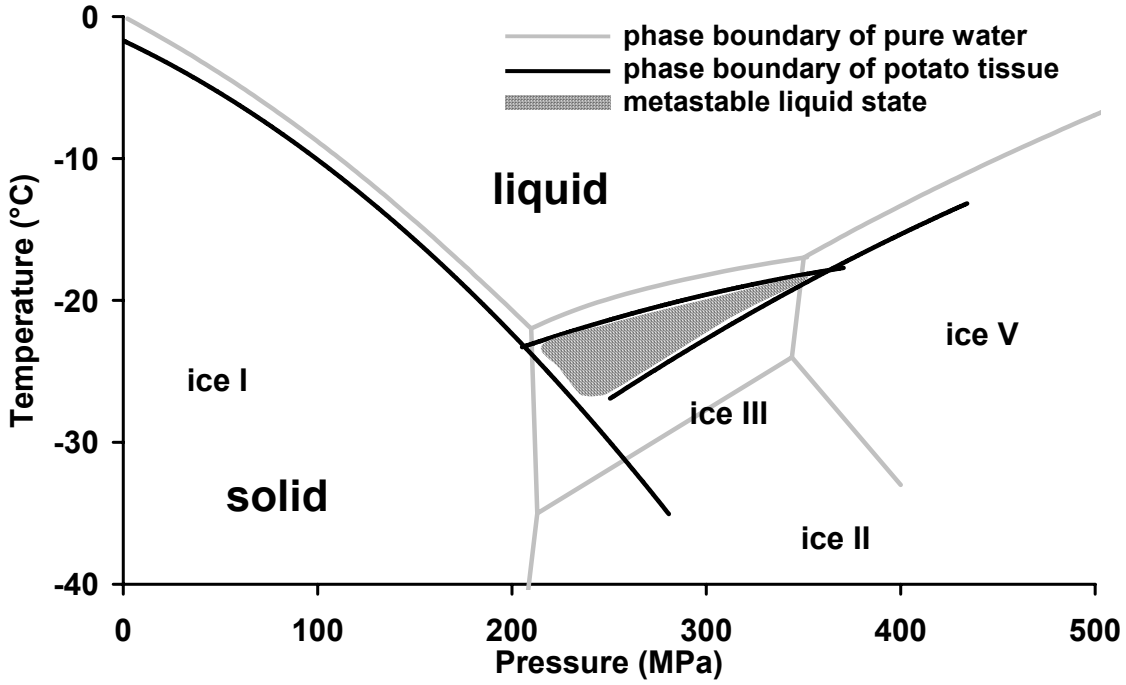

Figure 4.31. Schematic *pT*-diagram of water and melting curves for potato tissue. No nucleation of ice crystals was obtained by cooling within the metastable region of the liquid state.

4.2. Definition of processes: suggested terminology

Subzero cooling under pressure (SbC): Because of the anomalous phase behaviour of water, using moderately high hydrostatic pressure, liquid aqueous systems can be maintained at temperatures as low as –22 °C and therefore, advantage can be taken of the low temperature (microbial and/or enzymatic inactivation) while avoiding the disadvantageous effects of freezing (texture, drip loss, etc.). Therefore, subzero cooling under pressure (SbC) without freezing appears to be applicable to prolong the shelf life of foods while avoiding the damage caused by freezing. Figure 4.32a shows the schematic path to be followed in this process, and Figure 4.32b and Figure 4.32c present the corresponding experimental path and temperature profile. It should be noticed that the sample was kept for 48 hours in a metastable state (below the phase transition line of ice III) in the liquid state with no pressure decrease, as shown by the temperature profile and the experimental path. After the non-frozen state storage, a gradual pressure release was performed in order to avoid crystallization of ice I, to better study the influence of this process on product's quality, as described by Luscher, Schlüter and Knorr, 2004.

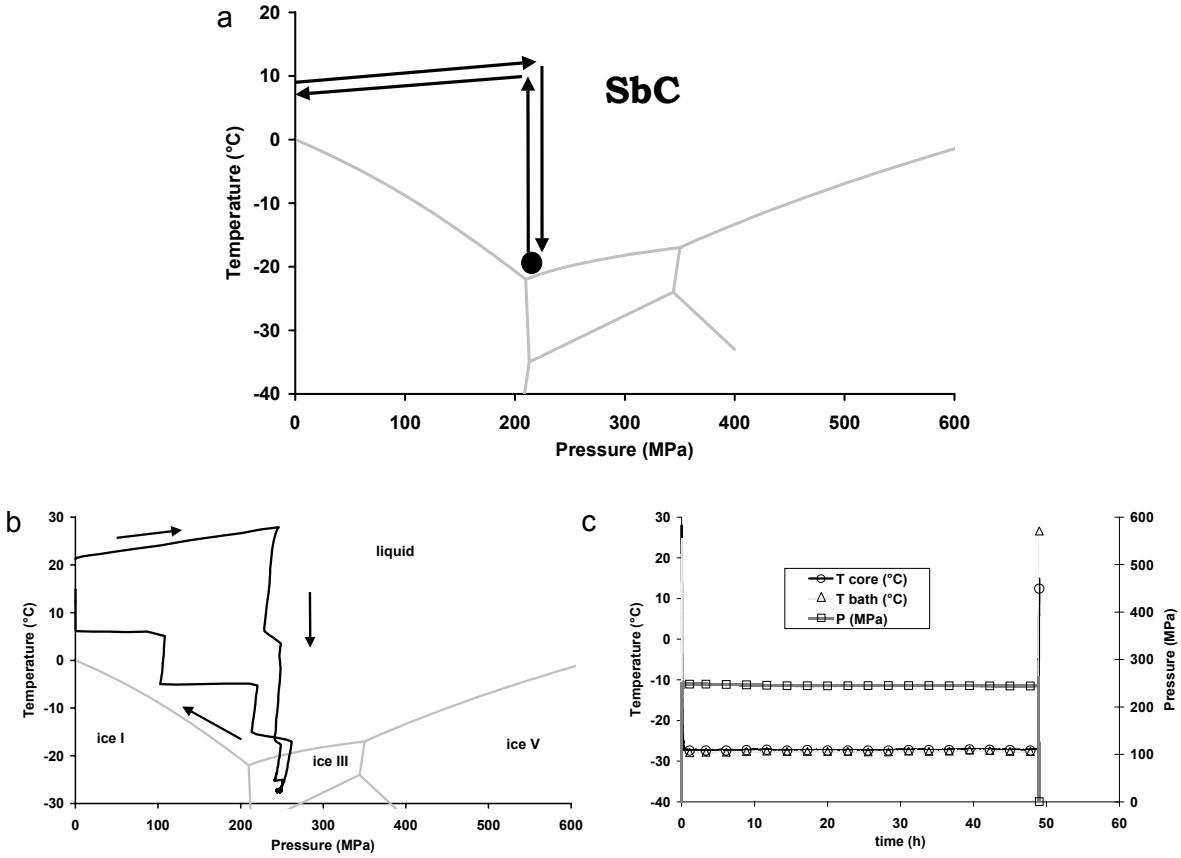

Figure 4.32. Subzero cooling without freezing: schematic path (a), experimental path (b) and temperature and pressure profile (c).

Pressure-assisted freezing (PAF) is a process in which an unfrozen sample is frozen after pressurization at a (nearly) constant pressure level, being the temperature gradient between cooling medium and sample the driving force for the process. In general, this definition is adopted for any ice modification, but the term, with no extra specifications, is usually used exclusively for pressure-assisted freezing to ice I. When a higher ice modification is obtained, it should be explicitly indicated. Figure 4.33a shows the theoretical schematic path for this process (continuous line) for ice I and a modification for a more real path (including adiabatic temperature increase during pressurization, dotted line), Figure 4.33b the experimental path for 140 MPa and Figure

4.33c shows the corresponding temperature profile. Depending on the **overall processing goal**, the process can be finished by decreasing the pressure to 0,1 MPa, or for instance followed by pressure assisted thawing under the same pressure conditions and final pressure decrease. In this work, global processes coming-from and finishing-in atmospheric pressure are considered, with the aim of describing general paths very closed to real profiles. As commented, in some cases, this is not possible, and the specific characteristics for each path will be described. Consequently the processes are described considering the main phase transition steps, e.g. pressure built up, cooling and completed phase transition shown in Figure 4.33.

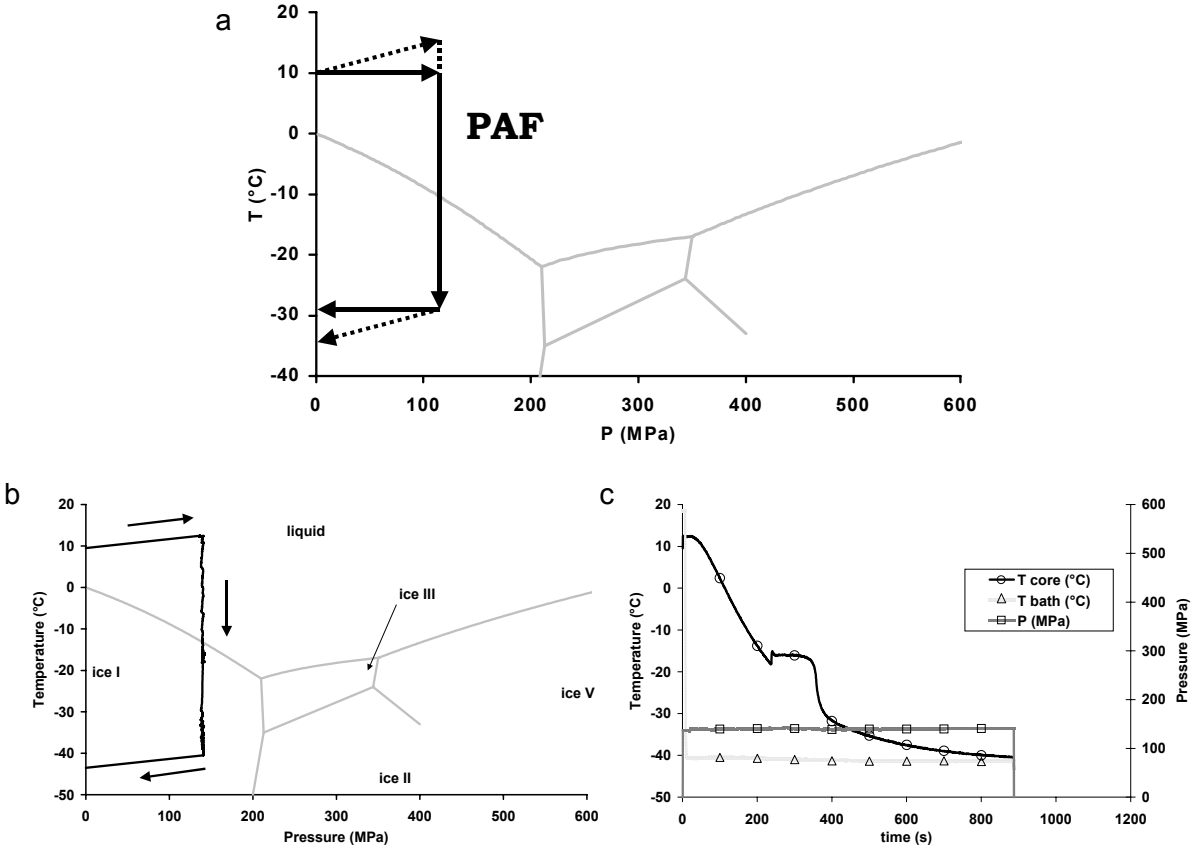

Figure 4.33. Schematic (continuous) and modified paths (dotted) (a), experimental path (b) and temperature and pressure profile (c), for pressure-assisted freezing (PAF).

A specific case of this process was described in a previous paper (Schlüter et al., 2004): the pressure-assisted freezing to metastable ice I. Although this process could lay, generally, in this category (PAF), its particular characteristics are explained. A metastable ice I modification can be obtained in the pressure range between 210 and 240 MPa, as the nucleation of ice I crystals can be reached in the thermodynamically stable region of ice III. In this case, a pressure-assisted freezing to metastable ice I could be defined as a particular case of PAF between 210 and 240 MPa, where the areas of nucleation of both ice modifications are superposed. Anyway, for the general aim of the standardization of terminology, this special case should just be referred to as PAF. Figure 4.34a shows a schematic path for this process, together with the areas of nucleation of ice I and ice III. It can be seen that there is a pressure range in which the nucleation areas are coincident and, therefore, both ice modifications are susceptible to crystallize. Figure 4.34b shows an experimental path and Figure 4.34c the corresponding temperature profile, for a pressure level of 225 MPa. The temperature curve in Figure 4.34c shows one of the metastable profiles obtained for this pressure range, in which initially ice I is nucleated but then, when the temperature in the sample

surface is low enough to reach the nucleation area of ice III, then ice III nucleates, leading to a double *plateau*, clearly indicating the metastable nature of the region.

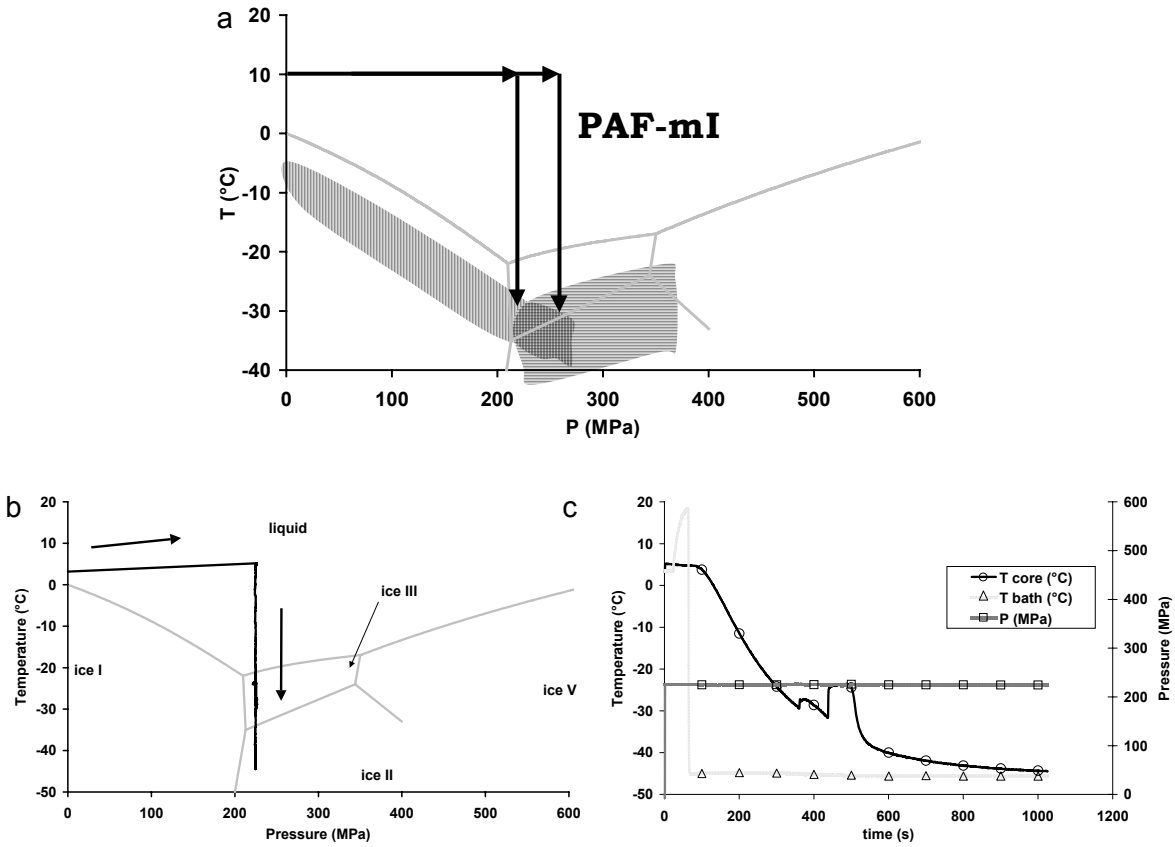

Figure 4.34. Pressure-assisted freezing (PAF): special case of freezing to metastable ice I: schematic path with the nucleation areas of ice I and ice III (a), experimental path (b) and temperature and pressure profile (c).

Pressure-assisted freezing to higher ice modifications (pressure-assisted freezing to ice III, PAF-III, or pressure-assisted freezing to ice V, PAF-V) are other cases of PAF processes in which unfrozen samples are first pressurized and then, due to a temperature gradient driving force, freezing takes place at a constant pressure. It seems that no novelties with respect to PAF are described, but after freezing the samples, two possible paths can be followed: a) samples are stored at high pressure and then, thawed at the same pressure level and b) pressure is released, leading to solid-solid phase transitions or re-crystallizations to other ice modifications. In the second case, the benefits obtained through the nucleation of higher density crystals are lost through the solid-solid phase transitions, in terms of microstructure damage and overall quality of the products. The exact limits at which ice III or ice V are expected to be obtained are not the scope of the present paper and should be defined for each product. Figure 4.35 shows the schematic paths for the two possibilities, with HP storage (a) and pressure release (b), an experimental path for PAF-III with HP storage (c) and the corresponding temperature profile for PAF-III at 300 MPa (d).

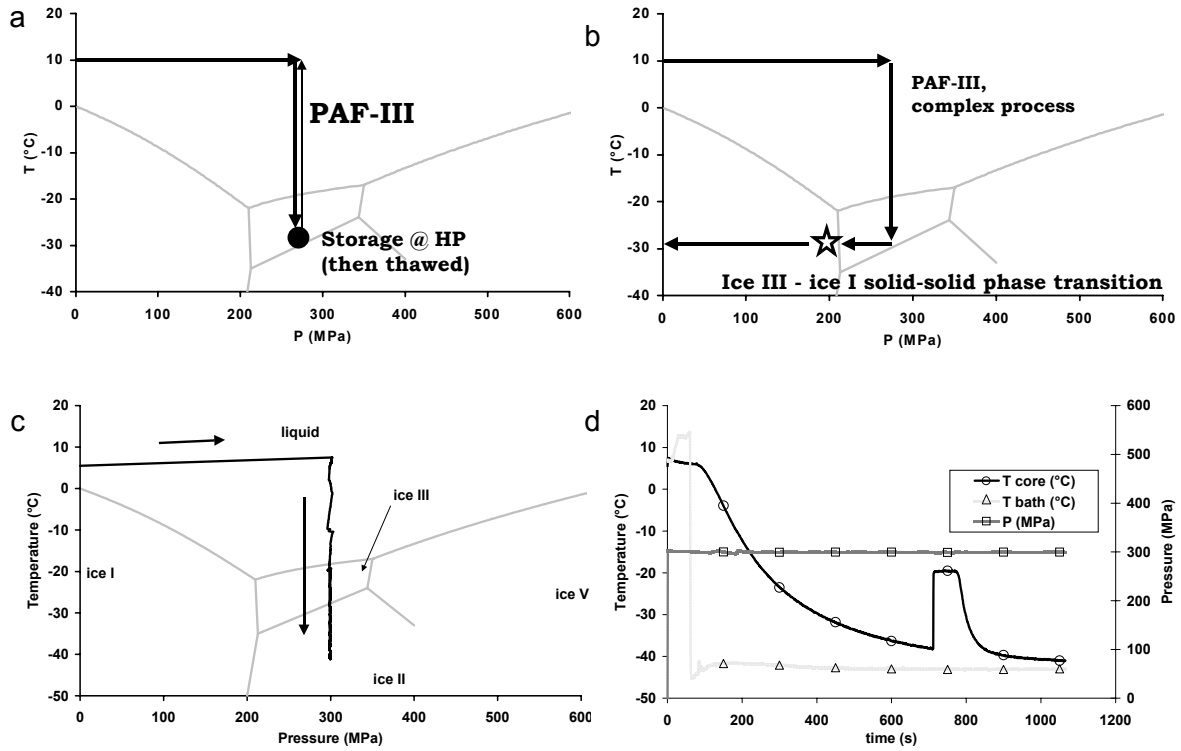

Figure 4.35. Schematic paths for PAF-III with storage at high pressure (a), complex process when pressure is released (b), experimental path for PAF-III (c) and the corresponding temperature and pressure profile for 300 MPa (d).

Pressure-shift freezing (PSF) means that a sample is frozen due to a pressure release, leading to an instantaneous crystallization of ice, homogeneously distributed throughout the sample, as a consequence of the isotropic nature of pressure. Ice I is the only ice modification susceptible to nucleate after a pressure release, because it is the only one with a negative slope in the phase transition line. While “assisted” processes are independent on the slope of the phase boundary, “induced” and “shift” processes are strictly dependent on it. Generally, the phase boundary can be crossed due to temperature or pressure changes, but the transformation of phases due to external manipulation of the pressure is of special interest since this manipulation can be realized faster and more homogenously compared to conventional temperature changes. Figure 4.36 shows the schematic (a) and experimental paths (b) and the corresponding temperature profile (c). In this figure, it is observed that the point at which the pressure release has already crossed the phase transition line of ice III, but the sample was still in an unfrozen state, due to the existence of a liquid metastable phase (see Figure 4.31). After reaching the desired *pT* coordinates, pressure was released and subsequently, the temperature decreased due to the adiabatic expansion process. After this first negative slope, the path shows that the sample temperature increases: the inflection point shows the start of nucleation of ice I, i.e., the area of nucleation of ice I was first reached. Then, the path follows the phase transition line of potato until pressure is completely released.

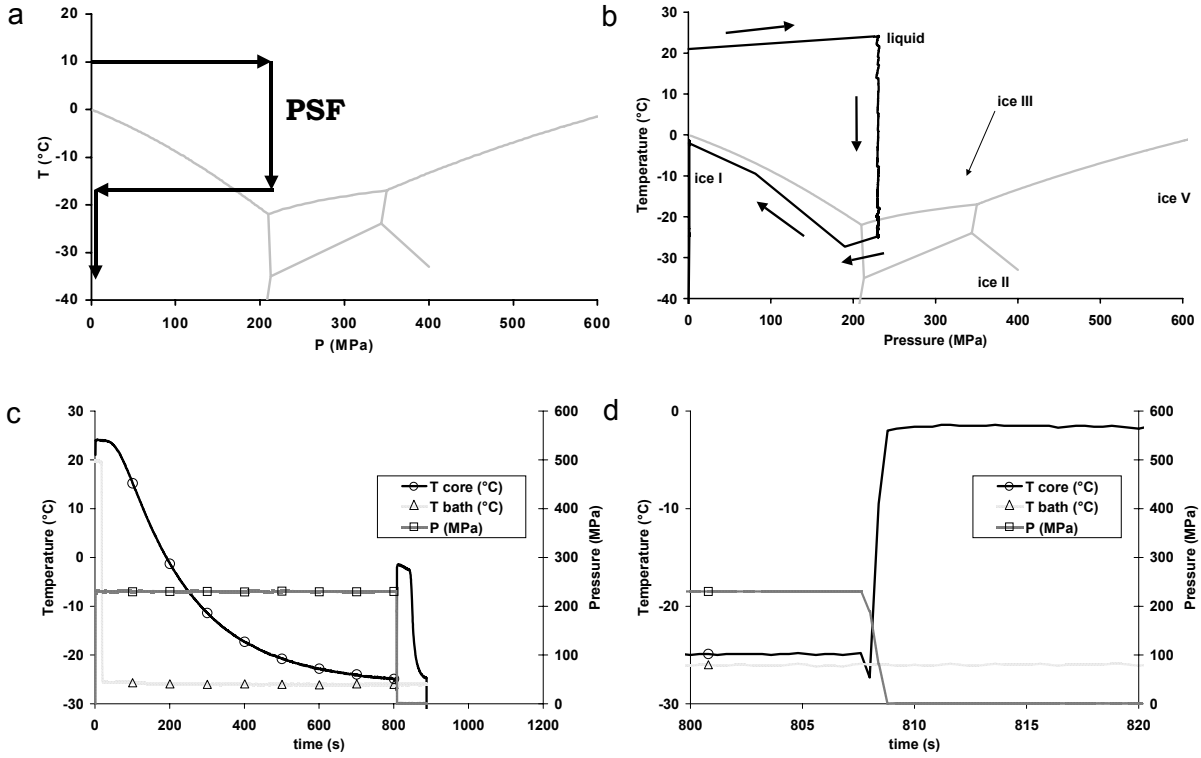

Figure 4.36. Schematic path for pressure-shift freezing (PSF) (a); experimental path (b), temperature and pressure profile (c) and detail of nucleation (d).

Pressure-induced freezing (PIF) is a process that involves the induction of a freezing phase change by pressure increase. Ice I cannot be obtained through this process, as the phase transition temperature decreases with pressure and, therefore, pressurization cannot induce ice I crystallization. This is a process only applicable for higher ice modifications. The schematic paths for this term are shown in Figure 4.37a. Figure 4.37b shows an experimental path for PIF to ice V. First, the sample was cooled to +10 °C and then pressurized to 200 MPa. A second cooling step was performed then in order to reach conditions of –24 °C and 220 MPa. From this point, the (still) unfrozen sample was pressurized until crystallization of ice V, occurred at 500 MPa. Then the frozen sample was thawed at constant pressure. Figure 4.37c shows the corresponding profiles and Figure 4.37d shows a detail of the crystallization of ice V, easy to identify through the jump to the corresponding freezing plateau.

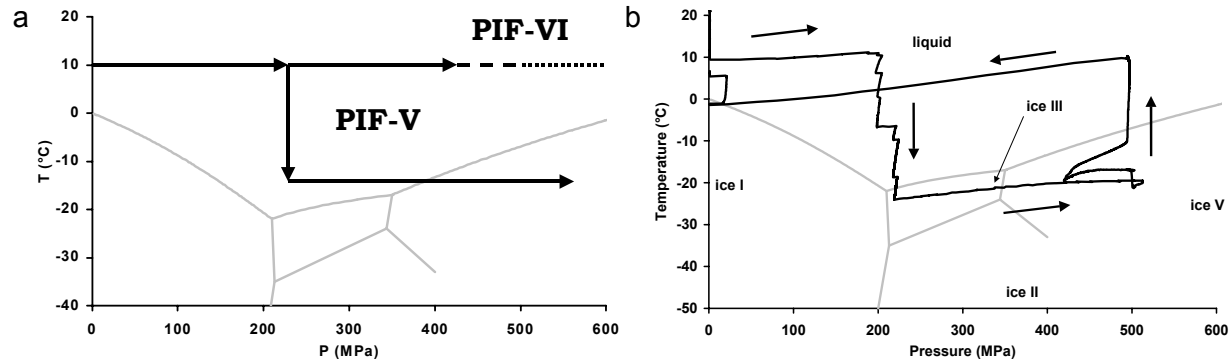

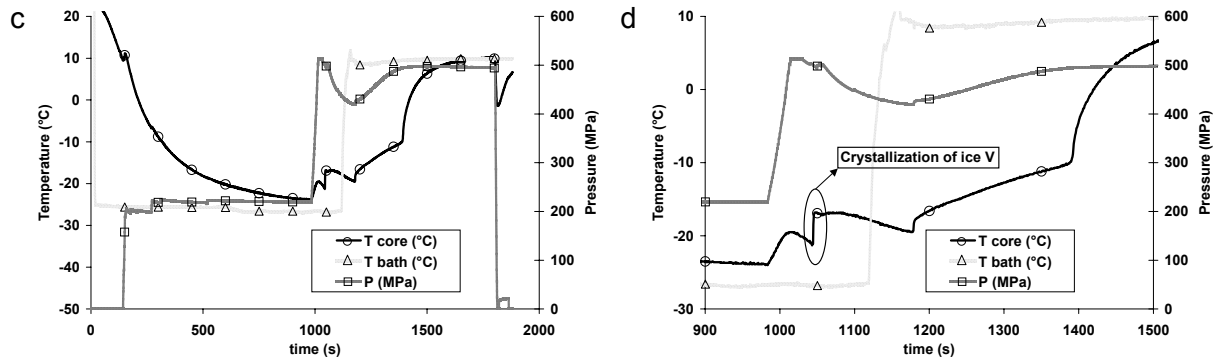

Figure 4.37. Schematic paths for pressure-induced freezing (PIF) to ice V and ice VI (a), experimental path for PIF-V (followed by pressure-assisted thawing, PAT) (b) and temperature and pressure profile (c) and detail of nucleation (d).

Pressure-assisted thawing (PAT) describes a process in which a sample is thawed at a constant pressure, the difference between the sample and the bath temperature being the driving force for this process. The term pressure-assisted thawing should be exclusively used for processes in which a frozen sample is heated under nearly constant pressure starting at a sample temperature below the melting curve of interest (e.g. ice I, ice III, ice V). Moreover, only the processes in which no melting of ice I is induced during pressurization have to be included into this category. Figure 4.38 shows the example of a schematic path of this process, together with the experimental curves, corresponding to the PAT of ice I at 100 MPa. The thawing process is considered completed when the temperature of sample centre achieves +10 °C. This criterion is taken after considering the adiabatic cooling of samples after pressure release. Samples should reach +10 °C to avoid crystallization of ice I after pressure release.

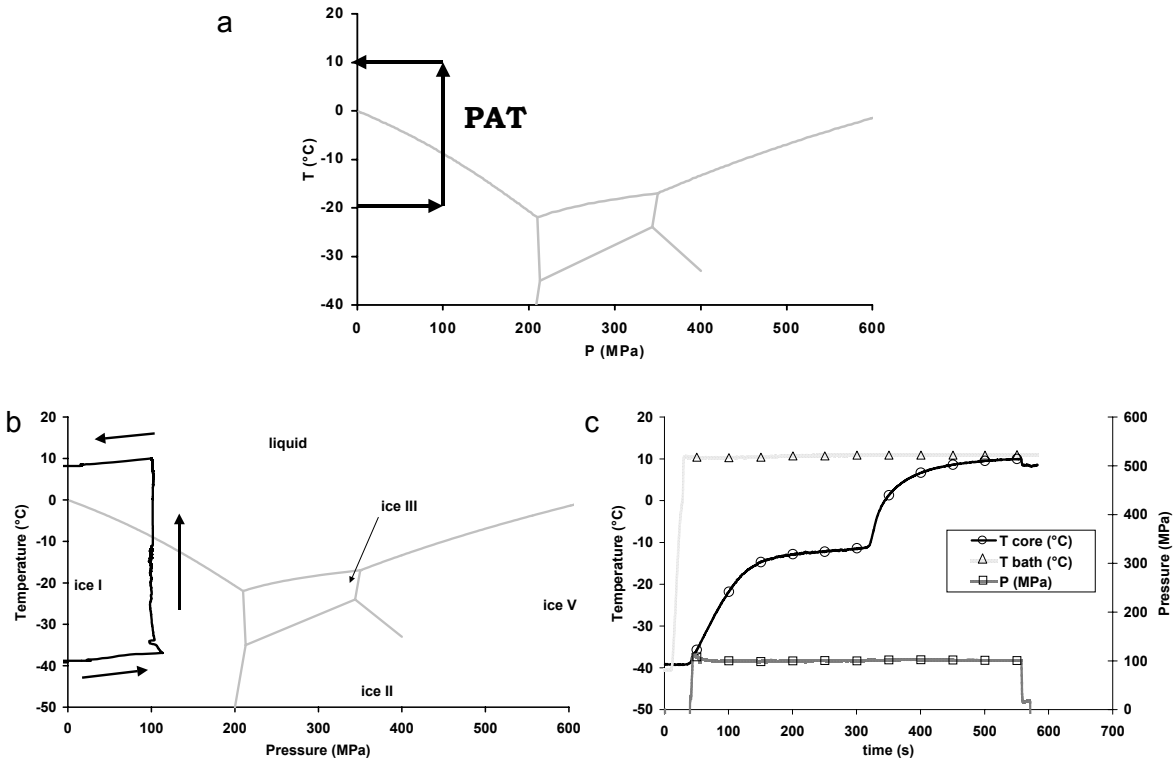

Figure 4.38. Pressure-assisted thawing (PAT), only valid for the domain of ice I: schematic path (a), experimental path (b) and temperature and pressure profile (c).

A special case of PAT is the one involving higher ice modifications. For example, the pressure-assisted thawing from ice III (PAT-III). This special case of PAT should involve a high pressure storage in the corresponding higher ice modification or solid-solid phase transitions. In the first case, samples which are previously frozen to ice III (for example) can be kept or stored at high pressure and then thawed at the same pressure level. In the second case (more feasible and realistic), the sample comes from a frozen state at atmospheric pressure and then, through a pressurization, a first solid-solid phase transition (ice I to ice III) takes place and then, PAT can occur starting from a frozen higher ice modification. Figure 4.39a and Figure 4.39b show the schematic paths for both processes and Figure 4.39c and Figure 4.39d, the experimental paths for the process with a solid-solid phase transition, with a pressure level of 300 MPa and an initial temperature of –40 °C. A frozen sample, in the domain of ice III, is thawed at constant pressure forced to a temperature gradient. The existence of ice III is obtained through the pressurization of a sample at atmospheric pressure to the domain of ice III, occurring a solid-solid phase transition ice I to ice III.

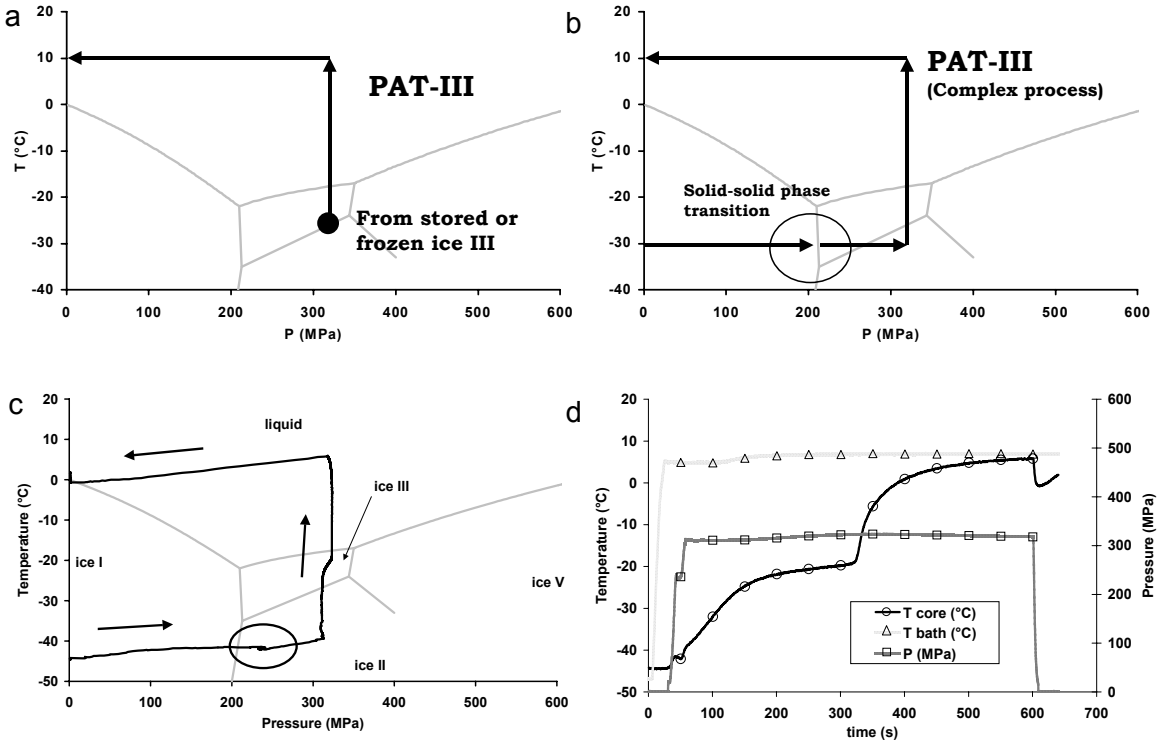

Figure 4.39. Pressure-assisted thawing from ice III (PAT-III): schematic path of the process after frozen or stored ice III (a); schematic path with a solid-solid phase transition remarked with a circle (complex process) (b); experimental path (c) and temperature and pressure profile (d) for the complex process.

Depending on the final pressure level and the initial temperature at which a frozen sample at atmospheric pressure is pressurized, a solid-solid phase transition or a partial melting of samples can occur. The exact limits of the *pT* combinations leading to one or to another process are out of the scope of this paper. Anyway, the possibility of "inducing" through pressurization the partial melting of ice I into liquid is considered as a process itself: a pressure induced thawing:

Pressure-induced thawing (PIT) describes a process based on the principle that, as opposed to pressure-shift freezing, a frozen product can be forced to a phase transition from ice to liquid water by applying pressure along the melting curve of ice I. Due to the prolongation of the melting curve of ice I in the domain of ice III, this process can be also obtained with pressure levels above 210 MPa. The process (PIT), as described, makes reference only to the melting of ice I during pressurization, but, after this

induced melting (that is often only partial, not homogeneous within the sample and depending on sample size and heat transfer conditions), further thawing should take place, at constant pressure (PAT). This second part of the process may be assumed as an assisted process, but **the term PIT includes both induction of melting by pressure increase and the subsequent thawing at constant pressure**. Figure 4.40 shows schematic and experimental paths, together with the corresponding temperature profile. Figure 4.40a shows two different paths: the dotted line refers to a PIT process in the domain of ice I; the continuous line shows a PIT in which the sample is in the metastable region of ice I. In this last case, the sample follows the extended phase transition line of ice I as often reported in the literature, but the same terminology will be used for such a case. The experimental paths from Figure 4.40b and Figure 4.40c are referred to the dotted line and the paths shown as Figure 4.40d and Figure 4.40e to the continuous line (in the domain of metastable ice I). Regarding the experiments, it can be summarized that samples pressurized from an initial temperature of –35 °C undergo a solid-solid phase transition and samples pressurized from an initial temperature higher than –25 °C undergo a partial melting of sample surface.

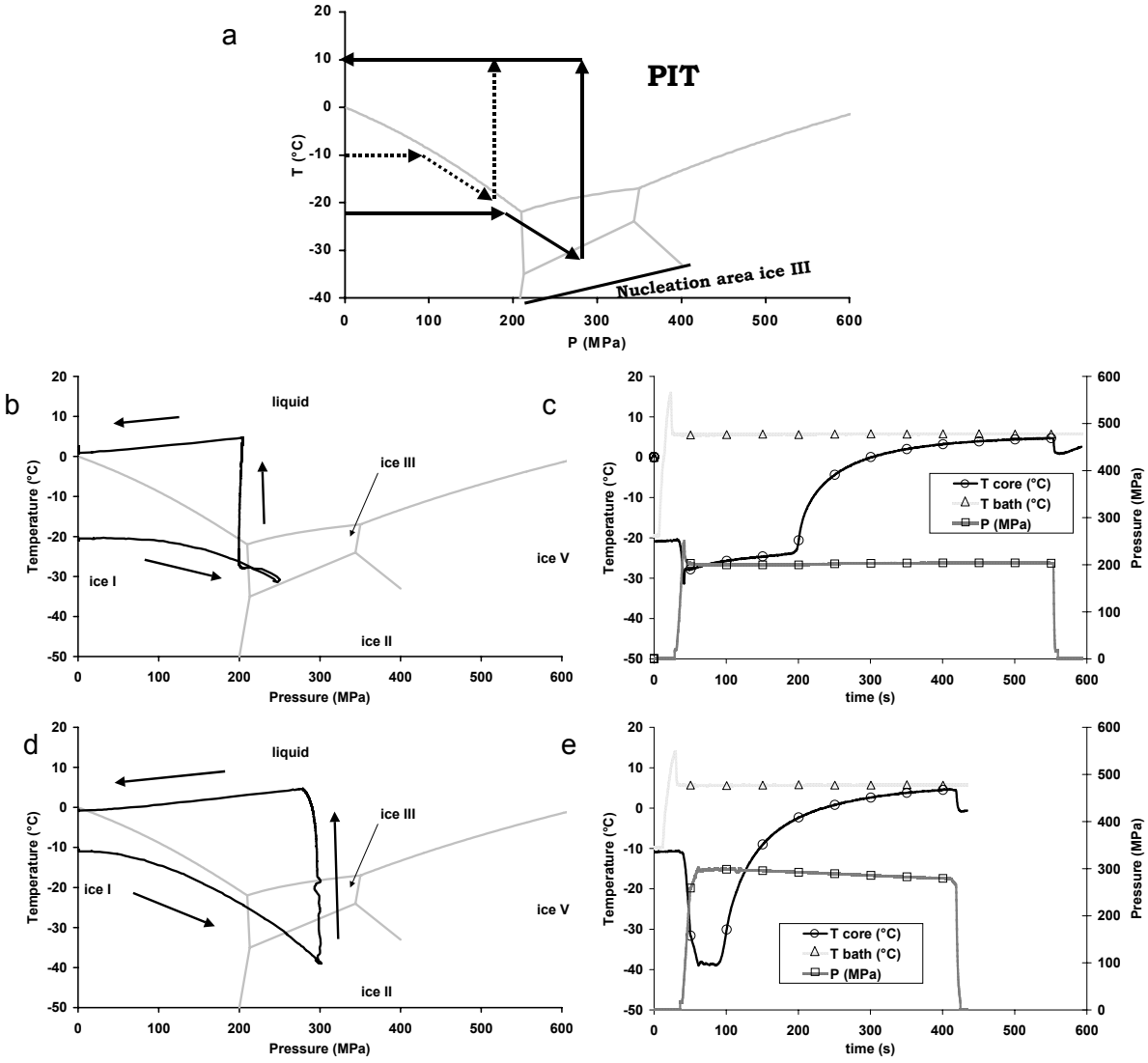

Figure 4.40. Pressure-induced thawing (PIT): schematic path of thawing of ice I (a) in the domain of ice I (dotted line, PIT) and in the domain of ice III (full line, PIT*), experimental path (b) and temperature and pressure profile (c) for the dotted line case and experimental path (d) and temperature and pressure profile (e) for the continuous line case.

The actual difference between PAT and PIT should be taken as the difference in the pressurization step. For PAT, the pressurization step does not lead to a partial melting of sample surface and for PIT, there is indeed a partial melting during pressure increase. Then, in both cases the process is completed by thawing at constant pressure. Therefore, PAT is composed of pressurization (without melting) and thawing at constant pressure, and PIT is composed of pressurization with partial melting and thawing at constant pressure. Although PIT is actually the sum of an induced partial thawing and an assisted thawing, the whole process is defined and named PIT.

A special case of PIT can be described if pressure is further increased. In this case, the sample temperature, following the extended melting curve of ice I, can reach the area of nucleation of ice III. In this case, ice III may be crystallized and, therefore, a jump in sample temperature is expected at the corresponding ice III transition line: a pressure-induced crystallization of ice III is then obtained. From this point, an assisted thawing of ice III is performed at constant pressure. Although the process is actually the combination of PIT + PIC-III + PAT-III, the whole process is named PIC-III (as special case of PIT). Figure 4.41 shows the schematic and experimental paths of this process. During pressurization, the sample surface melts. This liquid water at the surface is able to crystallize when the area of nucleation of ice III is reached. When ice III first nucleates, the amount of ice I in the sample seems to convert to ice III immediately probably adapting to the first nuclei. It has been experimentally recorded that the sample centre temperature reaches instantaneously the phase transition temperature of ice III for the corresponding processing pressure, as shown in Figure 4.41c.

The experimental curves obtained for PAT-III coming from atmospheric pressure (Figure 4.39c and Figure 4.39d), for PIT in the domain of ice III (Figure 4.40d and Figure 4.40e), and for PIC-III (Figure 4.41b and Figure 4.41c) are all related to a set of processes in which, actually, as these processes involve a pressure increase, then a positive temperature gradient, and finally a pressure release: $+\Delta P$, $+\Delta T$ and $-\Delta P$. The only difference between these three processes lies in the combination of initial temperature and working pressure. For PIT (in the domain of ice III), the initial temperature (-10 °C) is above a critical value (T_C), and for PAT-III the initial temperature (-40 °C) is below this T_C, occurring then a solid-solid phase transition. In both cases, the working pressure was 300 MPa, but in one case, starting form –10 °C, at a pressure around 40 MPa the temperature starts to decrease due to partial melting and in the case starting at –40 °C, the temperature increases with pressure with no melting until the phase transition line between ice I and ice III is reached. In the third case (PIC-III), a similar process as PIT is performed, with the only difference that here the area of nucleation of ice III was reached. The final pressure overcame a critical pressure (P_C) at which the extended phase transition line of ice I and the upper level of the area of nucleation of ice III are crossing. All these three processes are schematically explained in Figure 4.42.

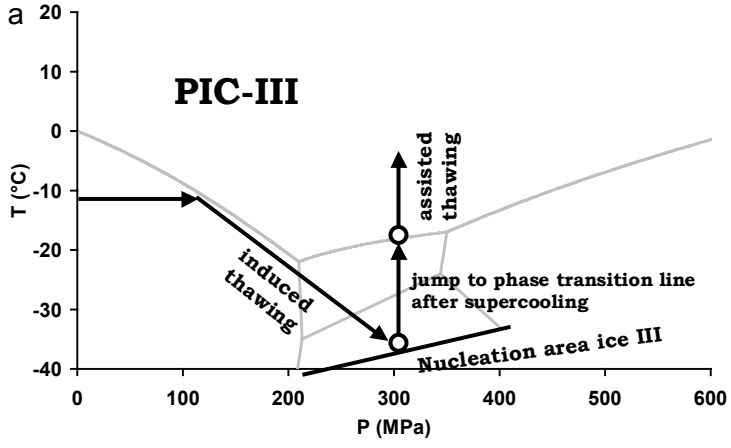

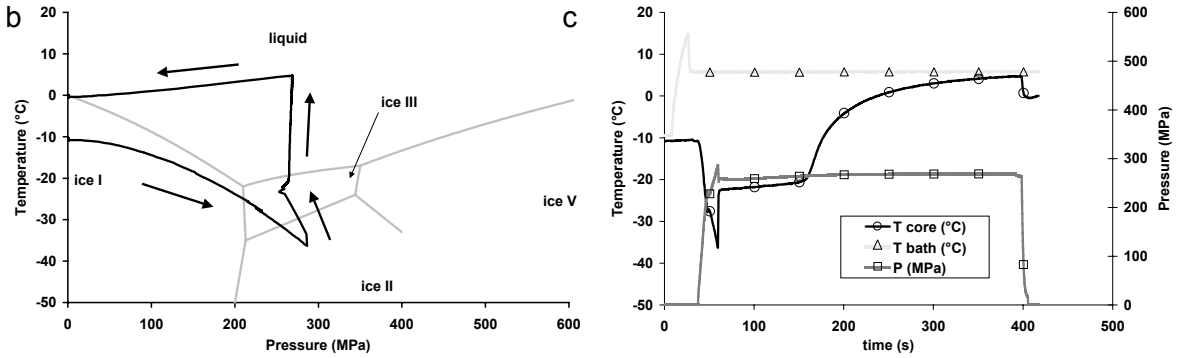

Figure 4.41. Pressure-induced crystallization of ice III (PIC-III): schematic path (a), experimental path (b) and temperature and pressure profile (c).

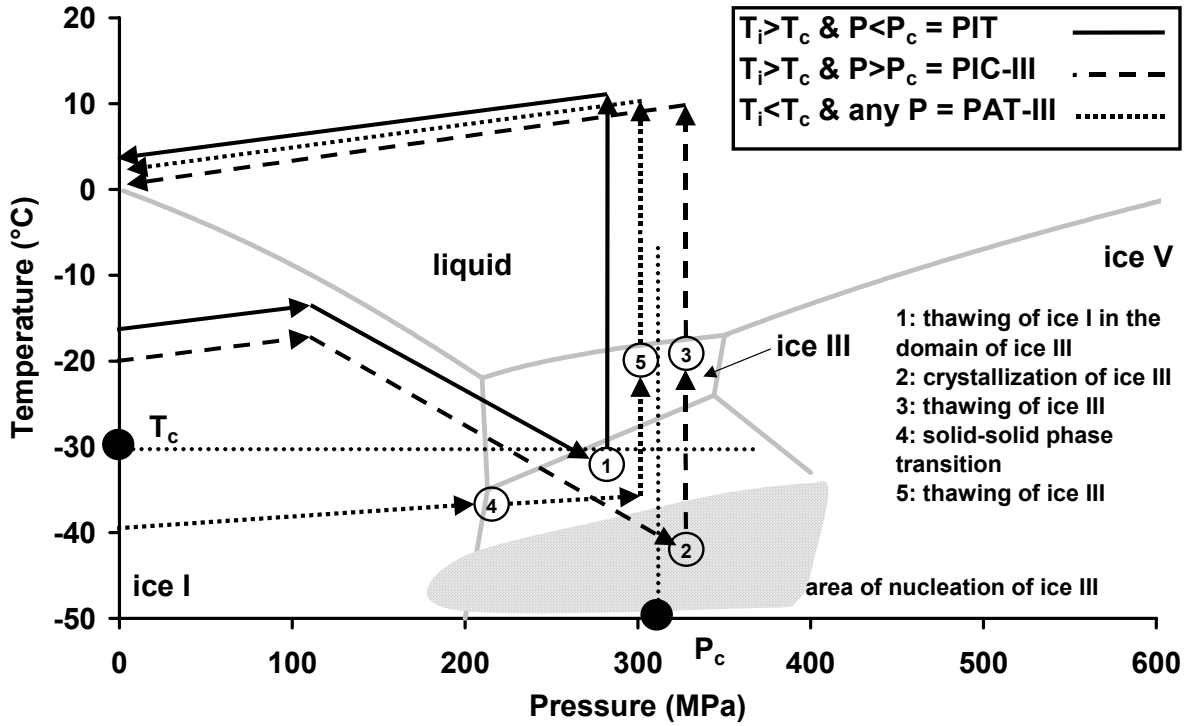

Figure 4.42. Influence of initial temperature and working pressure on the obtained paths: PIT (of ice I in the domain of ice I), PIC-III (special case of PIT) and PAT-III (with solid-solid phase transition).

Finally, the **pressure-shift thawing (PST)** will be described. As previously defined, (Cheftel et al., 2002) pressure-shift freezing is a process where crystallization is induced simultaneously in the entire sample by fast pressure release. Therefore, when thawing of an entire sample is induced by a fast pressure release, a new process should be defined: pressure-shift thawing. Figure 4.43a shows the schematic path for this new defined process. After performing a classical pressure-assisted freezing to ice V at 500 MPa (we first need a frozen sample in a high ice modification), pressure is instantaneously released. Then, the bath temperature was changed to thawing conditions and after the pressure release, the sample temperature follows the melting curve of ice V. This curve is followed through an extension into both ice III and ice I thermodynamically stable domains, in a similar way as ice I had an extension into ice III domain. Therefore, the sample thawing path follows this extended melting curve of ice V until the first nucleation area for another ice modification is reached, corresponding, in this case, to ice I. Figure 4.43b and Figure 4.43c show the path and temperature profile for this process. Relatively fast pressure release, lower depressurization rate

should lead to clearer results since then the equilibrium line should be reached by the sample temperature. To better observe this fact, Figure 4.43d shows the detail of the temperature decrease while the ice V phase transition line is followed and the instantaneous jump when ice I nucleates. The water in sample surface begins with ice I nucleation and then, the crystals appear in the whole sample: both sample surface and sample centre temperatures have the same values just after the nucleation of ice I, showing that nucleation took place uniformly in the whole potato cylinder. Finally, when pressure is completely released, an atmospheric pressure thawing process from ice I to water takes place (thawing temperature around -1 °C).

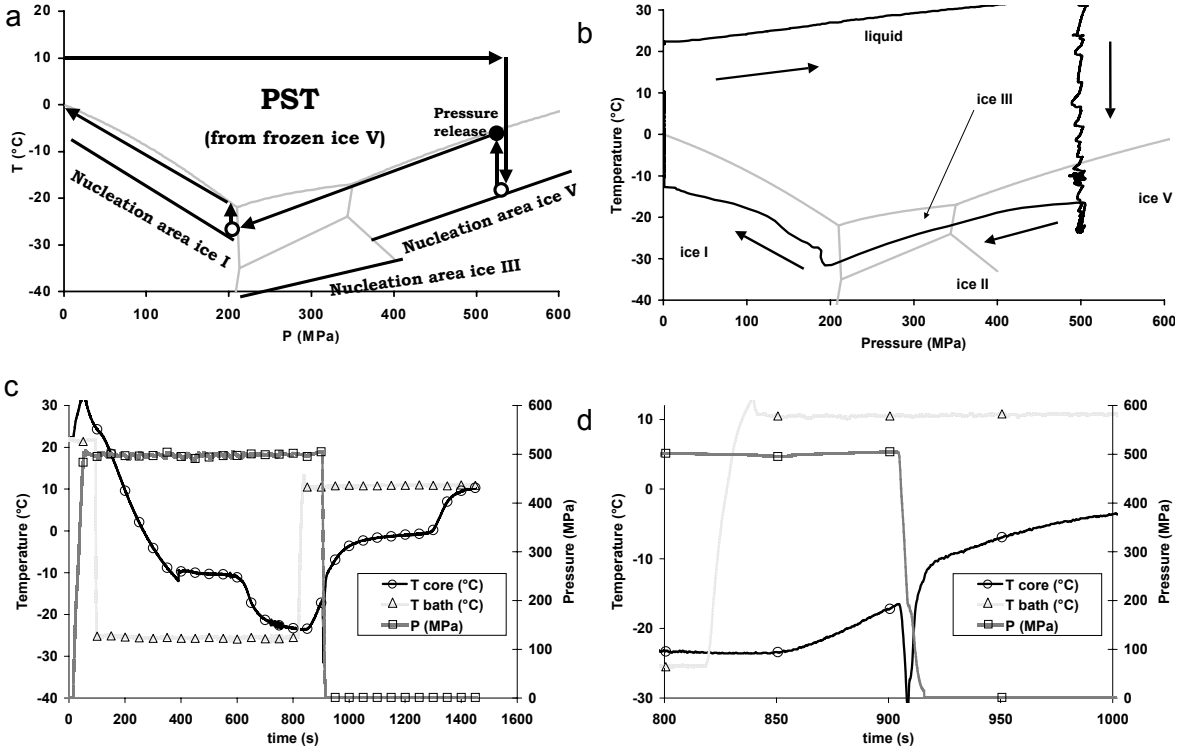

Figure 4.43. Pressure-shift thawing (PST): schematic path (a), experimental path (b), temperature and pressure profile (c) and detail of temperature and pressure profile (d).

Summarizing, Figure 4.44 shows the suggested nomenclature, with all the examples treated. The nomenclature suggested is shown in Table 4.1.

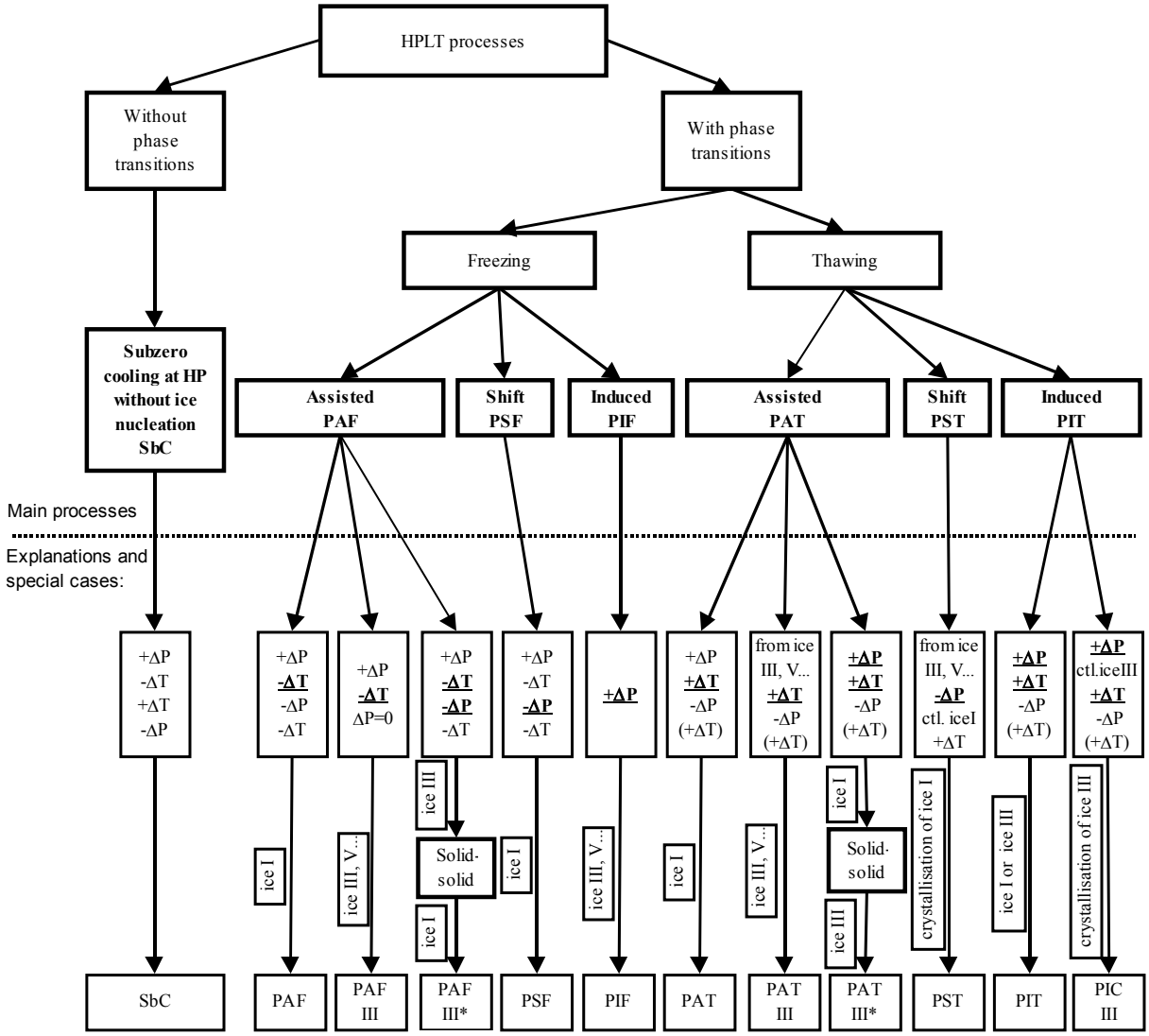

Figure 4.44. Schema of definition of processes, with all studied cases. The phase transition steps are underlined.

Table 4.1. Suggested nomenclature for HPLT processes

Name	Process description	Special cases
SbC	Subzero cooling at high pressure (without crystallization)	
PAF	Pressure-assisted freezing (to ice I)	PAF-I
	Pressure-assisted freezing to higher ice modifications	PAF-III, PAF-V
PSF	Pressure-shift freezing (only possible to ice I)	
PIF	Pressure-induced freezing (only possible for higher ice modifications)	PIF-III, PIF-V
PAT	Pressure-assisted thawing (from ice I)	PAT-I
	Pressure-assisted thawing from higher ice modifications	PAT-III, PAT-V
PIT	Pressure-induced thawing (in the domain of ice I)	PIT
	Pressure-induced thawing (ice I thaw in the domain of ice III)	PIT*
	Pressure-induced crystallization of ice III	PIC-III
PST	Pressure-shift thawing (only possible from higher ice modifications)	PST-III, PST-V

4.3. Modelling of HPLT processes

4.3.1. Thermodynamic properties

Understanding phase transition during high pressure processing of foods is important both with respect to optimizing the process and improvement of product quality, but scientific information available in this area is very limited (Zhu, 2004). Good knowledge of the thermophysical characteristics of a wide range of foodstuffs has a major importance in the accurate prediction of their unsteady-state temperature distribution, the process duration and energy consumption in cooling and freezing or heating and thawing (Kostadin, 1999). Tests have been carried out with potato tissue under isothermal conditions with constant pressure increase rate. In high pressure calorimetry the pressure change is used to obtain the desired phase change at constant temperature.

A typical isothermal pressure scan experiment (P-scan) consisted in placing sample and reference water in both cells of the calorimeter. The sample is first frozen at the initial set temperature and after stabilization of the signal, pressure was increased from atmospheric level to the set value at a constant rate of 0,5 MPa/min. During the pressure increase, the calorimetric signal was constant until a decrease appears when a partial melting of the sample occurs. This calorimetric signal is given by the temperature difference between the reference sample (water) and the potato tissue sample.

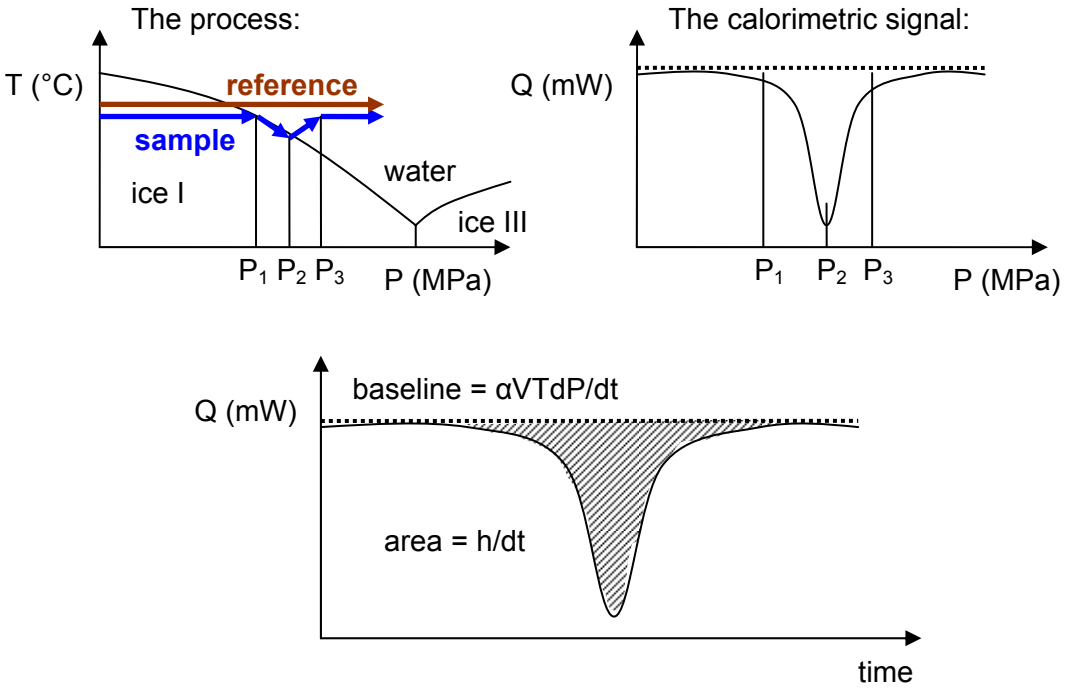

Figure 4.45. Schematic diagrams of a P-scan calorimetric experiment and the calculation of the corresponding latent heat.

The heat dissipated during temperature and pressure changes is given by the thermodynamic equation:

$$\partial Q = c_p \partial T + h \partial P \qquad (4.2)$$

where c_p is the heat capacity and h the latent heat.

For an isothermal process, the heat dissipated during compression, when phase changes occur is given by:

$$\frac{dQ}{dt} = \alpha VT\frac{dP}{dt} + h\frac{1}{dt} \qquad (4.3)$$

where α is the isobaric expansion coefficient, V the volume of the sample and h is a term expressed by $(dU/dP)_{Tconstant}+(dV/dP)_{Tconstant}$.

Figure 4.45 shows the typical way to calculate the latent heat of fusion from the area (integral) under the calorimetric signal curve.

Figure 4.46 shows two examples of experimental calorimetric curves.

a

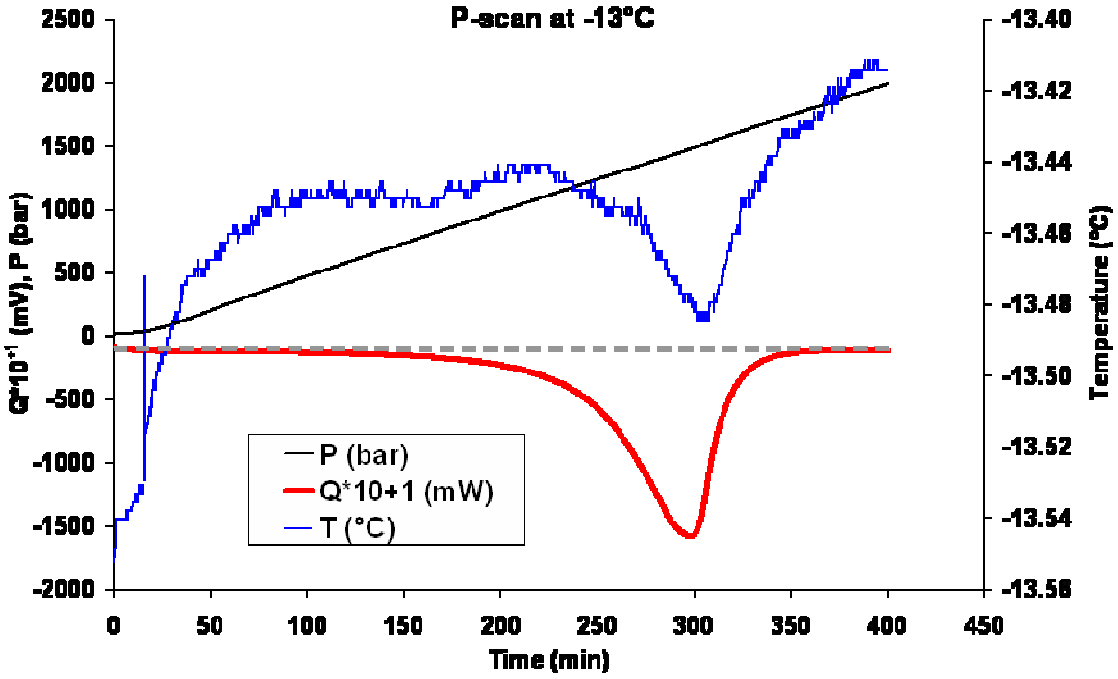

b

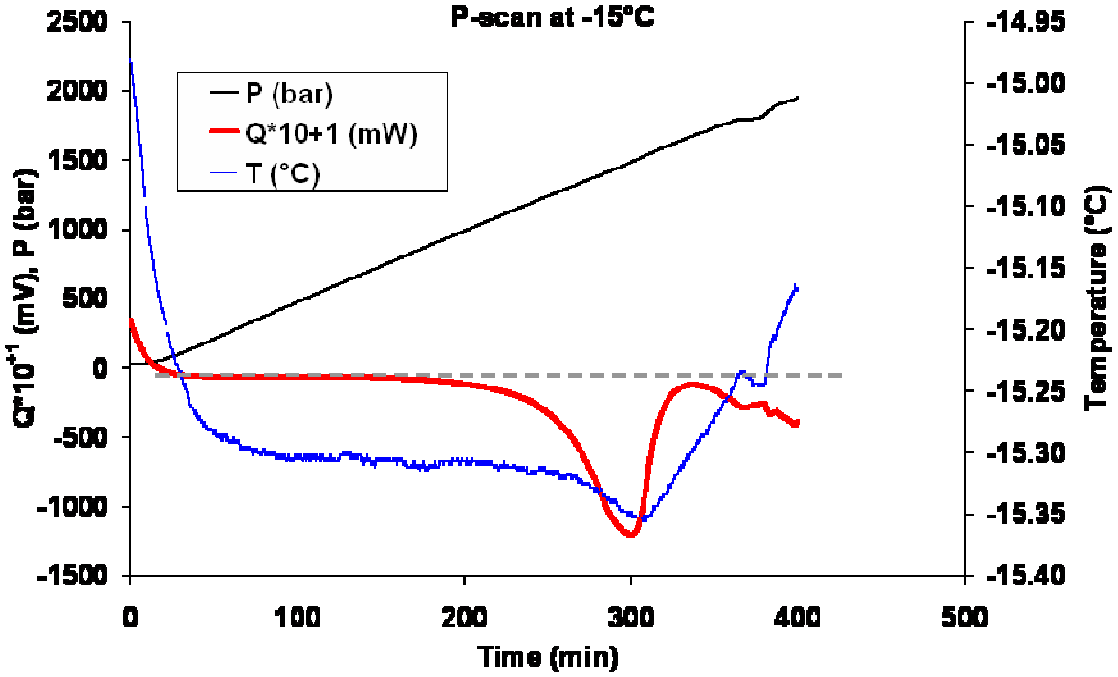

Figure 4.46. Experimental curves of calorimetric pressure scans at (a) -13°C and (b) -15°C.

A summary of the calculated values are shown in Table 4.2. Experimental values of latent heat of water and potato at high pressure..

Table 4.2. Experimental values of latent heat of water and potato at high pressure.

T (°C)	L water (kJ.kg^{-1})	L potato (kJ.kg^{-1})
-3,7	-313,4	-238,0
-10.0	-283,4	-280,4
-13.5	-268,0	-441,9
-15.0	-261,3	-289,8
-15.5	-259,2	-347,1
-18.0	-248,6	-292,2

4.3.2. Processing time definitions

4.3.2.1. Freezing

Related to the processing time, several numeric prediction methods were reported in the literature, but mainly for atmospheric conditions (Agnelli and Mascheroni, 2001, Mannapperuma and Singh, 1988, Pham, 1985, 1987, 1989 and 1996, Chung and Merritt, 1991, Sanz *et al.*, 1999, Cleland and Earle, 1984, Miyawaki *et al.*, 1989, Franke, 2000, Martens *et al*., 2001, Bon *et al.,* 2001). Few reports have been published for numerical modelling of high pressure supported freezing processes.

Denys *et al*. (1997 and 2000) used a numerical solution for two-dimensional heat transfer for finite tylose (23% (hydroxymethyl) cellulose gel) cylinders, at 66.4, 114.5, 168.6 and 230.8 MPa. Here, pressure-shift freezing was studied, thus, no higher ice modifications were obtained, and all the curves (therefore all the plateaus) had the same freezing temperature corresponding to atmospheric pressure. Schlüter *et al*. (1998) fitted pressure-assisted freezing curves obtained for potato cylinders during high pressure treatment at 50, 100 and 150 MPa by using a finite difference numerical procedure (radial symmetrical one dimensional heat conduction) and reported a necessity of modifying both the literature values of the apparent specific heat and the thermal conductivity of potato tissue. The peak value of the apparent specific heat function (Weibull) was markedly reduced at high pressure but the general shape of the applied distribution of the specific heat could be retained. Sanz and Otero (2000) applied a mathematical model in three steps (pre-cooling, phase change and tempering) based on Chung and Merritt (1991) transient state heat transfer equations for finite agar gel (99% water) cylinders and based on the Newmann's rule for finite geometry, at 92, 130, 180 and 210 MPa. In this case, as the model was divided in three steps, the predictability of the jump to the plateau temperature after super-cooling is lost, and only pressure-shift freezing was studied to compare the overall process times with higher or lower degree of super-cooling.

Divergent results concerning the processing time can be found in literature due to different definitions of the freezing time. Substantial reductions in the freezing times of high pressure-assisted freezing experiments have been described (Murakami *et al.*, 1992) in comparison with the times required to complete the same processes at atmospheric pressure, but the opposite has been also reported by Levy *et al.* (1999).

Consequently, to compare the various results a differentiation of "processing time", "freezing time" and "crystallization time" is required. Delgado and Sun (2001) suggested two definitions for freezing times: the "*nominal freezing time*" for a given product, with uniform initial temperature of 0 °C, is the time the thermal centre takes to

reach a temperature of 10 °C below the initial freezing point; the "*effective freezing time*", also known as "*standard freezing time*" or "*holding time*" is the total time required to lower the product temperature from its initial value to a given final one at the thermal centre. The former definition is related to the product quality since it considers the time for ice formation, while the latter is related to the total time in which the product remains in the equipment.

For pressure supported freezing processes the overall "processing time" can be defined as the sum of several time steps due to: loading (initial product temperature), pressure built up, pressure holding (temperature decrease, pressure-assisted freezing), pressure release (temperature decrease, pressure-shift freezing), taking out and subsequent storing (final freezing step, final product temperature). Since the phase transition is assumed to mainly affect the tissue especially the freezing step is of particular importance. The "*freezing time*" will be defined here (for all cases) as the time in which the temperature of the sample centre reaches a value 18°C lower than the corresponding phase transition temperature starting from the initial temperature experimentally set to 25 °C above the freezing point independent of the applied pressure level. This temperature difference would be more appropriate than the already reported 10 °C (Cleland and Earle, 1984) as food products are defined as frozen at temperatures below –18 °C.

The phase transition time ("plateau" time) will be defined as the time span between nucleation and reaching a sample temperature (centre) 5 °C below the corresponding initial freezing point. This definition is based on results given by Fikiin (1998) who calculated the ice content during freezing as a function of temperature using different models. An ice content of approx. 80 % can be estimated, when the product reaches a temperature 5 °C below the initial freezing point.

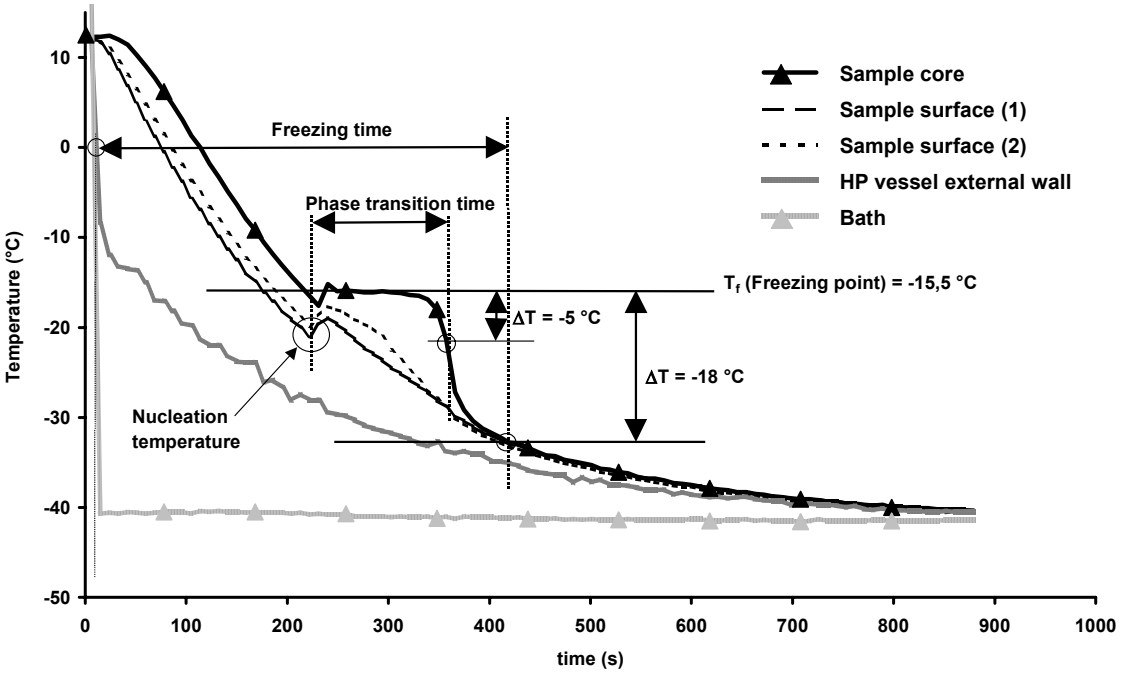

Figure 4.47. Definitions of phase transition time and freezing time on the example of a pressure-assisted freezing processes at 140 MPa.

The phase transition times were calculated from the time at which the wall temperature jumps (showing the beginning of nucleation) until the sample core temperature had reached –5°C with respect to the plateau temperature. The freezing time begins when the bath temperature goes to negative values and finishes when the sample core temperature reaches –18°C with respect to the corresponding plateau. In Figure 4.47,

an example of all the temperatures recorded is shown, together with the definitions for time calculations in the case of pressure-assisted freezing.

4.3.2.2. Thawing

The Thermistor-Cryoscope method (already described in previous paper, by Schlüter *et al*., 2004) was used in order to obtain the phase transition points in a p-T diagram. In every experiment, the sample temperature was recorded at three different points: once in the sample centre and twice in sample wall, in diametrically opposite points. Also, the temperature of the high-pressure vessel external wall and the bath temperature were recorded. An average value from the two wall temperatures was taken for further calculations in the mathematical model.

Thermistor-Cryoscope method will be used in order to obtain the phase transition points in a p-T diagram. In every experiment, the sample temperature was recorded at three different points: once in the sample centre and twice in the sample wall, in diametrical opposite points. Also, the temperature of the high-pressure vessel external wall and the bath temperature were recorded. An average value from the two wall temperatures was taken for further calculations in the mathematical model. In Figure 4.48, an example of all the temperatures recorded in a thawing process is shown. Together with the experimental recorded temperatures, the first derivative, in a 10-fold amplified order, of the core temperature is shown. The clear peak observed in the derivative is used as an accurate method to determine the phase change temperature.

In the case of pressure-supported thawing at $P>P_C$, a slightly different method to the one able for $P<P_C$ can be used to calculate thawing times and phase transition temperatures. The nucleation temperature of ice III is reached, and phase transition time should calculated from this point and until the pick obtained through the first derivative. Figure 4.48b shows the time definitions and the first derivative method for the cases in which crystallisation of ice III is induced during pressurisation.

The thawing times were calculated from the time at which the sample is introduced in the bath (start point of thawing in Figure 4.48), due to the pressure build-up process beginning, and until the sample core temperature has reached +10°C (final point in Figure 4.48).

a

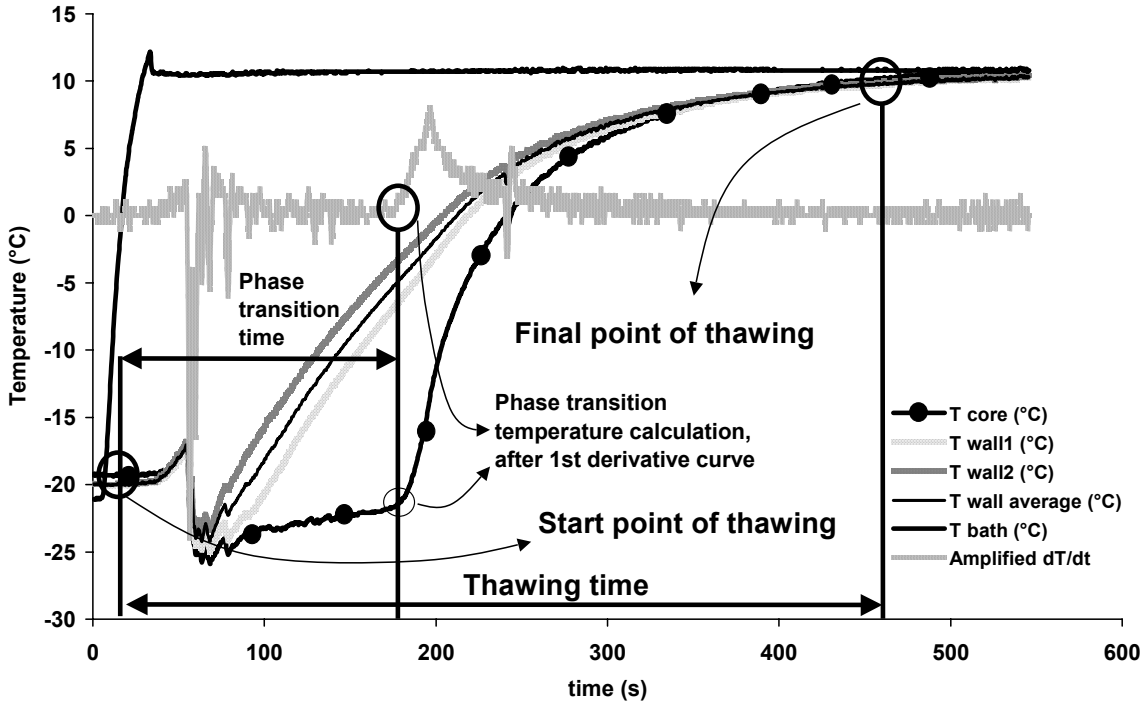

b

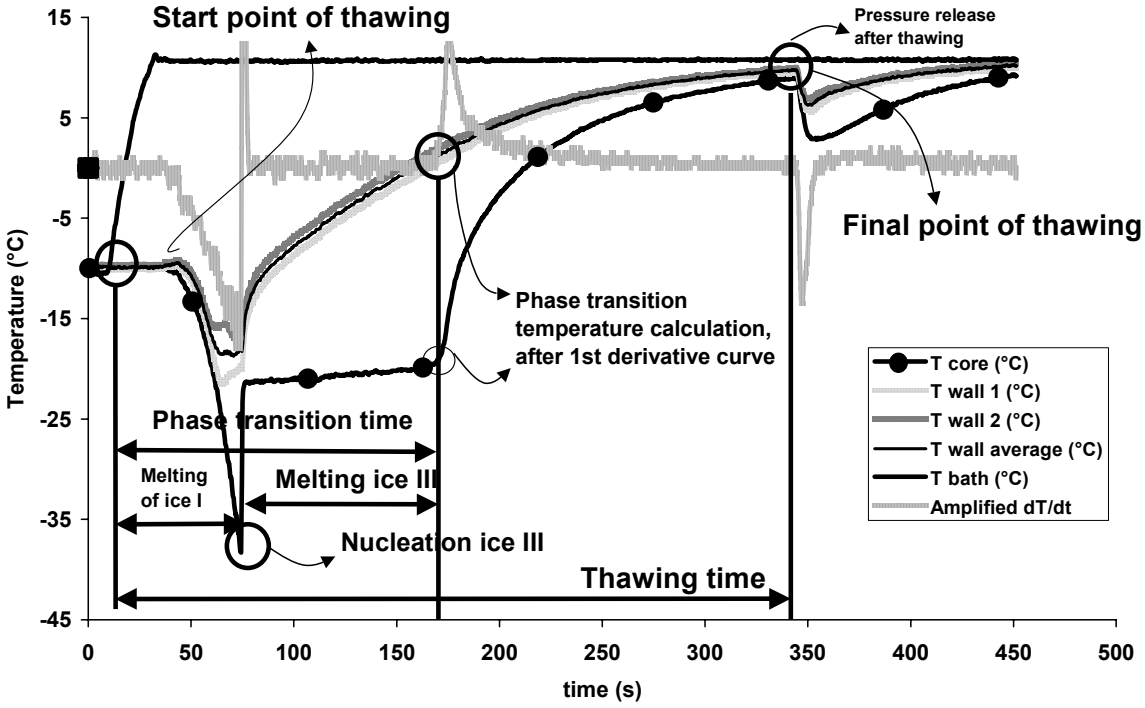

Figure 4.48. Definitions of thawing times with the Thermistor-Cryoscope method: criteria for time calculation, and method of the 1st derivative to determine phase transition time and temperature: a) for pressure-assisted thawing; b) for pressure-induced thawing.

4.3.3. Experimental results on freezing and thawing times

4.3.3.1. Freezing at laboratory scale

When studying the freezing time and the phase transition, the effect of the phase transition on food quality must be discussed, as this quality is directly related to the cell modifications and disruptions due to the formation of ice crystals. The faster the process of nucleation and propagation of the crystals, the lower the negative effects of the freezing process on food products' quality. This phase transition process speed is directly related to the degree of super-cooling. As reported by Luscher *et al*., 2003, freezing to ice III resulted in the lowest damaging effect on the tissue compared to the phase transition processes when ice I was involved. These results are thought to occur because of a decrease in volume during the phase transition and a lower latent heat of fusion.

Table 4.3. Experiments organization, experimental phase transition time, freezing time and experimental freezing temperature (T_f^{exp}) for laboratory scale experimental set.

		Experimental results			
Exp	P (MPa)	T_f^{exp} (°C)	Ice modif.	Ph. transition time (s)	Freezing time (s)
a	0.1	-1.0	I	88	390
b	140	-16.0	I	118	390
c	209	-24.5	I	109	595
d	255	-20.8	III	156	590

e	300	-20.0	III	76	845
f	225	-27.5	I	144	760
g	225	-22.9	III	150	511
h	225	-27.5/-23.5	I / III	328	671
i	240	-29.5/-23.0	I / III	158	443
j	PSF	-1.8	I	37	820

It can be concluded that as the freezing time grows with pressure (that is equivalent to the ice modification), the phase transition time ("plateau" time) reaches a maximum for ice modification I above 209 MPa (metastable zone) and has its minimum in ice III (for pressures lower than 209 MPa). The positive influence of applying high pressure on the time required to release latent heat was reported by Denys *et al*., 1997. This was explained as a combined effect of both the larger temperature gradient between high-pressure medium and sample and the higher nucleation rate (as a consequence of a higher degree of super-cooling). To understand this effect better, both the effect, both pressure and the degree of super-cooling must be related, as shown in Figure 4.49a.

However, in view of the faster and uniform nucleation, it was reported that crystallization occurs more homogeneously and that a better product is obtained in terms of texture (Fuchigami *et al*. 1997b and 1998). It should be noted that, since the sample has to be brought into the liquid state at negative temperature, the total time required for a high-pressure freezing process is larger compared to a classical freezing.

As mentioned before, a higher degree of super-cooling is assumed to lead to a shorter phase transition time, as the temperature gradient is then higher. Therefore, a correlation is expected between these two variables: phase transition time and degree of super-cooling. In Figure 4.49b, the experimental results for this correlation are shown.

It can be assumed that the effect of super-cooling is not beneficially affecting the reduction of phase transition times when ice I is crystallized, but a slightly positive effect is reached when ice III nucleates. These assumptions may fit with the calculation of instantaneous ice formed when the freezing temperature is first obtained after the super-cooling. After the considerations of Otero and Sanz (2000) and Chevalier *et al.* (2000b), the amount of ice instantaneously formed in a freezing process can be described after a heat balance:

$$m_w Cp_w \Delta T = L m_i \qquad (4.\ 4)$$

where m_w is the mass of liquid water, Cp_w is the specific heat capacity of liquid water at atmospheric pressure and 0 °C, ΔT is the super-cooling attained, L is the latent heat of water and m_i is the mass of ice. Taking these parameters with the corresponding values adapted for potato and the different pressures experimented, the results given in Figure 4.49c are obtained.

From this Figure 4.49a correlation can be described: the higher the pressure, the higher the super-cooling degree, specially for ice III crystallization (Figure 4.49a). Therefore, the higher the degree of super-cooling, the shorter the phase transition time, also clearly for ice III (Figure 4.49b), and finally, the amount of ice instantaneously formed in the freezing processes is always growing (both for ice I and ice III) as long as it does the degree of super-cooling (Figure 4.49c). It should be mentioned that the instantaneous amount of ice with respect to the degree of super-cooling for each pressure agree with those presented by Otero and Sanz (2000). Therefore, a direct

relation exist between pressure, degree of super-cooling, shortening of phase transition time, increase of product's quality and amount of ice instantaneously formed in the freezing processes.

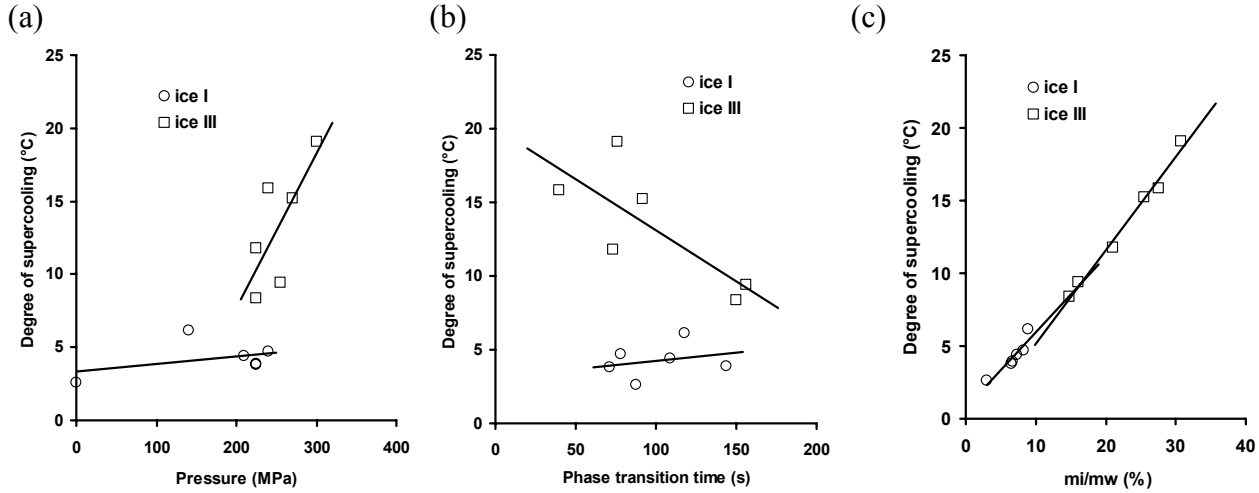

Figure 4.49. Correlation between super-cooling before freezing (to ice I and ice III) and (a): pressure level; (b): phase transition time; (c): ice content instantaneously nucleated (m_i/m_w).

4.3.3.2. Freezing and thawing at pilot scale

An experimental set performed for the evaluation of quality related parameters after processing has been also used to evaluate processing times in pilot scale.

Pressure, temperature and time were recorded every 0,2 seconds and some representative cases were already presented in Figure 4.50 in two type of diagrams: a time profile (left) and a process path (right) in the water phase diagram.

In Figure 4.50a and Figure 4.50b, the time profile for atmospheric freezing and thawing are shown. The corresponding paths on the phase diagram of water are not shown because only a vertical line at 0,1 MPa is observable for both cases. In the freezing profile, a little supercooling is observable and the corresponding little jump to the freezing temperature was obtained. Then, after the freezing plateau, the experiment was run until the sample temperature reached at least -18°C. In the case of thawing, after placing the frozen sample in the vessel, coming from storage chamber at -22°C, the temperature increased to a horizontal asymptote (thawing point). When melting was completed, the experiment was continued until the sample temperature reached +10°C.

In Figure 4.50c and Figure 4.50b the "conventional" PSF and PIT processes are shown and the paths clearly show that in the complete process, samples remain in the domain of ice I and liquid water.

Figure 4.50e and Figure 4.50f show PSF at 240 MPa and -28°C and PIT at 240MPa. In these cases it is already observable how, although the domain of ice III is reached, combinations of ice I and liquid water are still present in the whole process.

Finally, Figure 4.50g and Figure 4.50h show the PSF at 280 MP and -28°C and PIT at 290 MPa. For the PSF process, the temperature level reached before pressure release was the lowest reachable in the equipment used and the pressure level was selected not higher than 280 MPa to avoid possible ice III or ice V nucleation before pressure release. For the PIT process, the pressure level chosen is not higher than 290 MPa to avoid possible re-crystallization into ice III of the partial melted water in the sample surface during pressure build-up.

a) PSF at 200 MPa and -20°C

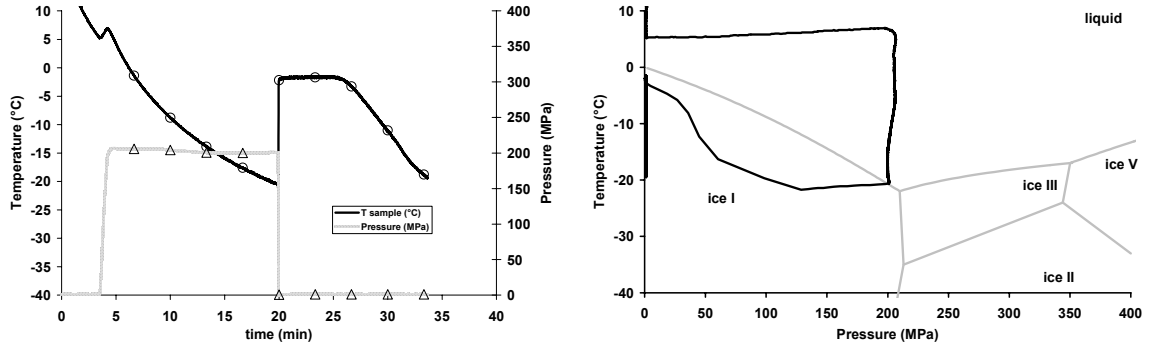

b) PIT at 200 MPa

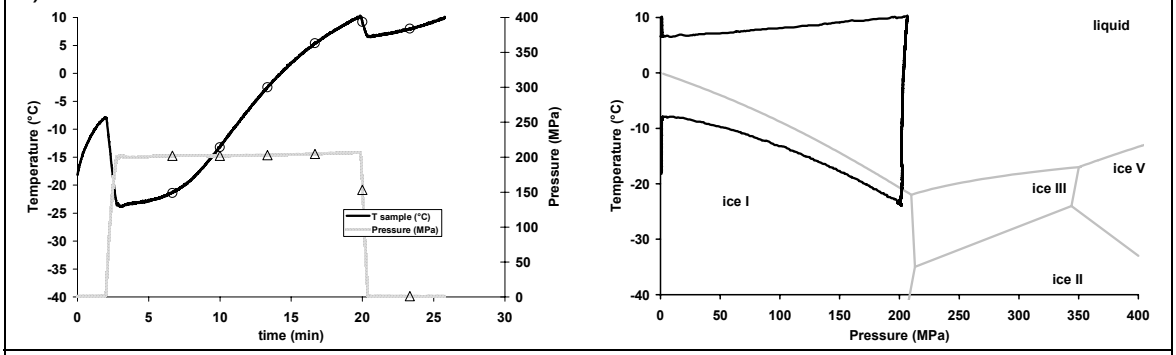

c) PSF at 240 MPa and -28°C

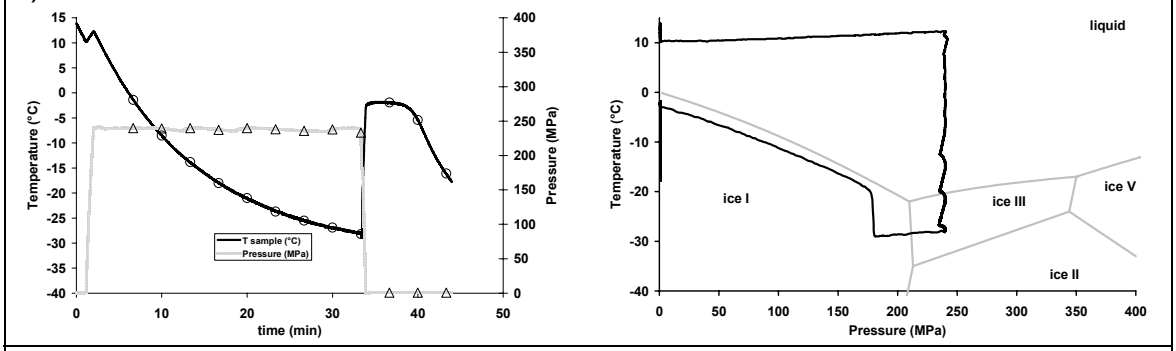

d) PIT at 240 MPa

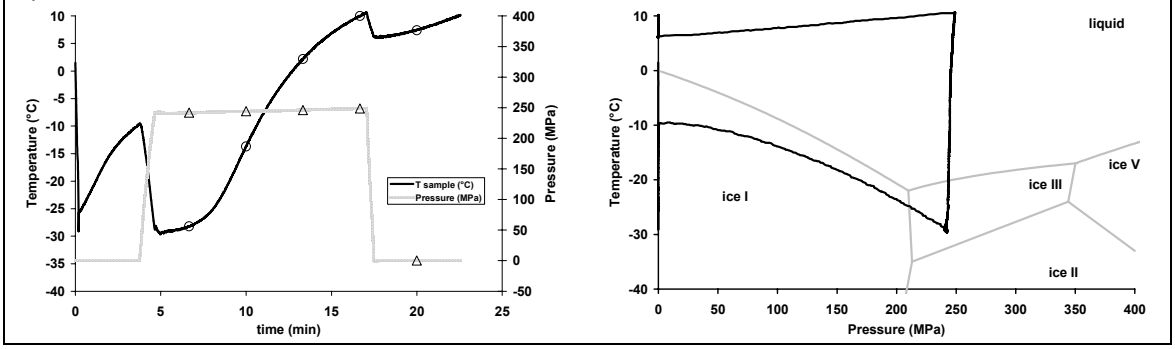

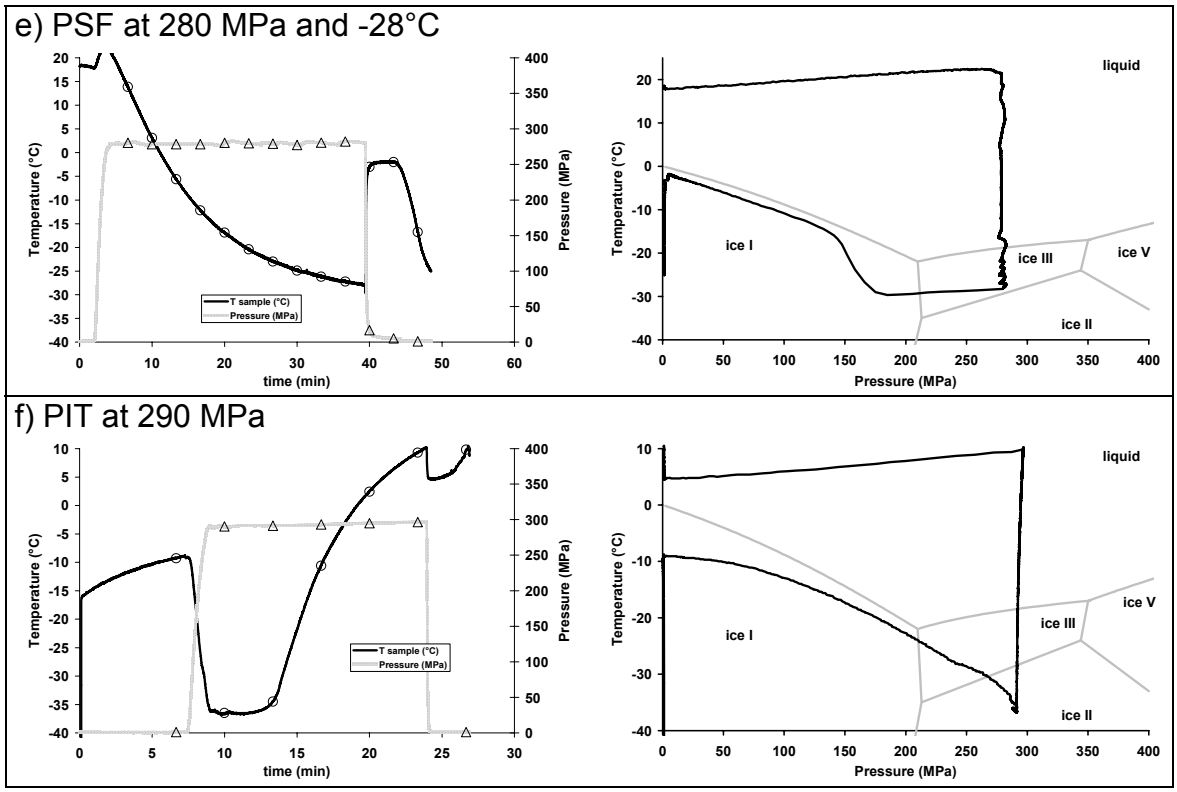

Figure 4.50. Representative examples of experimental time profiles (left) and paths on the phase diagram of water (right), for the pilot scale experiments.

In all cases, different processing times are calculated using time definitions introduced by Schlüter et al. (2004). The **freezing time** is defined as the time between data recording start (after placing the fresh sample in the vessel and proceeding to closure) and the time at which the sample temperature reaches -18°C, directly for atmospheric freezing or after pressure release for PSF processes. The **thawing time** is defined as the time between data recording start (frozen stored samples are first placed in the vessel and closure system is closed) and the time at which the sample temperature reaches +10°C, directly for atmospheric thawing processes or after pressure release for PIT. Finally, the **freezing plateau time** is defined as the time between the pressure release (for PSF processes) or the temperature jump (for atmospheric freezing processes) and the time at which the sample temperature reaches a level 5°C lower than the corresponding freezing temperature (in our case, for potatoes, -7°C at atmospheric pressure).

Using these time definitions, the freezing times, the freezing plateau times and the thawing times for all the recorded experiments (a total of 31 freezing-storage-thawing processes) are shown in Figure 4.51.

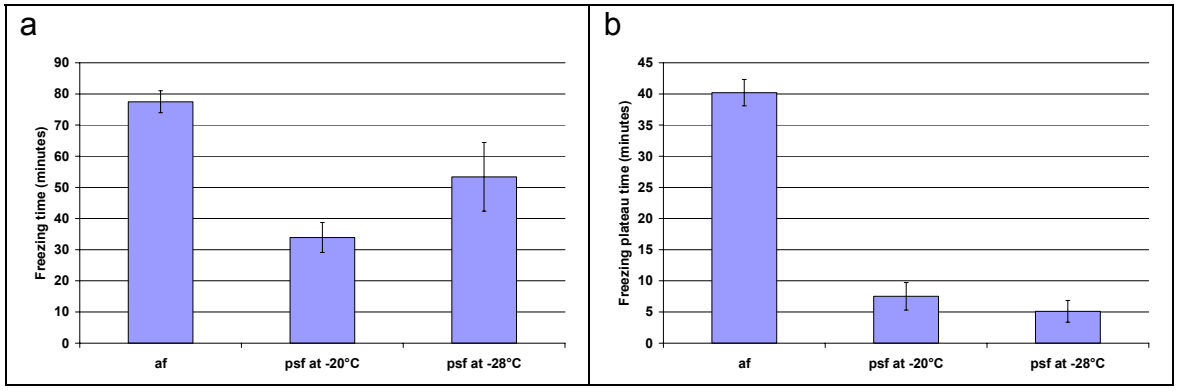

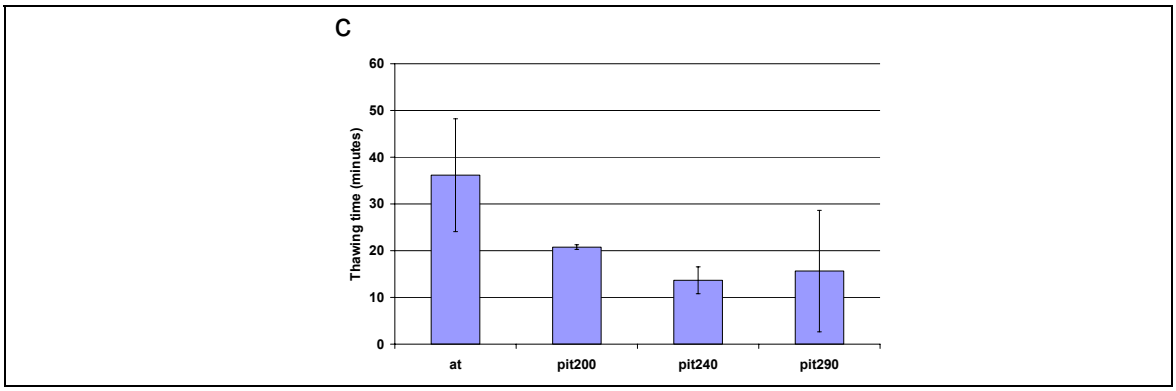

Figure 4.51. Processing times: freezing time (a), freezing plateau time (b) and thawing time (c) (see text for details on time definitions).

In the case of freezing times (Figure 4.51a), this value, for PSF processes, represents the 44% for PSF at -20°C and the 69% for PSF at -28°C with respect to the value for atmospheric freezing. This global process time reduction is of high interest for potential industrial applications, due to evident economical reasons. The freezing time for PSF -28°C is higher than the corresponding to PSF at -20°C due to the pre-cooling step (the step in which the set temperature must be reached at constant pressure before pressure release) because in both cases, the temperature of the cooling system was the same (the lowest available in the equipment used) and the time to reach -28°C is, evidently, longer than the time needed to reach -20°C.

Anyway, the direct relation between processed food quality and the freezing plateau time has been reported extensively in the literature: all disruptions of the cells and consequently, all texture damages occur during the phase transition from water to ice, that is, during the plateau. In Figure 4.51b the freezing plateau times are shown and it can be proved that the lower the set temperature before pressure release (freezing plateau time for PSF at -20°C represents the 19% and for PSF at -28°C the 13% with respect to atmospheric freezing), the lower the freezing plateau time (thanks to the higher temperature gradient reached), and therefore, the lower probability of cellular stresses and textural damages. This point must be proven through direct quality related parameters and these results are shown below.

Finally, in the case of thawing times (Figure 4.51c), the results obtained show that the thawing time is reduced with increasing applied pressure, thanks to the increased temperature gradient. To explain the highest value obtained for 290 MPa the standard deviation of the results must be taken into account. In both cases, 240 and 290 MPa, the thawing time is reduced more than a 50%, with respect to the atmospheric thawing value.

4.3.4. Profile time modelling

Knorr et al. (1998) already pointed out that HPLT processes offer various unique applications for food research and development. Improved quality characteristics have been reported for pressure-shift frozen or pressure-induced thawed products. However, systematic evaluations of the freezing or thawing processes and of the subsequent consequences for products during further processing or storage are still lacking. Therefore, a precise monitoring is needed to advanced process development. As next step, a mathematical model is also needed to reproduce experimental data as a tool to understand the kinetics related to HPLT processes, as well as to predict freezing and thawing profiles for new geometry, products and scales, in order to facilitate scale-up procedures, basic to develop an industrial process concept.

In this sense, Schlüter, Heinz and Knorr (2003) suggested a two step model based on a finite difference scheme, taking into considerations the often neglected supercooling phenomena, specially present when ice III freezes. Calculated curves were fitted to

experimental data using modified thermophysical properties from literature. Figure 4.52 shows the experimental and modelled freezing curves at 0,1 - 180 and 300 MPa, respectively, for potato cylinders.

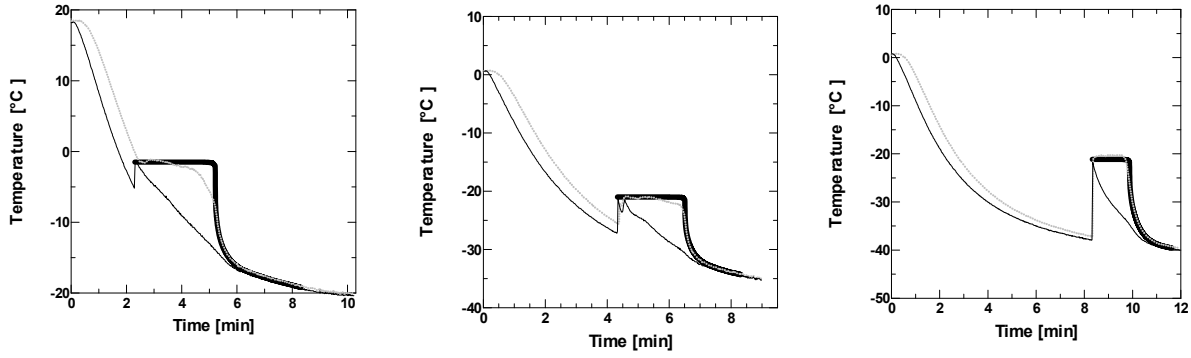

Figure 4.52. Application of the two-step mathematical model at 0,1 (left), 180 (middle) and 300 MPa (right).

Taking this previous work as starting point, a numerical explicit finite difference scheme was used to describe conductive heat transfer and thermal phenomena during the high pressure supported freezing processes. A one-step mathematical model based on the solution of differential equations governing the heat transfer was applied. This scheme is used to predict the temperature distribution inside the cylindrical potato samples through an explicit one-dimensional explicit finite volume scheme, and then, to predict the phase transition time and overall process time (two variables of relevance with different explanatory values). The model here used was applied to freezing process in which ice III was obtained, with a one-step modelling schema. This model has been implemented in a spread sheet with the help of Visual Basic program tool. The way this model is applied permits that a one-step calculation follows the experimental jump to the corresponding freezing point, also after significant supercooling as ice III is obtained. This one-step model is able to calculate then nucleation temperatures, freezing times and phase transition times. Figure 4.53 shows the application of this mathematical model for pressure-shift freezing (a), for pressure-assisted freezing of ice I and ice III at different pressures (b, c and d), for pressure-assisted freezing in the metastable region with a double plateau (e) and for a pressure-assisted thawing process (f).

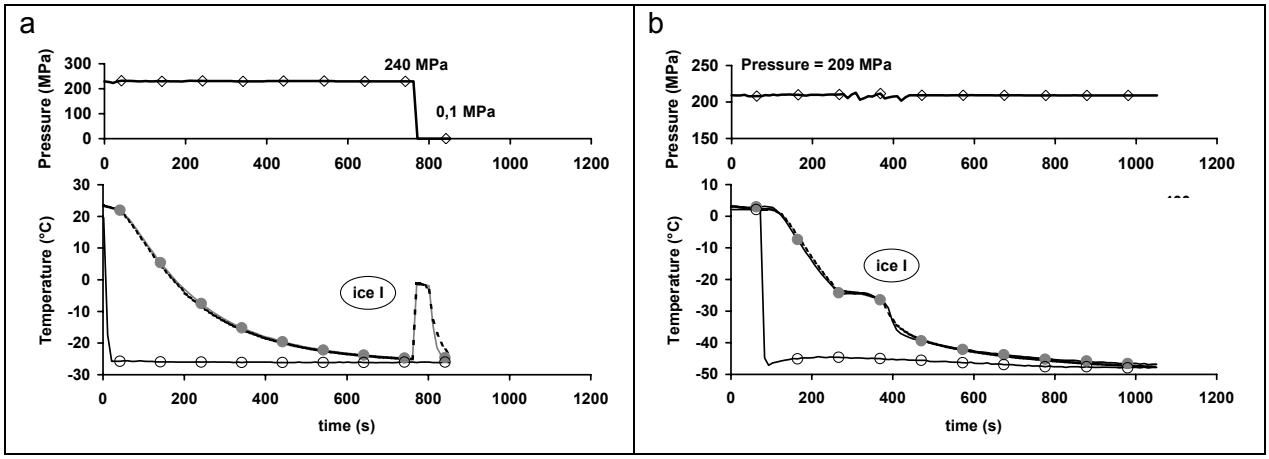

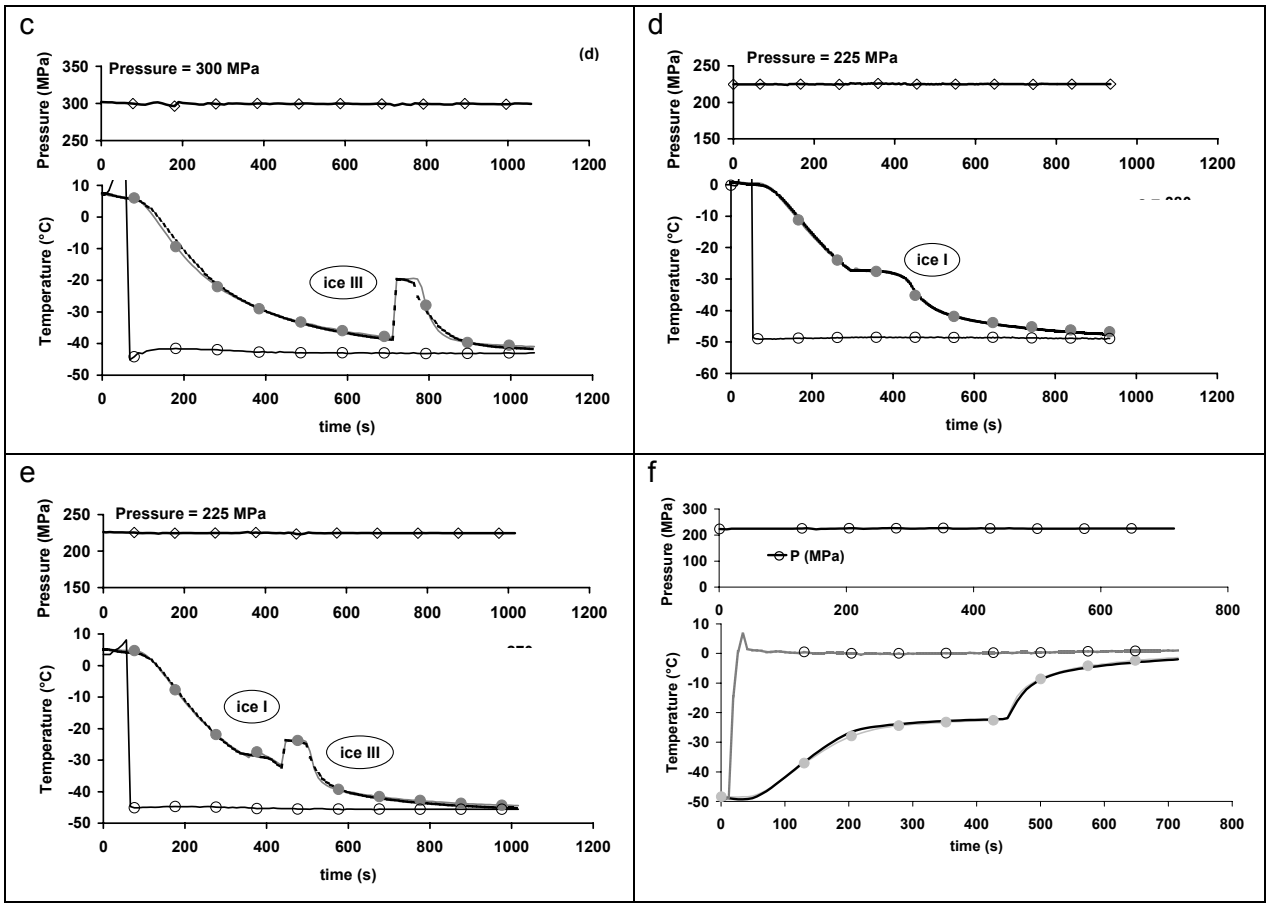

Figure 4.53. Mathematical model application for the cases of (a) PSF, (b) PAF of ice I in the domain of ice I, (c) PAF of ice III in the domain of ice III, (d) PAF of ice I in the domain of ice III, (e) PAF of ice I and ice III with double plateau in the metastable region and (f) the case of PAT. Processing pressure (MPa), temperature of the sample core (°C) (—●—), temperature of the cooling bath (°C) (—o—) and modelled core temperature (▬▬) are shown.

4.3.5. Influence of ΔT and L on thawing times

A double set of experiments was performed to study the influence of the temperature gradients (ΔT) and the values of latent heat of fusion (L) at constant temperature gradients) for pressure-assisted thawing processes:

Pressure-assisted thawing with constant medium temperature. In this case, the samples, already frozen at atmospheric pressure and –40°C, were placed (inside the pressure vessel) in a heating bath maintained always at +10°C, and then pressurised to the processing pressure (0.1, 100, 180, 210 and 300 MPa). Figure 4.54a shows the schematised paths for this set of experiments. The influence of the different temperature gradients is discussed after the obtained results.

Pressure-assisted thawing with constant temperature gradient. After freezing at atmospheric pressure and –40°C, the samples were tempered to a temperature 25°C lower than the corresponding phase transition temperatures for each pressure level. Then, they were pressurised (0.1, 190, 210 and 310 MPa) after placing them into the heating bath, with a medium temperature 25°C higher than the corresponding expected phase transition one. Being the temperature gradients equal for all cases, the impact of the latent heat of fusion can be discussed after the obtained curves. Moreover, the influence of the ice modification can also be discussed, as the pressures were selected in order to have a pair of experiments with equivalent values of the latent heat of fusion for both ice modifications. Figure 4.54b schematically shows the paths planned for this second set of experiments.

In all cases, the samples were frozen at atmospheric pressure, with a cooling bath temperature of –40°C, and then tempered to the different initial temperatures. The pressurisation rate was, in all cases, approximately, of 400MPa/min.

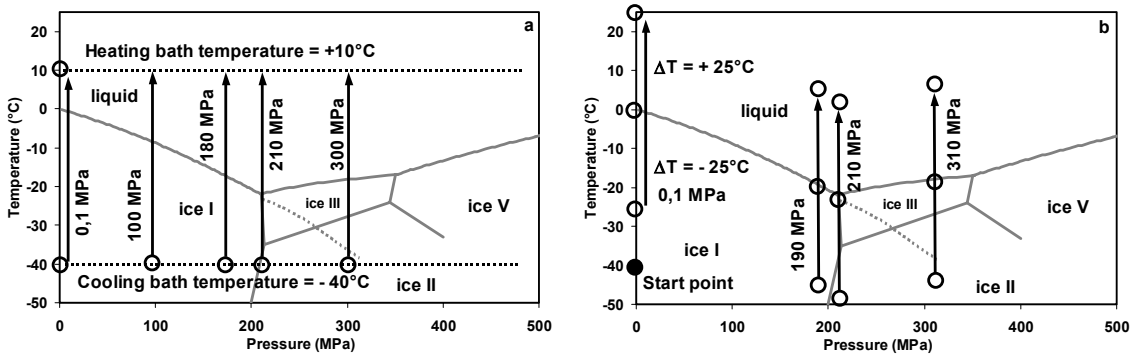

Figure 4.54. Schematic curves expected for each set of experiments.

a) Pressure-assisted thawing with constant heating bath temperature: influence of temperature gradient.

The results of this first set of experiments are shown in Figure 4.55. For the three experiments in which ice I thawed (0.1, 100 and 180 MPa), higher pressure levels, so higher temperature gradients, led to shorter thawing times and phase transition times (Figure 4.55a), due to the negative slope of the phase transition line between ice I and liquid. In the cases in which ice III was first obtained through a solid-solid phase transition and, then, thawing occurred, the higher the pressure level, the smaller the temperature gradient and, therefore, the longer the thawing time (Figure 4.55b). For ice III the slope of the phase transition line is positive and, therefore, the higher the pressure, the lower the temperature gradient.

In fact, we expected to have thawing from ice I at 210 MPa, but a solid-solid phase transition took then place. We could noticed it because of the behaviour of the experimental recorded pressure during the thawing process itself. When ice I is thawing, the differences in volume led to a decreasing tendency in pressure, whereas when ice III thawed (after ice I/ice III transition), pressure had the opposite tendency and was increased due to the higher volume of ice III compared to liquid water.

After atmospheric freezing, pressure was increased until the selected level: in the cases of atmospheric pressure and 100 and 180 MPa, the ice modification kept ice I, and then, when pressure was established, the samples were placed into the heating bath. The sample melts from surface until centre. This fact can be proved after Figure 4.55d, in which the temperature profiles of the sample centre and sample surface are shown. The surface temperature starts to increase before the centre temperature does, therefore it is clearly shown that when the surface is already melting, the centre remains frozen.

In the cases of 210 and 300 MPa, at the temperature (–40°C) in which pressure was built up, a solid-solid phase transition took place, and ice I transformed into ice III. Then, the pressure level was reached and the sample was placed into the heating bath. Then, ice III melted into water, as shown in Figure 4.55b. Here, the influence of the slope of each ice modification phase transition line is observed. In the case of ice I thawing (Figure 4.55a), as the slope of the phase transition line is negative, the higher the pressure, the higher the temperature gradient and shorter thawing times. In the case of ice III this slope is positive, and higher pressures suppose smaller temperature gradients, and therefore, longer thawing times (Figure 4.55b).

In Figure 4.56 the thawing time and the phase transition time for the different temperature gradients experimented (as a result from the different pressures applied)

are shown. It can be seen (especially clear for ice I) that the higher the temperature gradient, the shorter the phase transition time. In the case of the overall thawing time, this tendency is less clear.

It can also be stated that the influence of this temperature gradient is more accentuated when pressure is increased from atmospheric to 100 MPa and that the influence of the temperature gradient increase when increasing pressure until 180 MPa is less clear. That means that, in practise, and for potential future industrial applications of these processes, an optimum in the use of high hydrostatic pressure must be found, taking into account the costs of reaching higher pressures and the benefits in terms of processing time reductions. Both, phase transition and thawing times are slightly higher for the experiments carried out at 300 MPa, although the temperature gradient is higher than in the case of 180 MPa.

This surprising behaviour should be explained taking into account the fact that the ice modifications that are thawing are different. The solid-solid phase transition may have a key role in this processing time difference, as it takes extra time and, therefore, leads to a higher processing time for 300 MPa although the temperature gradient is higher. Then, for the cases in which ice III is thawed, again the clear tendency is observed: the higher the temperature gradient, the lower the obtained processing time.

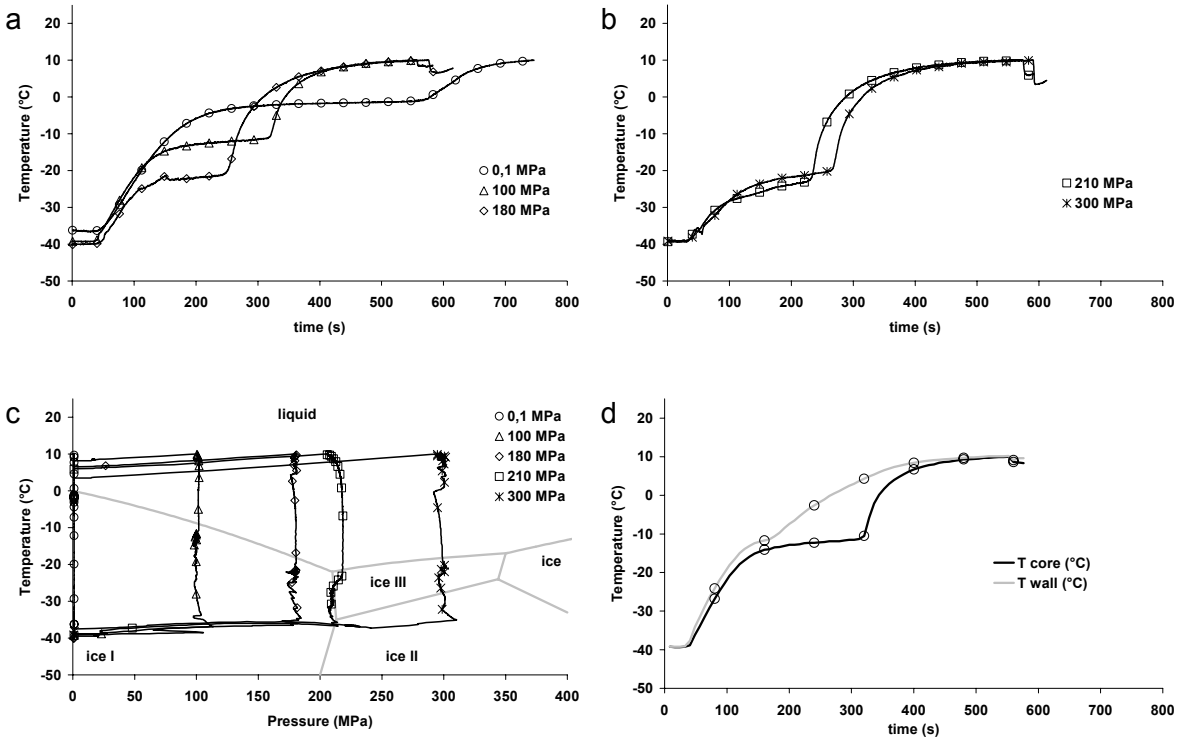

Figure 4.55. Experimental results for pressure-assisted thawing with constant heating bath temperature: a) temperature profiles of sample centre when thawing from ice I; b) temperature profiles of sample centre when thawing from ice III; c) thawing paths in phase diagram of water; d) temperature profiles of sample centre and surface at 180 MPa (ice I).

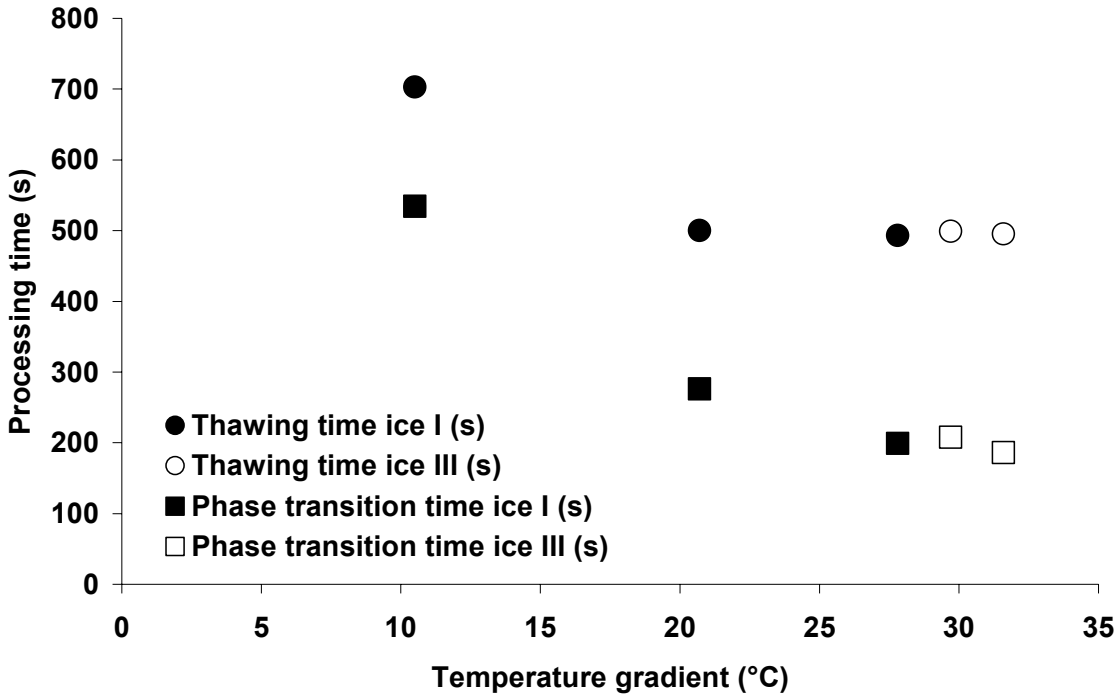

Figure 4.56. Influence of temperature gradient on phase transition and thawing times.

b) Pressure-assisted thawing with constant temperature gradient: influence of different ice modifications and different latent heats of fusion for ice I

Figure 4.57a for ice I and Figure 4.57b for ice III show the temperature profiles of the thawing processes carried out when the temperature gradients remained constant, at +25°C with respect to the corresponding phase transition temperature for each pressure level. For the different pressures experimented, the temperature gradient is equivalent, but the thawing times are different. The reason should therefore lie with different latent heats of fusion for each pressure level.

The corresponding values are re-printed or estimated after the results reported by Kalichevsky *et al*. (1995) and, for the cases studied here are:

ΔH (0.1 MPa) = +334 kJ/kg; ΔH (190 MPa, ice I) = +243 kJ/kg; ΔH (210 MPa, ice III) = +214 kJ/kg; ΔH (310 MPa, ice III) = +246 kJ/kg.

Nevertheless, in order to compare the obtained curves properly, the enthalpy of fusion or, better, the enthalpy of phase transition between ice I and ice III, when solid-solid phase transition takes place has to be considered. In the cases of 210 and 310 MPa these enthalpies should be added to those corresponding to the ice-liquid transition. These values are +17 kJ/kg for 210 MPa and –28°C and +6 kJ/kg for 310 MPa and –40°C. In fact the value for 310 MPa has been estimated at a pressure of 230 MPa and a temperature of –40°C, conditions at which the solid-solid phase transition actually took place (see circled phase transition on thawing path of Figure 4.57c). Therefore, the corresponding values are now:

ΔH (ice I➔liquid at 0.1 MPa) = +334 kJ/kg

ΔH (ice I➔liquid at 190 MPa) = +243 kJ/kg

ΔH (ice I➔ice III & ice III➔liquid at 210 MPa) = +17+214 = +231 kJ/kg

ΔH (ice I➔ice III at 230 MPa & ice III➔liquid at 310 MPa) = +6+246 = +252 kJ/kg

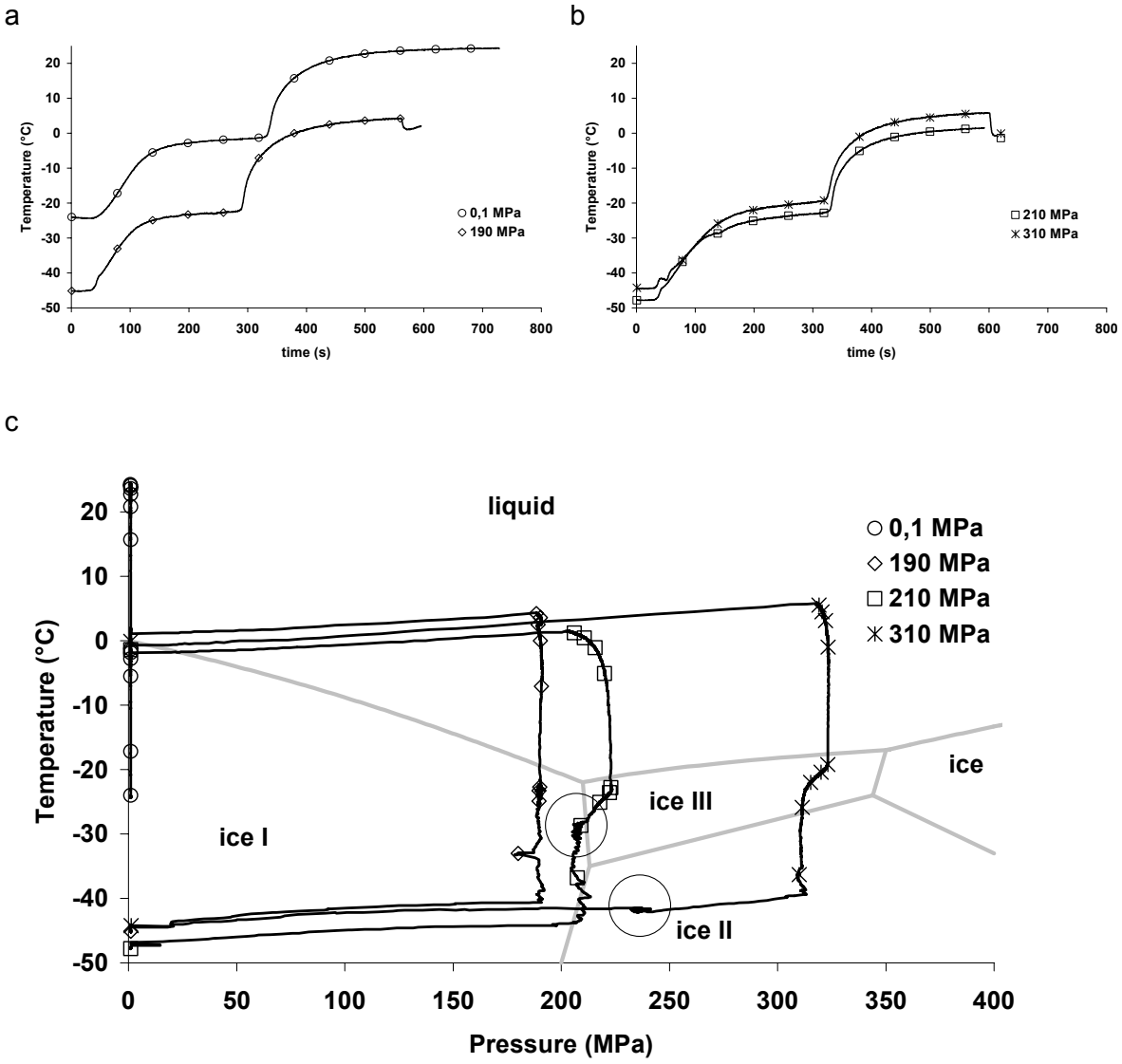

Figure 4.57. Experimental results for pressure-assisted thawing with constant temperature gradient: a) temperature profiles of sample centre for ice I; b) temperature profiles of sample centre for ice III; c) thawing paths on water phase diagram.

Figure 4.57c shows the four thawing paths on the phase diagram of water. In this figure, for the two cases in which a solid-solid phase transition occurred, this ice I/ice III transition is remarked with a circle. In the case of 310 MPa it was completely expected, but in the case of 210 MPa, as commented, the tendency of pressure to increase along the thawing *plateau* clearly showed that ice III and not ice I was thawing. Then, after the experimentation, we could see this fact in the obtained thawing path shown in Figure 4.57c.

Figure 4.58 shows the variation of the values of thawing and phase transition times with respect to the estimated enthalpies of fusion. In the cases where ice I was thawed, the influence of the enthalpy of fusion can be clearly stated: the higher the enthalpy of fusion, the longer the thawing and phase transition times, because the sample must transfer more calorific energy during the phase transition.

In the cases where a previous solid-solid phase transition took place, the values of the enthalpy of fusion, as already explained, are the addition of those corresponding to the consecutive processes: ice I – ice III phase transition and ice III – liquid water phase

transition. The values are similar for the two operated pressures (231 kJ/kg for 210 MPa and 252 kJ/kg for 310 MPa) and also similar to the corresponding for ice I thawing at 190 MPa. The fact that in the cases when ice III thawed, the processing times are similar corroborates that there is a direct influence of the enthalpy of fusion on the obtained processing times. Moreover, the lower value of phase transition time for ice I at 190 MPa, although the enthalpies of fusion are similar, show, as we obtained for the first set of experiments, that the existence of a solid-solid phase transition retards the thawing process.

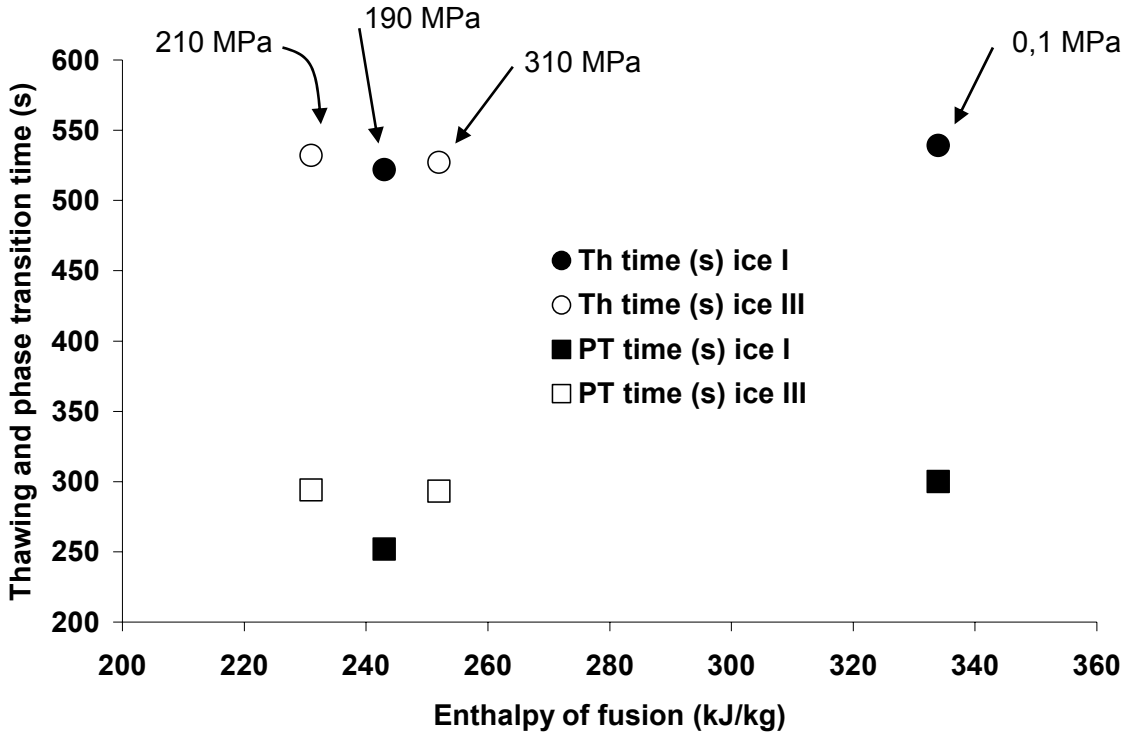

Figure 4.58. Thawing and phase transition times versus enthalpy of fusion.

Table 4.4 shows a summary of the experimental results obtained.

Table 4.4. Summary of experimental results for the influence of temperature gradients and latent heat of fusion on thawing times

Pressure-assisted thawing with constant heating bath temperature						
Pressure-assisted thawing with constant heating bath temperature: influence of temperature gradient						
Exp.	P (MPa)	T_f (°C)	Ice mod.	ΔT (°C)	Thawing time (s)	Phase transition time (s)
1	0,1	-0,5	I	10,5	703	534
2	100	-10,7	I	20,7	500	276
3	180	-17,8	I	27,8	493	199
4	210	-21,6	III	31,6	495	186
5	300	-19,7	III	29,7	499	208
Pressure-assisted thawing with constant temperature gradient						
Pressure-assisted thawing with constant temperature gradient: influence of latent heat of fusion						
Exp.	P (MPa)	T_f (°C)	Ice mod.	ΔH_f (kJ/kg)	Thawing time (s)	Phase transition time (s)
1	0,1	-0,7	I	+334	539	300
2	190	-21,8	I	+243	511	240
3	210	-22,2	III	+231	518	281
4	310	-18,7	III	+252	500	266

The samples thawed with a constant heating bath temperature showed an optimum for phase transition time at 210 MPa, where the maximum temperature gradient was reached, due to the depression of the phase transition line of ice I in the water phase diagram. At this level ice III was first obtained through a solid-solid phase transition and

then ice III thawed into water, within the cylindrical potato samples. The pressure increase from 210 MPa until 300 MPa did not mean a shortening of the processing times and, therefore, for a further scale-up study when industrial implementation should be performed, these higher levels of hydrostatic pressure should not be taken into account.

The difference in processing time when ice I or ice III was thawed is not high enough to recommend an optimum path in which a previous solid-solid phase transition takes place. Therefore, the optimum path for a potential industrial thawing process should be the one occurring in the vicinities of the triple point, where the maximum temperature gradient is reached.

In the case of thawing at constant temperature gradient, the optimum in terms of shortening the processing times is not clearly reached for a given pressure. However, a range of pressures have been obtained in which the time differences are not clear enough to give direct conclusions. But, taking into account that the higher the pressure to be held, the longer the pressurisation time and also the more expensive the process should be, then, an economic and technical optimum should be taken again for the vicinities of the triple point, where these best conditions for time are reached and where the pressure is as low as possible. It should also be noticed that a significant difference in the phase transition time was obtained for the curves at 190 and 210 MPa. Although the pressure difference was not so dramatic, in the case of 210 MPa ice III was thawed, and, therefore, a longer phase transition time was obtained. This behaviour leads to recommend the thawing from ice I as an optimum path for further industrial implementations.

Nevertheless, more accurate definitions of the processes (assisted, induced, etc.) should be addressed, as well as a detailed study on the pressure-temperature conditions leading to solid-solid phase transitions, or to induced thawing processes, etc. The great dependency of time results on the start and end point time definitions supposes as well that a full study of these initial conditions as control parameters for controlled thawing paths, should be still addressed.

4.3.6. Bench mark tests

Since the High-Pressure-Low-Temperature (HPLT) technology focused the attention of many food technologists for the study of freezing and thawing processes that could enhance the quality and safety of the products, and for the study of the microbial inactivation and of the enzymatic activity under such conditions, the number of laboratories investing resources in this research has increased considerably during the last two decades. However, the different research groups join scientists coming from chemical engineering, food technology, food biotechnology, biochemistry, etc. Together with the fact that each laboratory has begun research with no existing methodologies, procedures or methods to be followed, the collection of data present in the literature is quite heterogeneous and the validity of some of the results should be questioned, in terms of comparability with other results.

Given this situation, the consortium of the project SAFE ICE took the initiative of performing a bench-mark test in the equipment of three different laboratories: a HPLT laboratory vessel placed in the Department of Food Biotechnology and Process Engineering of the Technical University of Berlin (TUBER), a HP pilot plant placed in the Instituto del Frío – Consejo Superior de Investigaciones Científicas, Madrid (CSIC-1), a HP laboratory vessel also placed in the Instituto del Frío (CSIC-2) and a HP vessel placed in Ecole Nationale d'Ingénieurs des Techniques des Industries Agricoles et Alimentaires, Nantes (ENITIAA).

Benchmark testing examines the performance of systems. The notion of performance can be applied either to individual functions, to system modules or to a system as a whole. In the strict technical sense, a benchmark test is a measurement of system performance which cannot be affected by variables resulting from human involvement.

In this case, therefore, the benchmark tests can be used to check the performance homogeneity of a given process carried out in four different facilities, with the aim of checking the comparability of the results.

Taking advantage of the phase diagram of water various pathways can be followed using external temperature/pressure manipulations to change the physical state of biological systems. The main processes that have been studied were shown in Figure 4.28.

From all the possible paths, two of them have been selected to be the most representative processes, as described in the literature: Pressure-Shift-Freezing (PSF) and Pressure-Induced Thawing (PIT).

Pressure-shift freezing (PSF): 1-2-3-4-8. A crystallisation can be caused through a pressure release, with the particularity that pressure can be extremely quickly released (shorter phase transition time), and that pressure is an isotropic property (the crystallisation occurs within the whole sample at the same time). Due to the rapidity of the process, the size of the resulting crystals smaller than for conventional freezing, leading to a prevention of structural damages. Tofu (Kanda et al. (1993)), carrots (Fuchigami et al. (1997a,b)) or aubergines (Otero et al., 1998)) have been shown to maintain a better structural quality of frozen products after PSF. The reduction of the phase transition time for PSF, as well as the crystallisation in the whole sample volume has been demonstrated in oil-on-water emulsions (Levy et al. 1999). As long as the process is ended at atmospheric pressure, no added technical hurdles are involved.

Pressure-induced thawing (PIT): 8-4-3-2-1. The term induced makes reference to a process in which the phase change is "induced" by a pressure increase. In this case, after tempering the sample to an appropriate temperature (-20°C, for example), pressure is increased and, ideally, the melting curve is crossed until point 3. Then, before releasing the pressure, the liquid sample must be tempered to avoid re-crystallisation (3-2-1). This process, anyway, is an ideal path which is not obtained experimentally. In real experiments, during pressurisation, an induced partial thawing takes place at the sample surface, leading to a temperature decrease to compensate the energy of melting used for this partial melting. Then, the path "follows" an extended ice I melting line, and a metastable ice I is still present in the domain of ice III.

The tests were organized in two groups: pressure-shift freezing tests and pressure-assisted thawing tests. The experimental conditions for these tests are summarized in Table 4.5.

Table 4.5. Experimental conditions for the experimental tests

	FREEZING TESTS			
	TUBER	**CSIC-big**	**CSIC-small**	**ENITIAA**
Pressurisation liquid	Silicone oil	Water / Ethyl alcohol (50/50, v/v)	Silicone oil	Water / Ethyl alcohol (50/50, w/w)
Temp. of liquid medium	-20°C	-20°C	-20°C	-20°C
Target pressure	200 MPa		200 MPa	200 MPa
Pressurisation rate	18.4 MPa/s	1.7 MPa/s	5.8 MPa/s	3.5 MPa/s
Depressurisation rate	45 MPa/s	65 MPa/s	15 MPa/s	40 MPa/s
Initial temperature of tylose	20°C	0°C	20°C	0°C
Instruction to depressurise	-18°C	-20°C	-20°C	-18°C
Instruction to open vessel	-20°C	-20°C	-20°C	-20°C
	THAWING TESTS			
	TUBER	**CSIC-big**	**CSIC-small**	**ENITIAA**
Pressurisation liquid	Silicone oil	Water / Ethyl alcohol (50/50, v/v)	Silicone oil	Water / Ethyl alcohol (50/50, w/w)

Temp. of liquid medium	20°C	20°C	20°C	20°C
Target pressure	200 MPa	200 MPa	200 MPa	200 MPa
Pressurisation rate	20 MPa/s	1.6 MPa/s	5.5 MPa/s	3.5 MPa/s
Depressurisation rate	100 MPa/min	30 MPa/s	100 MPa/min	100 MPa/min
Initial temperature of tylose	-20°C	-45°C	-50/-25°C	-20°C
Instruction to depressurise	10°C	10°C	10°C	10°C
Instruction to open vessel	20°C	20°C	20°C	20°C

The experimental results are summarized in Figure 4.59 and Figure 4.60.

TUBER sample 1

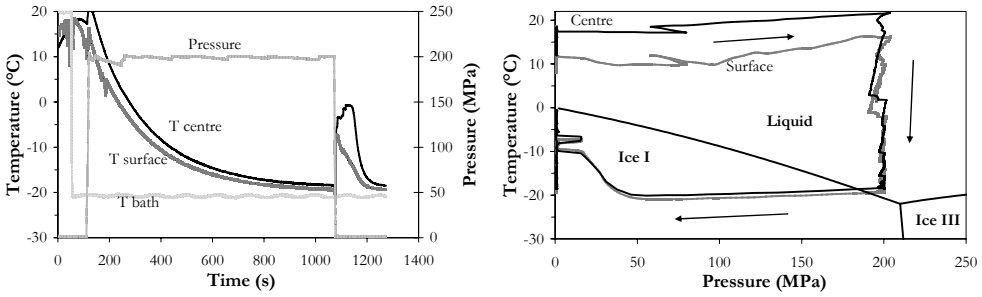

TUBER sample 2

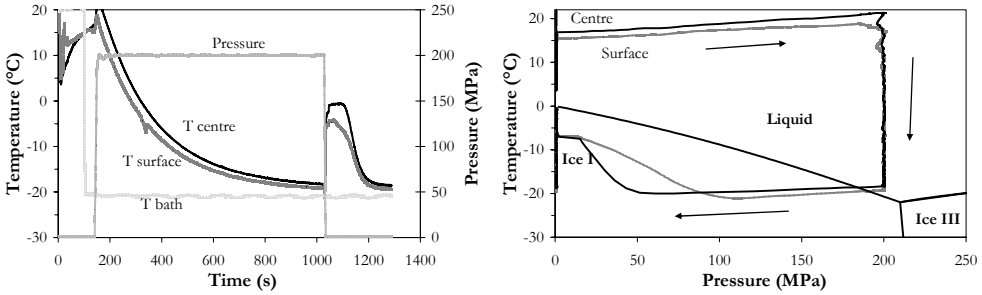

TUBER sample 3

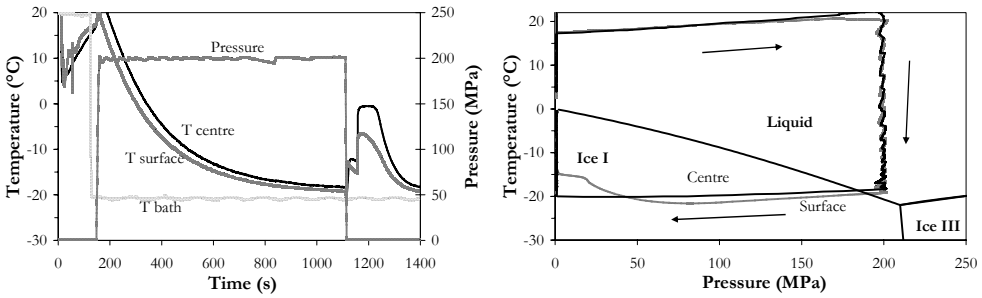

CSIC-small sample 1

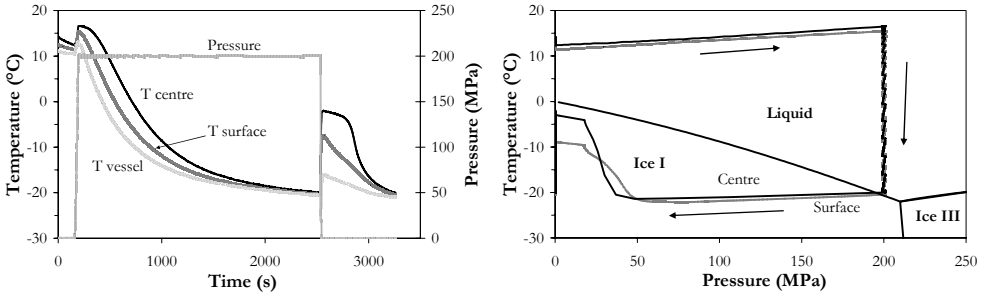

CSIC-small sample 2

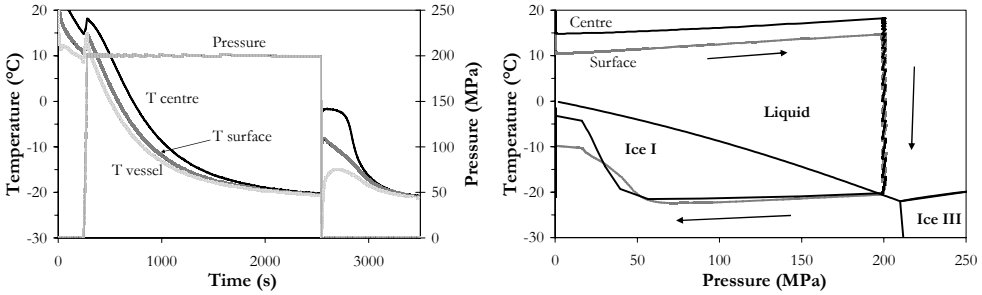

CSIC-small sample 3

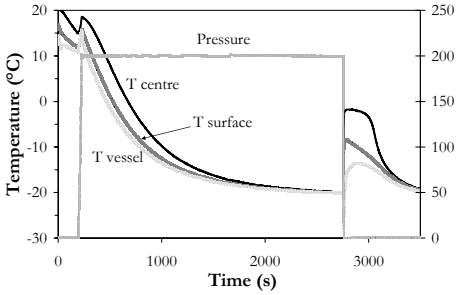

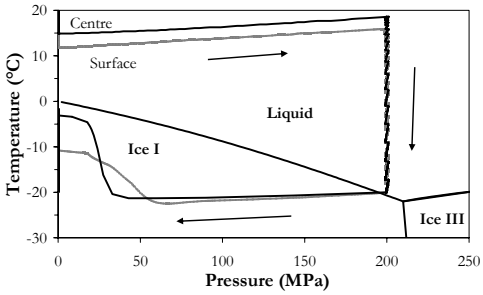

CSIC-big sample 1

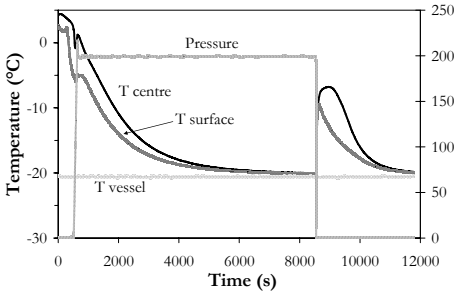

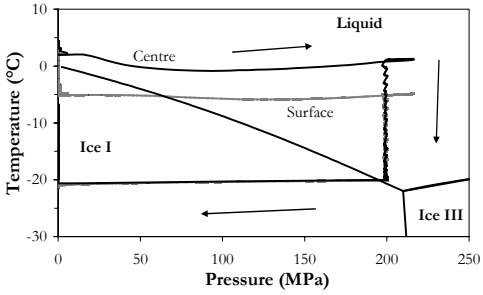

CSIC-big sample 2

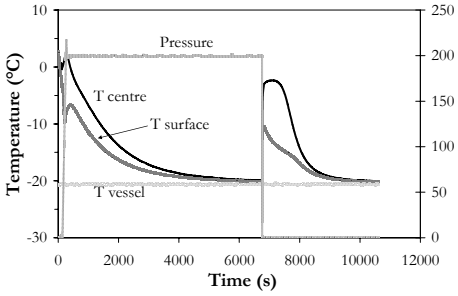

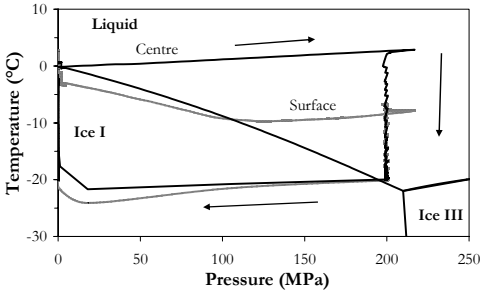

CSIC-big sample 3

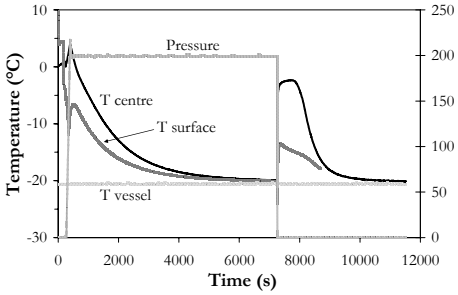

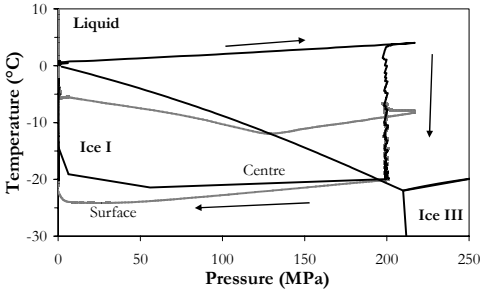

ENITIAA sample 1

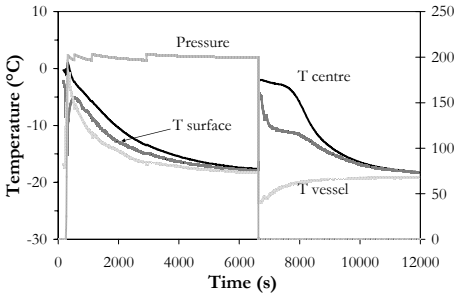

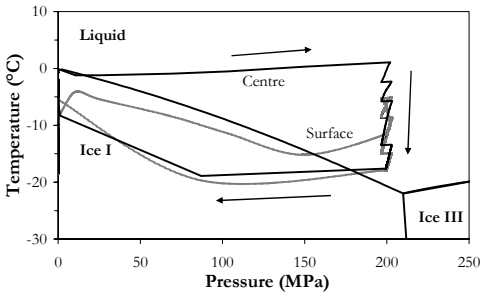

ENITIAA sample 2

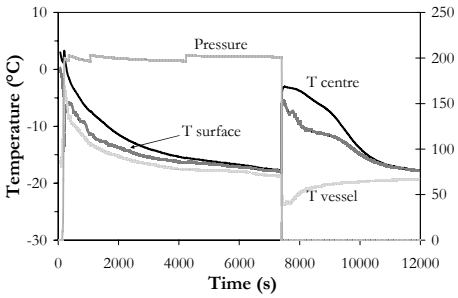

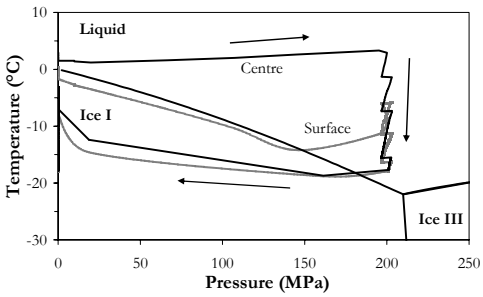

ENITIAA sample 3

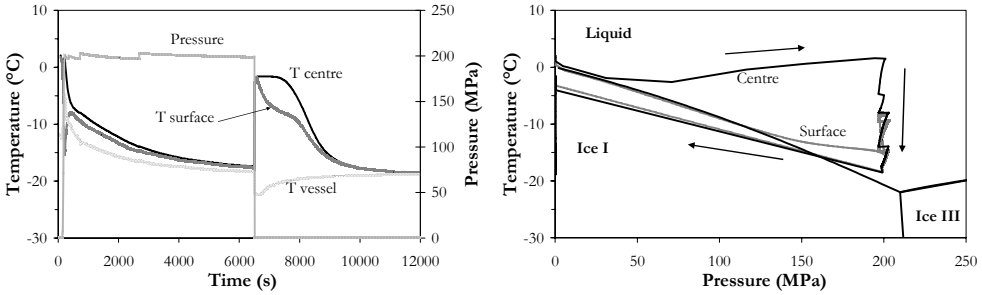

Figure 4.59. Bench-mark tests results for pressure-shift freezing.

TUBER sample 1

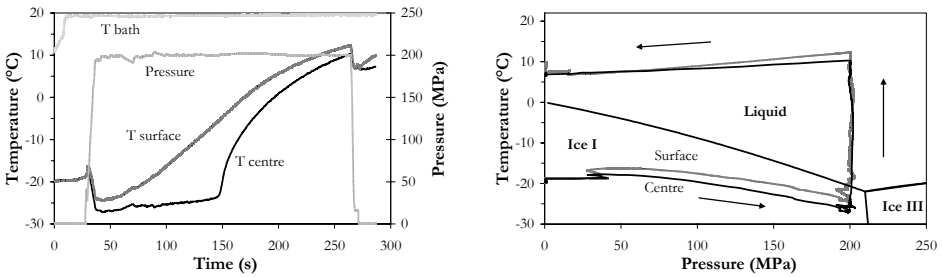

TUBER sample 2

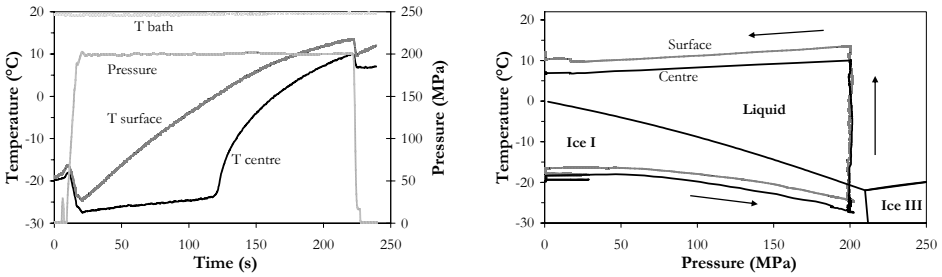

TUBER sample 3

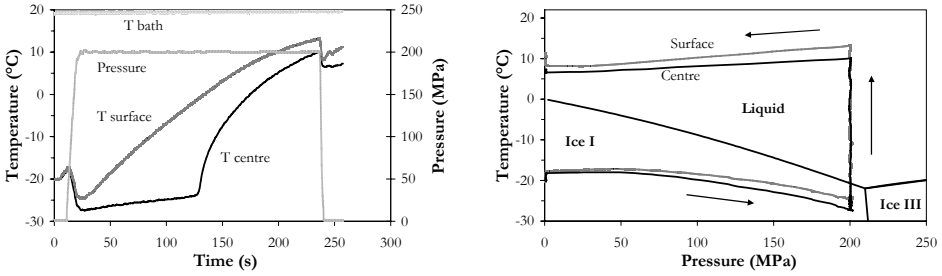

CSIC-small sample 1

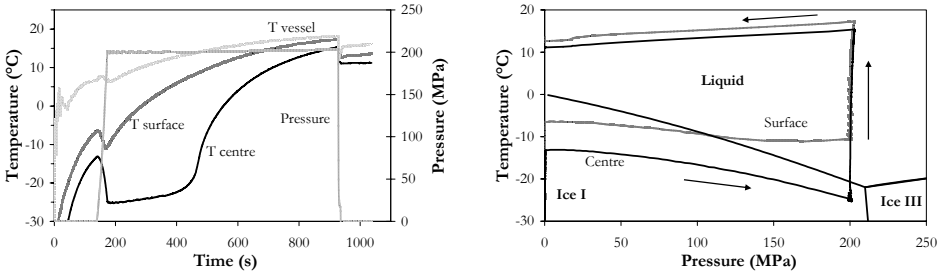

CSIC-small sample 2

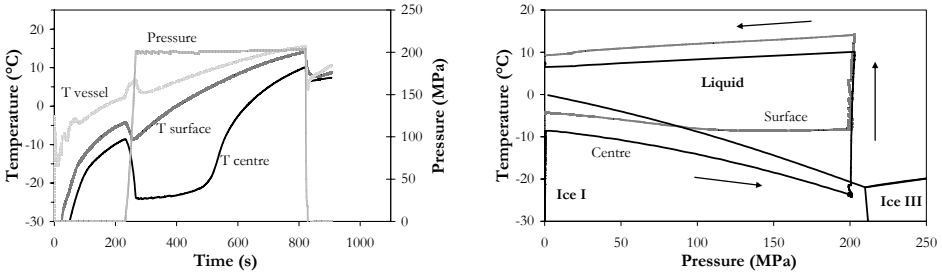

CSIC-small sample 3

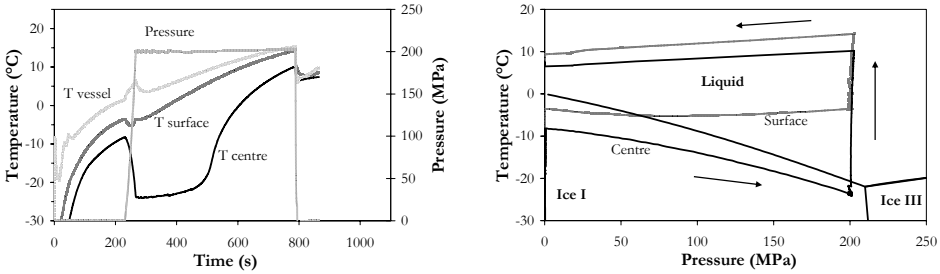

CSIC-big sample 1

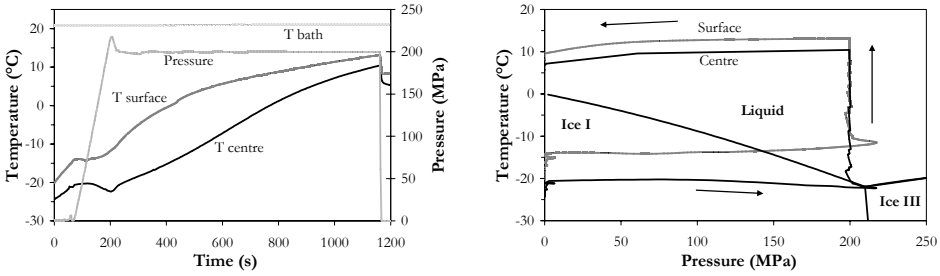

CSIC-big sample 2

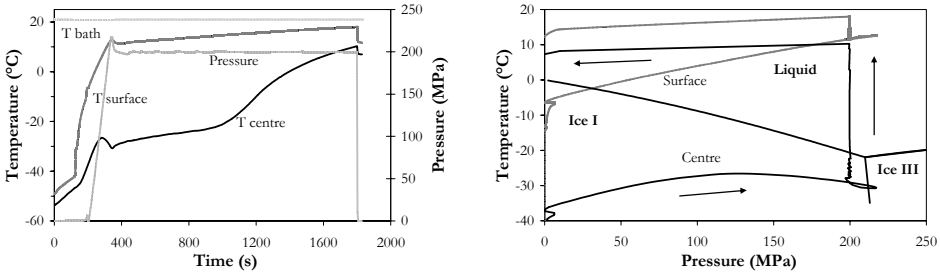

CSIC-big sample 3

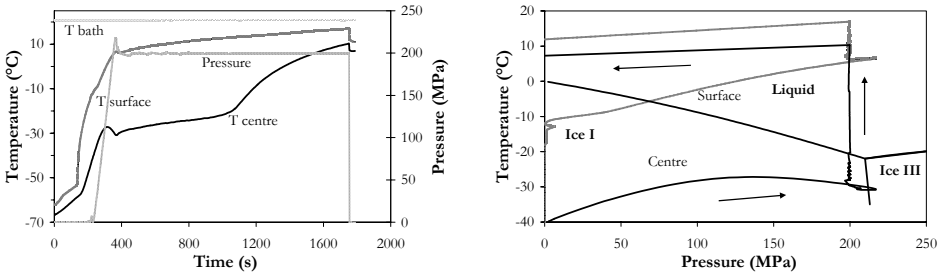

ENITIAA sample 1

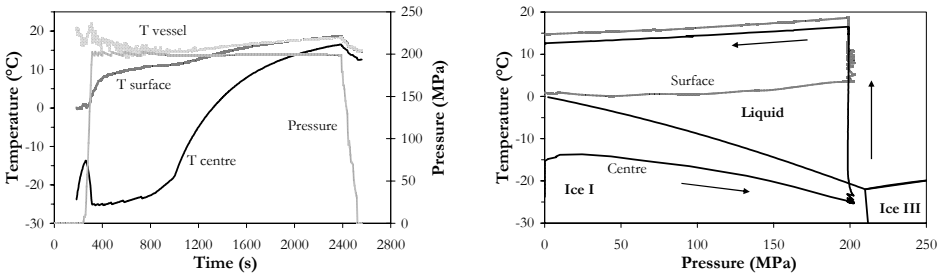

ENITIAA sample 2

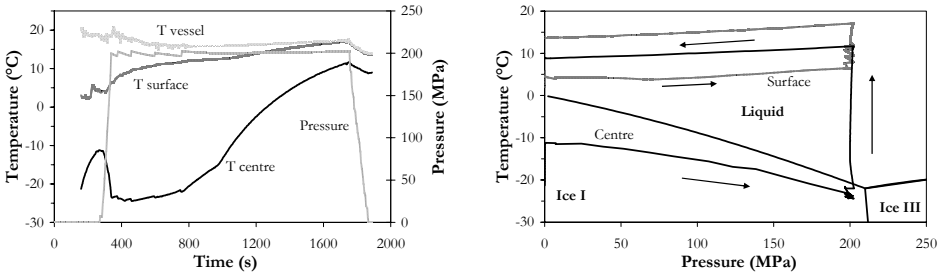

ENITIAA sample 3

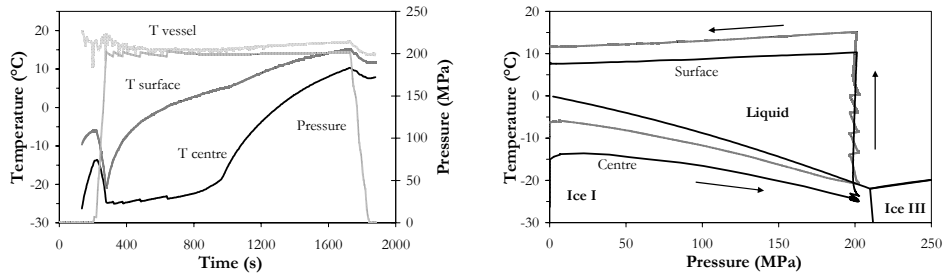

Figure 4.60. Bench-mark tests results for pressure-assisted thawing.

The different processing times for all these profiles are summarized in Table 4.6.

Table 4.6. Processing times for PSF and PAT processes.

		Freezing		Thawing
		Total time (s)	HP treatment time (s)	HP treatment time (s)
TUBER	Sample 1	1163	968	229
	Sample 2	1148	894	207
	Sample 3	1277	969	220
CSIC-big	Sample 1	11275	8035	1024
	Sample 2	10480	6622	1512
	Sample 3	11252	6997	1443
CSIC-small	Sample 1	3102	2386	764
	Sample 2	3305	2305	566
	Sample 3	3399	2568	529
ENITIAA	Sample 1	12270	6381	2120
	Sample 2	12100	7340	1456
	Sample 3	12780	6379	1499

The results from four different facilities from three different laboratories trying to run identical experiments permit a first evaluation of the influence of size, geometry and operational conditions on the final result of the essayed processes: PSF and PAT.

In the case of PSF, the influence of the sample volume, vessel volume and occupation ratio on the different processing times is shown in Figure 4.61. Clearly, an increasing volume of sample and vessel means higher overall processing times (t_T, for total time) and higher tempering time (t_A, for time, at atmospheric pressure, needed to reach final set point after pressure release), but not necessarily higher HP treatment time (t_P), this value being the time needed to reach the temperature level before the pressure release. t_A has been calculated as the difference between t_T and t_P.

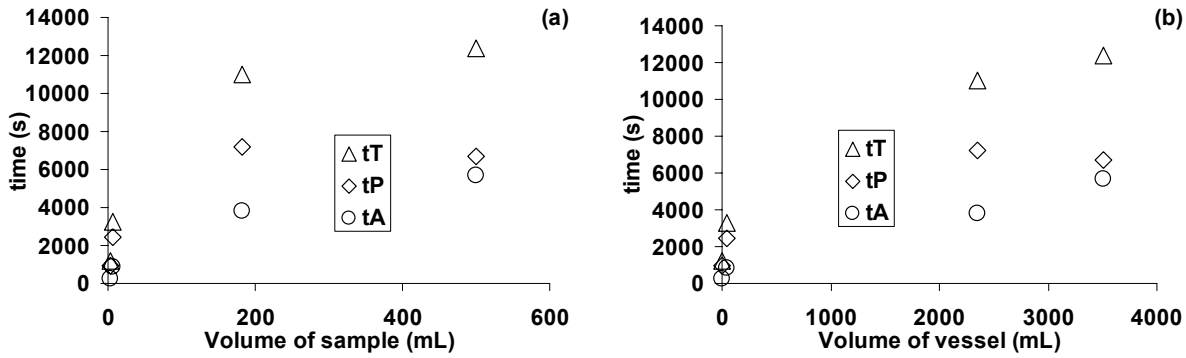

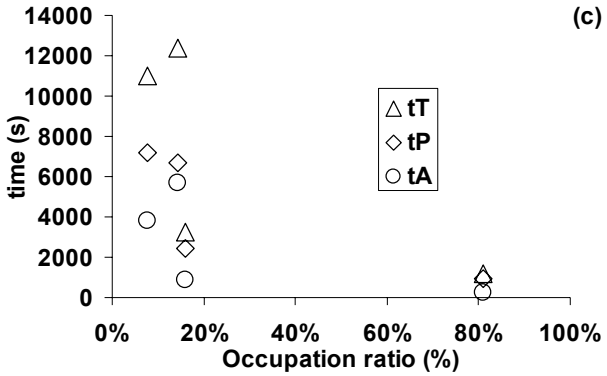

Figure 4.61. Influence of volume of sample, vessel and occupation ratio on processing times for PSF processes.

Depending on the purpose of the experiment, the best size and geometry to be recommended can change. For example, due to the temperature non-homogeneity of experiments carried out with big samples, if the aim is the study of the thermal gradients during freezing and thawing, it is recommendable to work with little samples or, if possible, with big samples placed in vessels so big that the occupation ratio is very low. Also, the solution of a big inner volume filled with a small sample, leaving large non-occupied spaces for the pressurisation fluid, permits a very accurate study of the heat transfer of samples, because the heat transmitting medium has space enough for free convection. For industrial purposes, pilot plants are recommended, as the size of the samples permits to observe the real handling problems of each sample type and geometry, like packing methods, 3-dimensional disposition, etc.

The differences between the curves presented by each facility are not only the result of different ways to run the experiments, but also the result of the differences between the equipments, the recording characteristics, etc.

For the curves obtained during the run of PSF processes, depending on the exact point in which the temperature of the pressurisation medium is recorded, one can obtain temperature profiles like the one for TUBER or the one for CSIC-big, in which this temperature is actually the temperature of the surrounding medium (immersion bath or cooling medium in jacket, respectively). In these cases, a horizontal profile for the "vessel" temperature is obtained, while for the other two cases, the temperature shows an evolution similar to the one for the samples. In these other two cases, the recording point was the pressurisation fluid just around the samples, but not the cooling medium itself. Therefore, sometimes, when trying to compare results coming from different laboratories, the comparison is difficult due to these differences. But, in fact, the processes are the same: it changes only the recording methods, as shown.

Related to the initial temperature for the PSF processes, in two cases this value was between +10 and +20°C, but in the other two cases (CSIC-big and ENITIAA), the initial temperature for the beginning of the pressure build-up was 0°C. In these cases, the sample surface was already frozen when the pressure build-up started, as shown by the fact that the temperature profiles are "following" the phase transition line, decreasing the temperature of the samples surfaces to give the necessary heat for the endothermic thawing of the frozen surface. This fact can affect the final results of the corresponding research, because this first partial freezing occurs at atmospheric pressure, and the final results (if, for example, texture, drip losses, microstructure, etc. are measured after processing) can be very affected from this first atmospheric partial freezing, as the effects of this process are different to the effects of the subsequent PSF. These kind of details should be taken into account when designing the PSF process, in order to be able to compare results with other laboratories, and in order to study singular influences of one process on the samples response - not partial

atmospheric freezing at the beginning, then thawing of the surface and finally the PSF itself, as happened in the above mentioned examples.

Another of the differences observed between the results from the different laboratories is the profile during pressure release. As this release is very fast, the recording frequency plays a key role in the presentation of final results. If this data recording frequency is too low, the shown results can show distortion with respect to the real case. The values of measuring rates were: 5.00 for TUBER, 0.33 for CSIC small, 2.00 for CSIC big and 1.00 for ENITIAA (values in Hz). The differences are big enough to be responsible for the differences observed in the temperature profiles. But also the rate of pressure release plays an important role here. Both parameters have to be adjusted to return enough data to properly represent the curve during release.

Concerning the experiments of PAT, for all the cases of experiments carried out at CSIC and for two of the curves shown from ENITIAA, a particularly interesting detail is observed. The temperature of the sample surface “crosses” the phase transition line, not agreeing with the often reported results in which the temperature profiles “follow” the phase transition line until the target pressure is reached (occurring during this process a partial melting of surface) and then thawing is completed at constant pressure. In the indicated cases, the fact that the surface temperature profile crosses the phase transition line indicates that a percentage of the sample was already melted before the pressure increase and, therefore, the liquid already present in the sample surface actually increases its temperature due to the heat of compression. Actually, this phenomenon should be avoided, because the process is then a mixture of atmospheric thawing with high-pressure-supported thawing and then the effect of the second process is not able to be analysed alone. In the experiments shown by TUBER and the sample 3 profiles from ENITIAA, the curves show the expected (and desirable) behaviour, reaching a minimum in temperature when pressurisation finishes (when target pressure is reached) and then, thawing is completed at constant pressure of 200 MPa.

The time during the high pressure holding step during thawing versus sample volume, vessel volume and occupation ratio is shown in Figure 4.62. Again, as shown for PSF experiments, the higher the volume of sample and vessel, the higher the necessary time to complete the thawing process, and, additionally, the smaller the occupation ratio, the higher the total thawing time.

These results should be corroborated for other samples and other facilities, but also new experiments should be run using the same facilities as here, but using different occupation ratios, to study the influence of the free spaces inside the vessel. Nevertheless, economic studies are also recommended in order to find an optimum of the vessel volume, for industrial purposes.

In this thesis, the results of the performance of these two processes in the mentioned facilities are shown. The comparability of the results will be discussed and the necessity of standardised protocols for the performance of HPLT processes, as well as the necessity for a homogeneous terminology is addressed.

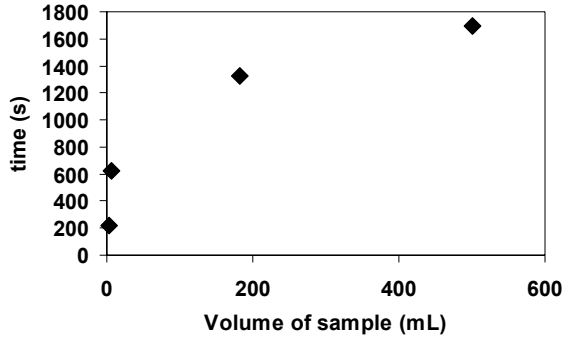

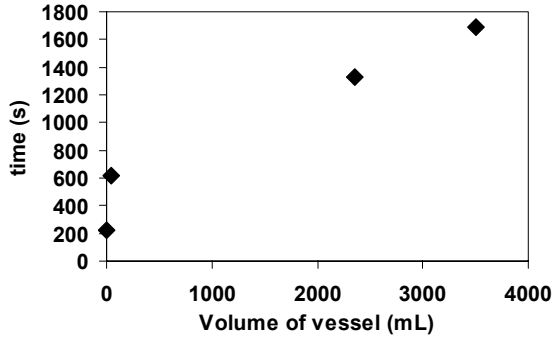

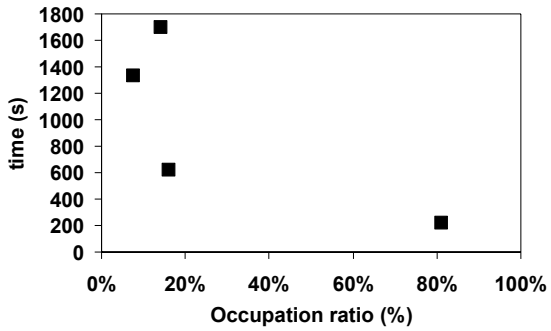

Figure 4.62. Influence of volume of sample, vessel and occupation ration on processing times for PAT processes.

4.4. Microscopic cell results

The study of vegetal tissues under the high-pressure, low-temperature microscope permits the visual observation of the tissues directly under pressure and during the different phase transition processes susceptible to occur in the working range of the facility, 0.1 to 700 MPa and +30 to -50°C.

The theory of ice crystallization or ice nucleation shows the existence of two types of nucleation: homogeneous nucleation and heterogeneous nucleation.

Homogeneous nucleation occurs in pure water in which there is no contact with any other foreign substance or surface. With homogeneous nucleation, the conversion of the liquid state to solid state is done by either lowering temperatures or by changes in pressure. However, temperature is the primary influence on the conversion of water to ice or ice to water. In homogeneous nucleation, the nucleation begins when a very small volume of water molecules reaches the solid state. This small volume of molecules, is called the embryo and becomes the basis for further growth until all of the water is converted. The growth process is controlled by the rate of removal of the latent heat being released. Molecules are attaching and detaching from the embryo at roughly equal and very rapid rates. As more molecules attach to the embryo, energy is released causing the temperature of the attached molecules to be lower than the temperature of the unattached molecules. The growth rate continues until all the molecules are attached. At this point, you have the solid state (ice). Most of us think that pure water freezes at 0°C. In fact, the nucleation event (freezing) for pure water will take place as low as -40°C (http://www.snowmax.com/education).

Heterogeneous nucleation occurs when ice forms at temperatures above -40°C due to the presence of a foreign material in the water. This foreign material acts as the embryo and grows more rapidly than embryos of pure water. The location at which an ice embryo is formed is called an ice-nucleating site. As with homogeneous nucleation, heterogeneous nucleation is governed by two major factors: the free energy change involved in forming the embryo and the dynamics of fluctuating embryo growth. In heterogeneous nucleation, the configuration of molecules and energy of interaction at the nucleating site become the dominating influence in the conversion of water to ice (http://www.snowmax.com/education).

Liquid-to-solid nucleation of a supercooled aqueous solution is a simple but profound example of the poorly understood process of evolution of a metastable state to its final equilibrium state (Heneghan, A.F., P. W. Wilson and A. D. J. Haymet (2002). Proceedings of the National Academy of Sciences of the USA., vol. 99, no. 15, 9631-9634). In the case of food materials, the type of nucleation is obviously heterogeneous, being the tissue cell walls the irregularities in which the nuclei are first formed. The use of the developed high pressure low temperature microscope enables us to obtain the answer to some key questions related to the phenomenon of freezing and thawing, both at atmospheric and at high pressure. One of the hypotheses most reported with

respect to the pressure-shift freezing process is that due to the rapidity of the process, the size of crystals results smaller than for conventional freezing, leading to a prevention of structural damages. Tofu (Kanda et al. (1993)), carrots (Fuchigami et al. (1997a,b)) or aubergines (Otero et al., 1998)) have been shown to maintain a better structural quality of frozen products after PSF.

Chevalier et al. (2001) reported that after PSF and air-blast freezing of turbot fillets and then stored at -20°C for 75 days, smaller and more regular intracellular ice crystals were observed in fillets frozen by PSF compared with air-blast frozen ones. Ice crystals area in PSF samples was approximately 10 times smaller than that of ABF samples, on average. For the microscopic observations, an indirect technique called isothermal freeze substitution was used to observe the spaces left by the ice crystals in tissue.

Zhu et al. (2005) reported that after pressure-shift freezing and conventional air freezing of cylindrical gelatine gel samples, PSF process promotes the production of larger numbers of smaller ice crystals in the frozen sample that help to retain a better texture in the product. A freeze-drying method was used to characterize the ovoid shape of the ice crystals formed.

Nevertheless, the direct observation obtained in the preliminary studies carried out with the HPLT microscope clearly show that there is no significant difference between the size and number of crystals obtained through atmospheric freezing and pressure-shift freezing. This can be demonstrated after observing the pictures in Figure 4.63 and Figure 4.64.

Figure 4.63 shows a sequence of pictures taken during atmospheric freezing of a suspension of tobacco cells. Figure 4.64 shows a sequence during pressure-shift freezing at 200 MPa and -20°C. In both cases, the size of the crystals is so small that the individual crystals are not observable for the magnification used (the maximal for the equipment). Nevertheless, the relative size of crystals with respect to the size of the tobacco cells clearly shows that there is no significant difference between both processes in terms of direct damage of the cell structures, given the extremely small size of crystals. This means that the often reported effect of atmospheric freezing on the cell's disruption must have another cause. Our suggested thesis is that the disruptions are mainly caused during storage or thawing. This thesis will be further discussed. Another of the most reported effects of PSF is the nucleation rate. It has been confused the phenomena of nucleation rate and phase transition. It has been shown that, after observation of the results in the HPLT microscope, that the velocity of nucleation, or the velocity of the nucleation front is not clearly faster for PSF and slower for AF. Figure 4.63 showed the image sequence (each image is taken 0,1 second after the previous one) for an AF process in tobacco cells. Figure 4.65 shows the same process, AF, also for tobacco cells suspension, in which the nucleation process is clearly slower than the case shown in Figure 4.63, where from one image to the next (that is, in less than 0,1 seconds), the whole sample was nucleated. For comparison, Figure 4.66 shows 0,1 seconds sequences of images for the PSF process shown in Figure 4.64.

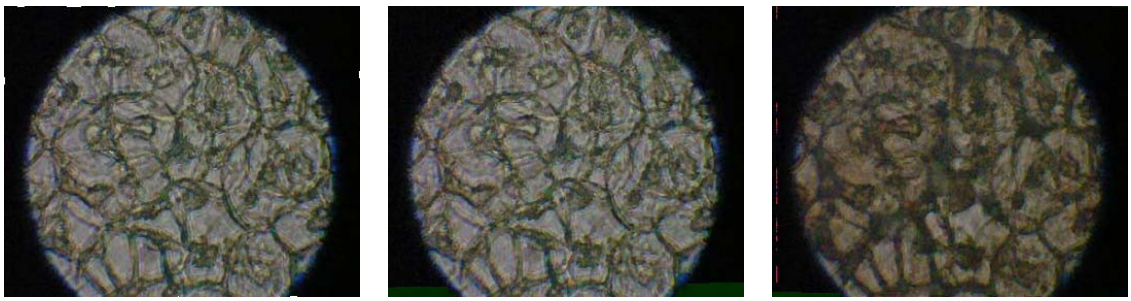

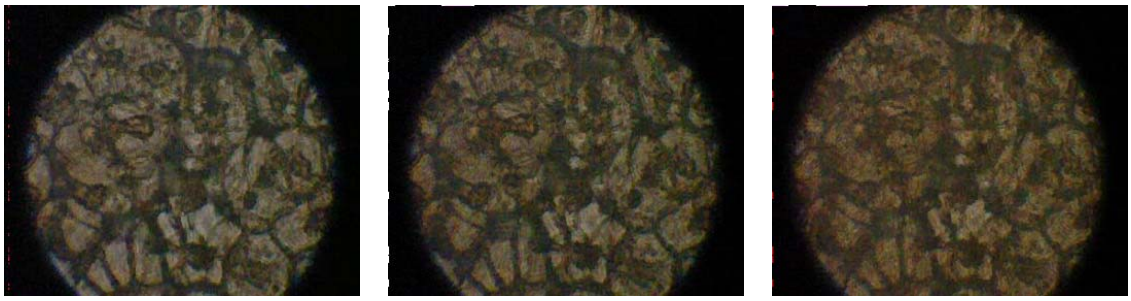

Figure 4.63. Pictures taken from the HPLT microscope during atmospheric freezing of tobacco cells suspension (sample 1)

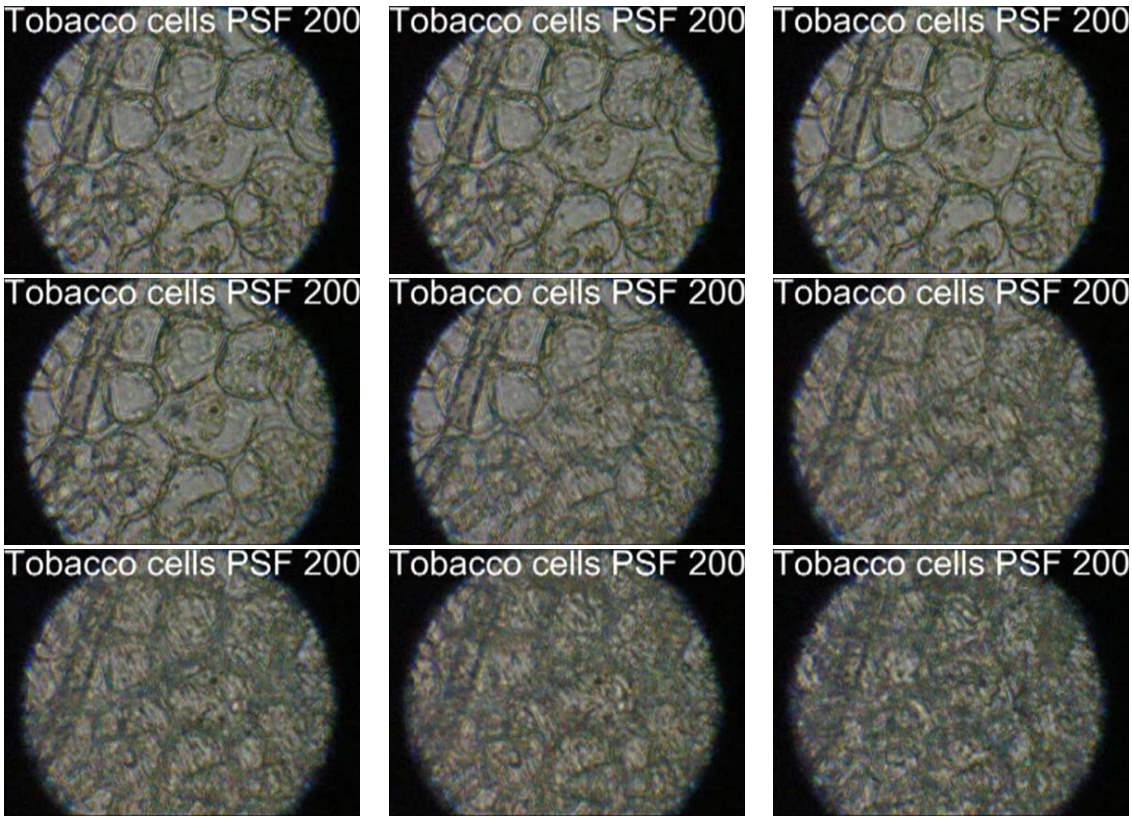

Figure 4.64. Pictures taken from the HPLT microscope during pressure-shift freezing of tobacco cells suspension at 200 MPa and -20°C (sample 2)

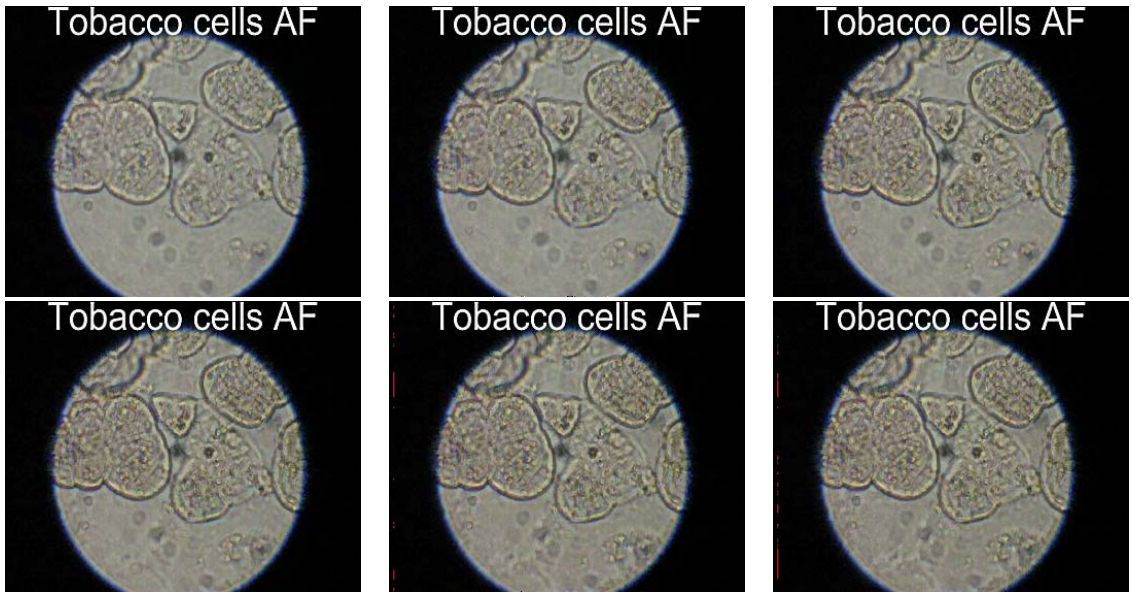

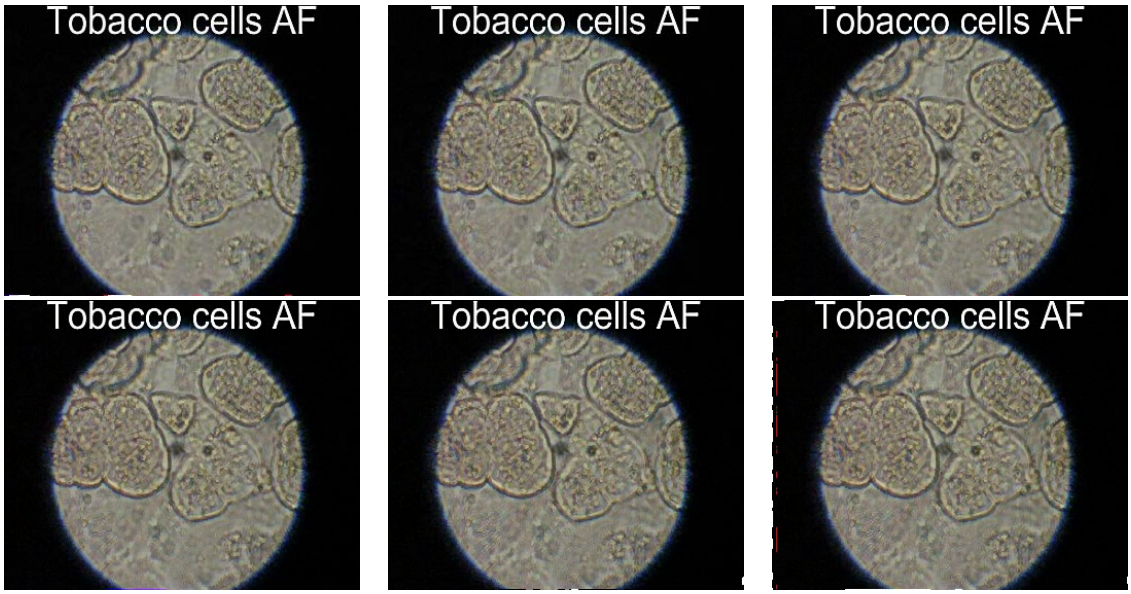

Figure 4.65. Sequence of images taken every 0,1 seconds during AF of tobacco cells suspension (sample 3)

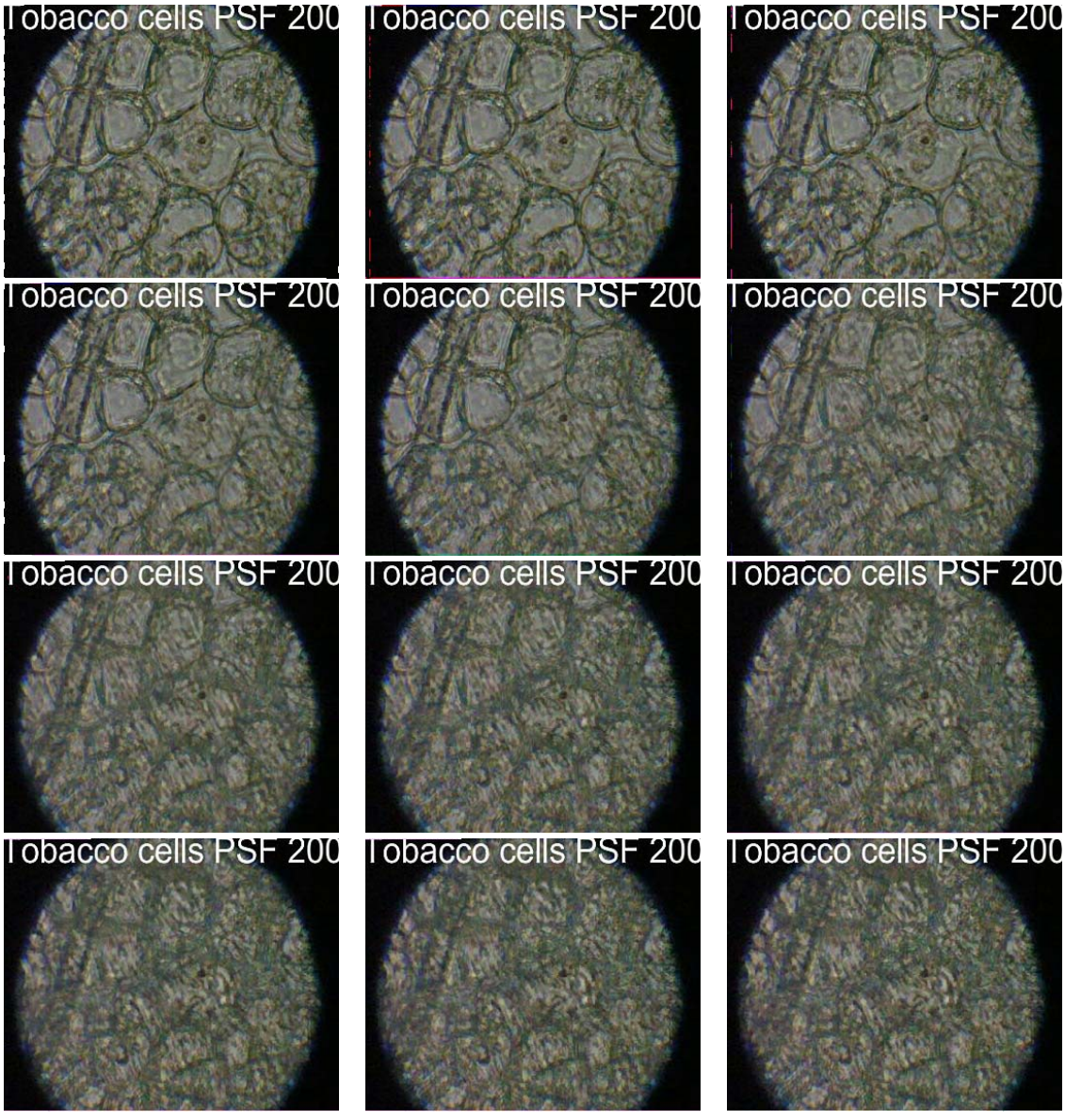

Figure 4.66. Sequence of images taken every 0,1 seconds during PSF of tobacco cells suspension (detail pictures from sample 2)

As mentioned before, it has been mentioned, we believe that the cell disruptions occur during storage in the frozen state or just before thawing processes. The reason may be the clustering or combination of ice crystals in bigger size crystals, due to a partial melting of their surface, which promotes this clustering. Experimental demonstration of this phenomenon has been obtained through the pictures taken in the HPLT microscope. Figure 4.67 shows the case of an AF process in the red onion sample, in which a crystal clustering is observed after the first nucleation (on(in a large scale of time). Figure 4.68 shows the case of an AT process, in which the clustering of ice crystals previous to the actual thawing process is clearly observable, in the case of lettuce tissue.

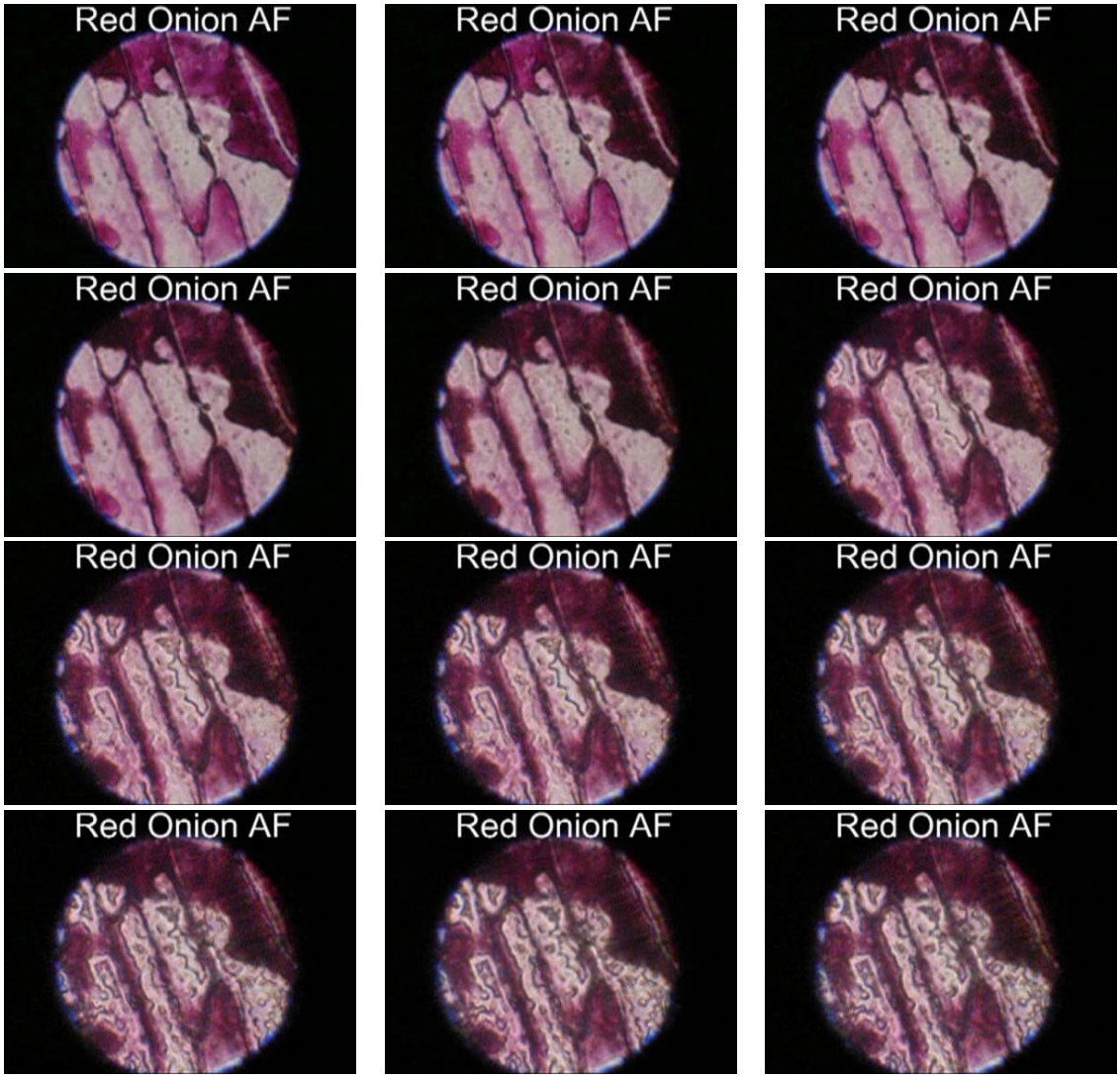

Figure 4.67. Sequences of AF of an onion sample, in which clustering of ice crystals after the first nucleation is observed

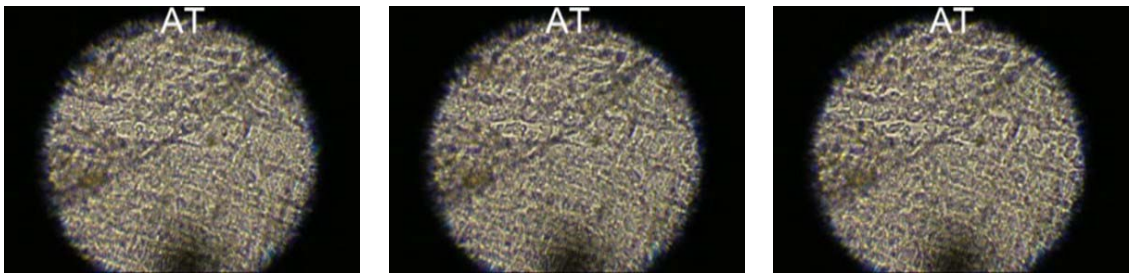

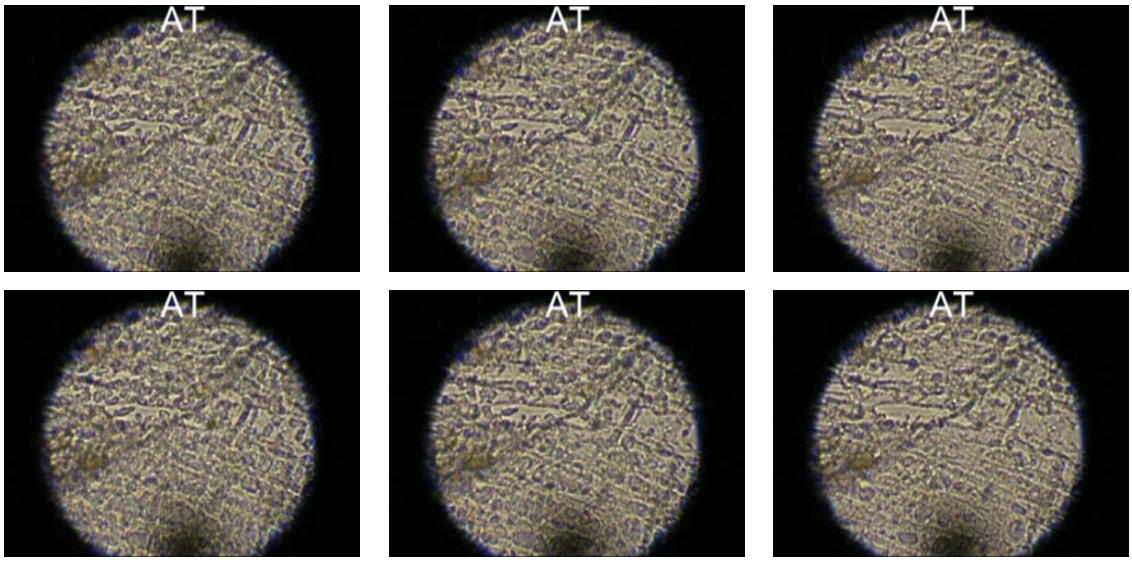

Figure 4.68. Sequences of images, previous to AT process of a lettuce sample, in which ice crystal clustering is observed before the actual thawing process

The solid-solid phase transitions are thought to create dramatic shear forces in cell structures, due to the great volume change between ice I and ice III. For example, Luscher et al. (2005) reported that the transient phase change of ice I to other ice polymorphs (ice II or ice III) during pressure cycles above 200 MPa resulted in an inactivation of about 3 log – cycles of Listeria inocua frozen suspensions, probably due to the mechanical stress associated with the phase transition. The first results obtained with the HPLT microscope are confirming that ice I to ice III phase transitions cause dramatic cell damages. Figure 4.69 shows solid-solid phase transition from ice I to ice III in onion tissue, Figure 4.70 shows ice III to ice V phase transition in onion tissue, Figure 4.71 shows ice V to ice III transition in apple tissue and Figure 4.72 shows ice III to ice I phase transition in apple tissue.

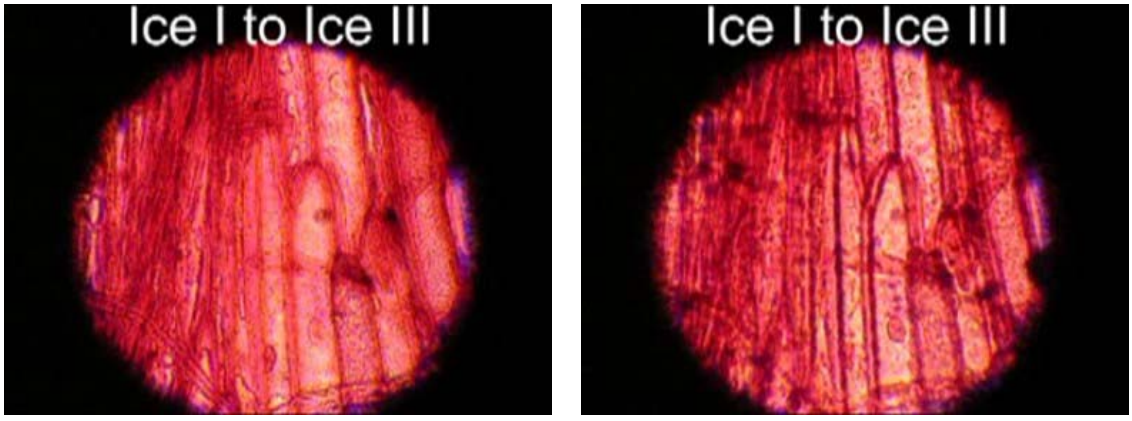

Figure 4.69. Sequence of images taken every 0,05 seconds from a solid-solid phase transition from ice I to ice III in coloured onion tissue.

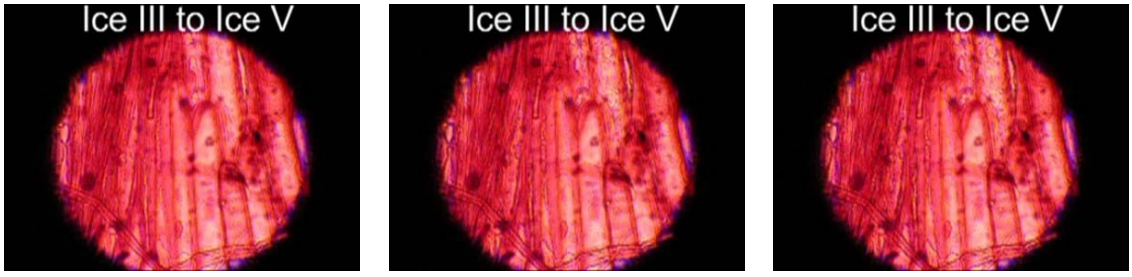

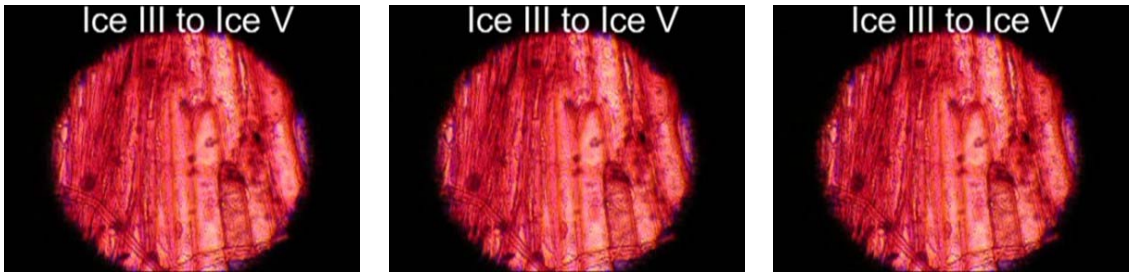

Figure 4.70. Sequence of images taken every second from a solid-solid phase transition from ice III to ice V in coloured onion tissue.

The ice I to ice III phase transition shown in Figure 4.69 shows an instantaneous process in which the cell size and form is dramatically changed due to the density variation from one ice modification to the following. In the case of ice III to ice V transition (Figure 4.70), the process is quite slow (the six-pictures sequence shown covers a total of 5 seconds) in which no cell size change is observed. The stress caused in ice I to ice III transition is, therefore, clearly high and the one cause in ice III to ice V not observable with the images taken in the HPLT microscope.

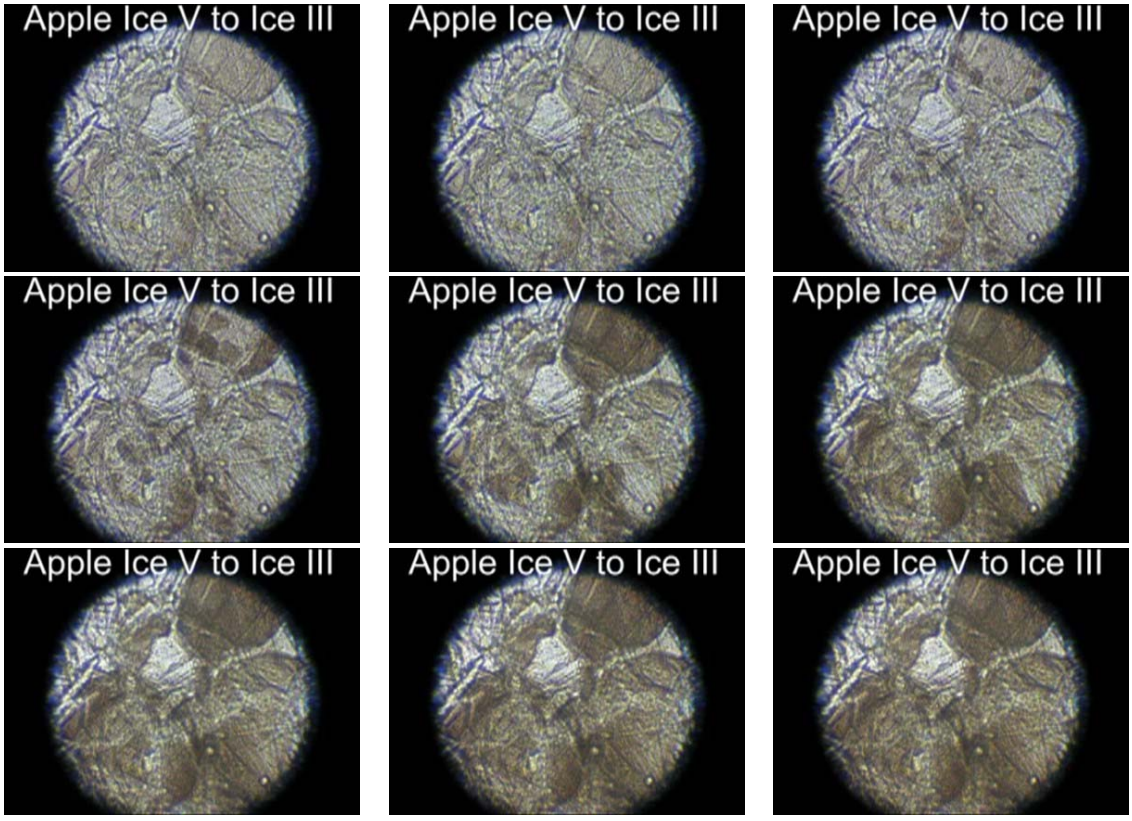

Figure 4.71. Sequence of images taken every second from a solid-solid phase transition from ice V to ice III in apple tissue.

In the opposite cases, that is, solid-solid phase transitions during pressure release, in both cases (ice V to ice III and ice III to ice I), the process is relatively slow (picture sequences of 8 seconds in the first case and 0,93 seconds in the second) and happens clearly first (or only) inside the cells. The cell walls are nor changed, after the images taken in the HPLT microscope, but the fact that there is a difference of the sate inside and outside the cells may cause stresses in the cell tissues.

The existence of metastable phases has been proved in potato tissue, as shown in Figure 4.73. At constant pressure of 260 MPa, between -26 and -28°C, the sample appearance changed in an unknown way (neither water nor ice) previous to the pressure release, after what a clear solid phase was observed. This metastable phase,

which density has been indirectly measured, as explained in the next chapter, seems to be a phase between water and ice, but being neither of them.

All the results shown in this chapter are the preliminary results obtained during the first experiments carried out in the prototype of HPLT microscopic cell and are actually opening more questions to be solved in the future than answers to some of the key phenomena involved in the HPLT technology.

One question to be studied in detail is the influence of the sample size on the results obtained. The differences observed between macroscopic and microscopic samples could be only the direct consequence of the specimen size and the nucleation phenomena can behave differently depending on the sample size. Therefore, the results presented here must be taken and discussed carefully. A methodical study of the differences of macroscopic and microscopic results on phase transition temperatures and pressures, nucleation points, existence of metastable phases and delimitation of their regions, etc. must be addressed in the future to better understand the freezing and thawing phenomena at high pressure. To obtain good images in a transmission light microscope, the samples must be very thin and therefore, the influence of the type of nucleation can be the key to explain the differences explained in this chapter between reported works (about nucleation rates, ice crystals size, etc.) and the first results obtained with the HPLT microscopic cell.

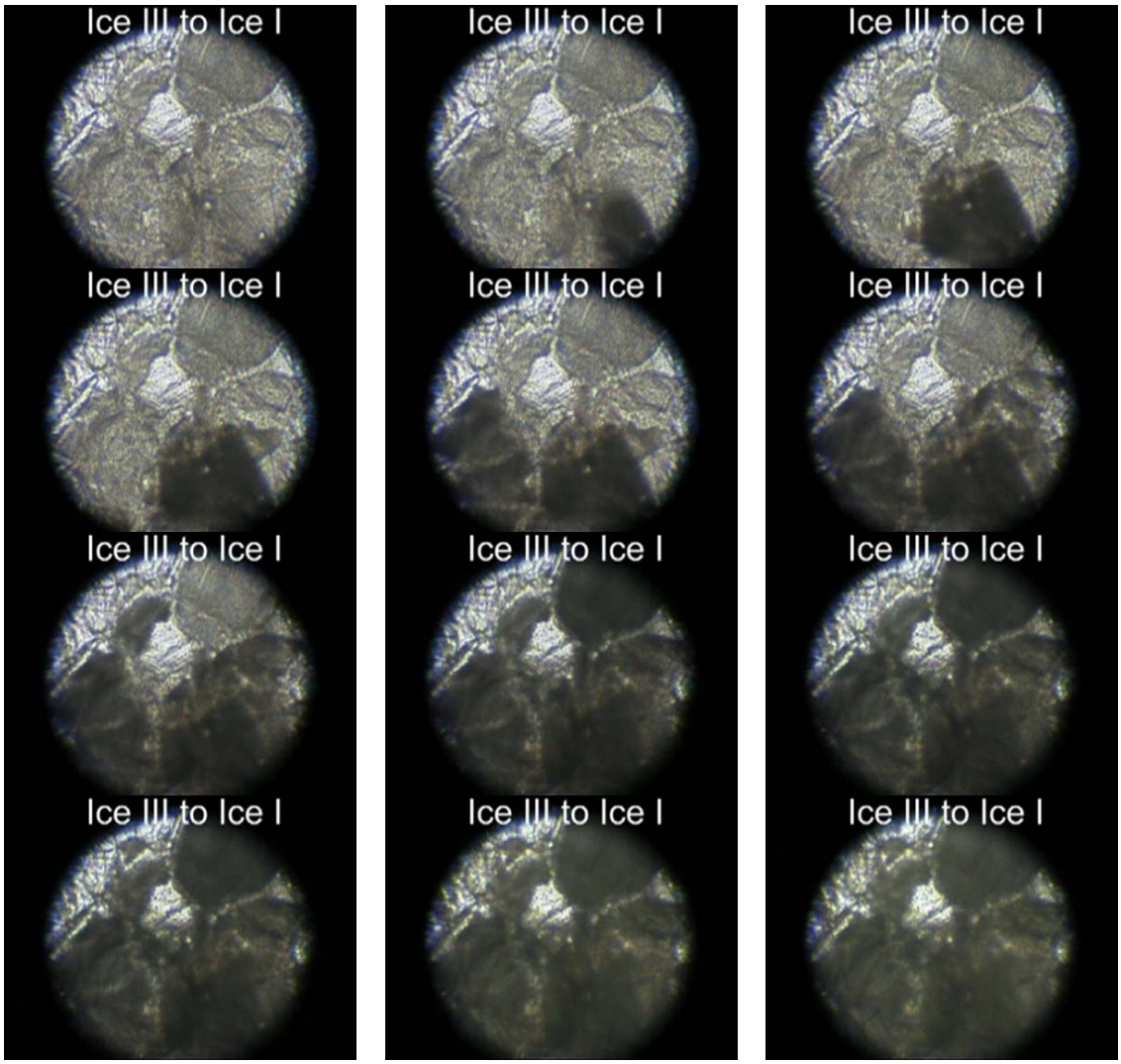

Figure 4.72. Sequence of images taken every 0,1 second from a solid-solid phase transition from ice III to ice I in apple tissue.

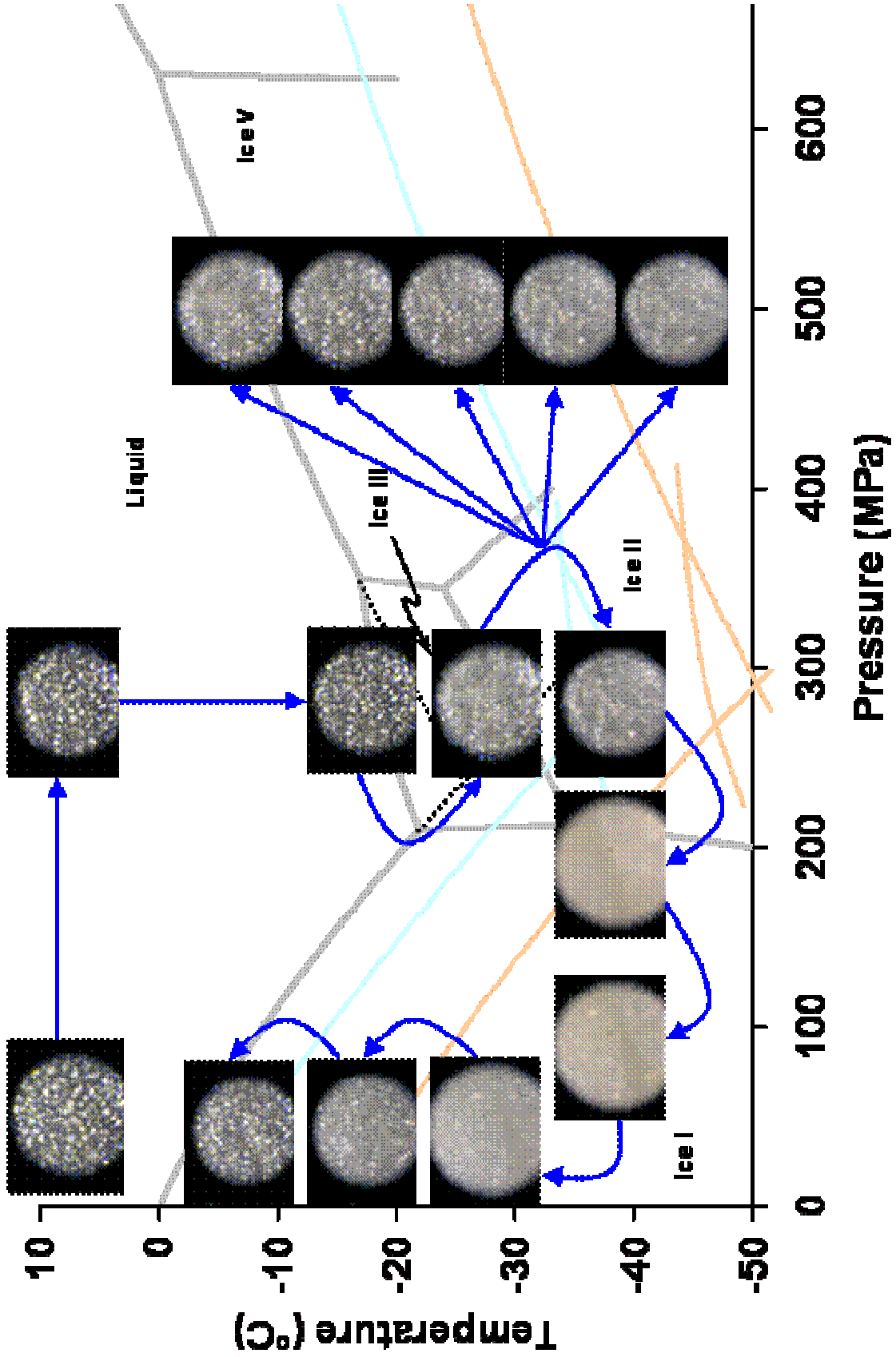

Figure 4.73. HPLT microscope images of potato during a pressure-assisted freezing process at 260 MPa, including a metastable liquid phase previous to pressure release.

4.5. Micro-organisms inactivation results

High hydrostatic pressure has attracted much interest as an alternative to heat as a means of inactivating microbes in food (Knorr, 1995). To ensure that pressure-treated foods are microbiologically safe, it is necessary to define pressure treatments that will ensure destruction of the pathogens of concern in different foods (Mackey et al., 1995). Although the use of high hydrostatic pressure technology as a pasteurization treatment is increasing (Schlüter et al., 2004), knowledge of the underlying mechanism of inactivation is limited (Hoover, 1989).

A vast amount of data exists on the kinetics of pressure inactivation of vegetative micro-organisms (Cheftel et al., 1995) at ambient and elevated temperatures (Heinz and Knorr, 1996; Heinz et al., 1998). In contrast, limited information has been gathered so far concerning microbial inactivation by means of high pressure in the low temperature range. Empirical data have shown that high pressure processing at low to ambient temperatures yielded improved microbial inactivation and better sensorial characteristics of vegetables (George, 2000; Brul et al.; 2000; Smelt et al., 2001). Preliminary data on selected pathogenic organisms suggest more effective inactivation under pressure at low (-10 to 5°C) temperatures as compared to ambient (20 to 40°C) ones (George, 2000).

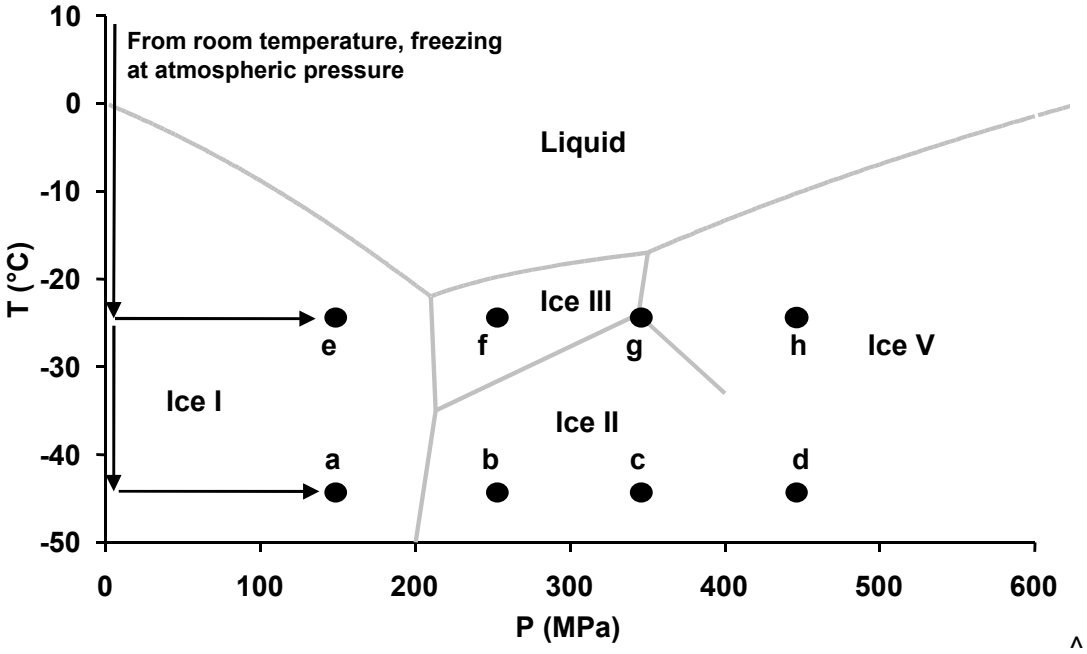

Figure 4.74. P/T conditions of experiments: (a) –45°C/150 MPa; (b) –45°C/250 MPa; (c) –45°C/350 MPa; (d) –45°C/450 MPa; (e) –25°C/150 MPa; (f) –25°C/250 MPa; (g) –25°C/350 MPa; (h) –25°C/450 MPa.

The different possibilities of processing food products in the high pressure - (subzero) low temperature (HPLT) range described by Urrutia et al. (2004) include ice phase transitions that should affect the viability of unwanted micro-organisms when present in treated products. A recent study from Luscher et al. (2004) indicated that inactivation of the gram-positive bacterium *Listeria innocua* is more effective after it had undergone Ice I-III solid-solid phase transition. In the current paper, *Bacillus subtilis* PS832 vegetative cells were selected as a model for spore-forming gram-positive bacteria. We chose this model, as we wanted to assess whether the HPLT treatment is also effective against vegetative cells of a spore-forming microbe. These micro-organisms are a challenge to the food industry since they can produce highly thermal resistant bacterial survival structures. Upon germination, these spores may give rise to biofilm formation for instance on piping of food manufacturing factories (den Aantrekker ED et al. 2003).

Such spores may survive the preservation treatment and can subsequently germinate in the product when distributed through the rest of the food chain. This causes economical loss and in some cases public health concern.

Here, the inactivation of *Bacillus subtilis* strain PS832, grown in TSB as culture medium, was studied for different pressure, temperature and time combinations. Some of these combinations lead to solid-solid phase transitions after freezing at atmospheric pressure and subsequent pressurisation. Depending on the pressure level, the samples may undergo solid-solid phase transitions from ice I into the domains of ice II, ice III or ice V (see Figure 4.74). We show that treatments of cells between 250 and 350 MPa at -25°C are the most effective in inactivating vegetative *Bacillus subtilis* cells. For these conditions, a double effect of extracellular solid-solid (Ice I-III) phase transition and possible intracellular solid-liquid phase transition is suggested to be key in mediating the observed drop in viability.

4.5.1. Determination of process parameters

In all cases, the samples were first frozen at atmospheric pressure and then pressurised until the corresponding set point. After the treatment time, pressure was released to atmospheric level, after which the samples were taken out from the pressure vessel. They were then kept at –25°C until further analysis of microbial survival. In the cases where pressure was applied at 2 cycles of 300 seconds, the samples were again pressurized after the first pressure release.

Given the different P/T combinations, at which the samples were treated, the *Bacillus* suspensions were subjected to different solid-solid and solid-liquid phase transitions. Depending on the rate of pressurization and pressure release, these solid-solid phase transitions were more or less easily observable in the pressure and temperature profiles. A slower rate of pressure release allowed us to obtain a clearer discontinuity in the P/T profiles. It must be pointed out that the temperature measurements correspond to the temperature of the surrounding pressurization medium and not are direct temperature measurement of the microbial suspension. Therefore, the pressure changes (due to phase changes) could not be directly inferred from the temperature changes. Nevertheless, the pressure changes, due to density changes between ice modifications, are still recognizable in most of the pressure profiles.

Different examples of P/T/t (pressure/temperature/time) diagrams reflecting the applied processes are shown in Figure 4.75. Phase transition events are circled.

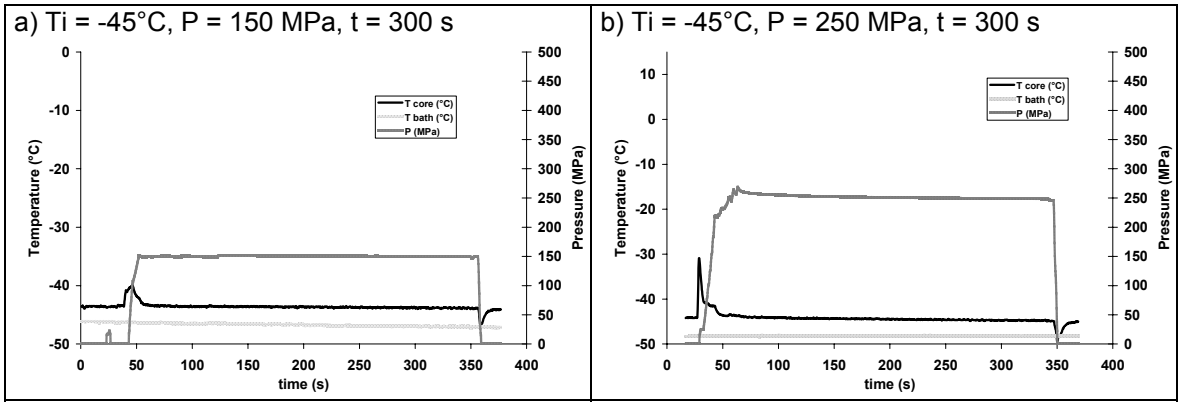

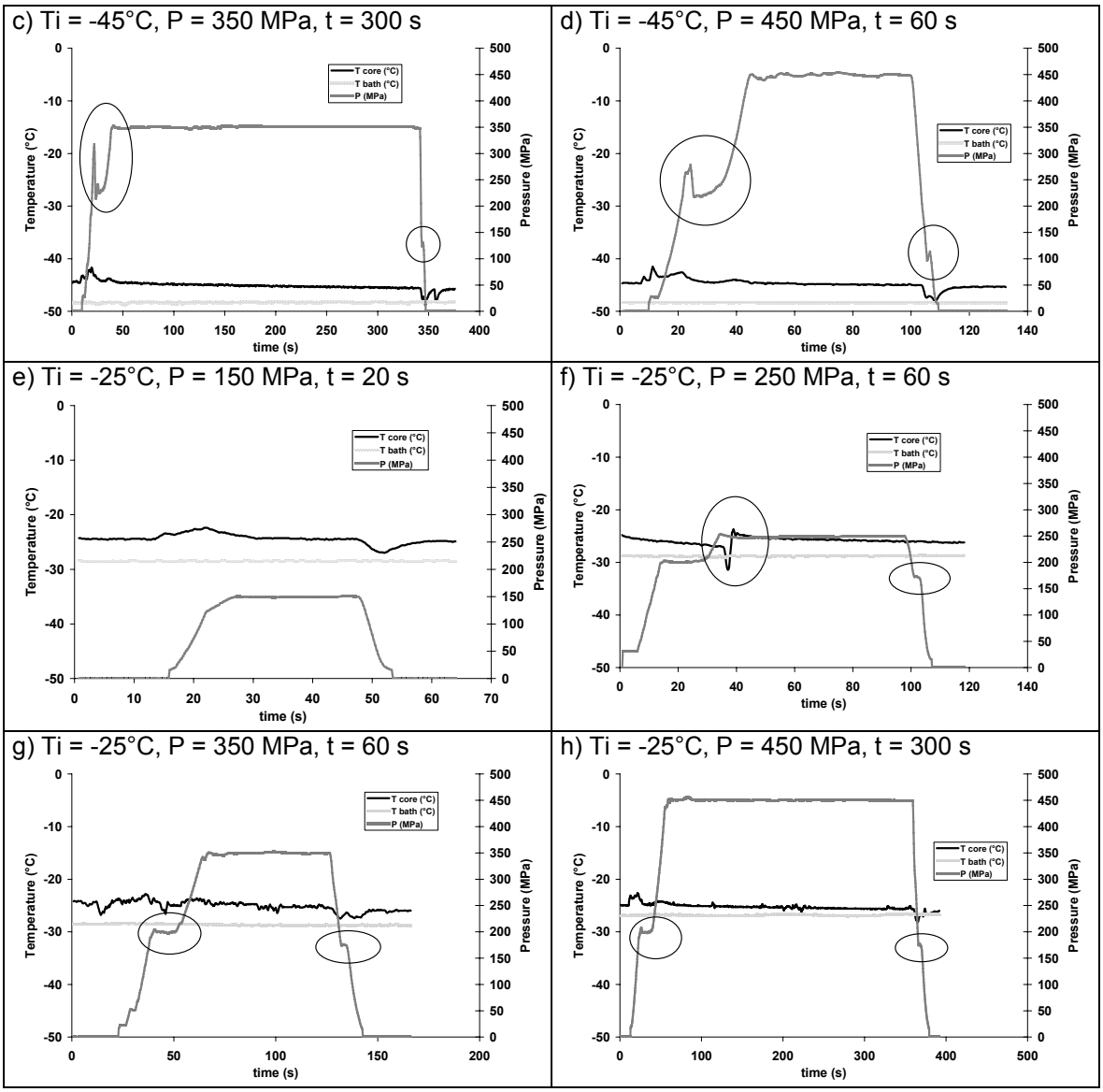

Figure 4.75. Examples of one-cycle P/T profiles. Bacillus subtilis overnight cell-suspensions in ACES buffer were treated at various time intervals, temperature and pressure levels as outlined in Materials and Methods. Phase transition events are indicated with a circle.

In the experiments described in Figure 4.75a, Figure 4.75b and Figure 4.75e, no solid-solid phase transitions took place, as no discontinuities in either pressure nor temperature profiles were detected. In these cases, the samples kept the initial ice I structure. The analysis of the other experimental conditions (Figure 4.75c, Figure 4.75f, Figure 4.75g, and Figure 4.75h) does show solid-solid phase transitions as indicated by the discontinuity in the individual traces (see circles in the figures). The singular points indicating the P/T conditions (Figure 4.74) for the different experiments lay in some cases in the domain of ice structures other than the ones expected on basis of the ideal behaviour of pure water. For instance the fact that ice V was never obtained throughout the experiment as shown in Figure 4.76 exemplifies the existence of metastable states of ice III. The specific cases are discussed below.

Figure 4.75a shows one of the experiments carried out for the P/T combination of –45°C and 150 MPa. For this P/T combination, as it can be seen in Figure 4.74, we expected to obtain ice I. The P/T profiles experimentally obtained confirmed this. The same is applicable for the example shown in Figure 4.75e (-25°C and 150 MPa). For

this P/T combination, the sample is still placed in the domain of ice I. No solid-solid phase transitions were observed.

Figure 4.75b shows an unexpected result. For this P/T combination (-45°C and 250 MPa), the sample is in the domain of ice II, but the experimentally obtained curves indicated that no solid-solid phase transitions occurred. This behaviour gives a strong indication for the existence of a metastable state of ice I in the domain of ice II. It should be taken into account that even the solid-solid phase transition lines for pure water as shown in Figure 4.74 are actually the average values from many data points that have an experimental variability of more than 100MPa in some cases. Figure 4.75f and Figure 4.75g show two examples of processes in which a solid-solid phase transition from ice I to ice III took place, just as on basis of the positioning of these processes in the phase diagram. In both cases, the phase transition was clearly observed both during pressurisation and upon depressurisation.

Figure 4.75h shows a treatment of cells at –25°C /450 MPa. For this P/T combination, as shown in Figure 4.74, it was expected that a second solid-solid phase transition from ice III to ice V would take place. However, as the P/T profiles show, only a phase transition from ice I to ice III was observed. This case again points to the existence of a metastable phase, in this case of ice III in the domain of ice V.

Figure 4.75c and Figure 4.75d show treatments of cells at -45°C/350 MPa and -45°C/450 MPa, respectively. Despite that the ice II stability area is the one present in these experiments, ice III is usually formed when pressurizing ice at about -45 °C above the transition pressure (see e.g. the Luscher et al. 2004). To assess the state of ice in our experiments, samples were warmed under constant pressure of 300 MPa above the ice II – ice III phase transition line until reached +10°C (unpublished data). No solid-solid phase transition was observed. Instead, the ice directly melted to water at the temperature of the phase transition line of ice III to liquid. This clearly indicated that the ice modification that was present was ice III. Therefore, we assume that ice III was formed in all cases in which solid-solid phase transitions took place.

For the experiments at -45°C, the fact that in all the experiments carried out at 250 MPa no-phase transition was observed, highlights the existence of a metastable area of ice I in the domain of ice III. Only when the set point pressure was higher than 250 MPa, did the phase transition occurred. Also, the fact that the points registered for the transitions during pressure increase differed significantly with those obtained during pressure decrease, demonstrate the existence of kinetically metastable phases, leading to hysteresis processes. In these situations the path of the process under study has an influence on the final registered phase transition points.

Finally, for the experiments at -25°C, the lack of a phase transition ice III to ice at 450 MPa is evidence for the existence of a metastable phase ice III in the domain of ice V.

Figure 4.76 summarises all the accumulated data of solid-solid phase transitions during our experiments. Clearly, depending on the direction of the path or pressurisation or pressure release, the positioning of the experimental phase transition points differed.

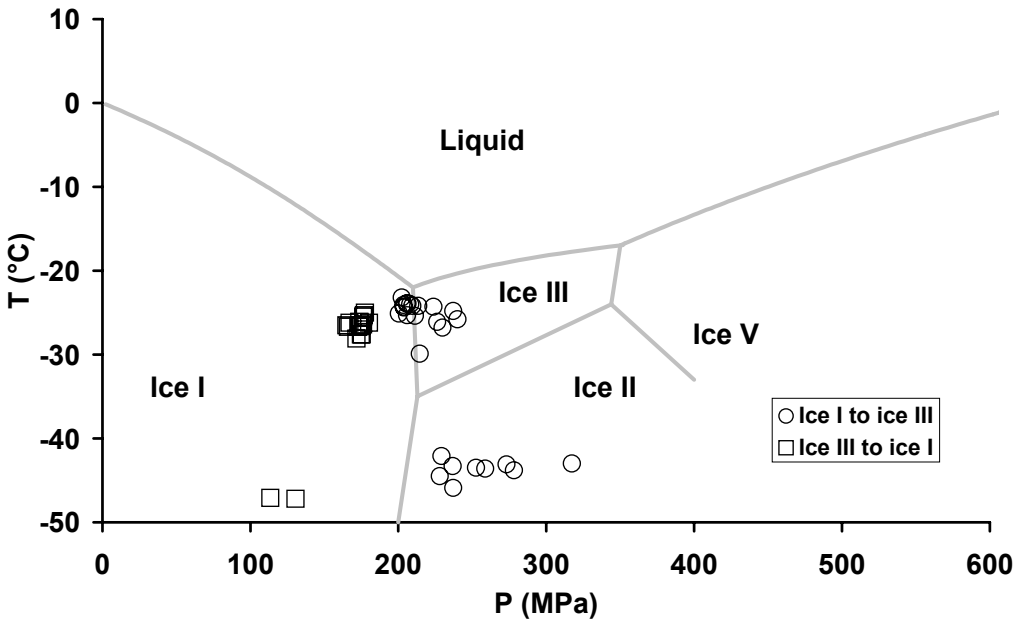

Figure 4.76. Solid-solid phase transition points for of Bacillus subtilis suspensions.

Summary for all the accumulated data of solid-solid phase transitions during our experiments. Depending on the direction of the path or pressurization or pressure release, the positioning of the experimental phase transition points differed. In this case, it should be pointed out that the lines shown for the pure water diagram are average values, as published from Bridgman (1912). Therefore, the range over which solid-solid phase transitions may be obtained can be very wide.

4.5.2. Influence of the HPLT on Bacillus subtilis cells

4.5.2.1. HPLT applied on Bacillus subtilis cells in the domain of ice I

To assess the bactericidal effect of freezing bacteria at atmospheric pressure, samples were frozen and kept for 40 minutes at –25°C or –45°C, respectively. Additionally, bactericidal effects of long term storage at –20°C (over 25 - 31 days) were also monitored. The number of survivors was assessed by colony counting of aliquots after 3 days of incubation under optimal conditions (37°C on TSA plates).

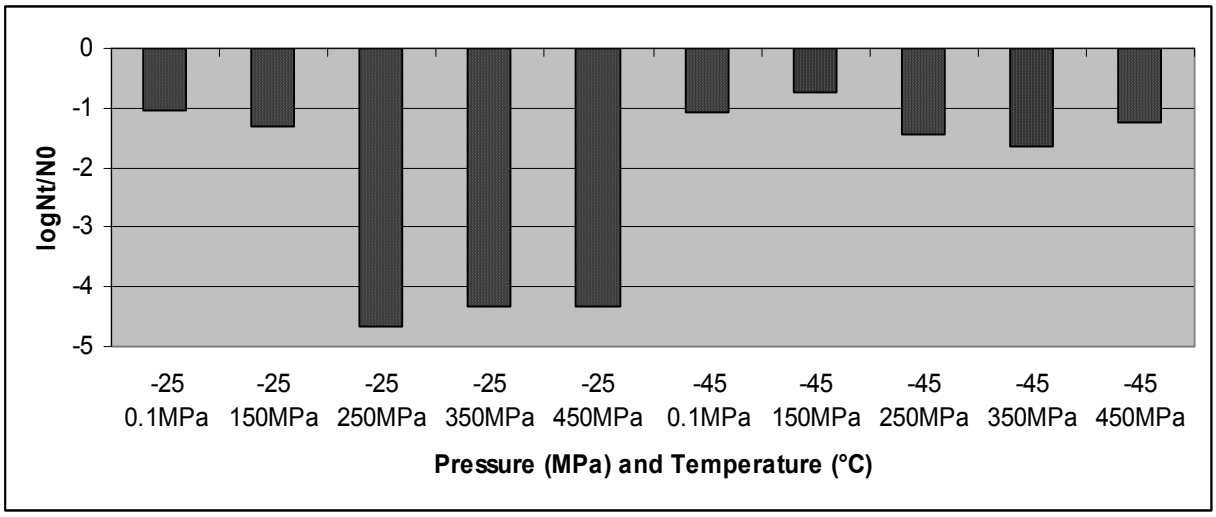

Figure 4.77. The effect of lowered temperatures on HPLT inactivation of Bacillus subtilis cells. B. Subtilis strain PS 832 was suspended in ACES buffer at appropriate dilutions. The cultures were then treated in sealed bags for 20

second at the indicated P/T combinations as described in Materials and Methods. Survival was measured through plate counting.

The viability of the cells was not affected by short-term storage at subzero temperatures. After 40 minutes freezing at –25°C and –45°C, only a small log_{10}-reduction in colony forming units (CFU's) was found (Figure 4.77). Even a long-term storage of up to 4 weeks did not lead to further substantial inactivation. A maximum of 1.4log-reduction in CFU's was found at 31 days of storage at –20°C.

Next we assessed what the effect was of applying pressure on deep frozen *Bacillus subtilis* cell. We found that 150MPa pressure at either –25°C or –45°C led to only a1 log-reduction in CFU's (Figure 4.77)

4.5.2.2. Effect of HPLT on microbial survival

Effect of temperature and pressure on inactivation: Figure 4.77 summarises the results of the inactivation levels observed in *Bacillus* subtilis cells subjected to a 20-seccond treatment at the various P/T combinations. All experiments carried out at 250MPa and higher and at an initial temperature of -25°C, resulted in strong inactivation. In Bacillus suspensions subjected to such conditions, a more than 4 log-reduction in cell viability was observed. Considering that the suspensions contained ca. 102 spores/ml, we concluded that a nearly full inactivation was achieved. Other cases (-45°C with various pressures, and -25°C/150MPa) resulted in mild to moderate inactivation, characterised by less than 2 log-reduction in viable cells. In addition, the inactivation showed a non-linear relation to treatment pressures at all the subzero temperatures. In contrast to what was observed at –25 and -45°C, the application of high pressure (200-250MPa) at 10°C up to 60 seconds led only less than one log reduction (Figure 4.78). An increasing difference in CFU's was obtained when the pressure treatment was above 250MPa, or treatment time above 60 seconds.

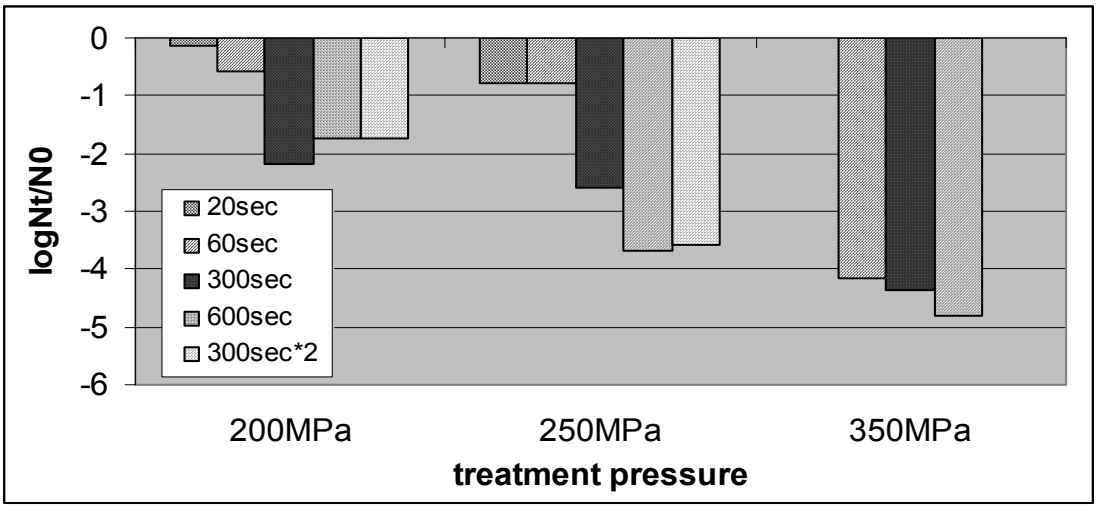

Figure 4.78. The effect on high-pressure inactivation of Bacillus subtilis cells at 10°C. B. Subtilis strain PS 832 was suspended in ACES buffer at appropriate dilutions. The cultures were then treated in sealed bags at the indicated P/t combinations as described in Materials and Methods. Survival was measured through plate counting.

Effect of the treatment time and application of two cycles of low temperature pressure treatment: In order to study in more detail the kinetics of the HPLT induced microbial inactivation, we then went on to assess the effect of treatment time on the inactivation of the cells. In these experiments, cells were exposed to –25°C or –45°C at elevated pressures and prolonged pressure holding times or with two cycles of pressure treatment. Unexpectedly, no significant correlation was found between treatment time and loss of viability at all experimental conditions. Figure 4.79 summarises the results

for the –25°C treatments. In a typical experiment, the inactivation of *Bacillus* cells that had undergone 600 seconds or a 2-cycles of 300 seconds treatment was not enhanced compared to a short-term treatment of after a few seconds only. A similar trend was observed for the –45°C treatments (data not shown). Interestingly, the inactivation at 10°C showed a clear time-dependence, with an increased loss of viability especially for a treatment time of up to 300seconds (Figure 4.79). The trend was mostly pronounced at pressures lower than 250MPa.

Temperature lowering alone has hardly any effect on the inactivation of *Bacillus subtilis* cells. High pressure alone has a minor effect on cell viability. The combination of high pressure and low temperature, especially when it led to phase transitions, turned out to be the most effective in inhibiting outgrowth of the *Bacillus* cells. In discussing our results, both solid-solid state transition and the phase transition from solid to liquid phase should be considered.

Phase transition from ICE I to III at temperature such as –25°C was observed. The change of the ice crystal configuration may induce denaturation of the cellular protein, which damages the integrity of the cell membrane, and could lead to enhanced inactivation of crucial intracellular enzymes.

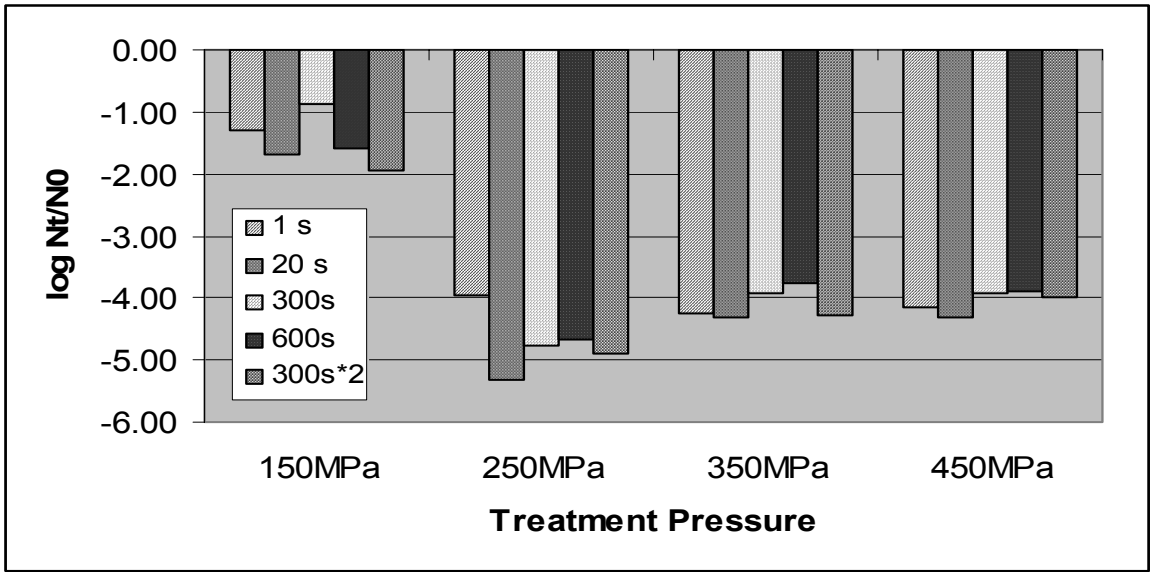

Figure 4.79. Influence of treatment time and repeated treatment on the inactivation of Bacillus subtilis at –25°C. B. Subtilis strain PS 832 was suspended in ACES buffer at appropriate dilutions. The cultures were then treated in sealed bags at the indicated P/T/t combinations as described in Materials and Methods. Survival was measured through plate counting.

In addition, partial thawing of structures inside the cells may occur as well. Osmotic active substances such as Na^+ and K^+ in *Bacillus* are reported to be present in vegetative exponentially growing cells at concentrations above 350mM and can easily reach 500mM or higher in stressed cells (Holtmann et al., 2002, and Whatmore et al., 1990). According to an ion-solvent interaction model proposed by Frank and Wen (1957), water structure around Na^+ ion resists making ice-like ordered water clusters while in the frozen environment. On the other hand, ions such as K^+, Rb^+, Cs^+ and NH^{4+} surrounded by the water are called structure-breaking ions, which make the structure of the ice crystal much “looser” than the ice made up of pure water. It is therefore hypothesized that at the above-mentioned conditions, thawing had already occurred inside the cells while the surrounding water (actually ice) was undergoing Ice I-III solid-solid phase transition. A double effect of extracellular solid-solid (Ice I-III) phase transition and possible intracellular solid-liquid phase transition is suggested to be a

key factor in mediating the observed large drop in viability at –25°C and ≥250MPa treatment.

On the other hand, *Bacillus* cells treated at –45°C had only Ice I-III phase-transition. More cells survived after treatment compared to the same treatment at –25°C because the intracellular surrounding was fully frozen. In contrast to the situation at –25°C, the high intracellular cation levels maybe help to protect cells by preventing protein denaturation (Kinsho et al., 2002).

In contrast to our results, Luscher et al. (2004) found, rather surprisingly, that inactivation of *Listeria* by the treatments at -45°C were almost as effective as the treatments at -25°C. This may be caused by the stationary phase *Listeria* not containing very high levels of osmotically active compounds (Fagerbakke et al., 1999).

Interestingly we found that inactivation showed a time-dependence only when the treatment was at 10°C, short-term and in the low-pressure range. All the other cases showed no time-dependence at all.

More than 4-log reduction was achieved after the treatment at 10°C and 350MPa. In this case, we considered it likely that most of the survivors are spores (ca. 10^2 ml^{-1}) since the initial inoculum was 10^{7-8} cfu/ml and contained up to 10^2 cfu/ml spores (see Materials and Methods). These results are in good agreement with the pressure resistance experiment on *Listeria monocytogenes* performed at 20°C (Tholozan et al., 2000).

To explain the cases at –25 and -45°C, as discussed above, phase transition (and possible partial thawing) caused the major inactivation when cells were treated with pressure while in the frozen state. The phase transition effect on cellular viability is much stronger than factors such as treatment time and pressure. Therefore the inactivation we observed was independent on the treatment time, and only slightly dependent on increased pressure too.. Moreover it is most likely that pressure, either. Moreover most likely susceptible cells had undergone (partial) intracellular thawing next to extracellular ice I-III phase transition, which may enhance the (all-or-nothing) effect. Therefore it would also explain why freeze-thaw-cycles did not lead to any additional inactivation.

Certainly results from the current study call for a mechanistic evaluation of the effects of applying high pressure at low temperatures as an anti-microbial treatment in the food industry. Such data are currently being gathered and will be very valuable in defining optimal cold pasteurisation process conditions.

4.6. Case study: Quality parameters of HPLT processed potatoes

The study of quality-related parameters in food models (tylose, gels from konjac glucomannans and calcium ions, agar gels, soy protein (tofu) or β-lactoglobulin gels) has been carried out over the last two decades, mainly in the domain of ice I (when sub-zero temperatures are used) and in small volumes of processed samples, for pressure-shift freezing (PSF) and pressure-assisted thawing (PAT) processes: the Fuchigami group studied the structural and textural changes in Kinu-Tofu and Kopmmyaku, but only in small volumes of vessel (40mL) and sample (13.5mL) (Fuchigami and Teramoto, 1997; Fuchigami, Teramoto and Ogawa, 1998; Teramoto and Fuchigami, 2000). The same group reported the changes in temperature and structure of agar gel in a larger vessel (712.5mL) but using a small sample volume (71.25mL), representing a 10% of occupation ratio (Fuchigami and Teramoto, 2003). In all cases, the studies were carried at pressure levels of 100 to 700 MPa, each 100 MPa, and temperatures always higher than -20°C. The Cheftel group reported the microstructure characteristics through ice crystal size distribution analysis of oil-in-water emulsions, in a large vessel (1105.8mL), but using very small samples (50g) and always pressure-shift freezing the samples in the domain of ice I (PSF at 207 MPa and -18°C) (Lévy, Dumay, Kolodziecczyk and Cheftel, 1999; Thiebaud, Dumay and Cheftel,

2002). Chevalier, Le Bail and Ghoul (2000) reported the ice crystal size in gelatine gel samples treated at 100, 150 and 200 MPa and at -20°C (domain of ice I in all cases) in a bigger scale (vessel volume of 3000mL and sample volume of 251mL). The Sanz group studied processes at different levels, 92 to 210 MPa and -8 to -21°C. The vessel volume was 2350mL and the sample volume 1208mL. Nevertheless, no quality related aspects were reported in this paper.

Also real products were studied after HPLT processing. Fuchigami, Kato and Teramoto studied the textural quality of carrots and Chinese cabbage (1997 and 1998, respectively), but the reported processes show that samples were already frozen before pressure build-up, so the results are not comparable with other reports. The process is, therefore, a pressurization at sub-zero temperatures, but, contrarily to other reports, the temperature of the sample did not decrease following the phase transition line of ice I, but increased during pressure build-up. The group of Le Bail studied the effects of PSF processes on the drip loss and physical properties of whiting fish, Norway lobster and turbot fish (Chevalier, Le Bail, Chourot and Chantreau, 1999; Chevalier, Sentissi, Havet and Le Bail, 2000; Chevalier, Sequeira-Munoz, Le Bail, Simpson and Ghoul, 2000). In all cases, a HP vessel of 3000mL was used, processing in each case, approximately, 500g of sample. Whiting fish was thawed at high-pressure (pressure-assisted thawing) at 50/100/150/200 MPa. Norway lobster PSF at 200 MPa and -18°C, and turbot fish PSF at 140 MPa and -14°C. The group of Sanz reported the microstructure of pork, eggplant, and mango and peach after processing with PSF at 200 MPa and -20°C (Martino, Otero, Sanz and Zaritzky, 1998; Otero, Solas, Sanz, Elvira and Carrasco, 1998; Otero, Martino, Zaritzky, Solas and Sanz, 2000). In all cases, the vessel volume was 2350mL and the sample volume, around 500mL. The group of Knorr described the impact of pressure assisted thawing on the quality of fillets from various fish species (redfish, salmon, whiting, haddock, rainbow trout and cod) through their sensory evaluation, texture, drip loss, colour, etc. (Schubring, Meyer, Schlüter, Boguslawski and Knorr, 2003). They treated the samples at 200 MPa in a 600mL HP vessel, processing in each batch 250 g of sample. Finally, Zhu, Ramaswamy and Simpson (2004) reported the effect of high-pressure versus conventional thawing on colour, drip loss and texture of Atlantic salmon. About 90g of fish sample were HP processed in a 4568mL vessel, performing a pressure-assisted-thawing process at 100/150/200 MPa.

All these studies were performed in the domain of ice I, that is, at temperatures higher than -22°C and at pressures up to 210 MPa. In the cases in which higher pressures were studied (the case of the group of Fuchigami), after reviewing this report, it seems that the samples were not actually frozen, because the temperature was not low enough to reach the area of nucleation (see definition in Schlüter *et al*., 2004). Therefore, no results are reported concerning the processing of food samples in other domains than ice I. The possibilities of processing taken into account in the present work are concerning the domain of ice III. A freezing process in which ice III is crystallized seems to be not feasible for the industry, because after nucleation of ice III crystals, the sample should be stored at high pressure, (which is not industrially performable) or depressurized. In the latter case, the solid-solid phase transitions are expected to lead to dramatic changes in the microstructure of samples. These processes are described in Figure 4.28.

The “classical” processes described are:

- Pressure-shift freezing (PSF) at 200 MPa (1➔2➔3➔4), the freezing process reported in most of the works published up-to-now;
- Pressure-assisted thawing to ice III (PAF-III) at around 280 MPa (1➔2➔5➔6➔7➔8), followed by high pressure storage (process stopped at point 6) and pressure-assisted thawing (6➔5➔2➔1) or followed by a solid-

solid phase transition during pressure release (point 6 to 7 and further to 8), which may cause dramatic damages in the cellular structure of vegetal tissues;

- PAT at 200 MPa (4➔3➔2➔1), the thawing process reported in most of the works published up-to-now; and
- PAT-III at around 280 MPa coming from atmospheric pressure (8➔7➔6➔5➔2➔1) or coming from high-pressure stored samples (6➔5➔2➔1).

The existence of metastable phases of ice I and liquid in the domain of ice III (as explained by Schlüter *et al*., 2004), permits the use of optimized paths for the processes PSF and PIT in the domain of ice III without actual crystallization of ice III. The experimental results shown in this paper demonstrate that when a process is carried out following the paths described in Figure 4.28, the ice modifications obtained are different to the expected ones. The novelty of the processes reported in this work is the use of the existence of these metastable phases to take advantage of maximum temperature gradients for freezing and thawing processes.

Pressure-shift freezing was performed at 240 MPa and around -24°C. At these conditions, although the stable phase is ice III, liquid water was still present in the samples before the pressure release. Lowering the temperature before pressure release means increasing the temperature gradient in the samples for the instantaneous nucleation, that is, the jump from this temperature level of -24°C to the plateau (at -1°C for potato, approximately). If the equipment is able to provide lower temperatures, a lower level can also be used, until around -28°C, without nucleation of ice III, due to the existence of a metastable liquid phase in this region (the cause of the supercooling phenomenon of around 15K when freezing to ice III).

Pressure-induced thawing was performed at 290 MPa. After placing samples in the high pressure vessel, pressure was increased until 290 MPa, and at this pressure level, the temperature profile “followed” the extension of the phase transition line of ice I into the domain of ice III, as shown in Figure 4.28 (path 4➔9). At this pressure level, the area of nucleation of ice III is not reached and, therefore, a metastable mixture of ice I and the partially melted water in the surface during pressurization is present in the samples. In this way, a higher driving force due to a higher temperature gradient was reached, being the difference between sample (around -35°C at 290 MPa) and the surrounding medium (+11°C) temperatures of 46K. Compared to the classical PAT, in which the temperature gradient is around 32K (from -21°C from the sample to +11°C from surrounding medium), the gradient is increased in 14K using this process, leading to a shorter processing time.

Up-to-now, storage processes of foodstuffs at subzero temperatures under pressure have not been carried out. The data on enzyme inactivation at subzero temperatures (Indrawati, et al., 1998, Indrawati, et al., 2000) suggest that denaturation of some enzymes under pressure might be enhanced by low temperature. Recently published data show that HPLT processes up to 210 MPa and -20°C are not enough to inactivate PPO enzymes from potato pieces treated by PSF, being pressure maintained for 1,5 to 3 hours (Préstamo et al., 2005). In this work, it has been reported that the combination of pressure and temperatures below zero produced a significant diminution by PSF treatment in the activity of PPO.

The action of polyphenol oxidase (PPO) in fruits and vegetables is connected to enzymatic browning of fresh and off-flavour generation in canned or frozen horticultural products, respectively (Vámos-Vigyázó, 1981). PPO is assumed to play a role not only in the brown discoloration of potatoes, but also in the formation of black spots following mechanical injury (Reeve et al., 1969; Amberger and Schaller, 1975).

Polyphenol oxidase (PPO, EC 1.14.18.1 and 1.10.3.1) catalyzes two types of reactions, both involving oxygen. The first reaction is the hydroxilation of monophenols to o-

diphenols and the second oxidation of *o*-phenolic substrates to *o*-quinones (Whitaker, 1972), which are subsequently polymerised to dark-coloured pigments. This copper containing enzyme, widely distributed in plants and animals, is considered to be the main contributor to undesirable browning, discoloration and darkening in fruits and vegetables (Mayer & Harel, 1979; Vámos-Vigyázó, 1981).

Several methods have been used to inhibit the enzymatic browning in foods. The traditional heat treatment is the most widely used food preservation method because of its faculty to destroy microorganisms and to inactivate enzymes. Steam blanching is very effective for controlling enzymatic browning in canned or frozen fruit and vegetables but not for fresh foods. In general, subjecting PPO to heat-treatment in the 70-90ºC range, results in the destruction of their catalytic activity (Vámos-Vigyázó, 1981). Blanching leads to losses in vitamins, flavours, colours, texture, carbohydrates and other water-soluble compounds. This method requires large amounts of water and energy and, additionally, waste disposal problems arise, making blanching technically disadvantageous (Marshall et al., 2000).

In the last few years numerous studies have been reported involving non-thermal – especially high-pressure – food preservation technologies. The effects of high-pressure related to food systems implies the modification of protein structure, that is, modification of enzymatic behaviour (Galazaka & Ledward, 1995) and inactivation of non-desirable microorganisms as well as retention of colour, favour and nutritional values. The other benefits of high-pressure, are the lack of environmental pollution, low energy usage and elimination of chemical additives. Knorr (1993) found that PPO is highly pressure resistant especially in potatoes. Pressures of 100-400 MPa led to a decrease in PPO activity at ambient temperature but it can not be inactivated even at 400 MPa, 50ºC for 15 min. treatment. Gomes and Ledward (1996) revealed after examining whole potato, mushroom and apple samples, that high-pressure alone is not realistic as a means of inhibiting PPO. This enzyme becomes inactivated at pressures which cause irreversible damage to the tissue itself.

Given this situation, the combination of high pressure with low temperatures, leading to the crystallization of ice, becomes one possible way to achieve enzyme inactivation. One of the most evaluated processes in this field is the “pressure-shift freezing”, PSF, whose aim is to improve the quality of frozen foods. In this process, the sample is cooled to sub-zero temperatures at high pressure without phase change and through an instantaneous pressure release, ice crystals nucleate homogeneously in the entire sample volume, due to the isotropy of pressure. Due to the high amount of ice instantaneously frozen during pressure release, the textural and structural damages caused by nucleation are minimized. The reported works are, nevertheless, only extended to pressure levels up to 210 MPa. Préstamo et al (2005) examined the PSF treatment of potato cubes. They point out that using high-pressure up to 210 MPa and temperatures of -8/-20ºC is not enough to inactivate the PPO, although the enzyme activity was reduced.

The use of High Pressure and Low Temperature (HPLT) processes for freezing and thawing purposes for food products have been object of various studies over the last years. A group of unique results in terms of quality, safety and stability related properties of products processed by HPLT technologies, with (freezing and thawing processes, solid-solid phase transitions) and without (sub-zero storage, chilling) phase transitions, has been collected within the European project SAFE ICE ((QLK1-2002-02230). The basic research concerned the determination of experimental phase diagrams of different food products and the experimental measurement of thermophysical properties which permitted a working model in which the potentials of self-developed industrial concepts (both for process and products) were analyzed. Given the potential of HPLT technologies for food processing obtaining a significant better quality of frozen products (specially in terms of texture) and better process conditions (lower use of water for thawing, shorter processing times for both freezing

and thawing), a study has been carried out on a pilot scale to determine the possibilities of processes like pressure-shift freezing (PSF) and pressure-induce thawing (PIT) (reference first paper). In this work, the preliminary results on a lab scale showed that the work in the metastable region of ice I in the domain of ice III (around 250 MPa and -25°C) has a positive consequence on the enzymatic activity shown in potatoes. Taking these results as a starting point, a new experimental set up was planed for a pilot scale equipment in which whole potatoes are treated under HPLT conditions for PSF and PIT processes.

The objective of the present work was to determine, on a pilot scale, the response of high-pressure-low-temperature processes on quality-related aspects (texture, colour and drip loss) and on PPO activity of whole potatoes. For this purpose, an experimental set was previously performed in laboratory scale to obtain preliminary results on the effect on enzymatic activity of PPO in potatoes for different high-pressure supported processes.

4.6.1. Laboratory-scale set: enzymatic activity of PPO

A previous experimental set had been performed at a laboratory scale to assess the enzymatic response of potato samples treated with PSF and PIT processes with pressure and temperature levels above the thermodynamic stable domain of ice I, i.e., in the metastable region of ice I (above 210 MPa and under -22°C). Figure 4.80 illustrates the time profiles and the phase diagram paths of one representative experiment.

The temperature profiles shown in Figure 4.80a correspond to a PSF process at -28°C and 260 MPa directly followed by a PIT process at 280 MPa. The sample temperature was recorded with a thermocouple in direct contact with the potato cylinder. During the freezing process (bath temperature -30°C) the pressure was built-up with the consequent adiabatic heating of the sample and pressure was kept constant until the sample temperature reached -28°C. When the sample centre reaches this temperature level, pressure is released and instantaneously, the sample temperature jumps to the atmospheric pressure corresponding to the phase transition temperature, for the potato, approximately, -2°C, and remains constant during the phase transition from liquid to ice I (freezing plateau). When the liquid is transformed into ice, the temperature decreases to the same level as before pressure release. At this point, the high-pressure vessel containing the potato cylinder is placed in the heating bath (temperature of +11°C) and the thawing process begins. First, the temperature of the sample increases at atmospheric pressure until a level of -10°C. At this point, pressure is built-up to 280 MPa and due to the endothermic partial melting of the sample, the temperature of the potato cylinder decreases to a level of -35°C, remaining constant until all the ice is transformed into liquid (thawing plateau) and then the temperature increases further at constant pressure until +9°C and then pressure is released, with the consequent adiabatic temperature decrease, until atmospheric level.

The freezing and thawing paths are shown in Figure 4.80b. The adiabatic heating during pressure build-up for the freezing process (full arrows indicate the direction of the freezing path) is followed by tempering at constant pressure until the set point (-28°C) is reached. Although the thermodynamic stable domain of ice III is reached, the sample remains liquid (no temperature jump is recorded) thanks to the phenomenon of supercooling, in which a metastable liquid phase is still present in the domain of solid phases before nucleation of ice (see Figure 4.28). When pressure is released, a first adiabatic temperature decrease is observed until the area of nucleation of ice I is reached, then the temperature of the sample jumps to the phase transition line and follows this line until reaching atmospheric conditions. After pressure release, the two steps occur nearly instantaneously. The temperature is decreased at atmospheric pressure. For the thawing path (dotted arrows indicate the direction of the thawing path), when the sample temperature reaches -10°C, pressure is built-up and instead of expected adiabatic heating, the temperature decreases, following the phase transition

line of ice I (background grey lines represent pure water phase transition lines) and even when pressure levels higher than 210 MPa are reached, although the sample enters the domain of ice III, still a mixture of ice I and melted ice I in the sample surface is still present. When the desired pressure level is reached (280 MPa), pressure is kept constant and the sample temperature is increased when the ice melting is completed. In this case, a metastable ice I present in the domain of ice III is observed experimentally (see Figure 4.28). When the temperature reaches +9°C, pressure is released with the following adiabatic temperature decrease. The temperature level before pressure release must reach a level high enough to avoid re-crystallization of the sample.

a

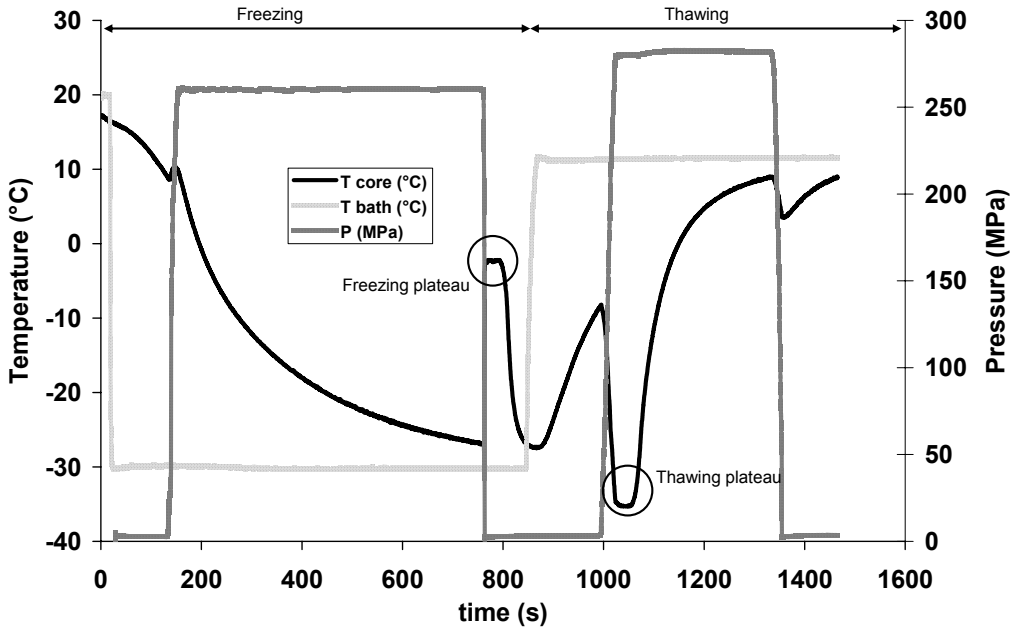

b

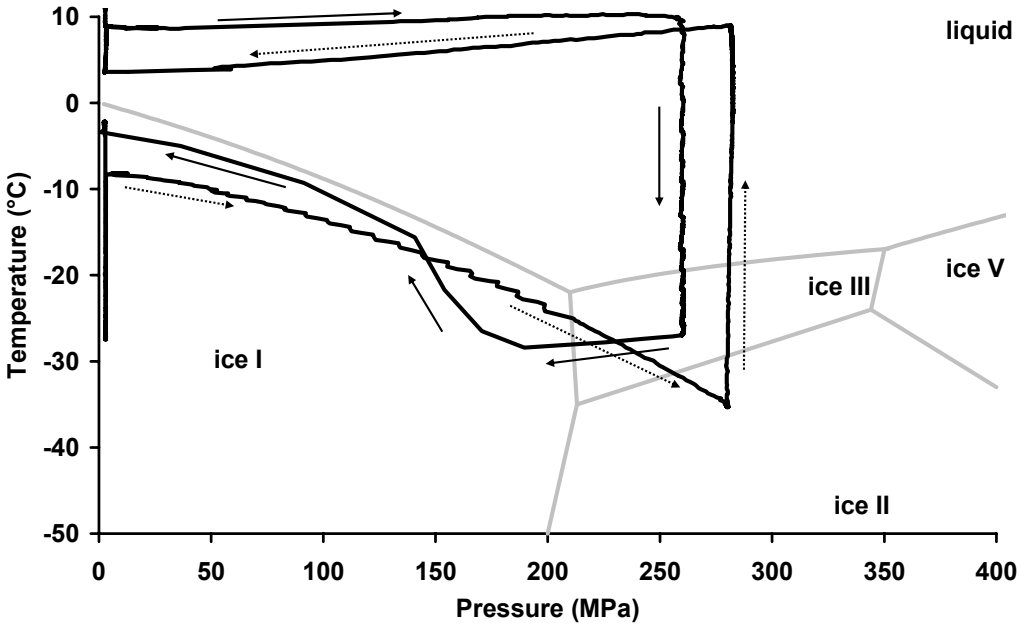

Figure 4.80. HPLT treatment time profiles (a) and paths on the phase diagram of water (b), with direction of paths for freezing (full lines) and thawing (dotted lines).

Observing the described freezing and thawing paths, the existence of both liquid and solid metastable phases can be used to increase the temperature gradients for freezing and thawing processes. Figure 4.81 shows these temperature gradient changes schematically.

In Figure 4.81a, the "conventional" (and most reported in the literature) PSF process is shown. Before the determination and explanation of the metastable phases (Schlüter et al., 2004), it was believed that -20°C and 210 MPa (point 3 in Figure 4.81a) was the lowest temperature and highest pressure possible before pressure release for PSF processes. The existence of a liquid metastable phase in the domain of ice I can be used to increase the real temperature gradient before pressure release (Figure 4.81b), therefore, minimizing the plateau time and consequently, minimizing the textural damage to food products. In the case of PIT, the limitation was believed to lie in the domain of ice I (point 3 in Figure 4.81c), but the existence of solid metastable phase in the domain of ice III can be used to maximize the temperature decrease until levels of -38°C at pressures higher than 260 MPa (point 3 in Figure 4.81d).

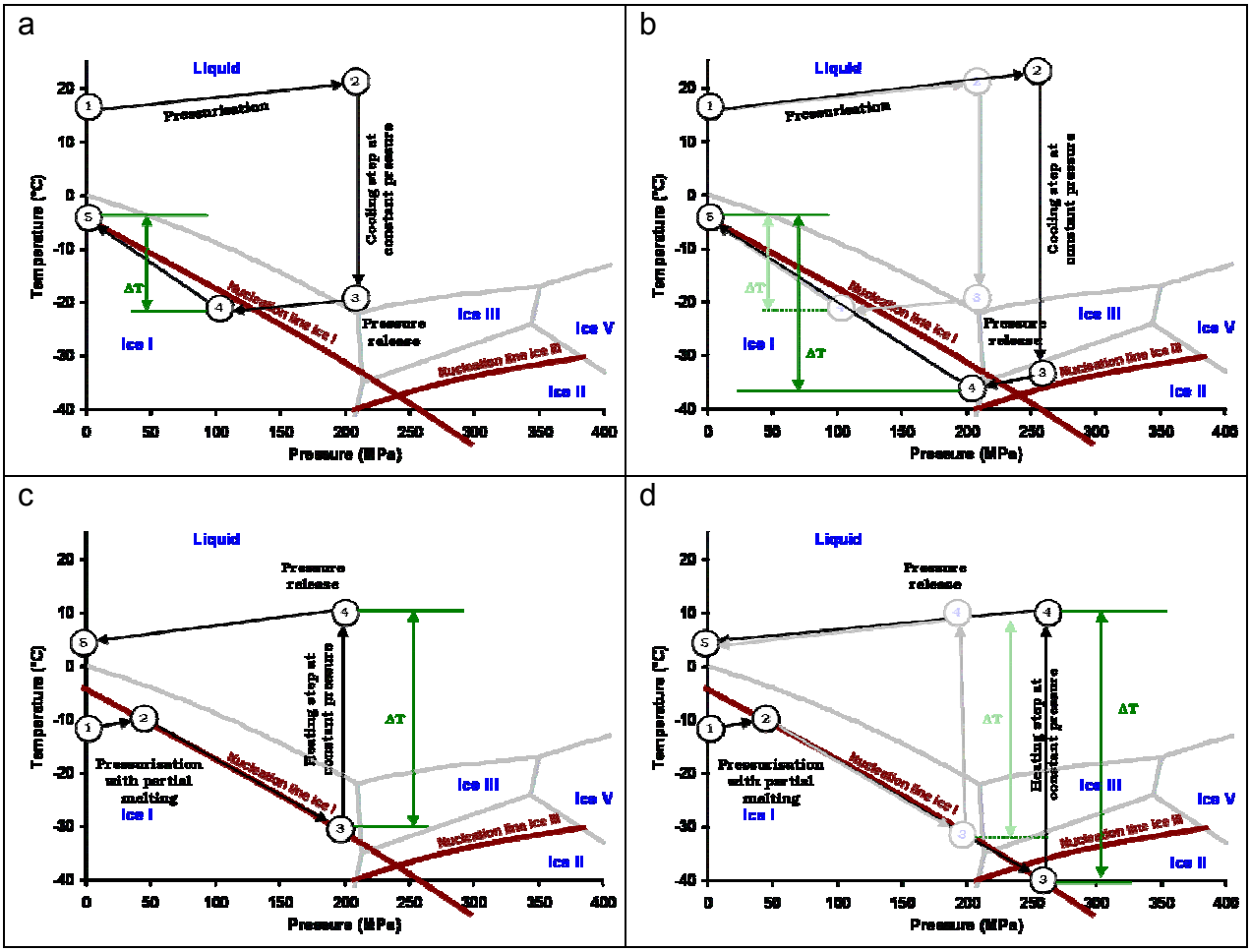

Figure 4.81. Schematic paths for "conventional" PSF (a), enhanced PSF (b), "conventional" PIT (c) and enhanced PIT (d).

The polyphenoloxidase content of a whole potato was chosen as a model system to assess the product's quality after pressure shift freezing followed by pressure-induced thawing processes. High-pressure assisted inactivation of quality determining enzymes requires relatively high pressures (700-800 MPa) combined with elevated temperature (40-50ºC). Seyderhelm et al. (1996) found that to inactivate most of the quality determining enzymes at least 800 MPa at 45ºC was needed. To preserve the quality whole vegetable products, high-pressure treatment alone is not enough (Gomes and Ledward 1996). Knorr (1993) carried out high-pressure treatments with potato cubes (400 MPa, 15ºC, 20 min.) with the changing of the pressure medium composition but

they only attained considerable decrease in PPO activity at 35 and 50ºC. The effect of high-pressure processing on enzyme kinetics, other chemical reactions such as the Maillard reaction (which causes browning) and lipid oxidation (which leads to off-flavours in fat-containing foods) are the focus of current research (Singh, 2001). High pressure treatments lead either to an activation or an inactivation of polyphenoloxidase (PPO) (Ludikhuyze and Hendrickx, 2002). To achieve considerable inactivation usually higher pressure – temperature combinations were required, but PPO from various plants differed in their activation / inactivation behaviour (Ludikhuyze and Hendrickx, 2002; Weemaes et al., 1998; Palou et al., 1999; Hernandez and Pilar Cano, 1998).

The effects of subzero temperature combined with high pressure processing on enzyme activity have been reported, but experiments were not designed to determine the extent of ice crystal formation, nor the relative effects of pressure-, cold- or freeze-denaturation (Cheftel et al., 2000). Enzymes solutions were frozen either by fast pressure release or under constant pressure, then thawed. In spite of long periods of time under pressure (80 to 135 minutes), PPO was not inactivated (Indrawati et al., 1998).

In the case of the preliminary experiments run on a laboratory scale, a summary of values of the enzymatic activity of each sample is shown (Figure 4.82a) together with a reference value, “fresh”, which shows the activity of fresh samples coming from the same potato rather than the treated sample. PSF 260 means pressure-shift shift freezing at 260 MPa and PIT 200 or PIT 280 means pressure-induced thawing at 200 or 280 MPa, respectively.

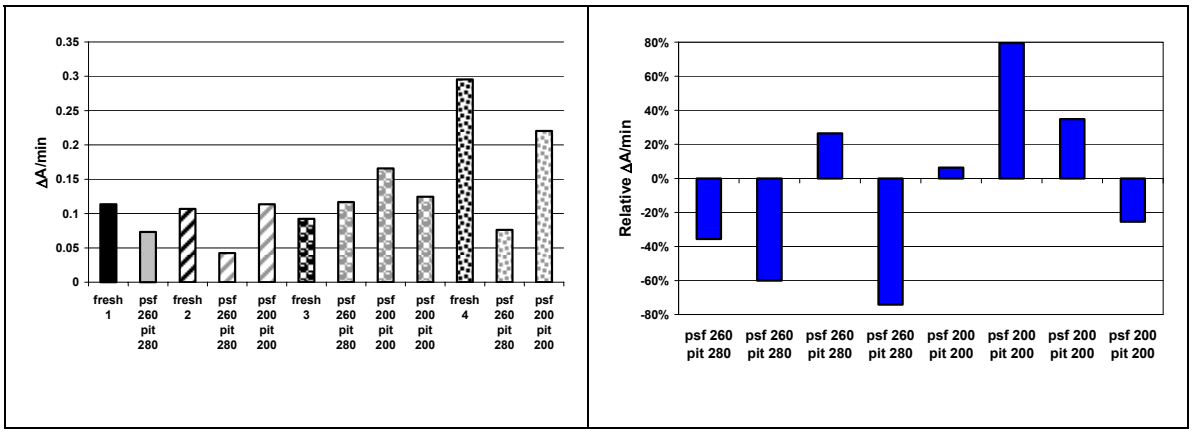

Figure 4.82. Enzymatic activity of polyphenol oxidase from fresh and HPLT treated potatoes (expressed as the linear increase of the absorbance per time unit at 420 nm) (a) and relative values for this activity with respect to corresponding fresh values (b).

To assess the effect of HPLT processing on enzymatic activity better, the results are also presented as the percentage of activity with respect to the corresponding fresh sample, eliminating results’ deviations due to the sample variability. Figure 4.82b shows a summary of relative values with respect to the corresponding fresh samples.

The values shown in Figure 4.82 as “enzymatic activity”, relate to the activity of extracted enzymes from the potato cells. The extractability of enzymes is directly related to cell damage and, therefore, this “enzymatic activity” shows the extraction capacity of enzymes from the samples cells. The higher the cell damage, the higher the extraction yield of enzymes, the higher the measured “activity”. In the cases of HPLT processed samples, an extra “inactivation” should take place, due to the effect of high pressures and low temperatures on the activity of such an enzyme, but, as reported in the literature (Indrawati et al., 1998), in spite of long pressure exposures (up to 135 minutes) at low temperatures, polyphenoloxidase is not inactivated. Recent studies (data not published) show that food quality related enzymes seem to be relatively insensitive concerning high pressure - low temperature processes. Only lipoxygenase

can be inactivated at high pressures in combination with low temperatures. In a limited way also polyphenoloxidase activity decreases. These results concern an HPLT treatment in which enzyme solutions are cooled at atmospheric pressure (therefore atmospheric freezing) down to -20°C and pressure is built-up. The processes performed here (PSF) deal with PT combinations that could lead to a slight PPO inactivation. This could explain the negative values in Figure 4.82b. These negative values are, therefore, the combination of a good quality preservation of the potato samples (low cellular damage and, therefore, no higher extraction yield of enzymes) together with a slight inactivation. The values for PSF at 260 MPa and PIT at 280 MPa show a slight inactivation (average value of -36%) and those for PSF at 200 MPa and PIT at 200 MPa show a slight increase in the activity (+24%). Repetition of experiments is especially recommendable in this case of analysis, given the high variability obtained.

4.6.2. Pilot-scale set (Nantes): colour changes, microstructure

In this work, optimized paths for PSF (at 240 MPa and -24°C) and PIT (at 290MPa) were performed for whole potatoes (bags of 6 vacuum packed potatoes) in a high pressure vessel placed in the laboratories of ENITIAA (Nantes, France), in order to assess the viability of these processes on a pilot scale and to study quality related parameters: microstructure (through microscopic study of embedded samples), drip loss, colour (colorimetric analysis) and visual aspect (evolution of aspect with time).

The following experimental plan was performed:

Sample	Freezing process	Storage	Thawing process
1	PSF at 200 MPa & -20°C	0 days	Atmospheric thawing
2	PSF at 240 MPa & -24°C	3 days	PIT at 200 MPa
3	PSF at 240 MPa & -24°C	3 days	PIT at 200 MPa
4	PSF at 240 MPa & -24°C	3 days	PIT at 290 MPa
5	PSF at 240 MPa & -24°C	3 days	PIT at 290 MPa
6	PSF at 240 MPa & -24°C	3 days	PIT at 290 MPa
7	Atmospheric freezing	3 days	Atmospheric thawing
8	Reference sample (fresh)		

For the freezing process, the samples packed in vacuum bags were installed in the HP vessel and pressure was built-up when the temperature of the sample centre reached 0°C. Then, pressure was maintained until the set point was reached (-18°C for 200 MPa and -22°C for 240 MPa) and during the fast pressure release, crystallization of ice I occurred. Therefore, the effective temperature gradient of the samples before pressure release was around 20K.

For thawing purposes, after 3 days storing, samples were placed in the high pressure vessel and pressure was immediately increased, leading to a partial melting of the sample surface ice.

Atmospheric freezing, PSF at 200 MPa and PSF at 260 MPa processes were performed in whole potatoes, followed by 3 days storage at -20°C and atmospheric thawing, PAT at 200 MPa or PIT at 290 MPa. Figure 4.83 shows examples of these processes in both, temperature-pressure profiles and on the phase diagram of water.

a) PSF at 240 MPa

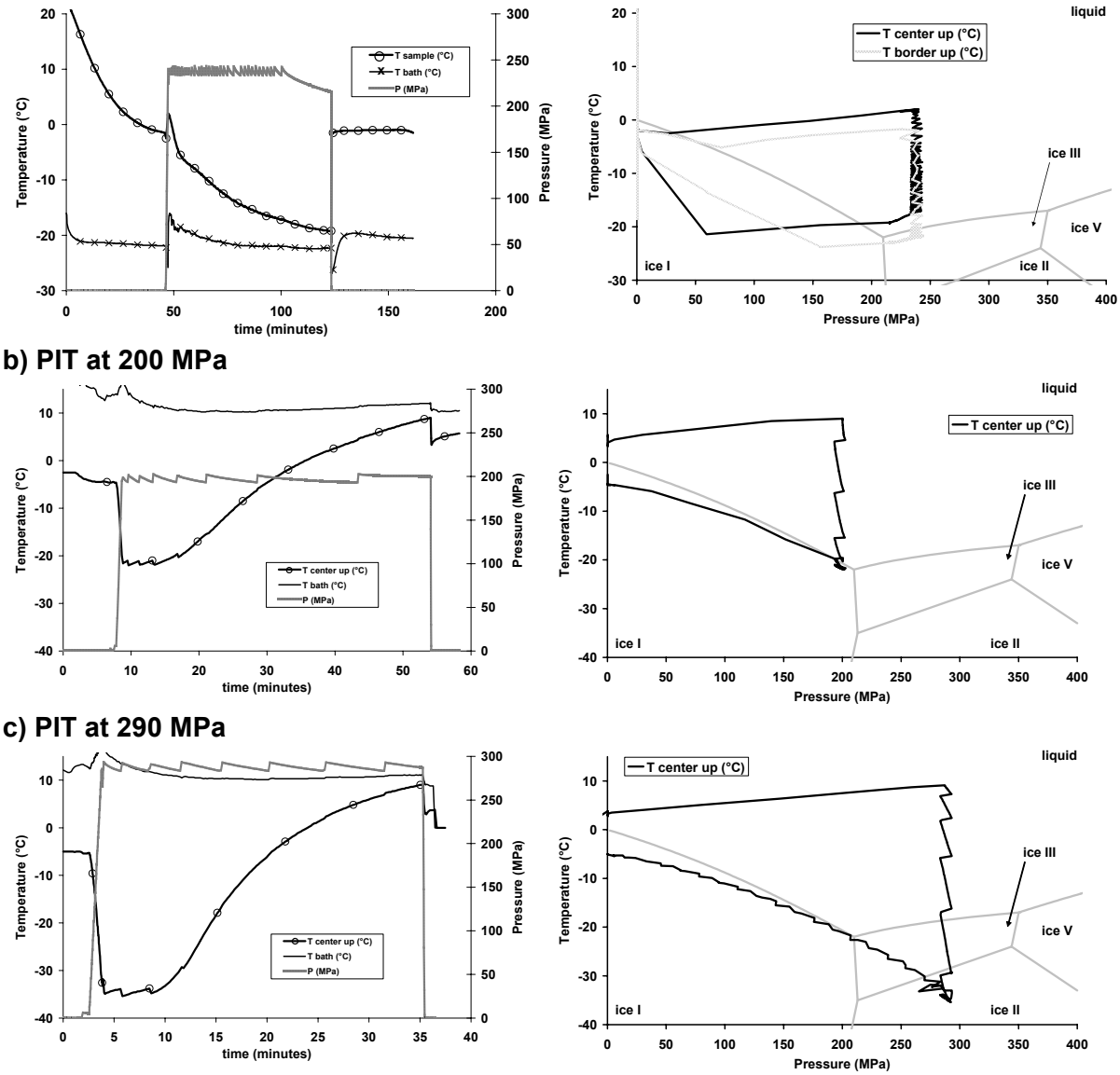

Figure 4.83. Temperature and pressure profiles (left) and process paths in the phase diagram of water (right) for three representative paths.

For freezing processes (Figure 4.83a), although the domain of ice III is reached, still water is present in the samples and the temperature gradient before pressure release can be optimized. In the case of the pressure-temperature diagram profile (right figure), two recorded temperatures are shown: one corresponding to the upper potato, recorded in the centre of the sample, and one corresponding to the lower potato, recorded in the border of the sample. These are the highest and lowest possible levels of the temperature during cooling at high pressure, because the sample borders have a lower temperature than the centre and samples in the lower part of the equipment are in contact with the incoming cooling medium.

For the thawing processes, the processing time in case c decreased in 20 minutes with respect to case b. The reason lies in the effective temperature gradient, which increases with pressure. After storing, samples were again packed in vacuum and placed in the HP vessel. During the time between the storing chamber and the beginning of the run, the temperature of the samples reached nearly 0°C. Then, pressure was built-up to the corresponding set point. In both cases, the path "followed" the phase transition line of ice I-liquid water, because a partial melting of sample surface takes place during pressurization, as explained by Schlüter et al. (2004). The difference between case a and b is that in case a the sample is in the domain of ice I in

the whole experiment, but in case b, the path goes to the domain of ice III and, nevertheless, no phase transition between ice I and ice III occurred. A metastable mixture of liquid water and ice I was obtained for a pressure level of 290 MPa and the temperature decrease due to the partial melting reached values around -35°C. That means that the effective temperature gradient was enhanced by 15K from case a to case b. In case b, this gradient is the difference between sample temperature (around --35°C) and the surrounding medium (at +10°C), so a total of 45K for the driving force.

For the visual aspect evaluation, a film was recorded over a period of 5 hours, taking images of 1 second every 10 minutes. The results are presented in Figure 4.84.

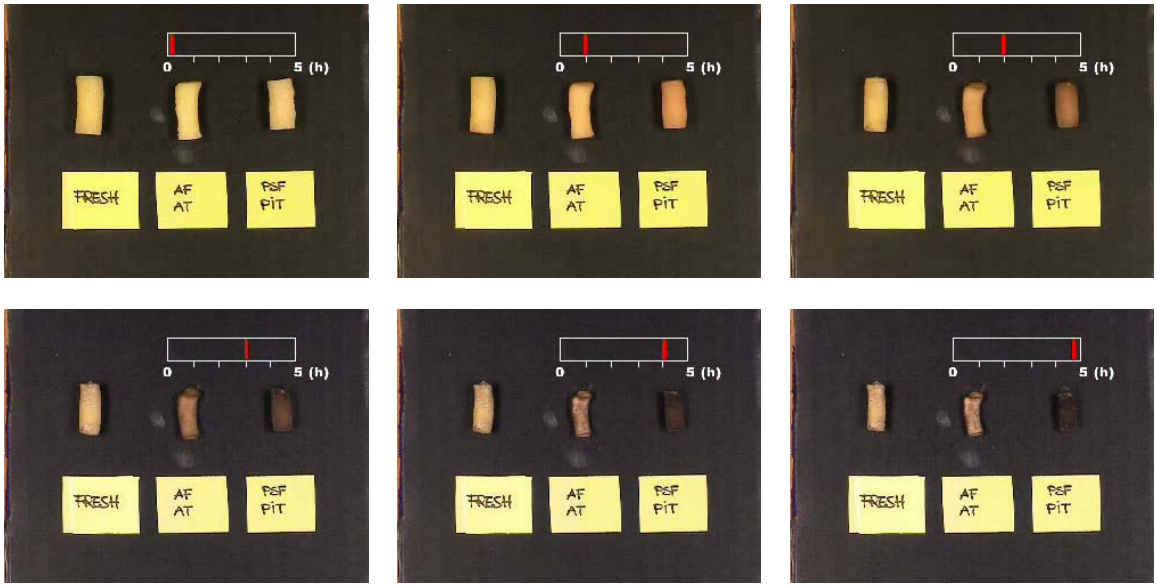

Figure 4.84. Sequences of the video of potato cylinders recorded over 5 hours. Left sample is a fresh potato, centre sample is a sample frozen and thawed at atmospheric pressure and right sample is PSF at 240 MPa and PIT at 290 MPa.

This sequence of images shows the evolution of the different samples with the time after the end of the thawing process. The left sample is a fresh one, the centre one is a sample frozen and thawed at atmospheric pressure and the right one corresponds to a sample PSF at 240 MPa and PIT at 290 MPa. The fresh sample changes its colour due to browning enzymatic oxidation and decreases its size (drip losses), although it maintains its shape (good microstructure). The atmospheric frozen and thawed sample does not maintain its shape (poor microstructure quality), loses more water than the fresh sample (higher drip losses), and the browning reaction takes place faster than for the fresh sample. In the case of pressure-supported processed sample, the shape is maintained (good microstructure quality), size is maintained better than the atmospherically treated one (lower drip losses), but the enzymatic inactivation is low, as seen by the high degree of browning of the sample.

The drip loss results are summarized in Figure 4.85. The results clearly show that the atmospheric freezing and thawing processes result in a higher drip loss in potato samples, when compared to the samples frozen and thawed with the support of pressure. Between the different pressure-supported processes, no clear conclusions can be made, as the values are very similar in all the cases.

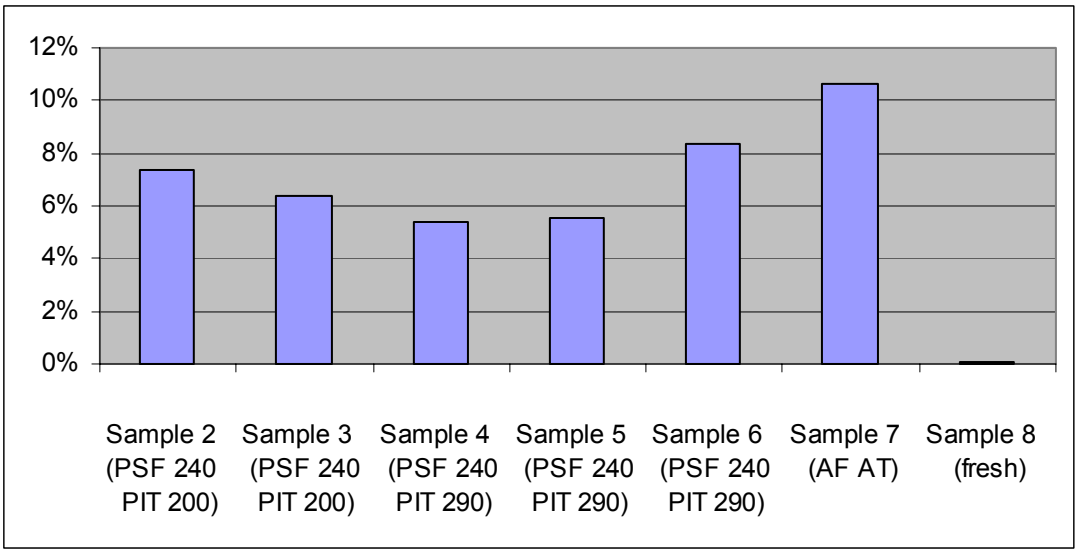

Figure 4.85. Drip loss (%) 2 hours after the end of thawing process.

The colour evolution in time is summarized through the colorimetric results in Table 4.7.

Table 4.7. Colour evolution in time of treated samples.

Freezing process	Thawing process	ΔL*	Δa	Δb	ΔE*
PSF at 240 MPa & -24°C	PIT at 200 MPa	-0.1723	0.8108	0.2643	0.870022
PSF at 240 MPa & -24°C	PIT at 200 MPa	0.0678	0.4558	0.1368	0.480692
PSF at 240 MPa & -24°C	PIT at 290 MPa	-0.6456	0.9782	0.0837	1.175024
PSF at 240 MPa & -24°C	PIT at 290 MPa	-0.709	1.175	0.0899	1.375277
PSF at 240 MPa & -24°C	PIT at 290 MPa	-0.5966	1.0819	0.0883	1.238643
Atmospheric freezing	Atmospheric thawing	0.4224	0.081	0.0302	0.431155
Fresh (reference)	Fresh (reference)	-0.4844	0.2997	0.1948	0.602005

The parameter ΔL^* shows the difference between the final (60 minutes after thawing) and initial (just after thawing) values of L* (lightness in a scale from black to white). The same difference is used for Δa (scale from red to green) and Δb (scale from blue to yellow). The colour difference, ΔE^* is defined as the square root of $(\Delta L^2+\Delta a^2+\Delta b^2)$. The results shown in Table 4.7 show a higher colour difference for the samples PSF at 240 MPa and PIT at 290 MPa than for the samples PSF at 240 MPa and PIT at 200 MPa. Reference sample (fresh) and AF, AT sample have also lower colour difference.

The microstructure results are summarized in Figure 4.86. Compared to the reference sample, the microstructure of atmospheric frozen and thawed sample shows broken cell walls and “wholes” originated from large ice crystals formed during a slow nucleation. The use of PSF and PIT accelerate the rate of nucleation and, consequently, the size of ice crystals formed is smaller. This leads to absence of broken cells or wholes on the microstructure, as clearly seen in the two cases shown in Figure 4.86c and Figure 4.86d.

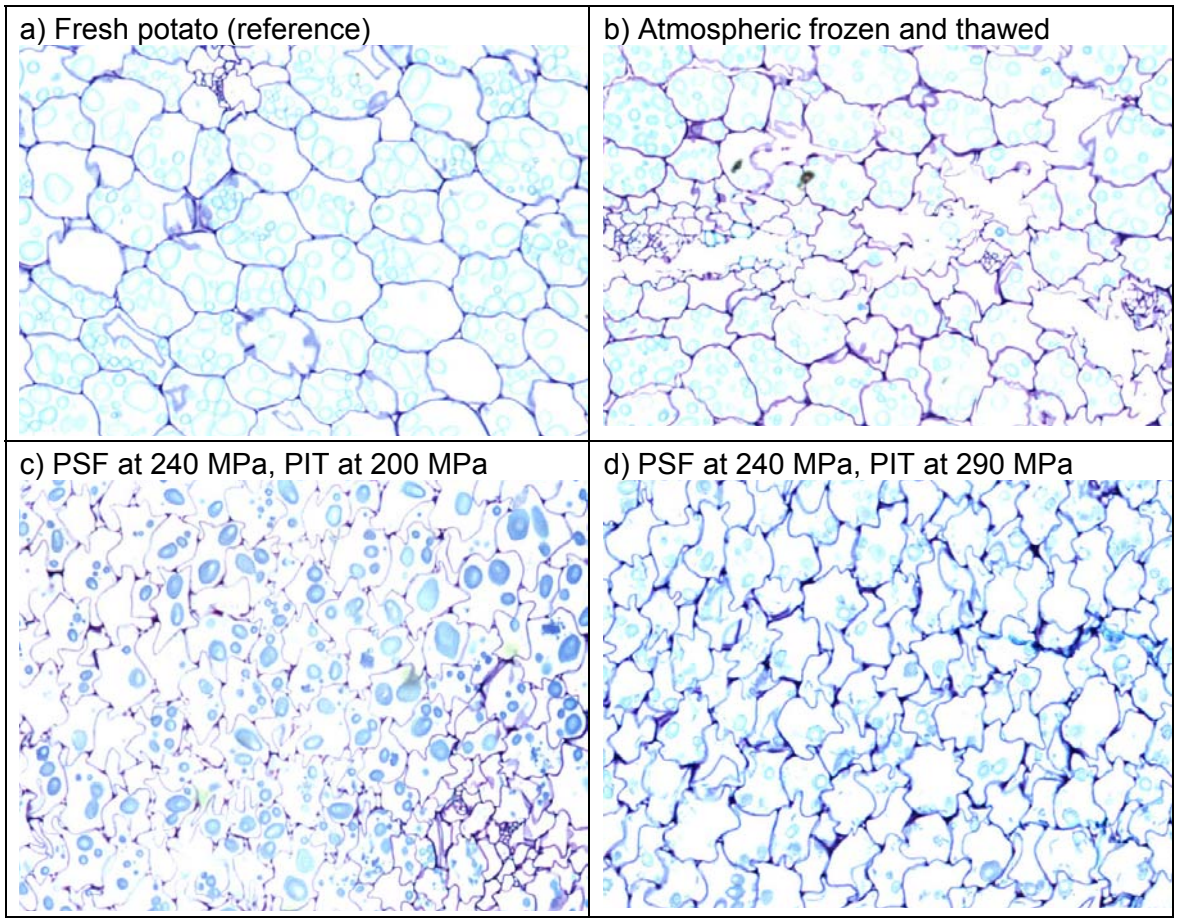

Figure 4.86. Microphotographs of potato tissue after different processing conditions.

Compared to the reference sample, the microstructure of atmospheric frozen and thawed sample shows broken cell walls and "holes" originated from large ice crystals formed during a slow nucleation. The use of PSF and PIT accelerate the rate of nucleation and, consequently, the size of ice crystals formed is smaller. This leads to absence of broken cells or holes on the microstructure, as clearly seen in the two cases shown in Figure 4.86c and Figure 4.86d.

The real opportunities for an industrial implementation of the HPLT technology depends on the quality of the processed products and the reliability of the related processes, from the process point of view and from the technical side (equipment limitations, etc.). It seems, after these first results that the technology has a promising future for the industry, as long as the quality of processed products are demonstrated to be enhanced with the use of high pressure at sub-zero temperatures, and given the already existing facilities which are industrially working.

4.6.3. Pilot-scale set (Berlin): activity of PPO, colour, texture, drip loss and microstructure

4.6.3.1. Enzymatic activity of polyphenol oxidase

After the tendency observed in the results corresponding to the laboratory scale, the use of pressures higher than 200 MPa and temperatures lower than -22°C seemed to be of high interest for PSF and PIT processes, in terms of enzymatic activity, as a quality-related parameter, consequence of the extractability of enzymes (cellular damage) and the possible slight inactivation of PPO.

The results obtained for the experimental set performed on the pilot scale equipment are summarized in Figure 4.87. The results shown in Figure 4.87 have a considerable standard deviation. This is evidence of the variability of results when working with real

products in which the matrix is affecting the final results. Even taking the high standard deviation of the data obtained, it seems clear that the application of pressures higher than 200 MPa (combined with PIT processes after storage) helps for a better control of enzymatic activity. Compared with the data of “conventional” PSF (at 200 MPa and -20°C) and “conventional” PIT (at 200 MPa), in which the enzymatic activity recorded is even higher than these for atmospheric freezing and thawing experiments, the enzymatic activity measured after processing for higher pressures is not higher than the corresponding to fresh samples. In some cases it has been even recorded a slight inactivation (reduction of the activity of processed samples with respect to the corresponding fresh samples).

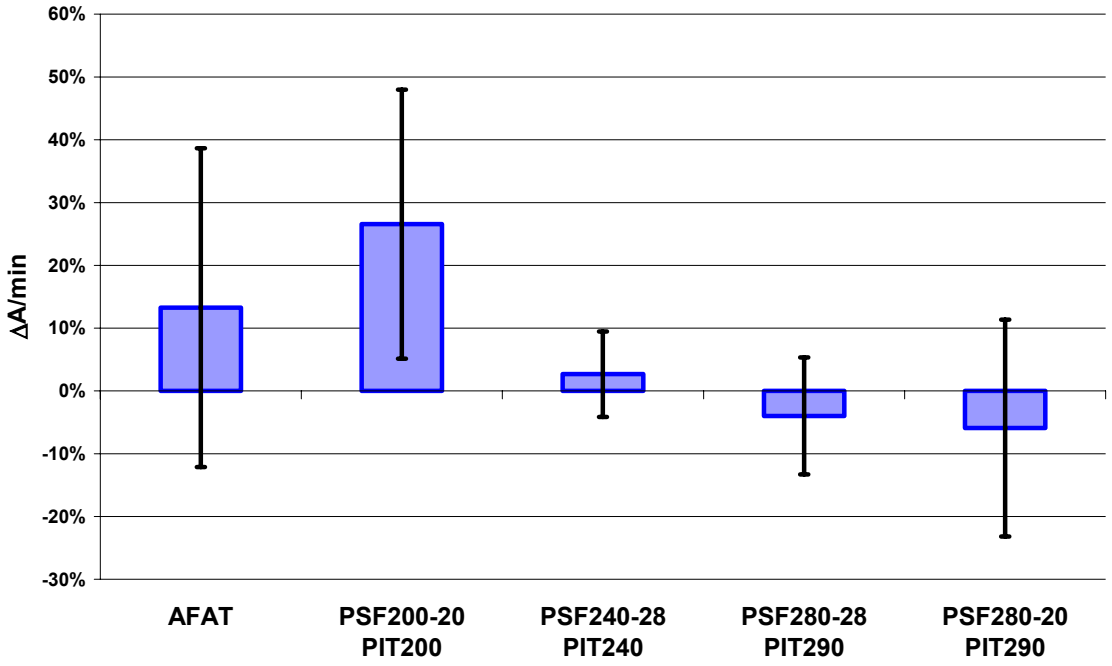

Figure 4.87. Relative enzymatic activity (with respect to fresh samples) of HPLT processed potatoes at pilot scale.

The results shown in Figure 4.87 have a considerable standard deviation. This is evidence of the variability of results when working with real products in which the matrix affects the final results. Even taking the high standard deviation of the data obtained, it seems clear that the application of pressures higher than 200 MPa (combined with PIT processes after storage) helps give a better control of enzymatic activity. Compared with the data of “conventional” PSF (at 200 MPa and -20°C) and “conventional” PIT (at 200 MPa), in which the enzymatic activity recorded is even higher than that for atmospheric freezing and thawing experiments, the enzymatic activity measured after processing for higher pressures is not higher than the corresponding to fresh samples. In some cases a slight inactivation (reduction of the activity of processed samples with respect to the corresponding fresh samples) has even been recorded.

The results presented here may appear to be in contradiction to those presented by Préstamo et al (2005). These authors found that PSF treatments of potato cubes (210 MPa at -20ºC, 180 MPa at -16°C, 150 MPa at -12°C or 120 MPa at -8°C) were not enough to inactivate the PPO, but a considerable decrease in PPO activity at 210 MPa and -20ºC was described: in comparison to control, only 30% of the PPO activity remained for the PSF at 210 MPa and -20°C.

Such high enzymatic inactivation seems to contradict the results shown in this paper, but a decisive difference lies between the two works in terms of procedures. In this paper, the results of the PPO activity in potatoes after PSF (or AF), then storage at -22°C for 7 days, then PIT (or AT) is shown. In the case of Préstamo et al (2005),

samples were treated by PSF and after pressure expansion, the treated samples were soaked in liquid nitrogen for 15 minutes and stored at -80°C. The frozen samples were then ground in a blender for one minute until powdered and then a similar analytical procedure for the determination of enzymatic activity to the one used in this work, was carried out. Therefore, the critical difference is that the results from Préstamo et al (2005) deal with frozen potatoes analyzed without thawing, but directly from the storage at -80°C, samples were rasped. In this work, all samples have been analyzed after a subsequent thawing process. The reason why this paper deals with AF/PSF-then stored-then AT/PIT is to simulate real situations of a potential industrial application of freezing-then storing-then thawing processes. Taking into account that our goal is to assess the best freezing method and not to obtain an enzymatic inactivation, the slight inactivation found already reaches our goal of, at least, not increasing the enzymatic activity after processing, or at least avoiding undesirable colour and texture changes. These textural and colour changes should be directly evaluated, together with the results presented for the enzymatic activity of samples after processing.

4.6.3.2. Quality-related parameters: colour, drip loss and texture.

The L*, a* and b* recorded values were used to obtain the parameter ΔE* (see equation 3.11) and a summary of the results obtained is shown in Figure 4.88.

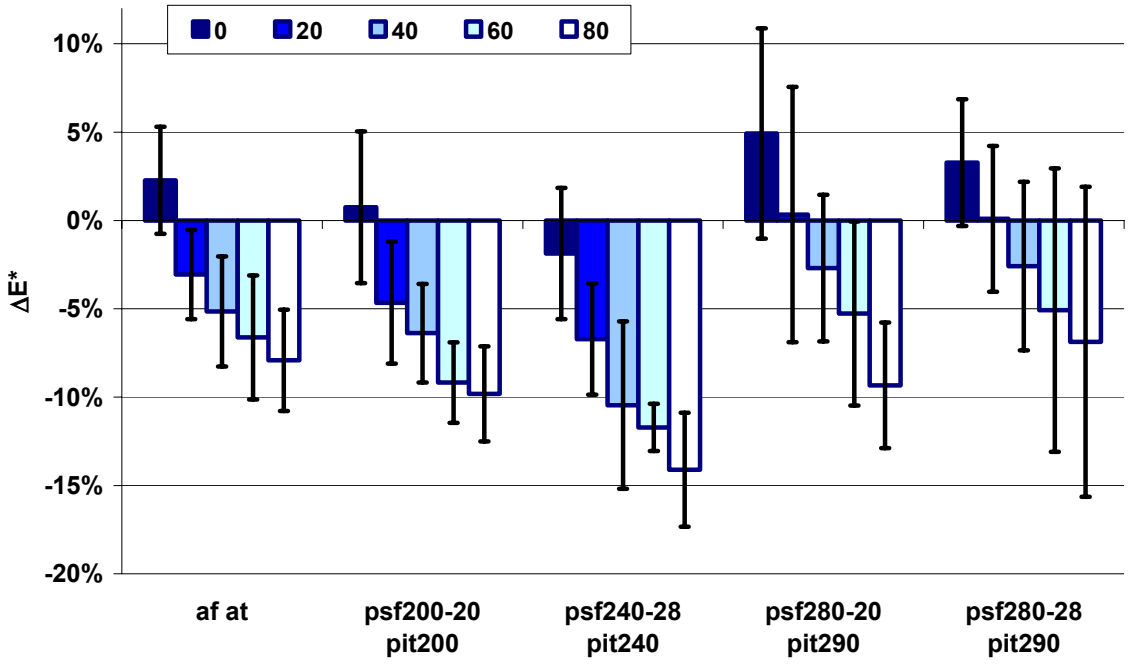

Figure 4.88. Relative colour changes on treated samples after 0, 20, 40, 60 and 80 minutes.

The values shown in Figure 4.88 correspond to the percentage difference between colour measurements 0, 20, 40, 60 and 80 minutes after the end of thawing for processed samples and the corresponding values of the fresh reference halves measured 0, 20, 40, 60 and 80 minutes after cutting. Equation (4.5) shows how the values in Figure 4.88 are obtained.

$$\Delta E_j\,*(\%) = \left(\frac{\Delta E_{treated} - \Delta E_{fresh}}{\Delta E_{fresh}} \right)_j \cdot 100 \quad j = 0,20,40,60,80\,(\text{minutes}) \qquad (4.5)$$

The phenomenon of browning is directly measurable through the evolution with time of the colour changes of samples after processing. In this sense, lower colour differences (the higher proximity to zero in the percentages shown in Figure 4.88) mean lower

degree of browning of the processed samples. Due to the high standard deviation of the results obtained, careful interpretation of results must be addressed. Nevertheless, there is a remarkable difference between the colour changes for the processes at lower pressures (PSF at 200 MPa and -20°C or PSF at 240 MPa and -28°C followed by PIT at 200 MPa or PIT at 240 MPa, respectively) and at higher pressures (PSF at 280 MPa and -20°C or -28°C followed by PIT at 290 MPa). The colour decrease, caused by browning, is clearly more accentuated in the two former cases than in the two later. This results seem to be in accordance with the enzymatic activity measured (see Figure 4.87). The colour was better maintained in samples processed at higher pressures than in those treated at lower pressures. It can be concluded that the colour measurement (even though the high deviation of results) can be used as an indirect indicator of the enzymatic activity. Nevertheless, the results for enzymatic activity correspond with a single set of measurements carried out just after the end of the thawing process and, therefore, only comparable with the results at time 0 for colour changes. The evolution of these colour changes is of high interest taking into account that the time of consuming food products after thawing is usually less than 30 minutes. In this time range (time 20 and time 40), the recorded colour changes for the samples treated at higher pressures are clearly lower (less browning) than those for samples treated at lower pressures or at atmospheric pressures.

In the case of drip loss, the summary of the results obtained are shown in Figure 4.89. In this figure, the data shown are the difference of the weight of the processed sample after 80 minutes minus the corresponding value at time 0, expressed in percentage of the same weight loss for the corresponding fresh samples, as expressed in equation 4.6.

$$Drip\ loss\ (\%) = \frac{\left[\left(w_{80} - w_0\right)_{treated} - \left(w_{80} - w_0\right)_{fresh}\right]}{\left(w_{80} - w_0\right)_{fresh}} \cdot 100 \qquad (4.6)$$

The results obtained for drip loss show that the level of lost water 80 minutes after the end of the thawing process is lower in all the cases in which HP was applied with respect to the cases at atmospheric pressure.

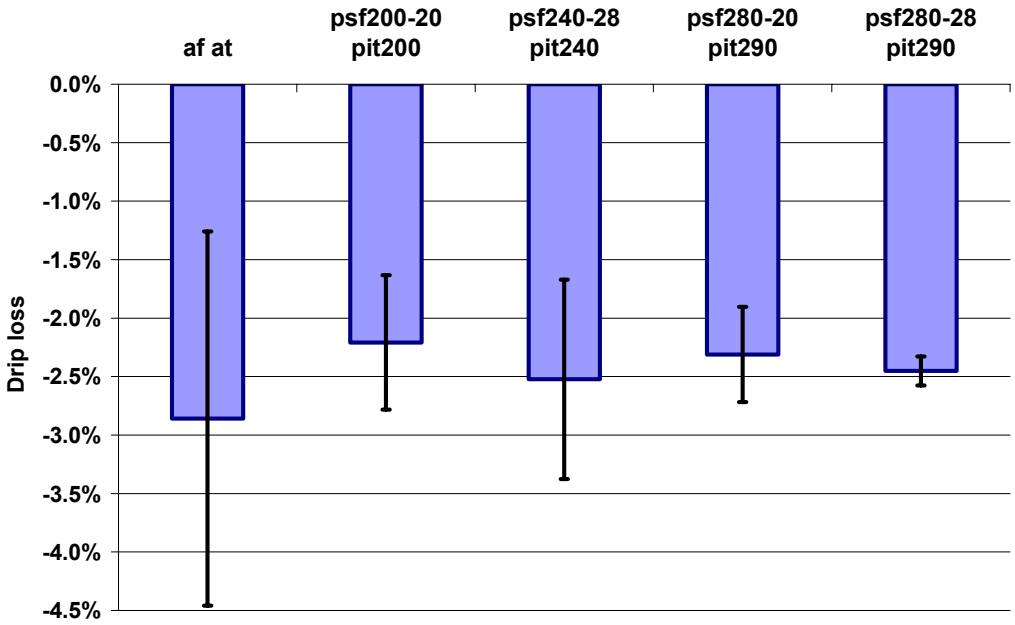

Figure 4.89. Drip loss results for processed samples in percentage of lost weight (with respect to fresh samples) after 80 minutes of thawing process end point.

Finally, the texture analysis results are summarized in Figure 4.90.

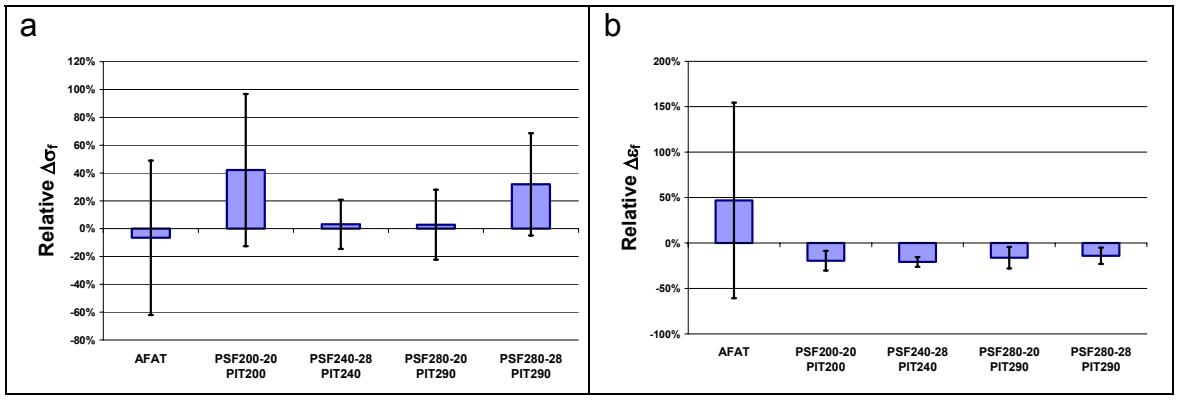

Figure 4.90. Relative failure stress (a) and relative failure strain (b) of treated samples as percentage of the corresponding fresh samples' values.

In the case of the relative failure stress (σ_f), the values shown are the difference between processed samples' values and the corresponding fresh values, as a percentage with respect to fresh values. Negative values mean a lower failure stress with respect to fresh samples, therefore, a texture detriment occurred. The positive values shown in Figure 4.90a mean that failure stress increased with respect to fresh samples, therefore, a texture enhancement occurred. In both cases, the lower the texture modification, the nearer we are to the fresh-like texture of processed samples. The results obtained clearly show again that all PSF/PIT processes applied maintained the texture response and the atmospheric treated samples showed a decrease in the texture, in both cases with respect to the corresponding fresh samples.

In the case of the relative failure strain (ε_f), Figure 4.90b shows the difference between processed values and the corresponding fresh samples' values, as a percentage with respect to fresh values. Positive results mean that failure strain increased for processed samples with respect to the corresponding fresh samples, that is, the sample was deformed during compressive test in a major grade. This is an indication of undesired gummy texture. Results shown in Figure 4.90b show again that all pressure treatments maintain the texture of processed samples, and the that atmospheric samples show a detrimental effect in texture, in both cases with respect to the corresponding fresh samples.

4.6.3.3. Microstructure analysis results

The embedded samples have been cut (5μm depth) and stained with blue colour which allows a better identification of the cell walls. The damage of the process on the cell walls can be analyzed through the photographs taken through the microscope. Examples of the images obtained are shown in Figure 4.91.

Taking as reference the fresh potato tissue shown in Figure 4.91a, the representative case in Figure 4.91b shows the structure of a sample frozen and then thawed at atmospheric pressure in which damaged cell walls are identifiable, as detailed in Figure 4.92.

a) Fresh potato

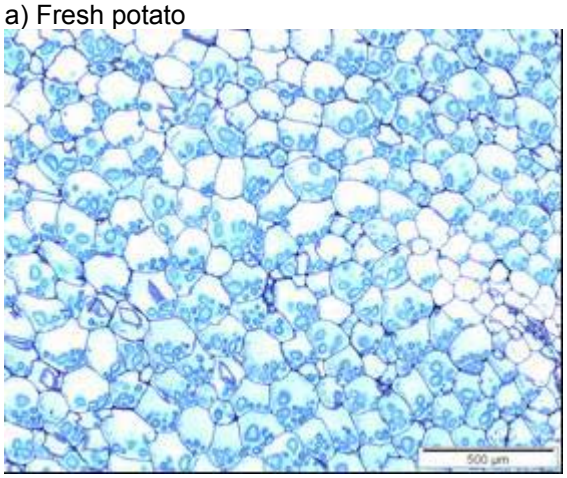

b) Atmospheric frozen and thawed

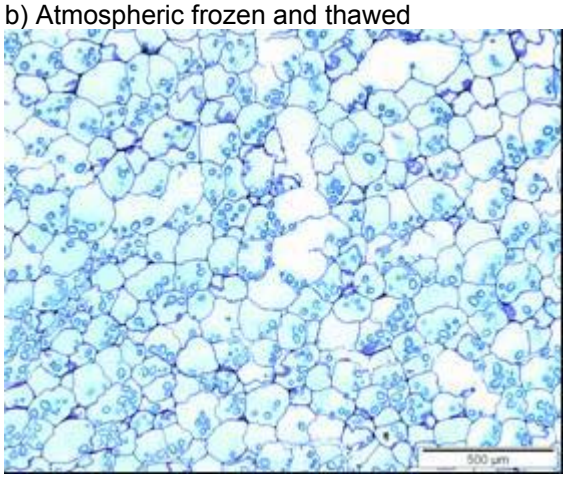

c) PSF 200MPa and -20°C and PIT 200 MPa

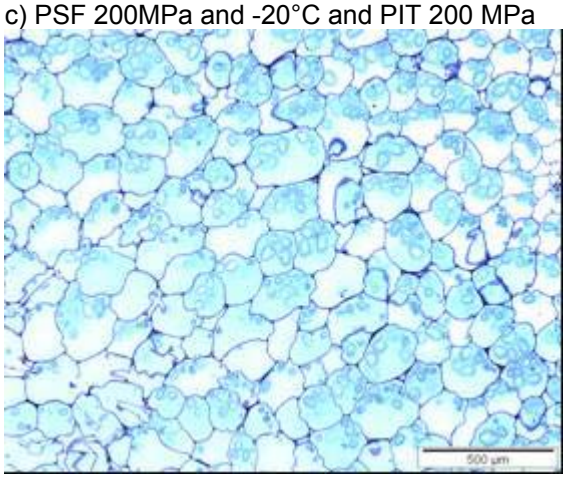

d) PSF 280MPa and -28°C and PIT 290 MPa

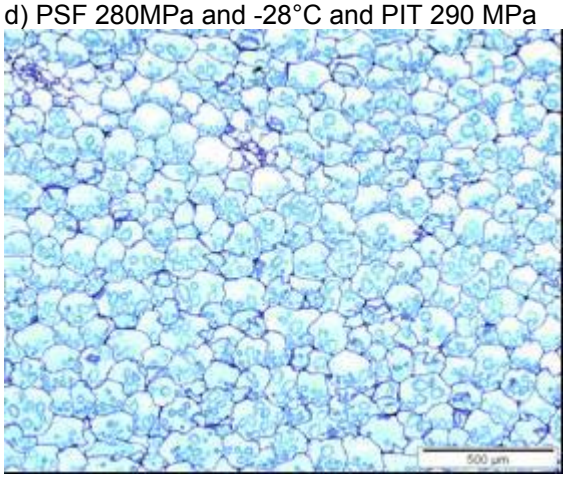

Figure 4.91. Micrographs of fresh (a), atmospheric (b) and high-pressure (c and d) processed potatoes.

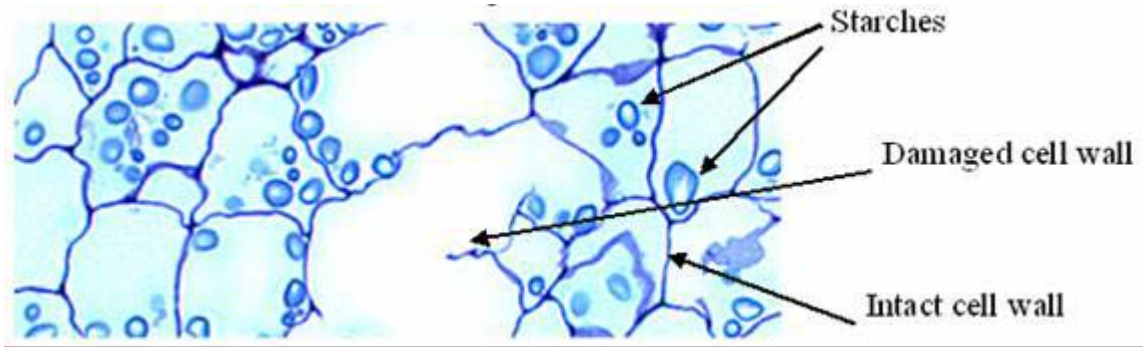

Figure 4.92. Detail of tissue structure of atmospheric frozen and thawed sample, indicating starch, intact cell wall and damaged cell wall examples.

The image shown in Figure 4.92 corresponds to the case of PSF at 200 MPa and -20°C and PIT at 200 MPa. In this case, no damaged cell wall is identifiable in the figure, meaning that no damage was caused by the ice crystal nucleation or develop. The form and size of the cells are maintained with respect to the fresh sample cases. Finally, the image shown in Figure 4.91d, corresponding to the case of PSF at 280 MPa and -28°C and PIT at 290 MPa, again shows no damaged tissues and, additionally, a change in the geometry of cells, as well as a reduction of cell size. The applied pressure may be the responsible for such an effect on the microstructure of processed samples at higher pressures.

Most of the reports dealing with HPLT processes and their consequences on quality-related properties (mainly texture), have concentrated on the domain of ice I (up to

pressures of 210 MPa and temperatures not lower than -22°C) and at a laboratory scale.

The use of a larger pressure vessel volume for HPLT freezing and thawing processing gives the opportunity of assessing the real possibilities of the industrial development of the HPLT technology for food products. In this work, the pressure-temperature combinations for HPLT processes of freezing and thawing have been performed as foreseen for potential industrial applications. The research has been done with a real product of high interest. The frozen potato market represented 15% of the total frozen food market in Germany in the year 2000 (Deutches Tiefkühlinstitut e.V., Köln – www.tiefkaaauehlinstitut.de). The product has been treated in whole samples, vacuum packaged (reproducing also potential industrial processes) and the occupation ratio product to inner vessel volume used was as high as possible (around 75%).

With respect to the temperature and pressure ranges, the impact of the existence of metastable phases in both liquid and solid states, mainly in the domain of ice III opens a new range of processing possibilities. Examples of such new processes have been shown here, and the reduction of processing times, thanks to the increase of temperature gradients has been proved. The effects on quality-related parameters are enhanced with respect to the cases of processes of pressure-temperature combinations used up-to-now (210 MPa, -22°C). The effects of different geometry dispositions and sizes, the pressurization rate, the pressure transmitting medium, the effect of different temperatures in the cooling and heating systems, etc. are processing parameters still to be studied for a proper analysis of the future industrial applications. Also, similar studies should be addressed for other key products for the frozen food industry, like fish products, frozen vegetables, etc.

Problems associated with the scale-up of a well studied process, like the temperature non-homogeneity, have been indirectly evaluated. It is reasonable to assume that during the pressurization and during the pre-cooling step at high pressure (for PSF) or the heating step at high pressure (for PIT) the temperature inside the HP vessel is not homogeneous (Hartmann et al., 2004). It can be assumed that the effects of the process on the enzymatic response for the samples 1 or 4, taken from the bottom or from the top of the vessel could be different. In fact, the high variability of the results for enzymatic activity (see Figure 4.87) could be explained through the different responses of samples placed in the bottom or in the top of the vessel. In this sense, further research must be addressed to deliver the influence of temperature inhomogeneities on the quality-related parameters of processed food products. It seems that high pressurization rates could help give a better temperature homogeneity in the vessel, due to the turbulences created through the high velocity inflowing liquid.

The results obtained for the enzymatic activity of PPO in HP treated potatoes show that a slight inactivation (up to 10%) was achieved at pressure levels of 280 MPa for freezing and 290 MPa for thawing. These results are in agreement with those presented by Indrawati et al. (1998), who found only a slight, reversible inactivation of mushroom PPO (around 15% at 200 MPa and -15°C). Both results should be compared carefully, given that the activity examined in this work is measured directly from a potato tissue and not from extracts or enzyme solutions, where no influence of cell damage plays a role on the measured activity. The benefits of HPLT treatment in all pressure and temperature range has been demonstrated in terms of texture, microstructure and drip loss, in accordance with the results published by Luscher et al. (2004). The benefit of HPLT treatment in pressure ranges higher than 240 MPa has been shown. Regarding the results on colour changes, the use of higher pressures than 240 MPa resulted in a lower colour change with time, of treated samples. These results seem to be in accordance with the enzymatic activity shown for samples treated at higher pressures and allow us to conclude that indirect measurements like colour changes are a good indirect indicator of the enzymatic activity, such as potato PPO.

4.7. Case study: Texture parameters of HPLT processed ice cream

4.7.1. Theory background

Ice cream is defined as a sweet frozen dessert, made from milk fat and solids, sugar, flavouring, a stabilizer (usually gelatine), and sometimes eggs, fruits, or nuts. The mix is churned at freezing temperature to attain a light, smooth texture (see V. Cobb, The Scoop on Ice Cream (1985); W. S. Arbuckle, Ice Cream (1986).)

The US has the highest consumption of ice cream in the world at around 24 litres per person per year, and a stabilized production per year (Figure 4.94) . The average consumption in Europe is around 6 litres per person[3]. The world's top 5 consumers of ice cream in order are: United States, New Zealand, Denmark, Australia, Belgium / Luxembourg[4], as shown in Figure 4.93.

Country	Litres per capita
New Zealand	26.3
United States	18.7
Australia	17.8
Finland	13.9
Sweden	11.9
Canada	9.5
Italy	9.2
Ireland	9
Denmark	8.7
United Kingdom	7.7
Chile	5.6
Malaysia	2
China	1.9
Japan	0.01

Figure 4.93. Consumption of ice cream per country (litres per capita), adapted from http://www.foodsci.uoguelph.ca/dairyedu/icdata.html, with permission.

Year	Production (Million Gallons)
1990	1175.9
1991	1204.4
1992	1194.3
1993	1191.5
1994	1234.7
1995	1262.9
1996	1286.2
1997	1340.1
1998	1384.6
1999	1393.3
2000	1383.7
2001	1372.6
2002	1371.1

Figure 4.94. US Production of ice cream, hard and soft, regular, low fat and non-fat, adapted from http://www.foodsci.uoguelph.ca/dairyedu/icdata.html, with permission.

---

[3] http://www.unilever.com/ourbrands/cookingandeating/articles/healthiericecream.asphttp://www.worldwatch.org/press/news/2004/01/06http://www.unilever.com/ourbrands/cookingandeating/articles/healthiericecream.asp

[4] http://www.ice-cream-recipes.com/ice_cream_facts.htm

The most frequently occurring textural defect in ice cream is the development of a coarse, icy texture. Iciness is also the primary limitation to the shelf life of ice cream and probably also accounts for countless lost sales through customer dissatisfaction with quality. There is no answer to the question "What is the shelf-life of ice cream?", it depends entirely on its conditions of storage. It might be one year, or it might be two weeks or less. Although the source of and the contributing factors to the problem of iciness are well known, it is also one of the defects about which I am most often asked.

To prevent iciness, temperature fluctuations during storage and distribution must be avoided as much as possible. Ice crystals need to be numerous and of small, uniform size so they are not detected when eaten. It is heat shock, large temperature fluctuations, which is the greatest culprit to the loss of these small, uniform ice crystal size distributions and resulting coarse, icy texture.

If the temperature during the frozen storage of ice cream increases, some of the ice crystals, particularly the smaller ones, melt and consequently the amount of unfrozen water in the serum phase increases. Conversely, as temperatures decrease, water will refreeze but does not re-nucleate. Rather, it is deposited on the surface of larger crystals, so the net result is that the total number of crystals diminish and the mean crystal size increases (Marshall et al., 2003).

Ice cream has the following composition: greater than 10% milk fat by legal definition, and usually between 10% and as high as 16% fat in some premium ice creams; 9 to 12% milk solids-not-fat: this component, also known as the serum solids, contains the proteins (caseins and whey proteins) and carbohydrates (lactose) found in milk; 12 to 16% sweeteners: usually a combination of sucrose and glucose-based corn syrup sweeteners; 0.2 to 0.5% stabilizers and emulsifiers; 55% to 64% water which comes from the milk or other ingredients.

Milk fat increases the richness of flavour in ice cream, produces a characteristic smooth texture by lubricating the palate, helps to give body to the ice cream, due to its role in fat destabilization, aids in good melting properties, also due to its role in fat destabilization and aids in lubricating the freezer barrel during manufacturing (Non-fat mixes are extremely hard on the freezing equipment). The limitations of excessive use of butterfat in a mix include cost, hindered whipping ability, decreased consumption due to excessive richness and high caloric value. During the freezing of ice cream, the fat emulsion which exists in the mix will partially destabilize or churn as a result of the air incorporation, ice crystallization and the high shear forces of the blades. This partial churning is necessary to set up the structure and texture in ice cream, which is very similar to the structure in whipped cream. Emulsifiers help to promote this destabilization process.

The serum solids or milk solids-not-fat (MSNF) contain the lactose, caseins, whey proteins, minerals, and ash content of the product from which they were derived. They are an important ingredient for the following beneficial reasons: improve the texture of ice cream, due to the protein functionality; help to give body and chew resistance to the finished product; are capable of allowing a higher overrun without the characteristic snowy or flaky textures associated with high overrun, due also to the protein functionality; may be a cheap source of total solids, especially whey powder. The limitations on their use include off flavours which may arise from some of the products, and an excess of lactose which can lead to the defect of sandiness prevalent when the lactose crystallizes out of solution. Excessive concentrations of lactose in the serum phase may also lower the freezing point of the finished product to an unacceptable level.

A sweet ice cream is usually desired by the consumer. As a result, sweetening agents are added to ice cream mix at a rate of usually 12 - 16% by weight. Sweeteners improve the texture and palatability of the ice cream, enhance flavours, and are usually the cheapest source of total solids. In addition, the sugars, including the lactose from

the milk components, contribute to a depressed freezing point so that the ice cream has some unfrozen water associated with it at very low temperatures typical of their serving temperatures, -15° to -18° C. Without this unfrozen water, the ice cream would be too hard to scoop.

The stabilizers are a group of compounds, usually polysaccharide food gums, that are responsible for adding viscosity to the mix and the unfrozen phase of the ice cream. This results in many functional benefits and also extends the shelf life by limiting ice re-crystallization during storage. Without the stabilizers, the ice cream would become coarse and icy very quickly due to the migration of free water and the growth of existing ice crystals. The smaller the ice crystals in the ice cream, the less detectable they are to the tongue. Especially in the distribution channels of today's marketplace, the supermarkets, the trunks of cars, and so on, ice cream has many opportunities to warm up, partially melt some of the ice, and then refreeze as the temperature is once again lowered. This process is known as heat shock and every time it happens, the ice cream becomes more icy-tasting. Stabilizers help to prevent this.

The basic steps in the manufacturing of ice cream are generally as follows: blending of the mix ingredients; pasteurization; homogenization; aging the mix; freezing; packaging and hardening. Figure 4.95 shows the Process flow diagram for ice cream manufacture.

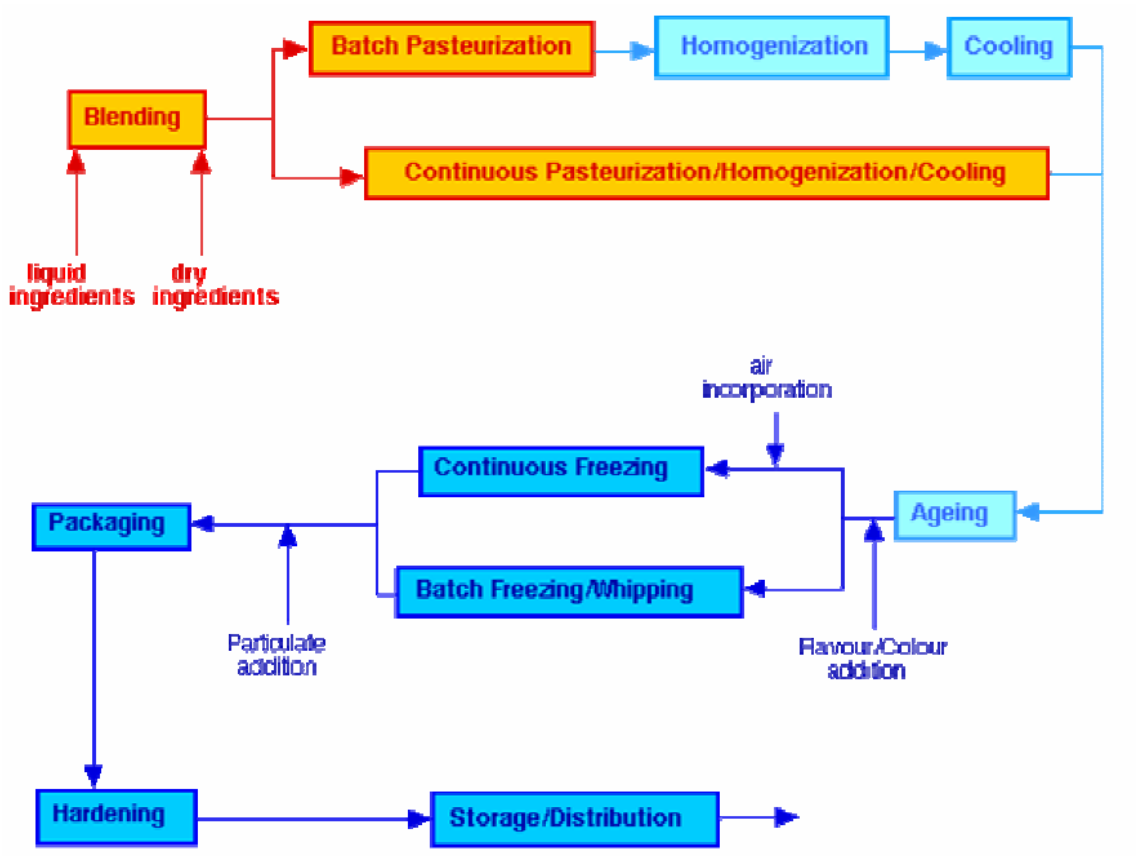

Figure 4.95. Process flow diagram for ice cream manufacture: the red section represents the operations involving raw, non-pasteurized mix, the pale blue section represents the operations involving pasteurized mix, and the dark blue section represents the operations involving frozen ice cream.

First the ingredients are selected based on the desired formulation and the calculation of the recipe from the formulation and the ingredients chosen, then the ingredients are weighed and blended together to produce what is known as the "ice cream mix".

The mix is then pasteurized. Pasteurization is the biological control point in the system, designed for the destruction of pathogenic bacteria. In addition to this very important function, pasteurization also reduces the number of spoilage organisms such as psychrotrophs, and helps to hydrate some of the components (proteins, stabilizers).

The mix is also homogenized, which forms the fat emulsion by breaking down or reducing the size of the fat globules found in milk or cream to less than 1 μm. Two-stage homogenization is usually preferred for ice cream mix. Clumping or clustering of the fat is reduced thereby producing a thinner, more rapidly whipped mix. Melt-down is also improved. Homogenization provides the following functions in ice cream manufacture: reduces size of fat globules; increases surface area; forms a membrane; makes possible the use of butter, frozen cream, etc. By helping to form the fat structure, it also has the following indirect effects: makes a smoother ice cream; gives a greater apparent richness and palatability; better air stability; increases resistance to melting.

Homogenization of the mix should take place at the pasteurizing temperature. The high temperature produces more efficient breaking up of the fat globules at any given pressure and also reduces fat clumping and the tendency to thick, heavy bodied mixes. No one particular pressure can be recommended that will give satisfactory results under all conditions. The higher the fat and total solids in the mix, the lower the pressure should be. If a two-stage homogenizer is used, a pressure of 2000 - 2500 psi (13,7 – 17,2 MPa) in the first stage and 500 - 1000 psi (3,4 – 6,8 MPa) in the second stage should be satisfactory under most conditions. Two-stage homogenization is usually preferred for ice cream mix.

The mix is then aged for at least four hours and usually overnight. This allows time for the fat to cool down and crystallize, and for the proteins and polysaccharides to fully hydrate. Aging improves whipping qualities of mix and body and texture of ice cream.

Following mix processing, the mix is drawn into a flavour tank where any liquid flavours, fruit purees, or colours are added. The mix then enters the dynamic freezing process which both freezes a portion of the water and whips air into the frozen mix. The "barrel" (see Figure 4.96) freezer is a scraped-surface, tubular heat exchanger, which is jacketed with a boiling refrigerant such as ammonia or freon. Mix is pumped through this freezer and is drawn off the other end in a matter of 30 seconds, (or 10 to 15 minutes in the case of batch freezers) with about 50% of its water frozen. There are rotating blades inside the barrel that keep the ice scraped off the surface of the freezer and also dashers inside the machine which help to whip the mix and incorporate air.

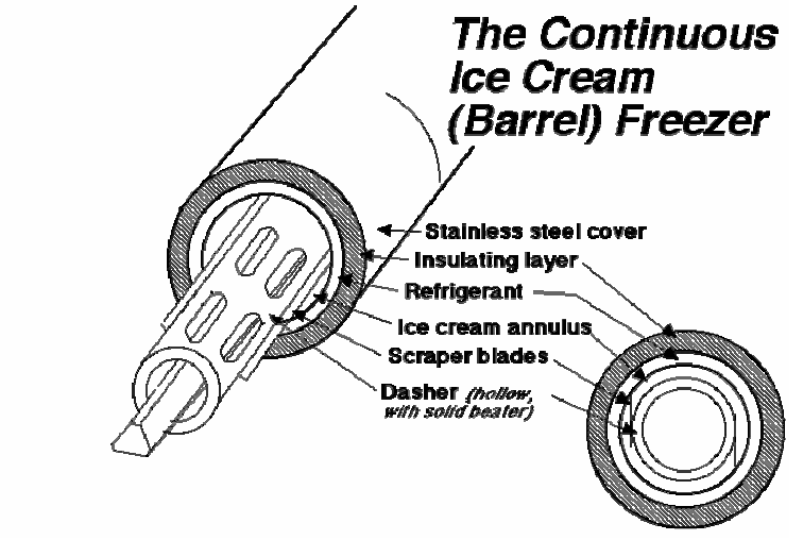

Figure 4.96. Schema of a barrel freezer used in the ice cream manufacture, adapted from http://www.foodsci.uoguelph.ca/dairyedu/icmanu.html, with permission.

Ice cream contains a considerable quantity of air, up to half of its volume. This gives the product its characteristic lightness. Without air, ice cream would be similar to a frozen ice cube.

After the particulates have been added, the ice cream is packaged and is placed into a blast freezer at -30 to -40°C where most of the remainder of the water is frozen. Below about -25°C, ice cream is stable for indefinite periods without danger of ice crystal growth; however, above this temperature, ice crystal growth is possible and the rate of crystal growth is dependant upon the temperature of storage. This limits the shelf life of the ice cream.

Hardening involves static (still, quiescent) freezing of the packaged products in blast freezers. The freezing rate must still be rapid, so freezing techniques involve low temperature (-40°C) with either enhanced convection (freezing tunnels with forced air fans) or enhanced conduction (plate freezers).

HP has been extensively used in the manufacturing of ice cream, but mostly only in the step of homogenization (Hayes and Kelly, 2003; Floury et al., 2000; Popper and Knorr, 1990). In recent years, advances in mechanical technology have allowed the development of homogenizers with higher pressure than the conventionally used, 50MPa (Hayes et al., 2003; Paquin, 1999).

Conclusions of Professor Douglas Goff[5] are that higher pressures (3000-4000 psi for the first step and 500 for the second, equivalents to 20,6-27,4 MPa and 3,4 MPa, respectively), create more and smaller fat globules (more surface area can create more fat networks), stabilize more air bubble surface area and slow down ice re-crystallization. These conclusions are particularly interesting for lower fat ice creams (lower than 10% fat content).

The application of high hydrostatic pressure, at levels of 100 to 800 MPa, may help the preservation, due to the inactivation of micro-organisms (already known and industrialized process for fruit and vegetable fruits, shellfish, ham and other meat products, etc. as seen in section 2.1.5). Additionally, an effect on the proteins present in ice cream (gelation), as well as on milk (casein micelles disruption, β-lactoglobulin denaturation, mineral balance shifting, pH increase, turbidity reduction, gelatinization of skim milk powder solutions with micellar casein, when pressurized in the presence of sugar) is expected.

Under these circumstances, and given the increasing demand on low-fat products, the application of high pressure to ice cream could play a significant role in enhancing the texture parameters of low-fat products, or even in products in which the storage temperature was not properly maintained constant. The idea under the set of experiments performed was to evaluate the organoleptic, textural and melting parameters of HP treated ice cream. The process aimed to obtain a re-crystallization of partially melted ice crystals due to a sudden pressure release (PSF). The process consisted in pressurizing a frozen ice cream sample and then instantaneously releasing the pressure. The details of the temperature and pressure profiles and the texture and melting down parameters are given below.

4.7.2. Experimental results

Conventional 9% fat in content ice cream (Nestlé Beauvais, Paris) was treated under high pressure at sub-zero temperatures with the aim of inducing solid-solid phase transitions or inducing a partial melting of ice I that is re-crystallized after the pressure release. In none of the trials, solid-solid phase transition was observed. In most of the cases, samples were pressurized up to 300 MPa and then de-pressurized back to atmospheric level without any re-crystallization (Figure 4.97a); in some cases, after

[5] http://www.idfa.org/meetings/presentations/douggoff.pdf

pressure release, a jump was observed, clearly indicating the re-crystallization of the partial melted water into ice I (Figure 4.97b).

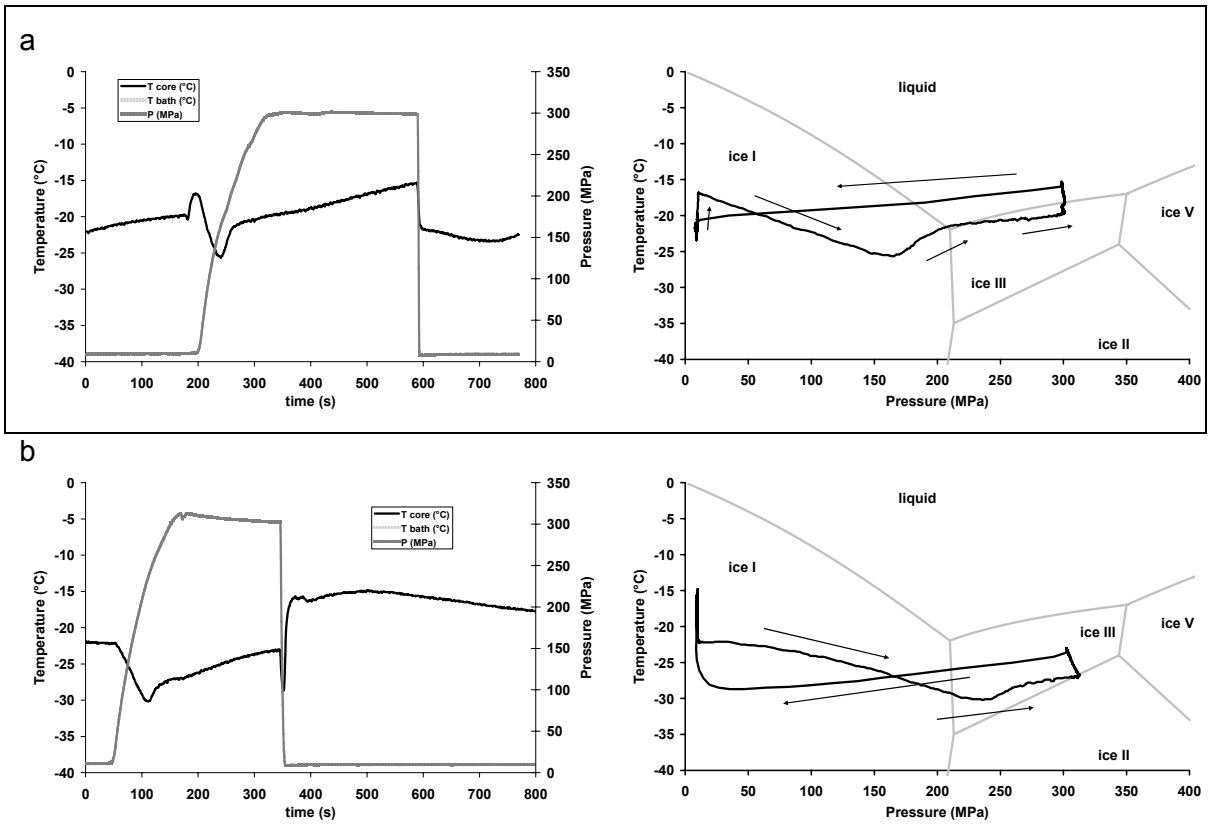

Figure 4.97. Time profiles (left) and processing paths (right) and of the high pressure treatment of ice cream samples at sub-zero temperatures: (a) without re-crystallization of ice I and (b) with re-crystallization of ice I.

In the processing path shown in Figure 4.97a, a first temperature increase is observed during pressurization, due to the adiabatic heat of compression, but quickly the temperature of the ice cream sample starts to decrease, due to the endothermic partial melting of ice I into water, arriving at a value of -25°C at 170 MPa. Then, the temperature increases again. To explain this behaviour (it could be expected, as happened with potato tissues, that the temperature of the sample decreases further until the pressure remains constant), it is suggested that the ice content of the sample is completely melted. Therefore, there is no more endothermic melting process and the whole sample, in liquid state, increases temperature due, again, to the adiabatic heat of compression. When the pressure level of 300 MPa is reached, pressure is released and temperature decreases following again the adiabatic slope, but no evidence of re-crystallization of the melted water is obtained, although the sample reaches values of -23°C after pressure release.

In the case of the trial shown in Figure 4.97b, a similar behaviour is obtained during the pressurization: a first temperature increase (barely appreciable in the figures) is followed by the temperature decrease caused by the partial melting of ice I into water. This processes seems to be finished at 240 MPa, for a temperature of -30°C and then, the temperature increases again, showing the probable existence of no more ice to melt in the sample. The difference between case b and a, is that in the second one, after pressure release, a freezing jump is clearly observed in the time profile. During pressure release, the temperature decrease (adiabatic decompression) and when a level of, approximately, -29°C is reached, the temperature of the sample jumps to a typical freezing plateau (between -15 and -20°C), clearly showing that the melted water is re-crystallized into ice I. The influence of these two kinds of results after HPLT treatment of ice cream samples on quality parameters has been studied on melting

curves and texture analysis. The results are given in Figure 4.98and, Figure 4.99, respectively.

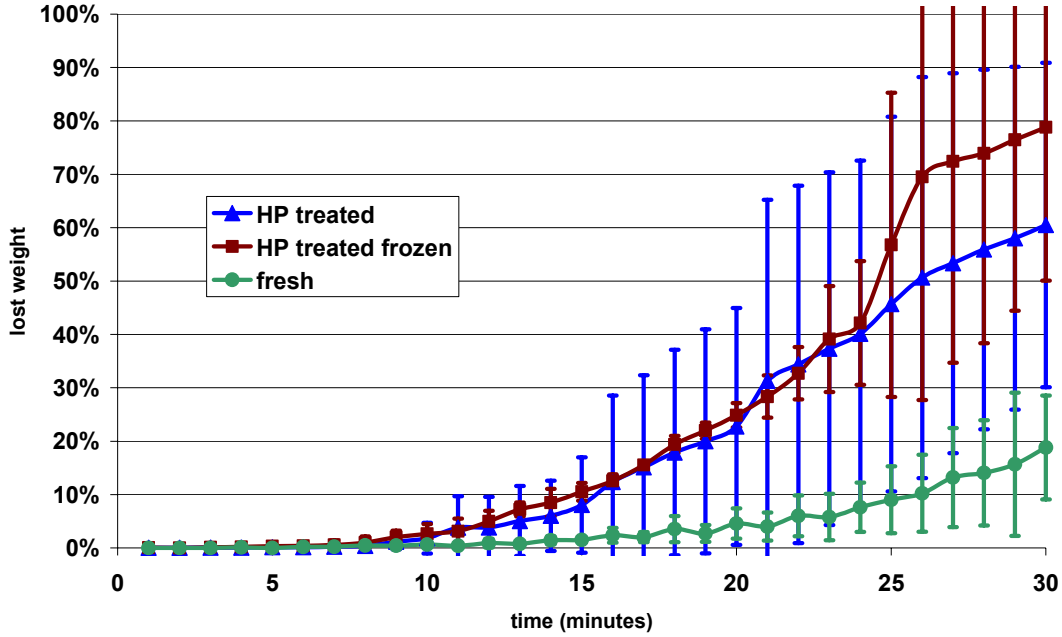

Figure 4.98. Melting curves of HPLT treated ice cream samples (compared to non-treated samples), expressed as percentage of lost weight in time. "HP treated" represents samples without re-crystallization of ice I and "HP treated frozen" represents samples with ice I re-crystallization.

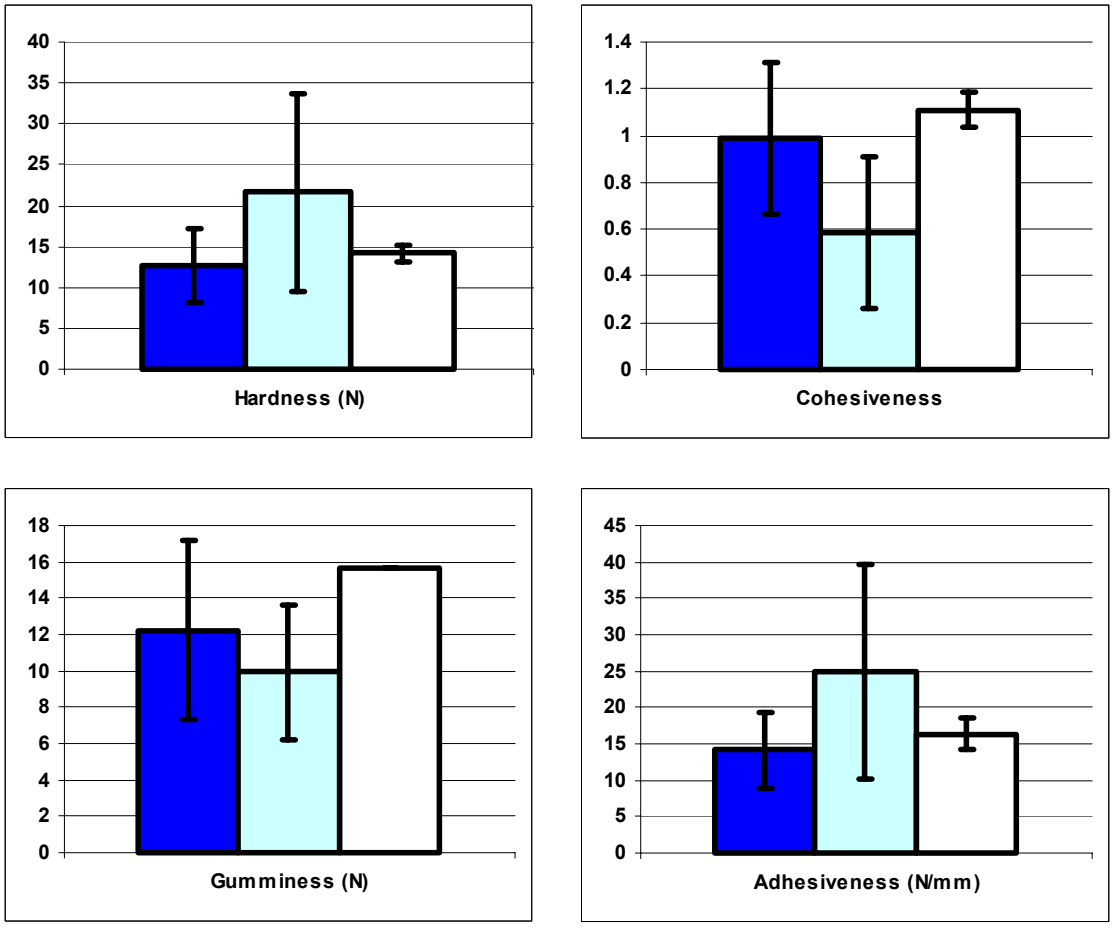

Figure 4.99. Texture analysis of ice cream: fresh (■), high pressure processed (■) and high pressure processed with re-crystallization (□).

The results obtained for melting curves clearly show that the application of high pressure to frozen ice cream samples is not enhancing the melting properties of the product. The aim of a good ice cream formulation is to obtain a product in which during consumption, the structure is not melting down. Therefore, the lower the weight loss percentage evolution in time, at room temperature, the better the product quality. The results shown in Figure 4.98 clearly show that for both cases of HPLT treated ice cream, the melting rate is higher than the corresponding for fresh (non-treated) samples.

In the case of the texture analysis, a clear enhancement of the textural properties of HPLT treated samples without ice re-crystallization is obtained (higher hardness, lower cohesiveness, lower gumminess and higher adhesiveness). These properties' changes are the consequence of a softer texture of the product, which is one of the aims of a good ice cream formulation. The results for samples in which ice was re-crystallized were not as good as expected. The results were also corroborated with sensorial analysis, that clearly conclude that the HPLT treated samples without re-crystallization had a much better mouth sensorial properties (softer, without any icy texture) than the non-treated samples.

5. Conclusion and perspectives

5.1. New challenges of the HPLT research

In the present dissertation, the results of the process optimization for freezing and thawing purposes at high pressure for processing times, quality and safety parameters taking potato mainly as a model product for vegetal tissues are shown. The first steps are done in terms of understanding the kinetics of phase transitions in the domain of high pressure low temperature region, implying freezing, thawing and solid-solid phase transitions. The existence of a metastable region has been experimentally proved and the consequences have been explained to obtain controlled and optimized freezing and thawing paths, in terms of processing time reduction, and product quality enhancement. The products treated were mainly potato, as a model of a vegetal tissue and ice cream, as an example of a product that must be necessarily treated at subzero temperatures and that seems to be the future of the industrial application of the HPLT technology.

The application of the studied processes in industrial scale facilities, the study of further products of interest and the economical study of the applicability of such processes are still challenges to be addressed in the HPLT field.

Examples of new challenges are:

(i) The study of the tenderization of animal tissues, specially meat, during frozen storage, through the application of high pressure. One of the main problems of the industry of frozen meat is the hard texture of the samples after long storage time and the microbial control of frozen specimens. The application of high pressure during the frozen storage of meats, implying a solid-solid phase transition, could mean the tenderization of the texture, thanks to the high stresses associated to a solid-solid phase transition between ice I and ice III. On the other hand, the microbial control of the stored samples could be enhanced, thanks to the already shown microbial inactivation in solid state when phase transitions occur. Additionally, the effect of solid-solid phase transitions in the control of prions, could open a new highly interesting field for the control of illness-related products.

(ii) The study of the texture of ice cream for low fat formulations. The main reason to increase the fat content in the formulation of ice creams (like, for example, Häagen Dazs, which products are of around 16% fat content, being the rest of around 12%) is to increase the texture properties, the smooth-like mouth sensation, to increase the flavours and aromas appreciation, etc. The use of low-fat formulations could be a new branch of demand for the European consumers, highly concerned on the low fat diet. The problem of bad texture and icy sensation of low-fat ice creams could be enhanced using high pressure, in both freezing (applying PSF) and homogenization steps, thanks to the re-distribution of smaller ice crystals in the sample, giving a soft texture.

(iii) The study of the application of high pressure to dairy products like eggs. The application of high pressure at room temperatures on eggs leads to similar protein changes than with the application of high temperatures. The application of high pressure combined with low temperature could lead to egg products in which the microbial control is ensured in a “half-cooked” state. The product could be then just heated on water and ready to eat. This could be a high interesting field for the market of eggs and egg-products, always limited for the fragility of the products and the low shelf-life. Increasing microbial control and handling the products in a half-cooked state could lead to a new branch of the food industry.

tissues. These three examples are just possible future challenges of the application of HPLT to the food industry. Many others could be written here, but the list would be as long as food products existing in the market.

5.2. Real potential of HPLT technology in industry

Scaling-up procedures needed for the industrial implementation of the, up-to-now laboratory scale developed, HPLT technology have been already started in several research groups from different focus:

- From a mathematical point of view, thanks to the development of mathematical models able to describe and predict thermophysical properties of water-based products at HPLT conditions, and to describe free and forced convectional fluid-dynamics during HPLT processes,
- From a bench mark test point of view, as explained in this work (chapter 4.2.6), being able to evaluate the reproducibility of results for different facilities, modes of operation and scales, and
- From an industrial concept development point of view, as explained in section 5.3.

The use of the technology of HPLT, implemented on an industrial scale, is still to be explored, but both the equipment facilities and the processing knowledge for real products in real processing paths are ready to jump from laboratory to industrial scale. Processing paths have been optimized in terms of process times, phase transition times and thermal gradients for freezing and thawing processes, thanks to the controlled use of the metastable phases.

Quality related parameters have been investigated in terms of microbial inactivation in both liquid and solid state, with special interest in the metastable region. Last results obtained in this field showed (data still not published) that the inactivation of Bacillus subtilis was similar for two paths (see): path a in solid state (sample from frozen storage was pressurized in solid state to 250 MPa at -25°C) and path b in liquid state (thawed samples were pressurized to 250 MPa and the tempered to -25°C without phase transition. Achieving the same point in the metastable region from solid and from liquid states, the results of microbial inactivation were the same: a level of 5 log was reached in both cases. This result can be used as an indirect way to measure the density of the solid and liquid metastable phases. Both values might be, given the similar microbial inactivation, of the same range. Supercooled water at 250 MPa and -25°C might therefore have a similar density than a metastable solid ice I (?) at 250 MPa and -25°C.

Safety related parameters have been also investigated in the frame of the SAFE ICE project: enzymatic inactivation in foods after HPLT processing have been investigated by Prof. Marc Hendrickxs, who obtained a great amount of data showing that blanching cannot probably be changed or omitted in industrial freezing processes, given that the application of HP during freezing does not inactivate enough quality and safety related enzymes, like peroxidase, polyphenoloxidase, etc.

5.3. Development of the industrial HPLT reactor concept

In the frame of the European Project SAFE ICE, a concept of reactor for HPLT continuous or semi-continuous processing of foods has been formulated in collaboration with UNIPRESS. The details of this invention are confidential, but the concept is as easy as designing a continuous tubular reactor for processing a product such as ice cream at high pressure and low temperature.

References

Agnelli, M. E., and Mascheroni, R. H. (2001). Cryomechanical freezing. A model for the heat transfer process. Journal of Food Engineering, 47, 263-270.

Alpas, H., N. Kalchayanand, F. Bozoglu, A. Sikes, C.P. Dunne and B. Ray, Variation in resistance to hydrostatic pressure among strains of food-borne pathogens, Applied and Environmental Microbiology 65 (1999), pp. 4248–4251.

Amberger,A. u. Schaller,K. (1975). Der Einfluß von Sorte und Standort auf die an der enzymatischen Verfärbung beteiligten Inhaltsstoffe; Potato Res. 18, 161-173.

Ananta, Edwin, Volker Heinz, Oliver Schlüter and Dietrich Knorr. (2001). Kinetic studies on high-pressure inactivation of Bacillus stearothermophilus spores suspended in food matrices. Innovative Food Science & Emerging Technologies, Volume 2, Issue 4, Pages 261-272.

Arbuckle, W.S. "Ice Cream." 4th Edition. Van Nostrand Reinhold, 1986. 0-87055-479-4.

Ashie, I. N. A. & Simpson, B. K. (1996). Application of high hydrostatic pressure to control enzyme related fresh seafood texture deterioration. Food Research International, Vol. 29, No.5-6, pp. 569-575.

Balny, C. and Masson, P. (1993). Effects of high pressure on proteins. Food Reviews International 9(4):611-628

Barbosa-Cánovas, G.V., Pothakamury, U.R., palou, E. and Swanson, B.G. (1998). Nonthermal preservation of foods. ISBN 0-8247-9979-8, Marcel Dekker, Inc., New York.

Barry, H., Dumay, E. M., and Cheftel, J. C. (1998a). Influence of pressure-assisted freezing on the structure, hydration and mechanical properties of a protein gel. In: High pressure food science, bioscience and chemistry, N. S. Isaacs, ed., Royal Society of Chemistry, London, 343-353.

Barry, H., E. Dumay, J. Lévy and J.C. Cheftel (1998b). Influence de la congélation assistée par la pression sur les caractéristiques d'un gel protéique. In « Structuration des Aliments », Lavoisier Tec. & Doc., Paris, pp. 303-312.

Barsotti L, Cheftel JC. Food processing by pulsed electric fields. II Biological aspects. Food Rev. Int. 1999; 15(2):181-213.

Bauer, B.A., M. Hartmann, K. Sommer and D. Knorr. (2004). Optical in situ analysis of starch granules under high pressure with a high pressure cell. Innovative Food Science & Emerging Technologies, Volume 5, Issue 3, Pages 293-298.

Behsnilian, D., M. Regier, M. Stahl: New Methods in Food Processing, INRA, 2003, ISBN 2-7380-1137-3

Bello, R.A., Luft, J.H. and Pigott, G.M. (1982). Ultrastructural study of skeletal fish muscle after freezing at different rates. Journal of Food Science 47:1389-1394.

Benito, A., G. Ventoura, M. Casadei, T. Robinson and B. Mackey, Variation in resistance of natural isolates of Escherichia coli O157 to high hydrostatic pressure, mild heat and other stresses, Applied and Environmental Microbiology 65 (1999), pp. 1564–1569.

Boderias,A.J., Perez-Mateas,M., Solas,M and Montero,P. (1998). Frozen storage of high-pressure- and heat-induced gels of blue whiting (Micromesistius poutassou) muscle: rheological, chemical and ultrastructure studies. Z. Lebensm Unters. Forsch. 205:335-342.

Bon, J., Benedito, J. Cárcel, J. and Mulet, A. (2001). Transferencia de calor en geometría cilíndrica considerando resistencia externa: método analítico. VIII Taller de herramientas de cálculo. Eds.: A. Mulet, C. Ordorica, J. Benedito, P. Fito. México.

Brauch, G., U. Hänsler and H. Ludwig, The effect of pressure on bacteriophage, High Pressure Research 5 (1990), pp. 767–769.

Bridgman, P.W. (1912). Water in the liquid and five solid forms under pressure. Proceedings of the American Academy of Arts and Science, XLVII(13):439-558.

Bridgman, P.W. (1914). The coagulation of albumen by pressure. *J. Biol. Chem.* 19:511-512.

Bridgman, P.W. (1935). The pressure-colume-temperature relations of the liquid, and the phase diagram of heavy water. Journal of Chemical Physics, 3:597-605.

Brul, S., A. J. M. Rommens and C. T. Verrips. (2000). Mechanistic studies on the inactivation of Saccharomyces cerevisiae by high pressure. Innovative Food Science & Emerging Technologies, Volume 1, Issue 2, Pages 99-108.

Butz, P., Habison, G., & Ludwig, H. (1992). Influence of high pressure on a lipid coated virus. In C. Balny, R. Hayashi, K. Heremans & P. Masson, High pressure and biotechnology (pp. 61–64). London: Colloque INSERM/J. Libby Eurotext Ltd.

Butz, P., R. Edenharder, A. Fernández García, H. Fister, C. Merkel and B. Tauscher. (2002). Changes in functional properties of vegetables induced by high pressure treatment. Food Research International, Volume 35, Issues 2-3, 2002, Pages 295-300.

Butz, P., R. Edenharder, H. Fister and B. Tauscher. (1997). The influence of high pressure processing on antimutagenic activities of fruit and vegetable juices. Food Research International, Volume 30, Issues 3-4, Pages 287-291.

Cano, P. (1996). Vegetables. In: Freezing effects on food quality, L. E. Jeremiah, ed., Marcel Dekker, New York, 247-298.

Cano, P., Martin, M.A. and Fuster, C. (1990) Effects of some thermal treatments on polyphenoloxidase and peroxidase activities of banana. J. Sci. Food Agric. 51, 223-231

Carl, K. and H. Ludwig, Pressure effects on bacteriophage, High Pressure Research 7 (1991), pp. 176–178.

Cheftel, J.C. (1991). Applications des hautes pressions en technologie alimentaire. Industries Alimentaires et Agricoles, 108, 143-153.

Cheftel, J.C. (1992). Effects of high pressure on food constituents. In "High Pressure and Biotechnology", C. Balny, R. Hayashi, K. Heremans, P. Masson, eds. J. Libbey Eurotext Ltd, London. Vol. 224, pp 195-209.

Cheftel, J.C. (1995). High pressure, microbial inactivation and food preservation. Food Sci Technol. Internat 1:75-90.

Cheftel, J.C., and Dumay, E. 1997. Les hautes pressions: Principes et potentialités. La conservation des aliments. In: Parmentier, M. (ed). Nouveaux procédés de conservation. 9:197-215.

Cheftel, J.C., Lévy, J., and Dumay, E. (2000). Pressure-assisted freezing and thawing: principles and potential applications. Food Reviews International, 16(4):453-483.

Cheftel, J.C., Thiebaud, M., and Dumay, E. (2002). Pressure-assisted freezing and thawing of foods: a review of recent studies. High Pressure Research, 22:601-611.

Chevalier D, Sentissi M, Havet M, Le Bail A. (2000c). Comparison Of Air-blast And Pressure Shift Freezing On Norway Lobster Quality. J. Food Sci., 65(2):329-333.

Chevalier, D., Le Bail, A., and Ghoul, M. (2000a). Freezing and ice crystalls formed in a cylindrical food model: part 1. Freezing at atmospheric pressure. J. Food Eng., 46:277-285.

Chevalier, D., Le Bail, A., Chourot, J.M. and Chantreau, P. (1999). High pressure thawing of fish (whiting): influence of the process parameters on drip losses. Lebensmittel Wissenschaft und Technologie, (32) 25-31.

Chevalier, D., LeBail, A., and Ghoul, M. (2000b). Freezing and ice crystals formed in a cylindrical food model: part 2. Comparison between freezing at atmospheric pressure and pressure-shift freezing. J. Food Eng., 46:287-293.

Chevalier, D., Sequeira-Munoz, A., Le Bail, A., Simpson, B.K. & Ghoul, M. (2000d). Effect of Pressure Shift Freezing, Air-blast Freezing and Storage on Some biochemical and physical properties of turbot (Scophthalmus maximus) Lebensmittel-Wissenschaft und-Technologie Vol. 33, No. 8, pp. 570-577.

Chilton, P., N.S. Isaacs, B. Mackey and R. Stenning, The effects of high hydrostatic pressure on bacteria. In: K. Heremans, Editor, High pressure research in the biosciences and biotechnology, Leuven University Press, Belgium (1997), pp. 225–228.

Chizov, V.E. and Nagornov, O.V. (1991). Thermodynamic properties of ice, water and their mixture under high pressure. Glaciers Ocean Atmosphere Interactions (Proceedings of the International Symposium); IAHS Publ., 208:463-470.

Chizov. V. E. (1993). Prikladnay Mekhanika i Tekhnicheskaya Fizika. 2. 113-123.

Chourot, J.M., Boillereaux, L., Havet, M., and Le Bail, A. (1997). Numerical modeling of high pressure thawing: application to water thawing. Journal of Food Engineering, 34:63-75.

Chourot, J.M., Lemaire, R., Cornier, G. and Le Bali, A. (1996). Modelling of high-pressure thawing. In: R. Hayashi & C. Balny, High pressure bioscience and biotechnology. (pp. 439-444). Amsterdam, Lausanne, New York, Oxford, Shannon, Tokyo. Elsevier.

Chung, S.L. and Merritt, J.H. (1991). Freezing time predictions for brick and cylindrical-shaped foods. J. Food Sci., 56(4):1072-1075.

Cleland, A.C. and Earle, R.L. (1984). Assessment of freezing time prediction methods. J. Food Science, 49:1034-1042.

Cleland, D.J. (1985). Prediction of freezing and thawing times for foods. Ph.D. Thesis. Massey University, Palmerston North, New Zeland.

Cobb, V. (1985). The Scoop on Ice Cream. Little.

Delgado, A. E., and Sun, D.-W. (2001). Heat and mass transfer models for predicting freezing processes - a review. Journal of Food Engineering, 47, 154-174.

Deliza, R. , A. Rosenthal, F.B.D. Abadio, Carlos H.O. Silva and C. Castillo. (2005). Application of high pressure technology in the fruit juice processing: benefits perceived by consumers. Journal of Food Engineering, Volume 67, Issues 1-2, March 2005, Pages 241-246.

den Aantrekker E.D., Vernooij W.W., Reij M.W., Zwietering M.H., Beumer R.R., van Schothorst M., Boom R.M. (2003). A biofilm model for flowing systems in the food industry. J. Food Prot. 66(8):1432-8.

Denys, S. (2000). Process calculations for design of batch high hydrostatic pressure processes without and with phase transitions. PhD Dissertation. Katholieke Universiteit Leuven. Belgium.

Denys, S., Ludikhuyze, L.R., Van Loey, A.M., Hendrickx, M.E. (2000). Modeling conductive heat transfer and process uniformity during batch high-pressure processing of foods. Biotechnology Progress, 16:92-101.

Denys, S., Schlüter, O., Hendrickx, M., Knorr, D. (2002). Effect of high pressure on phase transition of water, in Ultra High Pressure Treatment of Foods., M.H.a.D. Knorr, Editor. 2002, Aspen Publishers, Frederick, MD. p. 215-248.

Denys, S., Van Loey, A.M., Hendrickx, M.E., Tobback, P.P. (1997). Modeling heat transfer during high-pressure freezing and thawing. Biotechnoly Progress, 13:416-423.

Deuchi T., Hayashi R. (1990). A new approach for food preservation: use of non-freezing conditions at subzero temperature generated under moderate high pressure. In : Hayashi R. (ed.), Pressure Processed Food Research and Development, 37-51, San-Ei Shuppan Co., Kyoto, Japan.

Deuchi, T. and Hayashi, R. (1991). Pressure application to thawing of freezed foods and to food preservation under subzero-temperature. In High Pressure Science for Food. Ed. . Hayashi, pp.101-110. John Libbey Eurotext.

Deuchi, T. and Hayashi, R. (1992a). High pressure treatments at subzero temperature: application to preservation, rapid freezing and rapid thawing of foods. In C. Balny, R. Hayashi, K. Heremans & P. Masson (Eds.), High Pressure and Biotechnology. vol. 224, pp. 353-355, John Libbey Eurotext, Ltd.

Deuchi, T. Hayashi, R. (1992b). In High Pressure and Biotechnology, Eds. C. Balny, R. Hayashi, K. Heremans and P. Masson. 353-355. Montroge: INSERM/John Libbey Eurotext Ltd, England.).

Devine, C. E., Bell, R. G., and Lovatt, S. (1996). Red Meats. In: Freezing effects on food quality, L. E. Jeremiah, ed., Marcel Dekker, New York, 51-84.

Devlieghere, F. Vermeiren, L. and Debevere, J. (2004). New preservation technologies: Possibilities and limitations. International Dairy Journal, Volume 14, Issue 4, April 2004, Pages 273-285

Djaczenko, Wiktor, Martin Müller and Arrigo Benedetto. (1990). Ultra-rapid high pressure freezing in high resolution EM of cell-cell and cell-substrate interactions. Cell Biology International Reports, Volume 14, Supplement 1, Page 231.

Dobiáš, Jaroslav, Michal Voldřich, Miroslav Marek and Kamila Chudáčková. (2004). Changes of properties of polymer packaging films during high pressure treatment. Journal of Food Engineering, Volume 61, Issue 4, Pages 545-549.

Dogan, C. and O. Erkmen. (2004). High pressure inactivation kinetics of Listeria monocytogenes inactivation in broth, milk, and peach and orange juices. Journal of Food Engineering, Volume 62, Issue 1, Pages 47-52.

Dong U.L., Jiyong P., Jungil K., Ick H.Y., 1996. Effect of high hydrostatic pressure on the shelf life and sensory characteristics of Angelica keiskei juice. Korean J. Food Sci. Technol., 28, 105-108.

Donsi G., Ferrari G., Di Matteo M., 1996. High pressure stabilization of orange juice: evaluation of the effects of process conditions. Ital. J. Food Sci., 8, 99-106.

Dubochet, Jacques. (1995). High-pressure freezing for cryoelectron microscopy. Trends in Cell Biology, Volume 5, Issue 9, Pages 366-368.

Dumay, E., C. Lambert, S. Funtenberger and J. C. Cheftel. (1996). Effects of High Pressure on the Physico-chemical Characteristics of Dairy Creams and Model Oil/Water Emulsions. Lebensmittel-Wissenschaft und-Technologie, Volume 29, Issue 7, Pages 606-625.

Dumoulin, M., Ozawa, S., and Hayashi, R. (1998). Textural properties of pressure-induced gels of food proteins obtained under different temperatures including subzero. Journal of Food Science, 63(1), 92-95.

Dunn, J., Ott, T. and Clark, W. 1995. In J. Food Technology. 49(9):95-98.

Edwards, M. C. (1995). Change in cell structure. In: Physico-chemical aspects of food processing, S. T. Beckett, ed., Blackie Academic & Professional, London, 212-233.

Edwards, M., and Hall, M. (1988). Freezing for quality. Food Manufacture, (3), 41-45.

Erikson, M.C. and Y.C. Hung, Eds. (1997). Quality in frozen food. Chapman and Hall, New York.

Eshtiaghi, M.N. and Knorr D., 1993. Potato cubes response to water blanching and high hydrostatic pressure. J. Food Sci., 58, 1371-1374.

Estiaghi, M.N., Stute, R. and Knorr, D. 1994., In J. of Food Sci. 59, 1168-1170.

Evans, L. F. (1967a). Selective nucleation of the high-pressure ices. Journal of Applied Physics, 38, 4930-4932.

Evans, L.F. (1967b). Two-dimensional Nucleation of Ice. Nature. January. 28. 384-385.

Fagerbakke, K.M., Norland, S., Heldal, M. (1999). The inorganic ion content of native aquatic bactieria. Can. J. Microbiol. 45:304-311.

Farkas, D.F. and D.G. Hoover, High pressure processing, Journal of Food Science, Supplement-Kinetics of Microbial Inactivation for Alternative Food Processing Technologies 65 (2000), pp. 47–64.

Farr, D. 1990. High pressure technology in the food industry. Trends in Food Science & Technology July: 14-16.

Fennema, O. R., Powrie, W. D., and Marth, E. H. (1973). In: Low-temperature preservation of foods and living matter, Marcel Dekker, New York.

Fennema, O.R. (1975). Nature of freezing process. In: O.R. Fennema, W.D. Powrie and E.H. Marth (editors). Low temperature preservation of foods and living matter, Marcel Dekker, New York, p. 151-222.

Fikiin, K.A. (1998). Ice content prediction methods during food freezing: a survey of the eastern European literature. J. Food Sci., 38, 331-339.

Floury, J., A. Desrumaux and J. Lardieres. (2000). Innovative Food Science and Emerging Technologies, 1:127-134.

Franke, K. (2000). A new approach for the numerical calculation of freezing and thaqing processes of foods using a modified ficticious heat flow method. J. Food Eng., 44:23-29.

Freitas, T.R.P., L.P. Gaspar, L.A. Caldas, J.L. Silva and M.A. Rebello. (2003). Inactivation of classical swine fever virus: Association of hydrostatic pressure and ultraviolet radiation, Journal of Virological Methods 108, pp. 205–211.

Fuchigami, M. and Teramoto, A. (2003). Changes in temperature and structure of agar gel as affected by sucrose during high-pressure freezing. Journal of Food Science 68(2): 528-533.

Fuchigami, M. and Teramoto, A. (1997). Stuctural and textural changes in Kinu-Tofu due to high-pressure-freezing. Journal of Food Science, 62(4):828-832.

Fuchigami, M., and Teramoto, A. (1996). Texture and cryo-scanning elextron micrographs of pressure shift frozen tofu. In “High Pressure Bioscience and Biotechnology”, R. Hayashi and C. Balny, Elsevier Science, Amsterdam, pp. 411-415.

Fuchigami, M., Kato, N. & Teramoto, A. (1998a). High-Pressure-Freezing Effects on Textural Quality of Chinese Cabbage. Journal of Food Science-Vol. 63, No.1.

Fuchigami, M., Kato, N., and Teramoto, A. (1996). Effect of pressure-shift freezing on texture, pectic composition and histological structure of carrots, in High-Pressure

Bioscience and Biotechnology., R. Hayashi and C. Balny, Editors. 1996, Elsevier Science, B.V. p. 379-386.

Fuchigami, M., Kato, N., and Teramoto, A. (1997a). High-pressure freezing effects on textural quality of carrots. J. Food Sci., 62(4):804-808.

Fuchigami, M., Miyazaki, K., Kato, N., Teramoto, A. (1997b). Histological changes in high-pressure frozen carrots. J. Food Sci., 62(4):809-812.

Fuchigami, M., Teramoto, A., and Ogawa, N. (1998b). Structural and textural quality of kinu-tofu frozen-then-thawed at high pressure. J. Food Sci., 63(6):1054-1057.

Gaspar, L.P., A.C.B. Silva, A.M.O. Gomes, M.S. Freitas, A.P.D. Ano Bom and W.D. Schwarcz et al., Hydrostatic pressure induces the fusion-active state of enveloped viruses, The Journal of Biological Chemistry 277 (2002), pp. 8433–8439.

Gaspar, L.P., J.E. Johnson, J.L. Silva and A.T. Da Poian, Partially folded states of the capsid protein of cowpea severe mosaic virus in the disassembly pathway, Journal of Molecular Microbiology and Biotechnology 273 (1997), pp. 456–466.

George, R.M. (1993). Processes used in the food industry. Trends in food science & technology, 4:134-138.

George, S. (2000). Impact of high hydrostatic pressure on foods at sub temperatures: Phase Transitions, Modelling Temperature Distribution During Thawing and Inactivation of Micro-organisms. PhD Thesis, Berlin University of Technology.

Goff, D. (2005). http://www.foodsci.uoguelph.ca/dairyedu/freeztheor.html

Golden, D. A., and Arroyo-Gallyoun, L. (1997). Relationship of frozen-food quality to microbial survival. In: Quality in frozen food, M. C. Erickson and Y.-C. Hung, eds., Chapman & Hall, New York, 174-193.

Gomes, M. R. A. and Ledward, D. A. (1996). Effect of High-Pressure Treatment on the Activity of Some Polyphenoloxidases. J. Food Chemistry, 56(1):1-5.

Goularte, L. , C. G. Martins, I. C. Morales-Aizpurúa, M. T. Destro, B. D. G. M. Franco, D. M. Vizeu, B. W. Hutzler and M. Landgraf. (2004). Combination of minimal processing and irradiation to improve the microbiological safety of lettuce (Lactuca sativa, L.). Radiation Physics and Chemistry, Volume 71, Issues 1-2, September-October 2004, Pages 157-161.

Gow C.Y., Hsin T.L., 1996. Comparison of high pressure treatment and thermal pasteurization effects on the quality and shelf life of guava puree. Int. J. Food Sci. Technol., 31, 205-213.

Groß, P., & Ludwig, H. (1992). Pressure-temperature-phase diagram for the stability of bacteriophage T4. In C. Balny, R. Hayashi, K. Heremans & P. Masson, High pressure and biotechnology (pp. 57–59). London: Colloque INSERM/J. Libby Eurotext Ltd.

Hasselton, H.T., Jr., I-Ming Chou, Shen, A.H. and Basset, W.A. (1995). Techniques for determining pressure in the hydrothermal diamond-anvil cell: Behaviour and identification of ice polymorphs (I, III, V, VI). American Mineralogist, vol. 80, pp. 1302-1306.

Hayakawa, I., T. Kanno, K. Yoshiyama and Y. Fujio, Oscillatory compared with continuous high pressure sterilization of Bacillus stearothermophilus spores, Journal of Food Science 59 (1994), pp. 164–167.

Hayashi, R. (1989). Application of high pressure to food processing and preservation: philosophy and development. A: Spiess, W.E.L.; Schubert, H. (Eds.). Engineering and food. Vol. 2. Elsevier Applied Science. London. 815-826.

Hayashi, R. In Balny, C., Hayashi, R., Heremans, K. and P. Masson. 1992. In High Pressure and Biotechnology. Proceedings of the First European Seminar on High Pressure and Biotechnology.185-193.John Libbey and Company Ltd. London, England.

Hayashi, R., Kinsho, T. and Ueno, H. (1998). Combined applications of subzero temperature and high pressure on biological materials. In High Pressure Food Science, Bioscience and Chemistry. N.S. Isaacs, Ed., The Royal Society of Chemistry, Cambridge, UK, pp. 166-174.

Hayes, M.G. and A.L. Kelly (2003). J. Dairy Res.:70-307-313.

Hayes, M.G., A.C. Lefrancois, D.S. Waldron, H.D. Goff and A.L. Kelly (2003). Influence of high pressure homogenization on some characteristics of ice cream. Milchwissenschaft 58 (9/10), 519-523.

Heinz, V. and Knorr, D. (1996). High pressure inactivation kinetics of Bacillus subtilis cells by a three-state-model considering distribution resistance mechanisms. Food Biotechnol. 10:149-161.

Heinz, V.; Knorr, D. and Schlüter, O. (1998). Hochdruckbehandlung von Lebensmitteln. Spektrum der Wissenschaft 9/98:132-136.

Heremans K., 1992. From living systems to biomolecules. In : Balny C., HayashI R., Heremans K., Masson P. (eds.), High Pressure and Biotechnology, 37-44, John Libbey and Co. Ltd., London.

Hernandez, A., and Pilar Cano, M. (1998). High - pressure and temperature effects on enzyme inactivation in tomato puree. Journal of Agricultural and Food Chemistry, 46(1), 266-270.

Hite, B.H. (1899). The effect of preservation of milk. Bulletin 58, 15-35.

Hoa, Gaston Hui Bon, Pierre Douzou, Noël Dahan and Claude Balny. (1982). High-pressure spectrometry at subzero temperatures. Analytical Biochemistry, Volume 120, Issue 1, Pages 125-135.

Hobbs, P.V. (1974). In: Ice Physics. Clarendon Press, Oxford.

Hogan, E., Kelly, A.L. and Sun, D. (2005). High pressure processing of foods: an overview. In Emerging technologies for food processing, Sun, D. (editor). ISBN 0-12-676757-2. Elsevier Academic Press, London, UK.

Holtmann, G., Bakker, E.P., Uozumi, N. and Bremer, E. (2002). KtrAB and KtrCD: Two K+ uptake system in Bacillus subtilis and their role in adaption to hypertonicity. J. Bacteriol., 185.4.1289-1298.2003

Hoover, PG.; Metrick, C.; Papineau, A.M.; Farkas, D.F. and Knorr, D. (1989). Biological effects of high hydrostatic pressure on food micro-organisms. Food Technol. 43:99-107.

Hung, Y.-C., and Kim, N.-K. (1996). Fundamental aspects of freeze-cracking. Food Technology, 50(12), 59-61.

Indrawati, I., Ludikhuyze, L. R., Van Loey, A. M. & Henrickx, M. E. (2000). Lipoxygenase Inactivation in Green Beans (Phaseolus vulgaris L.) Due to High Pressure Treatment at Subzero and Elevated Temperatures. J. Agric. Food Chem., 48, 1850-1859.

Indrawati, van Loey, A., Denys, S. And Hendrickx, M. (1998). Enzyme sensitivity towards high pressure at low temperature. Food Biotechnology, 12(3), 263-277.

Isaacs, N.S., P. Chilton and B. Mackey, Studies on the inactivation of micro-organisms by high pressure. In: D.A. Ledward, D.E. Johnston, R.G. Earnshaw and A.P.M. Hasting, Editors, High pressure processing of foods, Nottingham University Press, UK (1995), pp. 65–79.

Jay, J.M. (1992). Modern Food Microbiology, 4th edition, an Nostrand Reinhold, New York.

Jeremiah, M.C., Ed. (1996). Freezing effects on food quality, Marcel Dekker, Inc., New York.

Jeyamkondan S, Jayas DS, Holley RA. Pulsed electric field processing of foods: a review. J. Food Protect. 1999; 62(9):1088-1096.

Jurkiewicz, K., M. Villas-Boas, J.L. Silva, G. Weber, G. Hunsmann and R.M. Clegg, Inactivation of simian immunodeficiency virus by hydrostatic pressure, Proceedings of the National Academy of Science United States of America 92 (1995), pp. 6935–6937.

Kalichevsky, M.T., Knorr, D. and Lillford, P.J. (1995). Potential food applications of high pressure effects on ice-water transitions. Trends on Food Science and Technology 6(8): 253-259.

Kanda, T., Kitagawa, K. and Fujinuma, K. (1993). Behavior of ice under pressure. For the basis of high pressure sterilization under low temperature. In High Pressure Bioscience and Food Science. Hayashi, R., Ed.; San-Ei Suppan Co. Kyoto; pp. 24-26.

Kanda, Y. and Aoki, M. (1993). Development of pressure-shift freezing method: Part I. Observation of ice crystals of frozen tofu. In High Pressure Bioscience and Food Science. Ed.: Hayashi, R. San-Ei Suppan Co., Kyoto, pp. 27-33.

Kanda, Y., Aoki, M. and Kosugi, T. (1992). Freezing of tofu (soybean curd) by pressure-shift freezing and its structure. Nippon Shokunin Gakkaishi, 39(7),608-614.

Karino, S., Hane, H, and Kosugi, T. (1994). Behavior of water and ice at low temperature and high pressure. In: High Pressure Bioscience, R. Hayashi, S. Kunugi, S. Shimada and A. Suzuki, eds., San-Ei Suppan Co, Kioto, 2-9.

Kennedy, C.J. (1998). Formation of ice in frozen foods and its control by physical stimuli. In “The Properties of Water in Foods. ISOPOW 6.” D.S. Reid, Ed. Blackie Academic, London, pp. 329-365.

Khadre, M.A. and A.E. Yousef, Susceptibility of human rotavirus to ozone, high pressure, and pulsed electric field, Journal of Food Protection 65 (2002), pp. 1441–1446.

Kimura K., Ida M., Yosida Y., Ohki K., Fukumoto T., Sakui N., 1994. Comparison of keeping quality between pressure-processed jam and heat-processed jam: changes in flavour components, hue, and nutrients during storage. Biosci. Biotech. Biochem., 58, 1386-1391.

Kingsley, D.H., D.G. Hoover, E. Papfragkou and G.P. Richards, Inactivation of hepatitis A virus and a calicivirus by high hydrostatic pressure, Journal of Food Protection 65 (2002), pp. 1605–1609.

Kinsho, T., Ueno, H., Hayashi, R., Hashizume, C., and Kimura, K. (2002). Sub-zero temperature inactivation of carboxypeptidase Y under high hydrostatic pressure. J. Biochem. 269, 4666-4674.

Kloczko I., Radomski M., 1996. Preservation of fruits, vegetables and juices by high hydrostatic pressure. Przemysl Spozywczy, 50, 25-26.

Knauf, G.M., K. Welter, M. Müller and K. Mendgen. (1989). The haustorial host-parasite interface in rust-infected bean leaves after high-pressure freezing. Physiological and Molecular Plant Pathology, Volume 34, Issue 6, Pages 519-530.

Knauf, Gertrude M., and Kurt Mendgen. (1988). Secretion systems and membrane-associated structures in rust fungi after high pressure freezing and freeze-fracturing. Biology of the Cell, Volume 64, Issue 3, Pages 363-370.

Knorr, D. (1993). Effects of high-hydrostatic-pressure processes on food safety and quality. Trends in Food Science and Technology, 4, 370-375.

Knorr, D. (1995). Hydrostatic pressure treatment of food: Microbiology. In: New Emerging Technologies for Food Preservation. Gould,G.W. (Ed) Blackie Academic & Professional.

Knorr, D., Schlüter, O., and Heinz, V. (1998). Impact of high hydrostatic pressure on phase transition of foods. Food Technology, 52:42-45.

Koch, H., Seyderhelm, I., Wille, P., Kalichevsky, M.T., Knorr, D. (1996). Pressure-shift freezing and its influence on texture, colour, microstructure and rehydration behaviour of potato cubes. Nahrung., 40(2):125-131.

Kolakowski, P., Dumay, E., and Cheftel, J.-C. (2001). Effects of high pressure and low temperature on β-lactoglobulin unfolding and aggregation. Food Hydrocolloids, 15, 215-232.

Kort, R., Brien, A.C.O., van Stokkum, I.H.M., Oomes, S.J.C.M., Crielaard, W. , Hellingwerf, H. J., and Brul, S. (2005). Assessment of heat resistence of bacterial spores from food product isolates by fluorescent monitoring of dipicolinic aicd release. Applied and Environmental Microbiology (in press).

Krebbers, Bregje, Ariette M. Matser, Sanne W. Hoogerwerf, Roy Moezelaar, Monic M. M. Tomassen and Robert W. van den Berg. (2003). Combined high-pressure and thermal treatments for processing of tomato puree: evaluation of microbial inactivation and quality parameters. Innovative Food Science & Emerging Technologies, Volume 4, Issue 4, Pages 377-385.

Lakshmanan, R., John R. Piggott and Alistair Paterson. (2003). Potential applications of high pressure for improvement in salmon quality. Trends in Food Science & Technology, Volume 14, Issue 9, Pages 354-363.

Lanier, T.C. (1998). High pressure processing effects on fish proteins. In: F. Shahidi, C.-T. Ho & N. van Chuyen. Process-induced chemical changes in food. 434, 45-55. Advances in experimental medicine and biology. New York. Plenum Press.

Le Bail, A., Chourot, J.-M., Barillot, P., Lebas, J.-M. (1997). Congélation-décongélation a haute pression. Rev. Gen. Froid, 972, 51-56.

Leadley C.E., Williams A., 1997. High pressure processing of food and drink-an overview of recent developments and future potential. In : New Technologies, Bull. No. 14, Mar., CCFRA, Chipping Campden, Glos, UK.

Lechaire Jean-Pierre , Marull Sylvie and Gaill Françoise. (1996). Ultrarapid freezing (quick-freeze or high-pressure) applied to reconstituted lipid bodies study in TEM after freeze-etching. Biology of the Cell, Volume 86, Issues 2-3, Page 189.

Lechaire, Jean-Pierre, Nicolas Gisèle, Muller Martin, Muller Theo and Gaill Françoise. (1993). Tem structure of collagen gels after slam of high pressure freezing. Biology of the Cell, Volume 79, Issue 1, Page 88.

Levy, J., Dumay, E., Kolodziejczyk, E., Cheftel, J.C. (1999). Freezing kinetiks of a model oil-in-water emulsion under high pressure or by pressure release. Impact on ice crystals and oil droplets. Lebensm.-Wiss. Technol., 32:396-405.

Li, J. and Sun, D.-W. (2002). Novel methods for rapid freezing and thawing of foods – a review. Journal of Food Engineering, 54:175-182.

Linton, M., J. M. J. McClements and M. F. Patterson. (2004). Changes in the microbiological quality of vacuum-packaged, minced chicken treated with high hydrostatic pressure. Innovative Food Science & Emerging Technologies, Volume 5, Issue 2, Pages 151-159.

Linton, M., J.M.J. McClements and M.F. Patterson, Inactivation of pathogenic Escherichia coli in skimmed milk using high hydrostatic pressure, Innovative Food Science and Emerging Technologies 2 (2001), pp. 99–104.

Londhal, L., and Goranson, S. “Quality differences in fast freezing.” 19th International Congress of Refrigeration, Sydney, 197-203.

López-Rubio, Amparo, José M. Lagarón, Pilar Hernández-Muñoz, Eva Almenar, Ramón Catalá, Rafael Gavara and Melvin A. Pascall. (2005). Effect of high pressure treatments on the properties of EVOH-based food packaging materials. Innovative Food Science & Emerging Technologies, Volume 6, Issue 1, Pages 51-58.

Lowry, P. D., Gill, C. O., and Pham, Q. T. (1989). A quantitative method of determining the hygienic efficiency of meat thawing processes. Food Australia, 41, 1080.

Lüdemann, H.D. (1994). Water and its solutions at high pressures and low temperatures. Polish Journal of Chemistry, 68, 1-22.

Ludikhuyze, L., and Hendrickx, M. E. G. (2002). Effects of high pressure on chemical reactions related to food quality. In: Ultra High Pressure Treatments of Foods, M. E. G. Hendrickx and D. Knorr, eds., Kluwer Academic/Plenum Publishers, New York, 23-51.

Lund, D. (2993). Predicting the impact of food processing on food constituents. Journal of Food Engineering, 56, 113-117.

Luscher, C., A. Balasa, A. Fröhling, E. Ananta, and D. Knorr. (2004). Effect of High-Pressure-Induced Ice I-to-Ice III Phase Transitions on Inactivation of Listeria innocua in Frozen Suspension. Appl. Environ. Microbiol. 70: 4021-4029.

Luscher, C., O. Schlueter and D. Knorr (2005). High pressure–low temperature processing of foods: impact on cell membranes, texture, colour and visual appearance of potato tissue. Innovative Food Science & Emerging Technologies, 6(1):59-71.

Mackey, B.M., K. Forestière, N.S.R.S. Isaacs and B. Brooker, The effect of high hydrostatic pressure on Salmonella thompson and Listeria monocytogenes examined by electron microscopy, Letters in Applied Microbiology 19 (1994), pp. 429–432.

Mackey, B.M.; Forestière, K. and Isaacs, N. (1995). Factors affecting the resistance of Lysteria Monocytogenes to high hydrostatic pressure. Food Biotechnology, 9: 1-11.

Maggi A., Gola S., Spotti E., Rovere P., Mutti P., 1994. High-pressure treatments of ascospores of heat-resistant moulds and patulin in apricot nectar and water. Ind. Conserve, 69, 26-29.

Makita, T. (1992). Application of high pressure and thermophysical properties of water to biotechnology. Fluid phase equilibrium. 76:87-95.

Mallett,C.P. 1994. Frozen Food Technology, Blackie Academic & Professional, London.

Mannapperuma, J.D. and Singh, R.P. (1988). Prediction of freezing and thawing times of foods using a numerical method based on entalphy formulation. J. Food Sci., 53(2):626-630.

Marquis, R.E., High pressure microphysiology, Advances in Microbial Physiology 14 (1976), pp. 159–241.

Marshall, Robert T., Goff, H. Douglas, Hartel, Richard W. “Ice Cream”, 6th ed., 2003, 366 p., ISBN: 0-306-47700-9.

Martens, M., Scheerlinck, N., De Belie, N., De Baerdemaeker, J. (2001). Numerical model for the combined simulation of heat transfer and enzyme inactivation in cylindrical vegetables. J. Food Eng., 47:185-193.

Martino, M.N., Otero, L., Sanz, P.D., Zaritzky, N.E. (1998). Size location of ice crystals in pork frozen by high-pressure-assisted freezing as compared to classical methods. Meat Science, 50 (3), 303-313.

Massaux, C., Bera, F., Steyer, B., Sindic, M. & Deroanne, C. (1999b). High hydrostatic pressure effects on freezing and thawing processes of pork meat. In: H. Ludwig, Advances in high pressure bioscience and biotechnology. (pp. 496-500). Berlin, Heidelberg. Springer-Verlag.

Massaux, C., Bera, F., Steyer, B., Sindic, M. and Deroanne, C. (1999a). High hydrostatic pressure freezing and thawing of pork meat: quality preservation, processing times and high pressures treatment advantages. In: H. Ludwig, Advances in high pressure bioscience and biotechnology. (pp. 485-488). Berlin, Heidelberg. Springer-Verlag.

Masschalck, B., van Houdt, R. and Michiels, C.W. (2001a). High pressure increases bactericidal activity and spectrum of lactoferrin, lactoferricin and nisin. Int. J. Food Microbiol. 64, 325-332.

Masschalck, B., van Houdt, R., Van Haver, E.G. and Michiels, C.W. (2001b). Inactivation of gram-negative bacteria by lysozyme, denatured lysocyme, and lysozyme-derived peptides under high hydrostatic pressure. Appl. Env. Microbiol. 67, 339-344.

Matheis, G. (1987). Polyphenol Oxidase and Enzymatic Browning of Potatoes (Solanum tuberosum), I. Properties of Potato Polyphenol Oxidase. Chem. Mikrobiol. Technol. Lebensm. 11, 5-12.

McClements, J.M.J., Patterson, M.F., Kinton, M. (2001). The effect of growth stage and growth temperature on high hydrostatic pressure inactivation of some psychrotrophic bacteria in milk. Journal of Food Protection, 64(4), 514-522.

Messens, W., J. Van Camp and A. Huyghebaert. (1997). The use of high pressure to modify the functionality of food proteins. Trends in Food Science & Technology, Volume 8, Issue 4, Pages 107-112.

Minerich, Phillip L. and Theodore P. Labuza. (2003). Development of a pressure indicator for high hydrostatic pressure processing of foods. Innovative Food Science & Emerging Technologies, Volume 4, Issue 3, Pages 235-243.

Miyawaki, O., Abe, T., and Yano, T. (1989). A numerical model to describe freezing of foods when supercooling occurs. J. Food Eng, 9:143-151.

Moerman, F. (2005). High hydrostatic pressure inactivation of vegetative micro-organisms, aerobic and anaerobic spores in pork Marengo, a low acidic particulate food product. Meat Science, Volume 69, Issue 2, Pages 225-232.

Moio L., La Pietra L., Cacace D., Palmieri L., De Martino E., Carpi G., Dall'Aglio G., MASI P., 1995. Application of high pressure treatment for microbiological stabilization of must. Vignevini, 22, 3-6.

Morason, R. Todd, Allan L. Allenspach and Richard E. Lee, Jr. (1993). Comparative ultrastructure of fat body cells of freeze-susceptible and freeze-tolerant Eurosta solidaginis larvae after chemical fixation and high pressure freezing. Journal of Insect Physiology, Volume 40, Issue 2, Pages 155-164.

Murakami, T., Kimura, I., Yamagishi, T., Yamashita, M., Sugimoto, M., Satake, M. (1992). Thawing of frozen fish by hydrostatic pressure., in High Pressure and Biotechnology; Coloquies INSERM., C. Balny, et al., Editors. 1992, John Libbey Eurotext Ltd.: Montrouge, France. p. 329-331.

Mussa, D.M. and Le Bail, A. (2000). High pressure thawing of fish: evaluation of the process impact on Listeria innocua, 2000 IFT Annual Meeting, June 10-14, Dallas, Texas, USA.

Nakagami, T., T. Shigehisa, T. Ohmori, S. Taji, A. Hase and T. Kimura et al., Inactivation of herpes viruses by high hydrostatic pressure, Journal of Virological Methods 38 (1992), pp. 255–262.

Niven, G.W., C.A. Miles and B.M. Mackey, The effects of hydrostatic pressure on ribosome conformation in Escherichia coli: An in vivo study using differential scanning calorimetry, Microbiology 145 (1999), pp. 419–425.

Okamoto, A.and Suzuki, A. (2001). Effects of high hydrostatic pressure-thawing on pork meat. Nippon Shokuhin Kagaku Kogaku Kaishi, 48(12), 891-898.

Oliveira, A.C., D. Ishimaru, R.B. Gonçalves, T.J. Smith, P. Mason and D. Sá-Carvalho et al., Low temperature and pressure stability of picornaviruses: Implications for virus uncoating, Biophysical Journal 76 (1999), pp. 1270–1279.

Oomes, S.J.C.M., and Brul, S. (2004). The effect of metal ions commonly present in food on gene expression of sporulating Bacillus subtilis cells in relation to spore wet heat resistance. Innov. Food Sci. & Emerg. Technol. 5, 307-316.

O'Reilly, Ciara E., Alan L. Kelly, Patrick M. Murphy and Thomas P. Beresford. (2001). High pressure treatment: applications in cheese manufacture and ripening. Trends in Food Science & Technology, Volume 12, Issue 2, Pages 51-59.

Otake, T., H. Mori, T. Kawahatta, Y. Izumoto, H. Nishimura and I. Oishi et al., Effects of high hydrostatic pressure treatment on HIV infectivity. In: K. Heremans, Editor, High pressure research in the biosciences and biotechnology, Leuven University Press, Belgium (1997), pp. 233–236.

Otero, L. and Sanz, P.D. (2000). High-pressure shift freezing. Part 1. Amount of ice instantaneously formed in the process. Biotechnol. Prog., 16:1030-1036.

Otero, L., Martino, M., Zaritzky, N., Solas, M. and Sanz, P.D. (2000). Preservation of microstructure in peach and mango during high pressure-shift freezing. J. Food Sci., 65:466-470.

Otero, L.; Solas, M. T.; Sanz, P. D.; de Elvira, C. and Carrasco, J. A. (1998). Contrasting effects of high-pressure-assisted freezing and conventional air-freezing on eggplant tissue microstructure. Z. Lebensm. Unters. Forsch., 206:338-342.

Pagan, R. and B. Mackey, Relationship between membrane damage and cell death in presssure-treated Escherichia coli cells: Differences between exponential- and stationary-phase cells and variation among strains, Applied and Environmental Microbiology 66 (2000), pp. 2829–2834.

Palmieri, L. and Cacace, D. (2005). High intensity pulsed light technology. In Emerging technologies for food processing, Sun, D. (editor). ISBN 0-12-676757-2. Elsevier Academic Press, London, UK.

Palou, E., Lopez-Malo, A., Barbosa-Canovas, G. V., Welti-Chanes, J., and Swanson, B. G. (1999). High-pressure treatment in food preservation. In: Handbook of Food Preservation, M. S. Rahman, ed., Marcel Dekker, New York, 533-575.

Paquin, P. (1999). Int. Dairy J. (9) 329-335.

Patterson, M.F., M. Quinn, R. Simpson and A. Gilmour, Sensitivity of vegetative pathogens to high hydrostatic pressure treatment in phosphate-buffered saline and foods, Journal of Food Protection 58 (1995), pp. 524–529.

Pehrsson P.E., 1996. Application of high-pressure pasteurization to citrus processing. In : Institute of Food Technologists Ann. Meet., Book of abstracts, p 108.

Peleg M. A model of microbial survival after exposure to pulsed electric fields. J. Science of Food and Agriculture. 1995; 67(1):93-99.

Petrenko, V.F. and Withworth, R.W. (1999). In: Physics of ice, Oxford University Press, New York.

Pham, Q.T. (1985). A fast, unconditionally stable finite-difference scheme for heat conduction with phase change. Inter.J.Heat Mass Transfer., 28:2079-2084.

Pham, Q.T. (1987). A note on some finite-difference methods for heat conduction with phase change. Numerical Heat Transfer., 11:353-359.

Pham, Q.T. (1989). Effect of supercooling on freezing time due to dendritic growth of ice crystals. Int. J. Refrig., 12:295-300.

Pham, Q.T. (1989). Effect of supercooling on freezing time due to dendritic growth of ice crystals. Int. J. Refrig., 12:295-300.

Pham, Q.T. (1996). Prediction of calorimetric properties and freezing time of foods from composition data. J. Food Eng, 30:95-107.

Pontes, L., L.A. Fornells, V. Giongo, J.R.V. Araujo, A. Sepulveda and M. Villas-Boas et al., Pressure inactivation of animal viruses: Potential biotechnological applications. In: K. Heremans, Editor, High pressure research in the biosciences and biotechnology, Leuven University Press, Belgium (1997), pp. 91–94.

Pontes, L., Y. Cordeiro, V. Giongo, M. Villas-Boas, A. Barreto and J.R. Araújo et al., Pressure-induced formation of inactive triple-shelled rotavirus particles is associated with changes in the spike protein VP4, Journal of Molecular Biology 307 (2001), pp. 1171–1179.

Popper, L. and D. Knorr (1990). Food Technology, 7:84-89.

Préstamo, G., Palomares, L. & Sanz, P. (2005). Frozen Foods Treated by Pressure Shift Freezing: Proteins and Enzymes. Journal of Food Science-Vol.70, No.1.

Qin BL, Pothakamury UR, Vega H, Martin O, Barbosa-Canovas GV, Swanson BG. Food pasteurization using high-intensity pulsed electric fields. Food Technology 1995; 49(12):55-60.

Rao, M.A. and R.W. Hartel, Eds. (1998). Phase/State Transitions in Food. Marcel Dekker, New York.

Rastogi, N.K., Raghavarao, K.S.M.S. and Niranjan, K. (2005). Developments in osmotic dehydration. In Emerging technologies for food processing, Sun, D. (editor). ISBN 0-12-676757-2. Elsevier Academic Press, London, UK.

Reeve RM, Hautala E, Weaver ML. (1969). Anatomy and compositional variation within potatoes. I. developmental histology of the tuber. American Potato Journal 46, 361–373.

Reid, D. S. (1993). Basic physical phenomena in the freezing and thawing of plant and animal tissue. In: Frozen food technology, C. P. Mallett, ed., Blackie Academic & Professional, Glasgow, 1-19.

Reid, D.S. (1998a). Freezing-nucleation in foods and antifreeze action. In “The Properties of Water in Foods”. ISOPOW 6. D.S. Reid, Ed., Blackie Academic, London, pp. 275-286.

Reid, D.S. (1998b). Crystallization phenomena in the frozen state. In “Phase/State Transitions in Foods. Chemical, Structural and Rheological Changes”. M.A. Rao, R.W. Hartel, Eds., Marcel Dekker, New York, pp. 313-326.

Reina LD, Jin ZT, Zhang, QH, Yousef AE. Inactivation of Listeria monocytogenes in milkby pulsed electric field. J. Food Protect. 1998; 61(9):1203-1206.

Reyns, Kristien M. F. A., Carine C. F. Soontjens, Kris Cornelis, Carla A. Weemaes, Marc E. Hendrickx and Chris W. Michiels.(2000). Kinetic analysis and modelling of combined high-pressure–temperature inactivation of the yeast Zygosaccharomyces bailii. International Journal of Food Microbiology, Volume 56, Issues 2-3, Pages 199-210.

Richter, Karsten. (1994). High-density morphologies of ice in high-pressure frozen biological specimens. Ultramicroscopy, Volume 53, Issue 3, Pages 237-249.

Ross, R. G., Andersson, P., and Bäckström, G. (1977). High Temp.- High Press. 9. 87-96.

Rouillé, J., Le Bail, A., Ramaswamy, H.S. and Leclerc, L. (2002). High pressure thawing of fish and shellfish. Journal of Food Engineering, 53(1):83-88.

Rovere P., Sandei L., Colombi A., Munari M, Ghiretti G., Carpi G., Dall'Aglio G., 1997. Effects of high pressure treatments on chopped tomatoes. Ind. Conserve, 72, 3-12.

Sale, A.J.H., G.W. Gould and W.A. Hamilton, Inactivation of bacterial spores by hydrostatic pressure, Journal of General Microbiology 60 (1970), pp. 323–334.

Sancho Félix, Yann Lambert, Gérard Demazeau, Alain Largeteau, Jean-Marie Bouvier and Jean-François Narbonne. (1999). Effect of ultra-high hydrostatic pressure on hydrosoluble vitamins. Journal of Food Engineering, Volume 39, Issue 3, Pages 247-253.

Sanz, P.D. and Otero, L. (2000). High-pressure shift freezing. Part 2. Modeling of freezing times for a finite cylindical model. Biotechnol. Prog., 16:1037-1043.

Sanz, P.D., de Elvira, C., Martino, M., Zaritzky, N., Otero, L. and Carrasco, J.A. (1999). Freezing rate simulation as an aid to reducing crystallization damage in foods. Meat Science, 52:275-278.

Sanz, P.D., L. Otero, C. de Elvira and J. A. Carrasco. (1997). Freezing processes in high-pressure domains. International Journal of Refrigeration, Volume 20, Issue 5, Pages 301-307.

Sanz, P.D., Solas, M.T. and Sanz, P.D. (1998). Microstructure of frozen large fruits. Pol. J. Food Nutr. Sci., 7/48(3):65-68.

Schlüter, O. (2004). Impact of High Pressure-Low Temperature Processes on Cellular Materials Related to Food. PhD Thesis. Technical University of Berlin.

Schlüter, O. and Knorr, D. (2002). Impact of the metastable state of water on the design of high pressure supported freezing and thawing processes. ASAE Meeting Paper No. 026024. St. Joseph, Mich.: ASAE.

Schlüter, O., George, S., Heinz, V. and Knorr, D. (1998). Phase transitions in model foods, induced by pressure-assisted freezing and pressure-assisted thawing. IIR Proceedings Series “Refrigeration Science and Technology”, 1998/6: 240-248.

Schlüter, O., George, S., Heinz, V. and Knorr, D. (1999). Pressure-assisted thawing of potato cylinders. In “Advances in High Pressure Bioscience and Biotechnology”. H. Ludwig, Ed. Springer Verlag, Berlin, pp. 475-480.

Schlüter, O., Heinz, V. und Knorr, D. (2003). Freezing kinetics due to ice III formation in potato tissue, in Advances in High Pres. Biosci. and Biotech.; Winter, R. Ed. 2002; Springer-Verlag, Heidelberg, Germany.

Schlüter, O., Urrutia Benet, G., Heinz, V and Knorr, D. (2004). Metastable states of water and ice during pressure-supported freezing of potato tissue. Biotechnology Progress, 20, 799-810.

Schubring, R., Meyer, C., Schlüter, O., Boguslawski, S. and Knorr, D. (2002). Thawing of frozen fish fillets by high hydrostatic pressure at 200 MPa. Presented in part at the

32nd Annual Meeting of the Western European Fish Technologists' Association, May 12-15 2002, Galway, Ireland.

Schubring, R.; Meyer, C.; Schlüter, O.; Boguslawski, S.; Knorr, D. (2003). Impact of high pressure assisted thawing on the quality of fillets from various fish species. Innov. Food Sci. and Emerg. Techn., 4 (2003) 257-267.

SeverinI C., Romani S., Dall'Aglio G., Rovere P., Conte L., Lerici C.R., 1997. High pressure effects on lipid oxidation of extra virgin olive oils and seed oils. Ital. J. Food Sci., 9, 183-191.

Seyderhelm, I., Boguslawski, S., Michaels, G & Knorr, D. 1996. Pressure induced inactivation of selected food enzymes. J. Food Sci., 61: 308-310.

Shen, T., Urrutia Benet, G., Brul, S. and Knorr, D. (2005). Influence of high-pressure-low temperature treatment on the inactivation of bacillus subtilis cells. Innovative Food Science and Emerging Technologies (in press).

Shigehisa, T., T. Ohmori, A. Saito, S. Taji and R. Hayashi, Effects of high pressure on the characteristics of pork slurries and inactivation of micro-organisms associated with meat and meat products, International Journal of Food Microbiology 12 (1991), pp. 207–216.

Silva, J.L. and G. Weber, Pressure induced dissociation of brome mosaic virus, Journal of Molecular Biology 199 (1988), pp. 149–161.

Silva, J.L., P. Luan, M. Glaser, E.W. Voss and G. Weber, Effects of hydrostatic pressure on a membrane-enveloped virus: Immunogenicity of the pressure-inactivated virus, Journal of Virology 66 (1992), pp. 2111–2117.

Simpson RK, Whittington R, Earnshaw RG, Russell NJ. Pulsed high electric field causes 'all or nothing' membrane damage in Listeria monocytogenes and Salmonella typhimurium, but membrane H+-ATPase is not a primary target. Int. J. Food Microbiol. 1999; 48(1):1-10.

Simpson, R.K. and A. Gilmour, The effect of high hydrostatic pressure in Listeria monocytogenes in phosphate-buffered saline and model food systems, Journal of Applied Microbiology 83 (1997), pp. 181–188.

Singh, R. P., and Heldman, D. R. (2001). In: Introduction to food engineering, Academic Press, London, UK.

Smelt, J.P.P.M, Hellemons, J. and Brul, S. (2001). Physiological aspects of modelling of high pressure inactivation of micro-organisms. Proceedings of high pressure meeting Japan, november 2000.

Smelt, J.P.P.M. (1998). Recent advances in the microbiology of high pressure processing. Trends in Food Science and Technology 9, 152-158.

Smelt, J.P.P.M., A.G.F. Rikje and A. Hayhurst, Possible mechanism of high pressure inactivation of micro-organisms, High Pressure Research 12 (1994), pp. 199–203.

Smelt, J.P.P.M., J.C. Hellemons, P.C. Wouters and S.J.C. van Gerwen, Physiological and mathematical aspects in setting criteria for decontamination of foods by physical means, International Journal of Food Microbiology 78 (2002), pp. 57–77.

Smelt, J.P.P.M., Recent advances in the microbiology of high pressure processing, Trends in Food Science and Technology 9 (1998), pp. 152–158.

Smout, C., Sila, D.N., Vu, T.S., Van Loey, A.M.L. and Hendrickx, M.E.G. (2005). Effect of preheating and calcium pre-treatment on pectin structure and thermal texture degradation: a case study on carrots. Journal of Food Engineering, 67, 419-425.).

Suthanthangjai, Winai, Paul Kajda and Ioannis Zabetakis. (2005). The effect of high hydrostatic pressure on the anthocyanins of raspberry (Rubus idaeus). Food Chemistry, Volume 90, Issues 1-2, Pages 193-197.

Takai, R., Kozhima, T.T. and Suzuki, T. (1991). Low temperature thawing by using high-pressure. Les actes du XVIIe Congrès International du Froid. Vol. 4, pp. 1951-1955.

Tammann, G. (1900). Über die Grenzen des festen Zustandes IV. Annalen der Physik, 4(2):1-31.

Tedford, L.A., D. Smith and C. J. Schaschke. (1999). High pressure processing effects on the molecular structure of ovalbumin, lysozyme and β-lactoglobulin. Food Research International, Volume 32, Issue 2, Pages 101-106.

Teramoto, A. and Fuchigami, M. (2000). Changes in Temperature, Texture, and Structure of Konnyaku (Konjac Glucomannan Gel) During High-pressure-freezing. Journal of Food Science, 65(3):491-497.

Tewari, G. , D. S. Jayas and R. A. Holley (1999). Science des aliments, 19: 619-661

Thevernot,R. 1979. A History of Refrigeration throughout the world, International Institute of Refrigeration, Paris.

Thiebaud, M., , E. Dumay, J. C. Cheftel (2002). Pressure-shift freezing of O/W emulsions: influence of fructose and sodium alginate on supercooling, nucleation, freezing kinetics and ice crystal size distribution. Food Hydrocolloids, 16, 13-31.

Tholozan, J. L., Ritz, M., Jugiau, F., Federighi, M. & Tissier, J. P. (2000). Physiological effects of high hydrostatic pressure treatments on Listeria monocytogenes and Salmonella typhimurium. Journal of Applied Microbiology 88 (2), 202-212. doi: 10.1046/j.1365-2672.2000.00917.x

Tian, S.-M., K.-C. Ruan, J.-F. Qian, G.-Q. Shao and C. Balny, Effects of hydrostatic pressure on the structure and biological activity of infectious bursal disease virus, European Journal of Biochemistry 267 (2000), pp. 4486–4494.

Torres, J. Antonio and Gonzalo Velazquez. (2005). Commercial opportunities and research challenges in the high pressure processing of foods. Journal of Food Engineering, Volume 67, Issues 1-2, Pages 95-112.

Trujillo, A.J., M. Capellas, M. Buffa, C. Royo, R. Gervilla, X. Felipe, E. Sendra, J. Saldo, V. Ferragut and B. Guamis. (2000). Application of high pressure treatment for cheese production. Food Research International, Volume 33, Issues 3-4, Pages 311-316.

Urrutia Benet, G., N. Chapleau, M. Lille, A. Le Bail, K. Autio and D. Knorr. (2005). Quality related aspects of high pressure low temperature processed whole potatoes. Innovative Food Science and Emerging Technologies, in press.

Urrutia Benet, G., O. Schlüter, D. Knorr. (2004). High pressure–low temperature processing. Suggested definitions and terminology. Innovative Food Science and Emerging Technologies, 5:413-427.

Urrutia-Benet, G, T. Balogh, J. Schneider and D. Knorr. (2006). Metastable phases during High-Pressure-Low-Temperature processing of potatoes and their impact on quality-related parameters. Journal of Food Engineering, in press.

Vali, G. Ed. (1995). “Biological Ice Nucleation and its Applications”, APS Press, St. Paul, MN.

Vámos-Vigyázó, L. (1981) Polyphenoloxidase and peroxidase in fruit and vegetables. CRC Crit. Rev. Food Sci. Nutr., 15, 49-127.

Van der Plancken, Iesel, Ann Van Loey and Marc E. Hendrickx. (2005). Combined effect of high pressure and temperature on selected properties of egg white proteins.

Innovative Food Science & Emerging Technologies, Volume 6, Issue 1, March 2005, Pages 11-20.

van der Rest, M.E., Kamminga, A.H., Nakano, A., Anraku, Y., Poolman, B. and Konings, W. (1995). The plasmamembrane of Saccharomyces cerevisiae: structure, function and biogenesis. Microbiology Reviews 59, 304-322.

Voldřich, Michal, Jaroslav Dobiáš, Lydie Tichá, Miroslav Čeřovský and Jana Krátká. (2004). Resistance of vegetative cells and ascospores of heat resistant mould Talaromyces avellaneus to the high pressure treatment in apple juice. Journal of Food Engineering, Volume 61, Issue 4, Pages 541-543.

Wagner, W., Saul, A.B., and Pruß, A. (1994). International equations for the pressure along the melting and along the sublimation curve of ordinary water substance. J. Phys. Chem. Ref. Data, 23:515-527.

Weemaes, C., Ludikhuyze, L., van den Broeck, I., and Hendrickx, M. E. G. (1998). High pressure inactivation of polyphenoloxidases. Journal of Food Science, 63(5), 873-877.

Whatmore, A.M., and R.H. Reed. (1990). Determination of turgor pressure in bacillus subtilis: a possible role for K+ in turgor regulation. J. Gen. Microbiol. 136:2521-2526.

Wilkinson, N., A. S. Kurdziel, S. Langton, E. Needs and N. Cook. (2001). Resistance of poliovirus to inactivation by high hydrostatic pressures. Innovative Food Science & Emerging Technologies, Volume 2, Issue 2, Pages 95-98.

Wouters, P.C., E. Galaasker and J.P.P.M. Smelt, Effects of high pressure on inactivation kinetics and events related to proton efflux in Lactobacillus plantarum, Applied and Environmental Microbiology 64 (1998), pp. 509–514.

Wouters, P.C., Glaasker, E. and Smelt J.P.P.M. (1998) Effects of high pressure on inactivation kinetics and events related to proton efflux in Lactobacillus plantarum. Appl. Env. Microbiol. 64, 509-514.

Wuytack, Elke Y. and Chris W. Michiels. (2001). A study on the effects of high pressure and heat on Bacillus subtilis spores at low pH. International Journal of Food Microbiology, Volume 64, Issue 3, Pages 333-341.

Yan, Hong and G. V. Barbosa-Cánovas. (2001). Density Changes in Selected Agglomerated Food Powders Due to High Hydrostatic Pressure. Lebensmittel-Wissenschaft und-Technologie, Volume 34, Issue 8, Pages 495-501.

Yoshioka, K., Yamada, A., Maki, T., Yoshimoto, C. and Yamamoto, T. (1999). Application of high pressurisation to fish meat: the ultrastructural changes and nucleotide in frozen carp muscle under high pressure thawing. In “Advances in High Pressure Bioscience and Biotechnology”, H. Ludkig, Ed. Springer Verlag, Berlin, pp. 501-504.

Zhang QH, Chang FJ, Barbosa-Canovas V, Swanson BG. Inactivation of micro-organisms in a semisolid model food using high voltage pulsed electric fields. Lebensm. Wiss. Technol. 1994; 27:538-543.

Zhang, Hongkang., Lite Li, Eizo Tatsumi and Sabir Kotwal. (2003). Influence of high pressure on conformational changes of soybean glycinin. Innovative Food Science & Emerging Technologies, Volume 4, Issue 3, Pages 269-275.

Zhao, Y., Flores, R.A. and Olson, D.G. (1998). High hydrostatic pressure effects on rapid thawing of frozen beef. Journal of Food Science, 63(2):272-275.

Zhu, S. (2004). Phase transition studies in food systems during high pressure processing and its applications to pressure shift freezing and high pressure thawing. PhD Thesis, McGill University, Montreal, Canada.

Zhu, S., H.S. Ramaswamy and A. Le Bail. (2005). High-pressure calorimetric evaluation of ice crystal ratio formed by rapid depressurization during pressure-shift freezing of water and pork muscle. Food Research International, Volume 38, Issue 2, Pages 193-201.

Zhu, S.; Ramaswamy, H.S.; Simpson, B.K. (2004). Effect of high-pressure versus conventional thawing on colour, drip loss and texture of Atlantic salmon frozen by different methods. Lebensmittel-Wissenschaft und –Technologie, 37(3):291-299.

List of publications and contributions to congresses

Journal publications

Schlüter, O., Urrutia Benet, G., Heinz, V and Knorr, D. (2004). Metastable states of water and ice during pressure-supported freezing of potato tissue. Biotechnology Progress, 20, 799-810.

Urrutia Benet, G., O. Schlüter, D. Knorr. (2004). High pressure–low temperature processing. Suggested definitions and terminology. Innovative Food Science and Emerging Technologies, 5:413-427.

Shen, T., Urrutia Benet, G., Brul, S. and Knorr, D. (2005). Influence of high-pressure-low temperature treatment on the inactivation of bacillus subtilis cells. Innovative Food Science and Emerging Technologies (in press).Technologies, 6:271-278.

Urrutia Benet, G., N. Chapleau, M. Lille, A. Le Bail, K. Autio and D. Knorr. (2005). Quality related aspects of high pressure low temperature processed whole potatoes. Innovative Food Science and Emerging Technologies, in press.

Urrutia-Benet, G, T. Balogh, J. Schneider and D. Knorr. (2006). Metastable phases during High-Pressure-Low-Temperature processing of potatoes and their impact on quality-related parameters. Journal of Food Engineering, in press.

Urrutia-Benet, G., O. Schlüter, J. Schneider and D. Knorr. (2006). Dynamic evaluation of pressure-supported thawing processes. Influence of metastable phases on thawing paths. Innovative Food Science and Emerging Technologies, submitted.

Contributions to congresses

Urrutia Benet, G., O. Schlüter and D. Knorr (2003). High pressure-low temperature safe processing of food: mathematical modelling of freezing and thawing of food products. Workshop on Nonthermal Food Preservation. Wageningen, The Netherlands, 7 –10 September 2003. (Poster).

High Pressure - Low Temperature Processing for Food Technology - Universitat de València - 3 March 2004. Invited lecture.

Urrutia Benet, G., O. Schlüter and D. Knorr (2004). Mathematical modelling of pressure-supported freezing processes through metastable states of water and ice. International Congress on Engineering and Food, ICEF 9, Montpellier, France, 7-11 March 2004. (Oral presentation).

Schlüter, O., G. Urrutia and D. Knorr (2004). Critical Process Parameters of Pressure-Supported Thawing of Plant Tissue. International Congress on Engineering and Food, ICEF 9, Montpellier, France, 7-11 March 2004. (Poster).

Urrutia Benet, G. and D. Knorr (2005). The impact of metastable phases on pressure-supported freezing and thawing processes. Intradfood 2005. Innovations in traditional foods, 25-28 October 2005, Valencia, Spain. (Oral presentation).

Shen, T., G. Urrutia Benet, S. Brul and D. Knorr (2005). Influence of high-pressure-low-temperature treatment on the inactivation of Bacillus subtilis cells. Intradfood 2005. Innovations in traditional foods, 25-28 October 2005, Valencia, Spain. (Oral presentation).

Otero, L., C. de Elvira, G. Urrutia Benet, A. Ousegui, A. Le Bail and P. Sanz (2005). Modelling industrial scale High-Pressure-Low-Temperature processes. Intradfood 2005. Innovations in traditional foods, 25-28 October 2005, Valencia, Spain. (Oral presentation).

Urrutia Benet, G., O. Schlüter and D. Knorr (2005). The impact of metastable phases on high pressure low temperature (HPLT) processing times. Intradfood 2005. Innovations in traditional foods, 25-28 October 2005, Valencia, Spain. (Poster).